Biologically active molecules from marine microalgae

Thesis

Biologically Active Molecules from Marine Microalgae

Giuliana d'Ippolito

Laurea in Chimica e Tecnologia Farmaceutiche

DOCTOR OF PHILOSOPHY

Sponsoring Establishment:
Stazione Zoologica "A. Dohrn", Naples, Italy

Collaborating Establishment:
Institute of Biomolecular Chemistry (ICB)-CNR, Pozzuoli, Italy

Director of studies
Adrianna Ianora

Internal advisor
Angelo Fontana

Second supervisors
Marcel Jaspars
Guido Cimino

December, 2005

Table of Contents

Abstract I

List of publications II

List of abbreviations III

Chapter 1

INTRODUCTION 1-14

1.1. The plankton 1

1.2. The diatoms 2

1.3. Effect of diatoms on copepod reproduction 6

1.4. Teratogenic effects of diatoms 8

1.5. Other inhibitory effects of diatoms 9

1.6. Reversibility of the negative effect of diatoms on egg hatching 10

1.7. Field evidence of the inhibitory effects of diatoms 10

1.8. The chemistry of diatom defence 12

1.9. Aims of this PhD thesis 14

Chapter 2

RESULTS 15-69

2.1. Derivatization procedure of aldehydes 15

2.2. *Skeletonema costatum* 19

2.2.1. Ecological effect of *S. costatum* on copepod reproduction 19

2.2.2. Aldehyde profile 19

2.2.3. Fatty acid composition 21

2.2.4. Biosynthesis of octadienal from 6,9,12-hexadecatrienoic acid 22

2.2.5. Incubation experiments with $^{3}H_{10}$-EPA 25

2.2.6. Lipid analysis 26

2.2.7. PUAs formation from glycolipids 28

2.2.8. Metabolism of complex lipids containing radioactive EPA 29

2.2.9. Characterization of MGDG 30

2.2.10. Structure elucidation of other oxylipins 31

2.2.11. Absolute stereochemistry of 9-hydroxy-7*E*-hexadecenoic acid 35

2.2.12. Absolute stereochemistry of 9-hydroxy-6*Z*,9*E*12*Z*-hexadecatrienoic acid 35

2.2.13. Absolute stereochemistry of 15-HEPE methyl ester and
5-HEPE methyl ester 36

2.3. *Thalassiosira rotula* 38

2.3.1. Ecological effect of *T. rotula* on copepod reproduction 38

2.3.2. Aldehyde profile 38

2.3.3. Production of octadienal and its intermadiates from HTrA 39

2.3.4. Production of decatrienal and its intermediates from $^{3}H_{10}$-EPA 41

2.3.5. Substrate specificity 44

2.3.6. Subcellular localization of enzymatic activities involved
in the synthesis of aldehydes 45

2.3.7. Lipid analysis 47

2.3.8. Metabolism of complex lipids by cell preparations 47

2.3.9. Free/bound fatty acids ratio 49

2.3.10. Glycolipid composition 50

2.3.11. Preliminar characterization of lipolytic activity 50

2.3.12. Structure elucidation of other oxylipins 52

2.3.13. Metabolism of HTrA 55

2.3.14. Identification of lipoxygenase activities on SDS-PAGE 55

2.4. *Pseudonitchshia delicatissima* 57

2.4.1. Ecological effect of *P. delicatissima* on copepod reproduction 57

2.4.2. Structure elucidation of oxylipins 57

2.4.3. Incubation experiments with $^{3}H_{10}$-EPA 61

2.5. The genus *Chaetoceros* 63

2.5.1. Effect of *C. socialis* and *C.affinis* on copepod reproduction 63

2.5.2. Oxylipins in *C. socialis* and *C. affinis* 64

2.5.3. Comparison of LOX activity between the two species 65

2.6. Antimitotic assay of oxylipins 66

Chapter 3

DISCUSSION 70-94

3.1. Chemistry 70

3.2. Biochemistry 75

3.2.1 Biosynthesis of oxylipins 75

3.2.2 Molecular characterization of lipoxygenases in *T.rotula* 83

3.2.3 Lipolytic activity in marine diatoms 86

3.2.4 Dynamics of oxylipin pathway in marine diatoms 89

3.3 Biochemical ecology 92

Chapter 4

CONCLUSION 95-98

Chapter 5

MATERIALS AND METHODS 99-114

5.1. General 99

5.2. Cell culturing 99

5.3. Extraction of aldehydes 100

5.4. Derivatization procedure of aldehydes 100

5.5. Purification of CET-aldehydes 101

5.6. GCMS analysis of CET-aldehydes 101

5.7. Total fatty acid composition 101

5.8. GCMS analysis of FAME 101

5.9. Isolation of HTA form *S. costatum* 101

5.10. Synthesis of d_6-HTrA 102

5.11. Incubation experiments with d_6-HTrA 102

5.12. Incubation experiment with $^3H_{10}$-EPA in *S. costatum* 102

5.13. Incubation experiment with $^3H_{10}$-EPA in *T. rotula* 103

5.14. Inactivated enzymatic preparations 104

5.15. Localization of LOX/HPL in *T. rotula* 104

5.16. LOX assay in *T. rotula* 104

5.17. Substrate specificity in *T. rotula* 105

5.18. Lipid extraction 105

5.19. Composition of complex lipids 106

5.20. Direct in vivo preparation of labelled TAG, GL, PL in *S. costatum* 106

5.21. Incubation experiments with $^3H_{10}$-EPA-containing lipids in *S. costatum* 106

5.22. Incubation experiments with aldehyde-depleted homogenates of *S. costatum* cells 107

5.23. Incubation experiments of lipids in ultrafiltered fractions of *T. rotula* 107

5.24. Quantification of lipid hydrolysis in lysed diatoms of *T. rotula* 108

5.25. Fractionation of the lipolytic activity of *T. rotula* 109

5.26. Preliminary characterization of the lipolytic activity and zymograms in *T. rotula* 109

5.27. Native gel filtration of 102'000 g supernatants in *T. rotula* 110

5.28. Extraction, purification and analysis of oxylipins 111

5.29. Absolute stereochemistry of 9-hydroxy-7E-hexadecenoic acid in *T. rotula* 111

5.30. Absolute Stereochemistry of 9-HHTrE in *T. rotula* 112

5.31. Chiral analysis of 6-hydroxyhexadecatrienoic acid in *T. rotula* 112

5.32 Conversion of d_6-HTrA into d_6-HHtrE in *T. rotula* 112

5.33. Absolute stereochemistry of 11-HEPE, 15-HEPE, 9-HEPE and 5-HEPE 113

5.34. Incorporation of $^3H_{10}$-EPA in *P. delicatissima* 113

5.35. Autoxidation of EPA 114

5.36. Antimitotic assay on sea urchin embryos of *Paracentrotus lividus* 114

Chapter 6

REFERENCES 115-120

ABSTRACT

Diatoms are unicellular photosynthetic microalgae responsible for approximately 40% of marine primary productivity. This algal class has traditionally been regarded as providing the bulk of the food that sustains the marine food chain to top consumers and important fisheries. However, this beneficial role has recently been questioned on the basis of laboratory and field studies showing that although dominant zooplankton grazers such as copepods feed extensively on diatoms, the hatching success of eggs thus produced is seriously impaired. Short chain polyunsaturated aldehydes, such as 2,4,7-decatrienal and 2,4-decadienal, were correlated to the antiproliferative effect of diatoms on copepod reproduction. After establishing a method of analysis, the aldehyde profile of some ecologically relevant species of marine diatoms was assessed. The results showed that the production of aldehydes is species-specific. Detailed chemical analysis revealed the presence of fatty acid derivatives other than aldehydes such as hydroxyacids, ketoacids, oxoacids and epoxyalcohols, increasing the complexity of a chemical defence of diatoms mediated only by aldehydes. All these compounds belong to a class of compounds called oxylipins, that are oxygenated compounds biosynthesized from fatty acids by oxygenase-catalyzed oxygenation. Marine diatoms are able to produce the major antiproliferative oxylipins by a novel oxygenase-dependent oxidation of C_{16} fatty acids hexadecatrienoic acid (16:3 ω-4) and hexadecatetrenoic acid (16:4 ω-1), and C_{20} eicosapentaenoic acid (20:5 ω-3). This process is triggered by lypolitic acyl hydrolase activity, that feeds the downstream lipoxygenase pathway. The ecological meaning of the oxylipin pathway in the diatom-copepod interactions is discussed, showing that attention should move from single compounds to complex biochemical process. The deleterious effect on copepod reproduction could be due to a biochemical process such as the generation of an high oxidative potential, rather than only by aldehydes or other secondary oxygenated products, that when present can co-occur to produce the final effect.

List of publications:

1. **d'Ippolito, G.**, Romano,G., Iadicicco, O., Miralto, A., Ianora, A., Cimino, G., Fontana, A. New birth-control aldehydes from the marine diatom *Skeletonema costatum*: characterization and biogenesis. *Tetrahedron Lett.* 2002, 43, 6133-6136.

2. **d'Ippolito, G.**, Romano, G., Iadicicco, O., Fontana, A. Detection of short-chain aldehydes in marine organisms: the diatom *Thalassiosira rotula. Tetrahedron Lett.* 2002, 43, 6137-6140.

3. **d'Ippolito, G.**, Romano, G., Caruso, T., Spinella, A., Cimino, G., Fontana, A. Production of octadienal in the marine diatom *Skeletonema costatum. Org. Lett.* 2003, 5, 885-887.

4. **d'Ippolito G.**, Tucci S., Cutignano A., Romano G., Cimino G., Miralto A., Fontana A. The role of complex lipids in the synthesis of bioactive aldehydes of the marine diatom *Skeletonema costatum. BBA,* 2004, 1686, 100-107.

5. Paffenhöfer G-A., Ianora A., Miralto A., Turner J.T., Kleppel G.S., Ribera d'Alcala M., Casotti R., Caldwell G.S., Pohnert G., Fontana A., Müller-Navarra D., Jonasdottir S., Armbrust V. Båmstedt U., Ban S., Bentley M.G., Boersma M., Bundy M., Buttino I., Calbet A., Carlotti F., Carotenuto Y., **d'Ippolito G.**, Frost B., Guisande C., Lampert W., Lee R.F., Mazza S., Mazzocchi M.G., Nejstgaard J.C., Poulet S.A., Romano G., Smetacek V., Uye S., Wakeham S., Watson S., Wichard T. Colloquium on diatom-copepod interactions, *Mar. Ecol. Prog. Ser.* 2005, 286, 293-305.

6. **d'Ippolito G.**, Cutignano A., Briante R., Febbraio F., Cimino G., Fontana A. New C_{16} fatty acid-based oxylipin pathway in the marine diatom *Thalassiosira rotula. Org. Biomol. Chem.* 2005, 3, 4065-4070.

7. **d'Ippolito G.**, Cutignano A., Tucci S., Romano G., Cimino G., Fontana A. Biosynthetic intermediates and stereochemical aspects of aldehyde biosynthesis in the marine diatom *Thalassiosira rotula. Phytochemistry*, 2006, 67 (3), 314-322

8. Cutignano A., **d'Ippolito G.**, Romano G., Lamari N., Cimino G., Febbraio F., Nucci R., Fontana A. Chloroplastic galactolipids fuel the aldehyde biosynthesis in the marine diatom *Thalassiosira rotula. ChemBioChem*, 2006, 7(3), 450-456.

List of Abbreviations:

AA, Arachidonic acid; APCI, atmospheric pressure chemical ionization; CET, carbethoxyethylidene; COSY, correlation spectroscopy; DGDG, digalactosyldiacylglycerol; e.e., enantiomeric excess; DIBAL, diisobutylaluminium hydride; EPA, 5Z,8Z,11Z,14Z,17Z-eicosapentaenoic acid; $^{3}H_{10}$-EPA, [5,6,8,9,11,12,14,15,17,18-^{3}H]-eicosapentaenoic acid; ESI, electron spray ionization; FAME, fatty acid methyl ester; FFA, free fatty acid; GCMS, gas chromatography-mass spectrometry; GL, glycolipid; HMBC, heteronuclear multiple bond coherence; HSQC, heteronuclear quantum coherence; HPL, hydroperoxide lyase; HPLC, high performance liquid chromatography; HTrA, 6,9,12-hexadecatrienoic acid (C16:3 ω-4); d_6-HTrA, [6,7,9,10,12,13-$^{2}H_6$]-6,9,12-hexadecatrienoic acid; HTA, 6,9,12,15- hexadecatetraenoic acid (C16:4 ω-1); IEF, isoelectric focusing; LCMS, liquid chromatography-mass spectrometry; LOX, lipoxygenase; MGDG, monogalactosyldiacylglycerol; MUF, 4-methylumbelliferone; NMR, nuclear magnetic resonance; PL, phospholipid; PUA, polyunsaturated aldehyde; PUFA, polyunsaturated free fatty acid; RP-HPLC, reverse phase-HPLC; SP-HPLC, staight phase-HPLC; SQDG, sulfoquinovosyldiacylglycerol; TAG, triacylglycerol; TOCSY, totally correlated spectroscopy; TMP, trimethylphosphite.

5-HEPE, 5-hydroxy-6*E*,8*Z*,11*Z*,14*E*,17*Z*-eicosapentaenoic acid;

6-HHTE, 6-hydroxy-7*E*,9*Z*,12*Z*,15-hexadecatetraenoic acid;

6-HHTrE, 6-hydroxy-7*E*,9*Z*,12*Z*- hexadecatrienoic acid;

6-KHTE, 6-keto-7*E*,9*Z*,12*Z*,15-hexadecatetraenoic acid;

6-KHTrE, 6-keto-7*E*,9*Z*,12*Z*-hexadecatrienoic acid;

9-HEPE, 9-hydroxy- 5*Z*,7*E*,11*Z*,14*E*,17*Z*-eicosapentaenoic acid;

9-HHTrE, 9-hydroxy-6*Z*,10*E*,12*Z*-hexadecatrienoic acid;

9-HPHTrE, 9-hydroperoxy-6*Z*,10*E*,12*Z*-hexadecatrienoic acid;

11-HEPE, 11-hydroxy-5*Z*,8*Z*,12*E*,14*Z*,17*Z*-eicosapentaenoic acid;

11-HPEPE, 11-hydroperoxy-5*Z*,8*Z*,12*E*,14*Z*,17*Z*-eicosapentaenoic acid;

14-HEPE, 14-hydroxy-5*Z*,8*Z*,11*Z*,15*E*,17*Z*-eicosapentaenoic acid;

15-HEPE, 15-hydroxy- 5*Z*,8*Z*,11*Z*,13*E*,17*Z*-eicosapentaenoic acid;

15-HPEPE, 15-hydroperoxy- 5*Z*,8*Z*,11*Z*,13*E*,17*Z*-eicosapentaenoic acid.

1. INTRODUCTION

1.1. The plankton

The plankton are a group of organisms subject to the movement of the water in which they live. While many are capable of small-scale movement, their large scale movements and distribution are determined by currents, thus they are "drifters" in the sea. At this level, "plankton" includes ZOOPLANKTON, or animal drifters (non-photosynthetic, heterotrophic organisms such as copepods, and many larval forms of sessile animals, and jellyfish), BACTERIOPLANKTON, bacteria (including both photosynthetic cyanobacteria and non-photosynthetic, or heterotrophic, bacteria), and PHYTOPLANKTON, which refers primarily to microalgae. More than 5000 species of marine microalgae are known to date; these are separated into five major divisions: Chlorophyta (green-algae) Chrysophyta (golden-brown, yellow algae and diatoms) Pyrrophyta (dinoflagellates) Euglenophyta and Cyanophyta (blue-green algae). The taxonomy of microalgae is subject of controversy. For instance, cyanobacteria (division Cianophyta) are prokaryotic bacteria sometimes included in bacterioplankton, sometimes in phytoplankton because they photosynthesize. Another pending issue is whether non-photosynthetic organisms should be included in the microalgae or not. For example, a great number of dinoflagellates lack chlorophylls and live heterotrophically, eating bacteria and other microalgae.

Phytoplankton have been called the grasses of the sea. Through the process of photosynthesis, these microscopic, single-celled plants nourish the entire food web of the oceans. The lives of all animals that live in the sea, with the exception of hydrothermal vent organisms, depend on phytoplankton for energy and minerals (Figure 1.1). The global carbon cycle, which regulates the temperature of our planet, and life-sustaining oxygen, essential to the metabolism of all aerobic organisms, is controlled by the activity of the phytoplankton. Perhaps no other group of organisms plays such a major role in the maintenance of life on Earth.

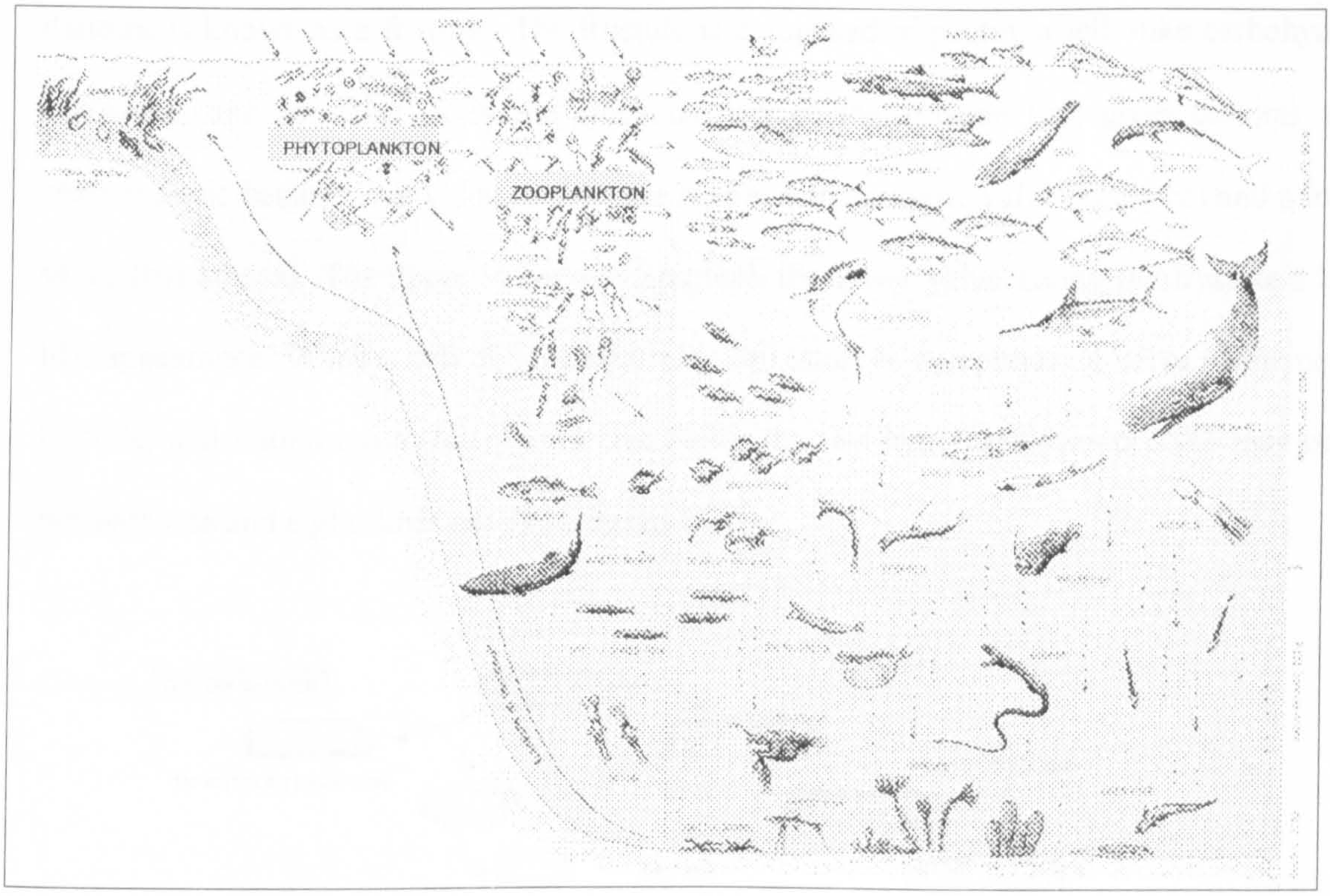

Figure 1.1: The marine food chain (from Isaacs, 1969)

Marine phytoplankton represent the major contributors of marine carbon fixation. In some regions of the ocean, these organisms can fix approximately the same amount of carbon, a few grams per square meter per day, as a terrestrial forest (Smetacek, 2001). Today, the oceans cover 70% of the Earth's surface, and on a global scale they are thought to contribute approximately one half of the total primary productivity of the planet.

1.2. The diatoms

Diatoms are one of the most important group of eukaryotic phytoplankton colonizing the oceans down to depths to which photosynthetically available radiation can penetrate. The diatoms are responsible for approximately 40% of marine primary productivity (Falkowski et al., 1998). They also play a key role in the biogeochemical cycling of silica (Treguer et al.,1995) owing to their requirement for this mineral for cell wall biogenesis. The cell wall of

diatoms is known as a frustule. The frustule is composed of pectin, a jelly-like carbohydrate substance, and of silica. It is the siliceous part of the frustule that gives diatoms their characteristic beauty. Every diatom frustule is split into an upper valve (epitheca) and a lower valve (hypotheca). The upper valve overlaps with the lower valve giving the frustule a box-like appearance. When a cell divides each new cell takes as its epitheca a valve of the parent frustule, and within ten to twenty minutes builds its own hypotheca; this process may occur between one and eight times per day (Figure 1.2).

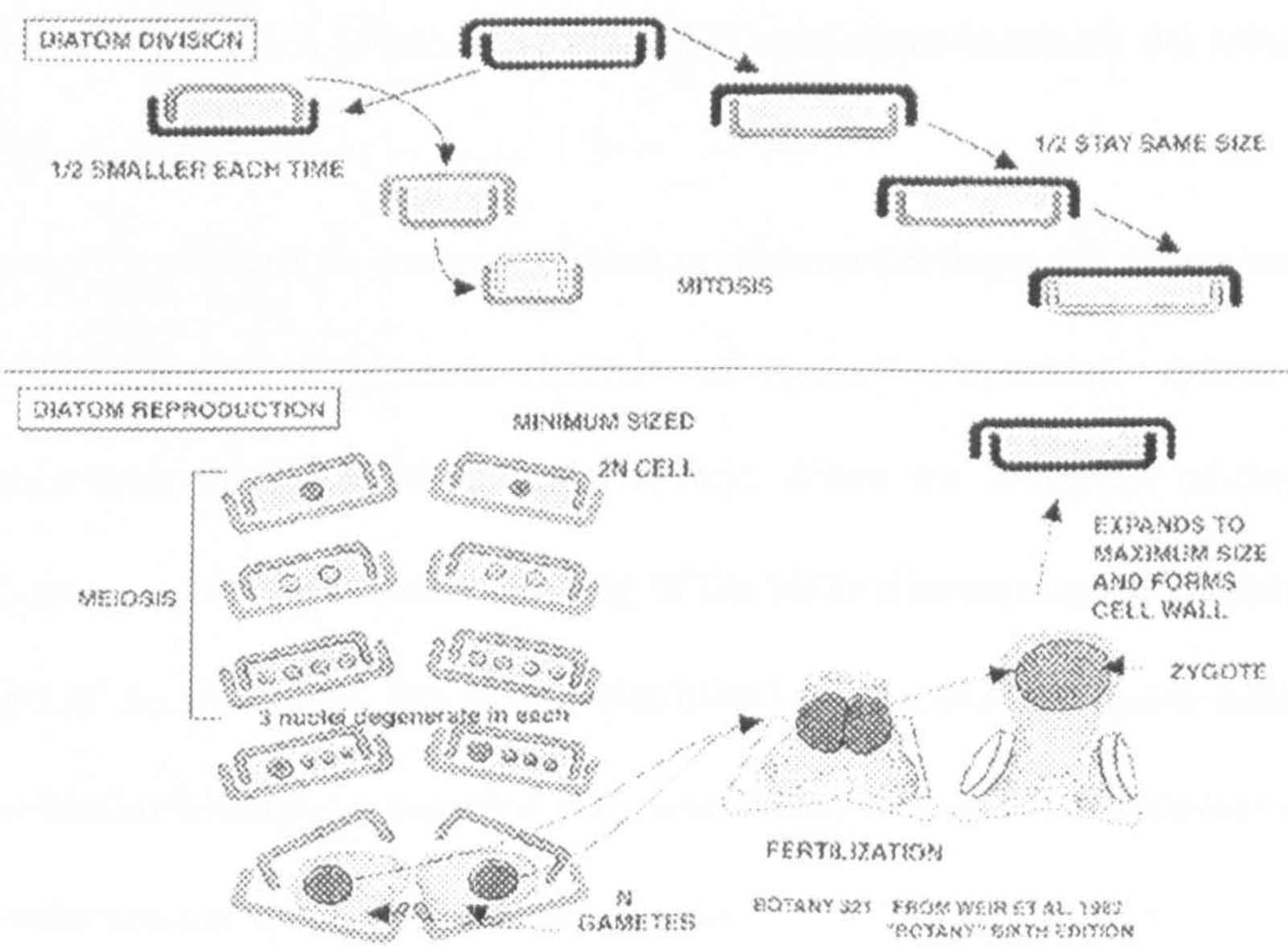

Figure 1.2: Life cycle of diatoms (from Weir et al., 1982)

This means that the original lower valve now becomes the upper valve (of the daughter cell) and that the size of the diatom is reduced. If this process continued, the diatom would shrink out of existence. However, when a certain minimum size is reached, diatoms form a reproductive spore, known as an auxospore. This spore gives rise to a full-size diatom and the process starts all over again. Many planktonic diatoms alternate between a vegetative

reproductive phase and a thicker walled resting cyst or statospore stage. The siliceous resting spore commonly forms after a period of active vegetative reproduction when nutrient levels have been depleted. An increase in nutrient levels and/or length of daylight cause the statospore to germinate and return to its normal vegetative state. Seasonal upwelling is therefore a vital part of many diatoms life cycle as a provider of nutrients and as a transport mechanism which brings statospores or their vegetative products up into the photic zone. Since the frustules persist after death, they are also the subject of paleoclimate research as frustules from sediments can be identified. Knowing who lived in the waters above the sediment can give clues to past environmental conditions based on the tolerance range of the species that are found.

The taxonomy of diatoms is mainly based on the morphology of the opaline frustule, its shape, its fine structure, the presence-absence of special elevations, spines and processes, in accordance with the classical Linnean method. Since the invention of the Scanning Electron Microscope a much better understanding of the three dimensionality of the diatom frustule and the shape of its processes has been established. But more and more research is being done using molecular biology to examine the genetic relationships. Sometimes two species that look quite similar are not closely related genetically.

Diatoms are divided into two subgroups, Centrales and Pennales, based on the symmetry of their frustules (Figure 1.3). Centric diatoms are radially symmetrical, appearing round like pillboxes or baskets. Pennate diatoms have bilateral symmetry, appearing slender and curved like rods. Because of their shape, centric diatoms float better than pennate diatoms and, thus, centric diatoms tend to be strictly planktonic while pennate diatoms tend to be primarily benthic. There are well over 250 genera of extant diatoms, with perhaps as many as 100,000 species (Norton et al., 1996) ranging across three orders of magnitude in size (about as many as land plants) and exhibiting a remarkable variety of shapes.

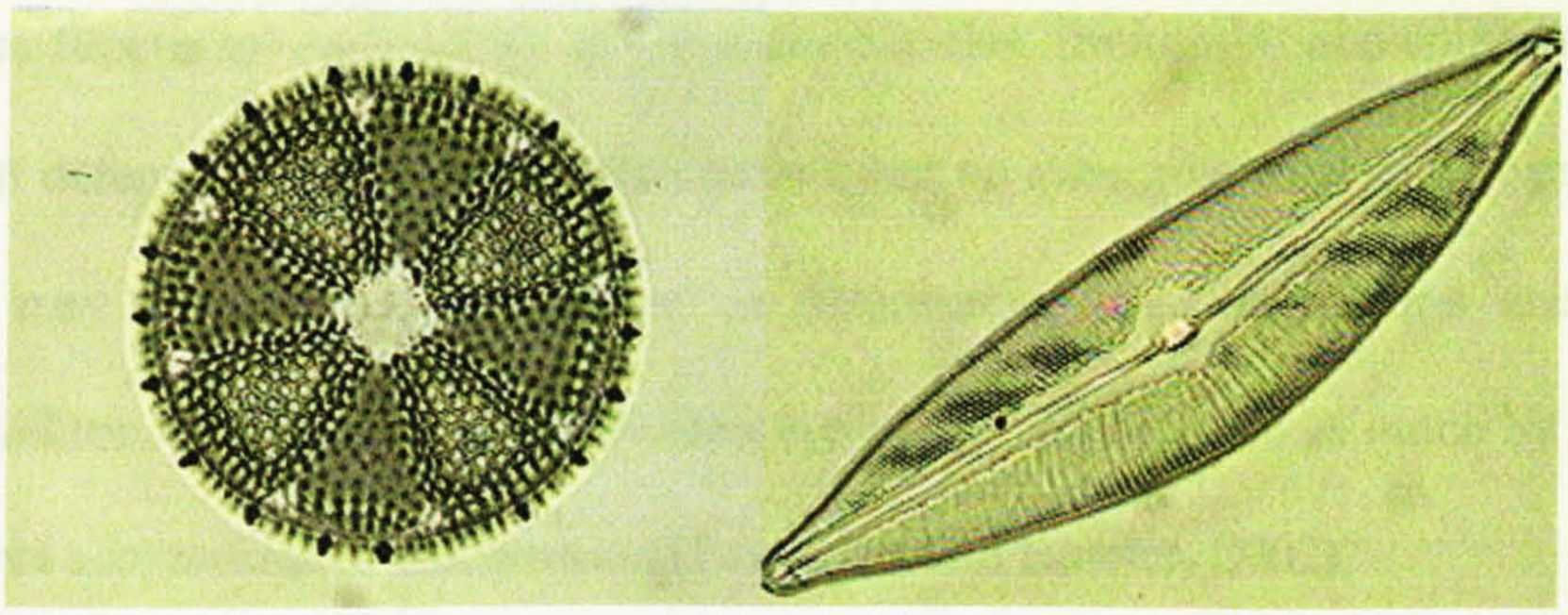

Figure 1.3: Typical centric (left) and pennate (right) diatom.

The well-studied small-celled species (5–50 μm) tend to be most abundant at the beginning of spring and autumn, when nutrients are not limiting and when light intensity and day length are optimal for diatom photosynthesis. When nutrients run out they will often aggregate into flocks that sink quickly out of the photic zone. The giant diatoms (which can reach 2–5 mm in size) are ubiquitous in all oceans, and their abundance shows less seasonal variability. Their silica cell walls predominate in the sediments of the ocean floor, thus making them serious players in ocean biogeochemistry over geologically significant timescales (Kemp, 2000). Besides planktonic diatoms, which are found in all open water masses, there are many benthic forms, growing on sediments or attached to rocks or macroalgae, and some species can also be found in soil (Lee, 1999). Diatoms also constitute a large proportion of the algae associated with sea ice in the Antarctic and Arctic.

In spite of their ecological relevance, very little is known about the basic biology of diatoms (Scala and Bowler, 2001). What are the molecular secrets behind their success? One possibility is that they have an extraordinary capacity for finding different adaptive solutions (e.g., physiological, biochemical, behavioural) to different environments. It has also been proposed that the major factor behind ecological success is their siliceous cell wall. Smetacek (Smetacek 1999 and 2001) has argued that the many different shapes and sizes of diatoms evolved to provide a robust first line of defence against various type of grazers, therefore

being the functional equivalents of the waxy cuticles, trichomes, and spines of higher plants. Plankton defense systems are poorly studied, but an emerging idea is that protection against grazers may be an important factor in determining the composition and succession of phytoplankton. If this is the case plankton evolution may be ruled as much by protection as by short-term adaptations or competition (Falciatore and Bowler, 2002).

1.3. Effects of diatoms on copepod reproduction

There is at present considerable debate in the biological oceanography community as to whether diatoms are a good or poor food for copepod reproduction and development. The idea that diatoms were therefore at the base of the marine food chain, and constituted a suitable food source for copepods, largely persisted until the 1990s. Various copepod species have been successfully grown with unialgal diets of diatoms, even though there is some evidence that diatoms are not an optimal food for copepod growth, because they lengthen the generation time and increase mortality rates (e.g. Paffenhofer, 1970). Kleppel (1993) was the first to point out that diatoms have been ascribed too much importance in the past and that, although copepods do consume diatoms to a large extent, they also eat many other kinds of organisms. It was originally shown by Ianora & Poulet (1993) that a diatom diet induced high egg production rates in the copepod *Temora stylifera* (Dana), even though hatching success was seriously impaired, with a four- to six-fold difference in hatching success between a diatom and a nondiatom diet. However, when Ianora & Poulet screened different biochemical components in the diatom *Thalassiosira rotula* and the dinoflagellate *Prorocentrum minimum* (including proteins, free amino acids, vitamins and fatty acids), they found no substantial differences between them. Later, Poulet *et al.* (1994) proposed that the inhibitory effect of diatoms on copepod egg-hatching success was not caused by a nutritional deficiency of diatoms, but by the presence of antimitotic compounds blocking copepod embryogenesis. They showed that, when the copepod *Calanus helgolandicus* (Claus) was fed the diatom *T.*

rotula, hatching success was dramatically reduced, dropping to 20% after 4 days of feeding on this diatom. The same type of inhibition was also observed using crude diatom extracts, which not only blocked development of newly spawned *C. helgolandicus* eggs, but also arrested cleavage in the classic sea urchin bioassay.

Several examples of how diatoms reduce hatching success with time, derived from a variety of studies. However, the data also indicated that not all copepods showed the same sensitivity to diatom metabolites, and that not all diatoms induced the same inhibitory effects on copepods. For example, diatoms had different effects on egg production rates in different copepods.

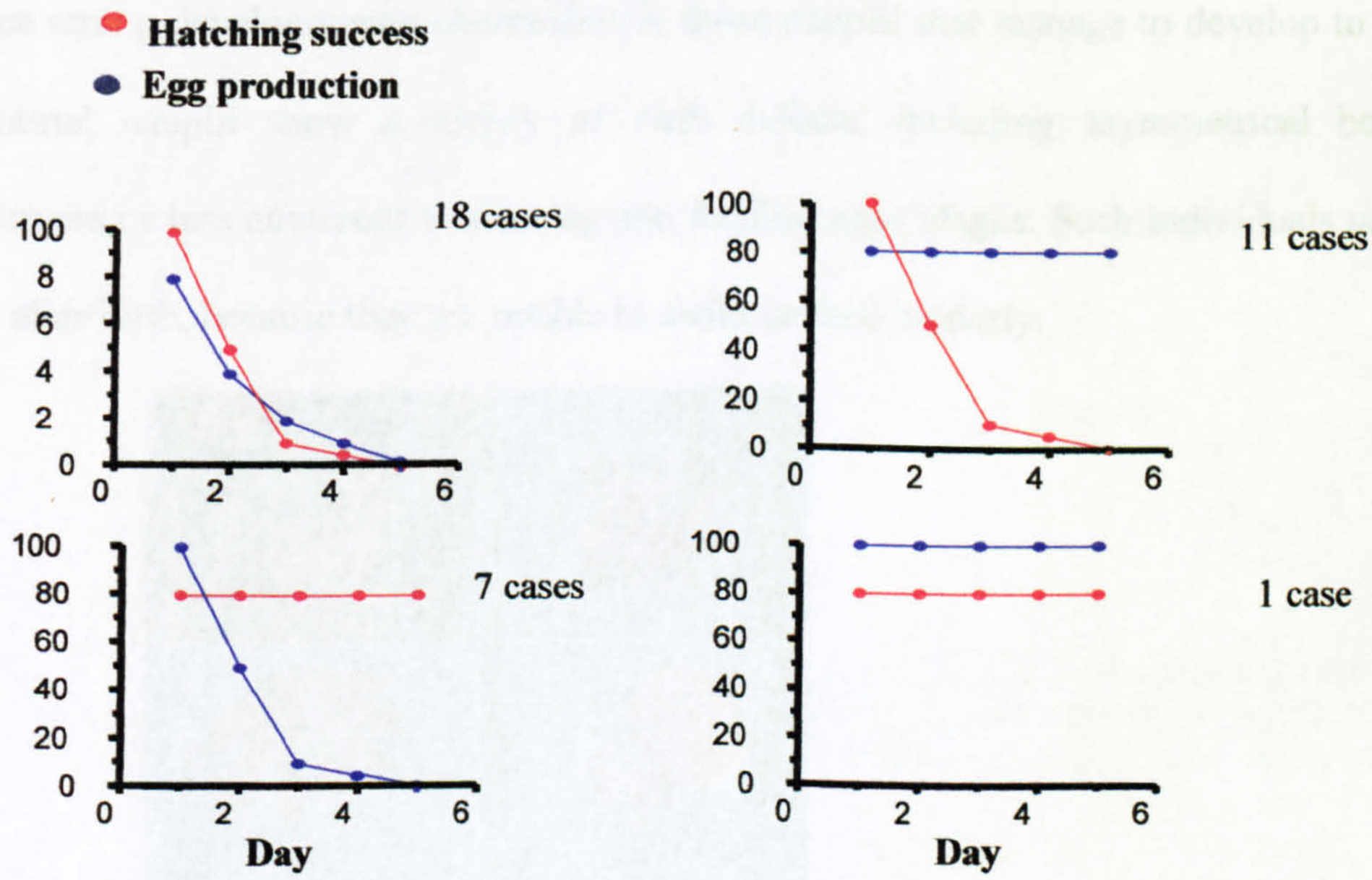

Figure 1.4: Thirty-seven selected combinations of copepod -diatom species (from Ban et al., 1997).

In an exceptional study intended to add more information about diatom-copepod interactions, fifteen laboratories located worldwide in twelve different countries and representing a variety of marine, estuarine and freshwater environments joined together to test combinations of different copepod species with different diatoms species (Ban et al., 1997). Among 37 diatom-copepod combinations examined, diatoms supported either lower copepod fecundity (7 cases)

or hatching success (11 cases) or both (18 cases) (Figure 1.4). Thus, while diatoms may provide a source of energy and materials for copepod growth, they often reduce fecundity and/or hatching success. These observations constitute the paradox of diatom-copepod interactions in the pelagic food web (Ban et al., 1997).

1.4. Teratogenic effects of diatoms

By definition, 'teratogens' are substances that induce congenital malformations in the offspring of organisms exposed to them during gestation. Teratogenesis is therefore the result of developmental toxicity, which can ultimately elicit embryo or fetal mortality (i.e. abortion). Diatoms have been shown not only to interfere with copepod embryogenesis, but also to induce strong developmental aberrations in those nauplii that manage to develop to hatching. Abnormal nauplii show a variety of birth defects, including asymmetrical bodies and malformed or less numerous swimming and feeding appendages. Such individuals usually die soon after birth, because they are unable to swim or feed properly.

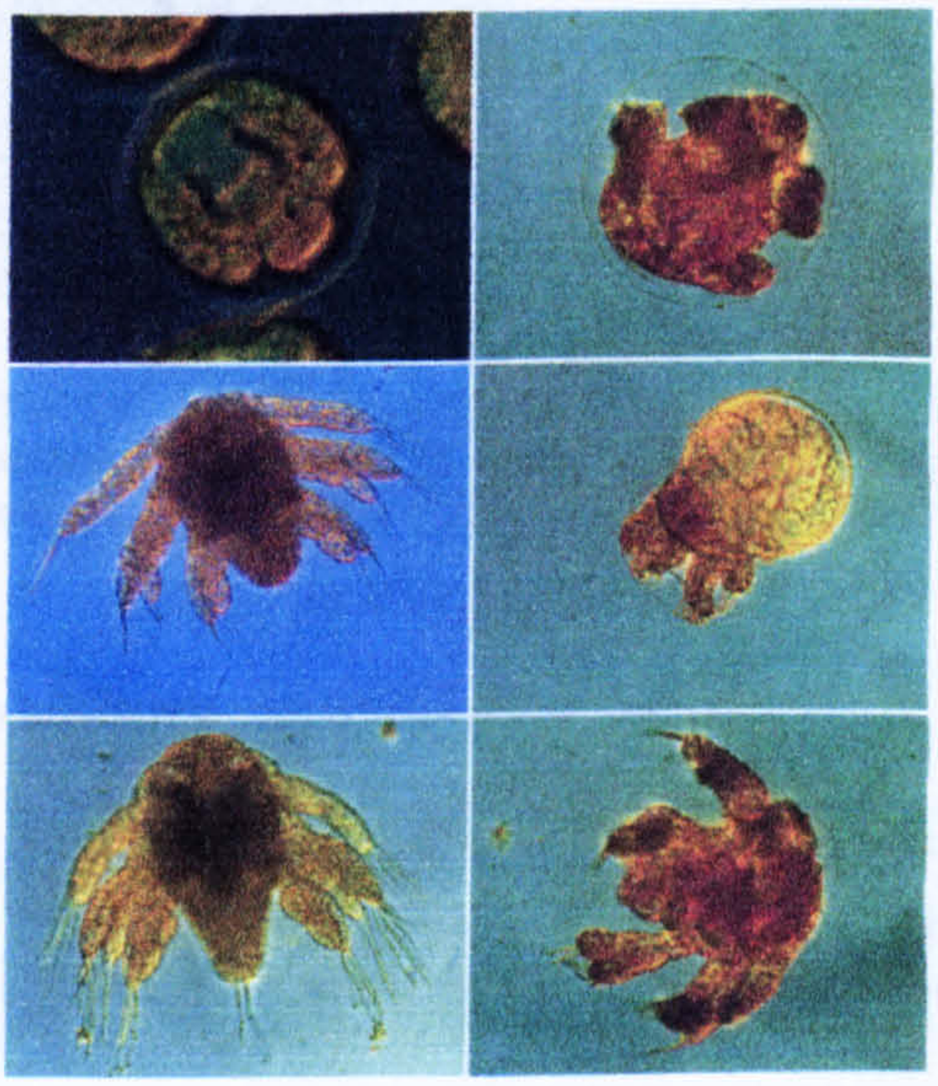

Figure 1.5: Images of *Calanus helgolandicus* regarding the development from embryos to nauplii of normal copepod (left) and copepod fed on toxic diatoms (right) (from Poulet et al., 1995).

The production of malformed nauplii was first reported by Poulet *et al.* (1995) for eggs spawned by wild *C. helgolandicus* females in various seasons of the year, and for eggs

spawned by females maintained on a diet of the diatom *Phaeodactylum tricornutum* (Figure 1.5). Abnormal nauplii were also recorded by Uye (1996) in *C. pacificus* and Starr *et al.* (1999) in *Calanus finmarchicus* fed on different diatom diets. Cell death through apoptosis occurred in many tissues of the body and especially in limbs having strong structural malformations, as revealed using confocal laser microscopy and the fluorescent probe terminal deoxynucleotidyl transferase–mediated deoxyuridine triphosphate nick end labelling (TUNEL) (Boehringer), specific for apoptosis (Figure 1.6).

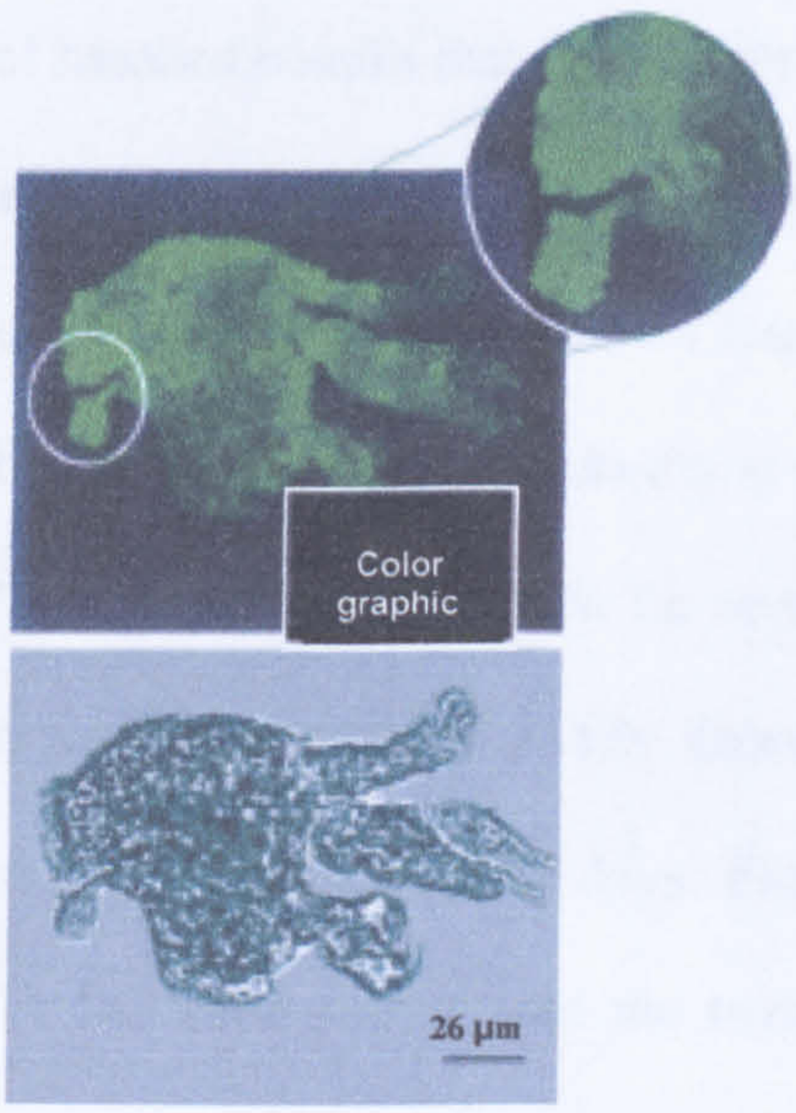

Figure 1.6: Abnormal *Calanus helgolandicus* nauplius generated from females that had been fed the diatom *Skeletonema costatum* for 5 days and observed in bright-field microscopy (lower panel); deformed limbs were positive for apoptosis, giving green fluorescence with TUNEL labelling (upper panel) (from Ianora et al., 2003)

1.5. Other inhibitory effects of diatoms

Reduced hatching success has been shown to be caused by diatom cells and not by the bacteria associated with diatom cultures. To demonstrate this, Ianora *et al.* (1996) rendered their *T. rotula* strain axenic and showed that this strain induced even stronger effects on hatching than the nonaxenic strain. Toxicity is not caused by anoxia. Miralto *et al.* (1995) have shown that, in containers with high concentrations of diatom (*T. rotula*) and dinoflagellate (*P. minimum,* as control) diets, oxygen did not modify hatching rates in *Centropages typicus*. With or without

bubbling, hatching success was 100% with dinoflagellate extracts but reduced with diatom extracts. Inhibition of egg-hatching success has been shown to be dependent on diatom density (Chaudron *et al.* 1996). The greater the number of cells ingested, the greater the inhibition, and *vice versa.* Starr *et al.* (1999) also found that the adverse effects of diatoms were density-dependent. At 10^2 cells ml^{-1} of *Thalassiosira nordenskioldii,* egg production rates in *C. finmarchicus* were low but hatching success was high. At higher concentrations of 10^4 cells ml^{-1}, the opposite was true, egg production being higher but hatching success lower; the number of hatched nauplii that were abnormal increased.

1.6. Reversibility of the negative effect of diatoms on egg hatching

In a series of laboratory experiments, Laabir *et al.* (1995) and Lacoste *et al.* (2001) showed that inhibition of egg-hatching success is reversible. When *C. helgolandicus* was first fed the diatom *P. tricornutum* or *T. rotula* for several days, and then switched to the dinoflagellate *P. minimum,* hatching success initially decreased dramatically to 0%, after which it increased sharply to >75% in only a few days. From new experiments conducted on the copepod *T. stylifera,* it has been shown that the reversibility of diatom inhibition may not necessarily apply for all copepod species. Hatching success diminished when *T. stylifera* was fed the diatom *T. rotula,* but despite some initial recovery after switching copepods to a nondiatom food, hatching success never returned to the initial values. These results suggest that some species of copepods, probably those that are more sensitive to diatom metabolites, never fully recover from the negative effects of a diatom diet in terms of egg-hatching success.

1.7. Field evidence of the inhibitory effects of diatoms

The first convincing field evidence of inhibitory effects of diatoms on copepod reproduction was reported by Miralto *et al.* (1999) who found that hatching success in *A. clausi* was greatly modified during two major diatom blooms in February 1997 and 1998 in the north Adriatic Sea. Egg viability in these periods was only 12% and 24%, respectively, of the total number of

eggs produced, compared with 90% after the bloom in June. Two diatom species, *Skeletonema costatum* (66.3%) and *Pseudonitzschia delicatissima* (23%), dominated the bloom in 1997, whereas in 1998 the bloom was almost entirely composed of *P. delicatissima* (80.6%). Neither of these two diatom species lowered egg production rates in *Acartia clausi,* which were, in fact, higher during the bloom. Notwithstanding the positive effect on fecundity, however, hatching success was dramatically reduced in both years.

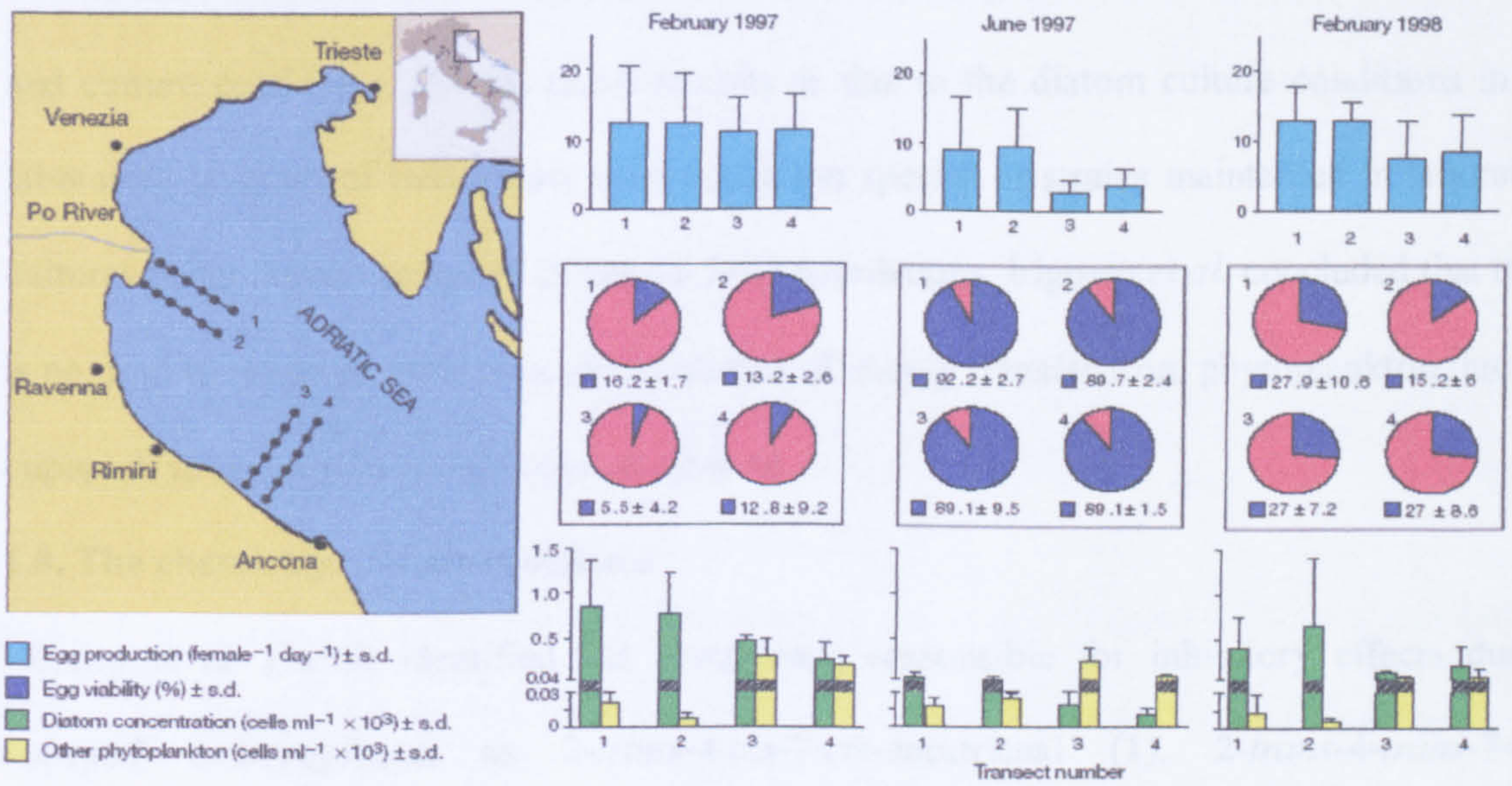

Figure 1.7 1 In situ relationship between diatom densities and copepod reproductive success during three cruises along four transects in the North Adriatic Sea during 1997±1998. Although the diatom bloom (green histograms) in February of both years promoted higher copepod fecundity (turquoise histograms), corresponding values for hatching success (blue portion of pie diagrams) were minimal in these periods compared with post-bloom conditions in June when the microbial food web was established (from Miralto et al., 1999).

There have been other studies indicating that diatoms induce deleterious effects on copepod reproduction in the wild. Mesocosm experiments off the Norwegian coast indicated a drop of 95% in the reproductive success of *C. helgolandicus* during a diatom bloom, even though feeding rates were high and alternate prey were available (Nejstgaard *et al.* 2001). A high incidence (20–40%) of abnormal nauplii of *Pseudocalanus newmani* was recently reported during a diatom bloom in the Sea of Japan (Ban *et al.* 2000). By contrast, other studies have

not found a negative relationship between egg-hatching viability and diatom concentrations. Ohman & Hirche (2001) concluded that mortality of *C. finmarchicus* eggs was caused mainly by cannibalism, and was a function of the abundance of females and juveniles, rather than diatom concentrations. Irigoien *et al.* (2002) too did not observe a negative relationship between copepod hatching success and either diatom biomass or diatom dominance in the microplankton from 12 globally distributed areas. They suggested that a possible explanation for the differences between laboratory and field results might relate to the diatom assemblage and culture conditions; that is, either toxicity is due to the diatom culture conditions in the laboratory or cases of toxicity are exceptions, the species or strains maintained in laboratory cultures being unrepresentative of natural field populations. Irigoien *et al.* concluded that there is no need to revise existing conceptual models of energy transfer from phytoplankton through copepods to fish, in diatom-dominated systems.

1.8. The chemistry of diatom defence

Miralto et al. (1999) identified the compounds responsible for inhibitory effects during copepod embryogenesis as 2-*trans*-4-*cis*-7-*cis*-decatrienal (**1**), 2-*trans*-4-*trans*-7-*cis*-decatrienal (**2**), and 2-*trans*-4-*trans*-decadienal (**3**) (Miralto *et al.* 1999). Although all three aldehydes were already known from other sources (Harkes & Begemann 1974), Miralto *et al.* were the first to report the presence of these compounds in marine diatoms. Decatrienals had been identified in the freshwater diatom *Melosira varians* C. Agardh (Wendel & Jüttner 1996), although the biological function of these molecules was unknown at the time. The anti-cell-growth activity of diatom aldehydes was tested on three animal models.

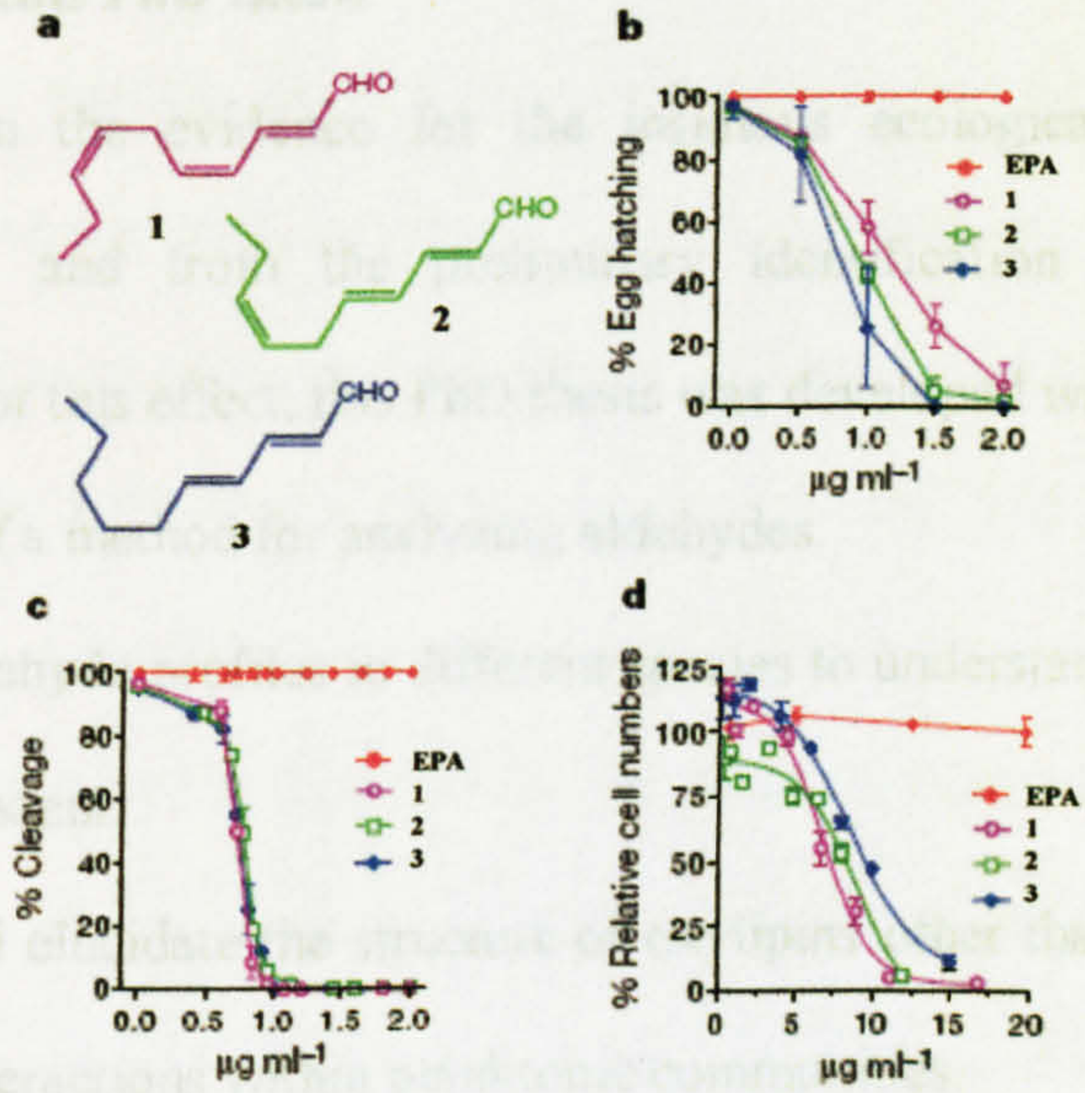

Figure 1.8 Effect of aldehydes on cell division. 2-*trans*-4-*cis*-7-*cis*-decatrienal (**1**) (pink), 2-*trans*-4-*trans*-7-*cis*-decatrienal (**2**) (green), and 2-*trans*-4-*trans*-decadienal (**3**) (blue) (a) markedly reduced the percentage hatching success of newly spawned copepod (b), cleavage of sea urchin embryos (c), and growth of Caco2 cells (d). The related compound EPA (red), used as a negative control, had no effect on cell division (from Miralto et al., 1999).

All three aldehydes reduced egg hatching rates in copepods (Figure 1.8b) and inhibited cleavage of sea urchin embryos (Figure 1.8c) when concentrations were >0.5 $\mu g/ml^{-1}$. In Caco2 cell lines derived from a human colon adenocarcinoma7, the concentration required to arrest cell growth was 11±17 $\mu g/ml^{-1}$ (Figure 1.8d). Similar concentrations of the fatty acid 5*Z*,8*Z*,11*Z*,14*Z*,17*Z*-eicosapentaenoic acid (EPA), an inactive related compound used as a negative control because of its presence in diatoms, had no effect on cell division. Aldehydes have been shown to arrest cell proliferation and induce apoptosis in cultured cell lines. It was suggested that these aldehydes were the probable agents of copepod reproductive failure when diatoms were the major source of food.

1.9. Aims of this PhD thesis

Starting from the evidence for the insidious ecological effect of diatoms on copepod reproduction, and from the preliminary identification of C_{10} aldehydes as molecules responsible for this effect, this PhD thesis was developed with the following aims:

1) Develop of a method for analyzing aldehydes.

2) Assess aldehyde profiles in different species to understand if the production of aldehydes is species-dependent.

3) Isolate and elucidate the structure of oxylipins other than aldehydes, probably involved in ecological interactions within planktonic communities.

4) Clarify oxylipin biosynthetic pathway and characterize enzymatic activities involved, to better understand the regulating factors of the process, and to develop suitable enzymatic tools to address in the future the study of phytoplankton bloom at Sea.

5) Understand the biochemical and ecological dynamics of oxylipin pathway in marine diatoms.

2. RESULTS

Plan of work

The first step was the development of a suitable method of derivatisation of aldehydes. This method was initially developed on commercially available standards, and then applied directly on diatom extracts. Five centric diatoms were choosen for the chemical ecology studies of this PhD thesis: *Skeletonema costatum*, *Thalassiosira rotula*, *Pseudonitschia delicatissima*, *Chaetoceros socialis* and *Chaetoceros affinis* (Fig....).The results were presented separately for each species and faced together into the discussion.

The selected diatoms were initially tested for their effect on copepod reproduction and screened for aldehyde composition. Then biosynthetic studies were conducted. First of all the fatty acid composition of some diatoms was assessed to understand the possible substrates involved in the oxidative processes. The biosynthetic pathways were elucidated using commercially available radioactive fatty acids or synthesizing deuterated fatty acids. After assessing the fatty acid precursor of aldehydes, their distribution in complex lipids was investigated, in order to understand the role of each lipid class in the generation of aldehydes. Biosynthesis from complex lipids was investigated using either partially purified enzymatic systems or radiolabelled substrate.

For each species, the presence of oxylipin derivatives other than aldehydes was investigated, and complete structure elucidation and stereocemical analysis were presented. Finally, the biological activity of studied oxylipins was investigated using a sea urchin embryos bioassay as a model.

2.1. Derivatization procedure of aldehydes

In order to detect polyunsaturated aldehydes in marine diatoms, a new procedure was developed based on the conversion of aldehyde into ethyl ester by the Wittig reaction with (CarbethoxyEThylidene)-triphenylphosphorane [CET-triphenylphosphorane] (Scheme 2.1). The method was designed to allow the GCMS detection of compounds with alkyl

chains ranging from 7 to 16 carbon atoms, but the procedure is also suitable for NMR and HPLC applications (d'Ippolito *et al.*, 2002b).

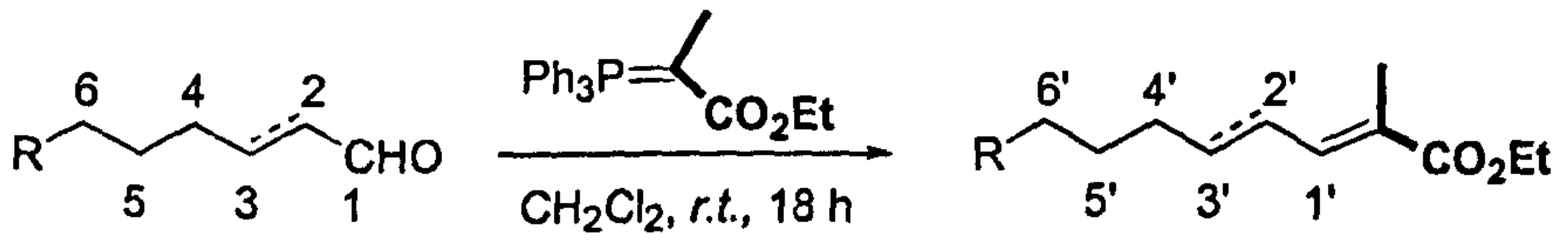

Scheme 2.1: Derivatisation procedure of aldehydes with CET-triphenylphosphorane.

The effect of temperature (16°-70°C), solvent (CH_2Cl_2, C_6H_6) and reaction time (1h-36h) was carefully evaluated in order to establish the most advantageous conditions for derivatization (data not shown). Reaction with 1.1 equivalent of derivatizing agent in CH_2Cl_2 at room temperature for 18 hours was found to be a good balance between yield and product alteration. Under these conditions, CET derivatives were formed almost quantitatively (about 98% of yield) with unconjugated aldehydes (**5-10** and **12**), whereas lower yields (87% of yield) were found with α,β-unsaturated homologues (**1-4** and **11**).

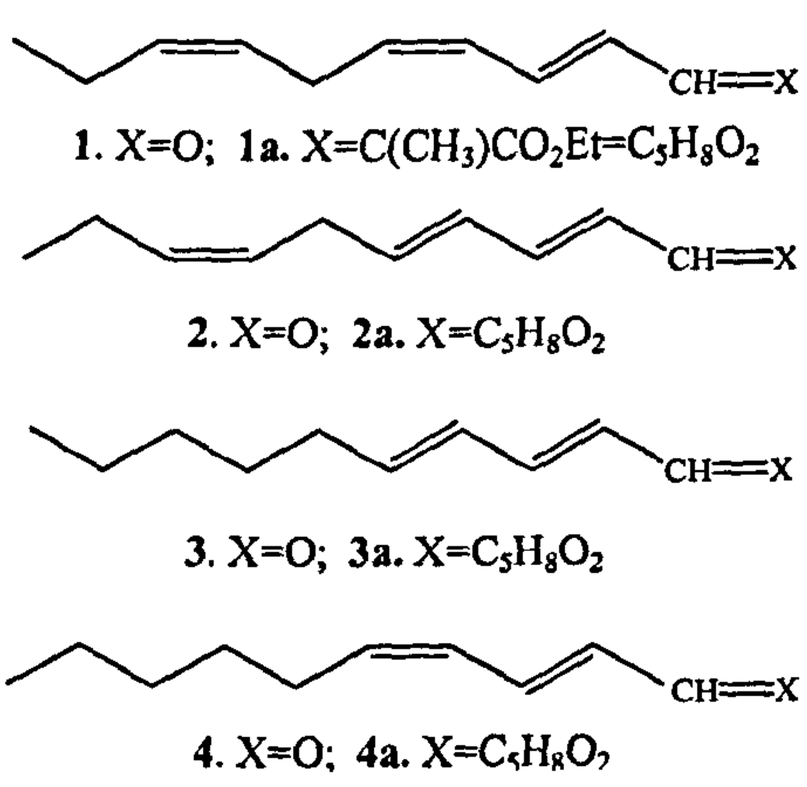

1. X=O; **1a.** X=$C(CH_3)CO_2Et$=$C_5H_8O_2$

2. X=O; **2a.** X=$C_5H_8O_2$

3. X=O; **3a.** X=$C_5H_8O_2$

4. X=O; **4a.** X=$C_5H_8O_2$

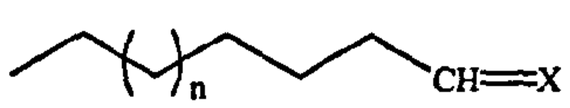

5. n=2, X=O; **5a.** n=2, X=$C_5H_8O_2$
6. n=4, X=O; **6a.** n=4 X=$C_5H_8O_2$
7. n=5, X=O; **7a.** n=5, X=$C_5H_8O_2$
8. n=6, X=O; **8a.** n=6 X=$C_5H_8O_2$
9. n=7, X=O; **9a.** n=7, X=$C_5H_8O_2$
10. n=8, X=O; **10a.** n=8 $C_5H_8O_2$

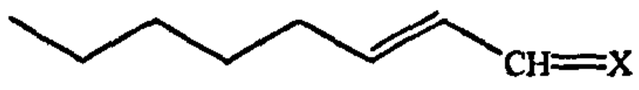

11. X=O; **11a.** X=$C_5H_8O_2$

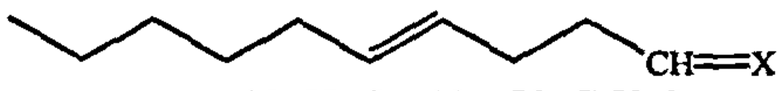

12. X=O; **12a.** X=$C_5H_8O_2$

The new generated double bond showed almost exclusively *E* configuration (95-98 %), even if the fraction of *Z* isomers increased proportionally with the amount of derivatizing agent and reaction temperature. For GCMS analysis, the reaction mixture was evaporated to dryness and dissolved in *n*-hexane or CH_2Cl_2 in order to obtain a final concentration of 0.1 or 1 μg/μL. These solutions were directly analyzed by GCMS, thus preventing any loss of material due to further sample manipulation. Alternatively, the sample was applied onto a SepPack SiO_2- cartridge and the derivatized compounds were purified with petroleum

ether/Et_2O 95:5. An average recovery of 90% was obtained in this latter case. Gas chromatographic elution of CET derivatives required a slow temperature gradient that led to separate saturated compounds at intervals of 2-3 min (Table 2.1).

	Parent aldehyde	Time (min.)	*m/z*
5a	C8:0	9.6	212 (25), 167 (45), 141 (30), 115 (80), 102 (100), 87 (65)
6a	C10:0	15.6	240 (15), 195 (35), 141 (15), 115 (85), 102 (100), 87 (50)
8a	C12:0	21.9	268 (15), 223 (25), 141 (15), 167 (60) 115 (80), 102 (100)
9a	C13:0	25.5	282 (15), 237 (40), 171 (15), 141 (20), 117 (75), 102 (100)
11a	C8:1 (2*E*)	11.7	210 (45), 165 (25), 139 (100), 111 (70), 81 (50), 79 (55)
12a	C10:1 (4*E*)	14.8	238 (10), 193 (15), 128 (100), 100 (45), 69 (65)
4a	C10:2 (2*E*,4*Z*)	17.9	236 (30), 207 (25), 291 (65), 290 (70), 161 (70), 109 (80), 93 (100)
3a	C10:2 (2*E*,4*E*)	20.8	236 (70), 207 (35), 191 (15), 137 (40), 133 (65), 93 (100), 79 (55)
1a	C10:3 (2*E*,4*Z*,7*Z*)	19.8	234 (60), 205 (15), 189 (25), 159 (40), 131 (65), 91 (100), 79 (90)
2a	C10:3 (2*E*,4*E*,7*Z*)	21.0	234 (30), 205 (10), 189 (15), 159 (25), 131 (55), 91 (100), 79 (80)

Table 2.1. GC–MS (EI, 70 eV) data of selected CET derivatives.

On the other hand, in agreement with the number of double bonds, derivatives of conjugated aldehydes were eluted later than the saturated homologues (Figure 2.1). Unambiguous characterization of each component was facilitated by the very characteristic fragmentation pattern in the high mass range of the MS spectra (Table 2.1).

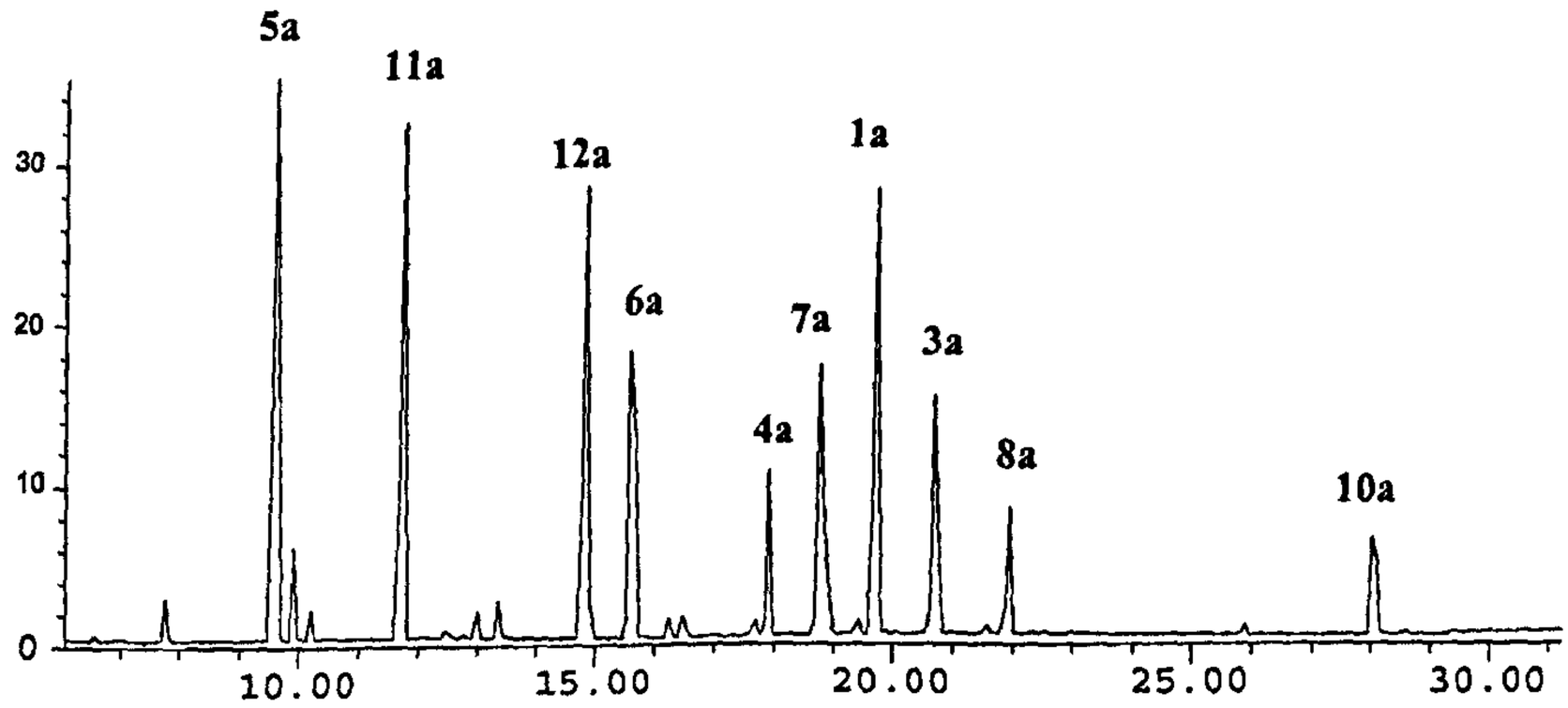

Figure 2.1: GC profile of CET derivatives of octanal (**5a**), 2*E*-octenal (**11a**), 4*E*-decenal (**12a**), decanal (**6a**), 2*E*,4*Z*-decadienal (**4a**), undecanal (**7a**), 2*E*,4*Z*,7*Z*-decatrienal (**1a**), 2*E*,4*E*-decadienal (**3a**), dodecanal (**8a**), tetradecanal (**10a**).

These included the intense molecular ion (M^+), and ions formed by loss of $CH_3CH_2O^\bullet$ ($M\text{-}45^+$) and of $CH_3CH_2^\bullet$ ($M\text{-}29^+$). However, the analysis of the MS spectra proved to be rather simple since most of the peaks could be explained by fragments of the ($M\text{-}45^+$) ions (Figure 2.2).

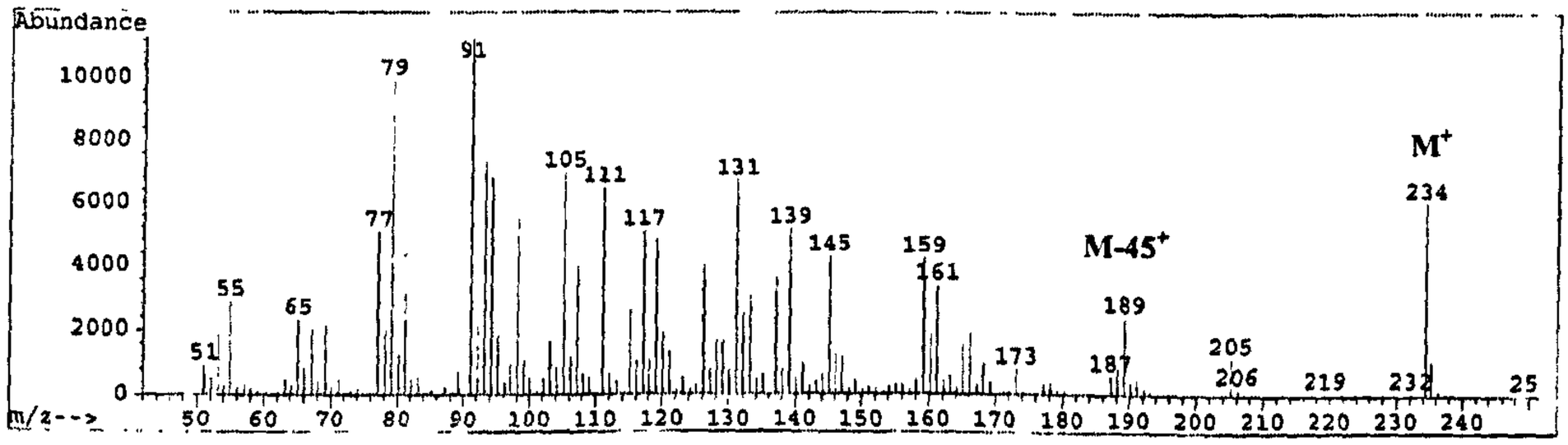

Figure 2.2: MS spectrum of CET-decatrienal (**1a**).

It is noteworthy that there was no double bond isomerization as a consequence of the derivatization procedure. The method was totally faithful even with very unstable compounds, such as *trans,cis,cis*-2,4,7-decatrienal (**1**) and *trans,cis*-2,4-decadienal (**4**), that have the intrinsic instability of double bond geometry (Spiteller and Spiteller, 2000). In this regard, an unambiguous determination of the double bond configuration of CET derivatives was obtained by NMR spectroscopy, since introduction of the carboxyethylidene group produced a strong regio-differentiation of hydrogens in α, β and γ to the carboxylic group. Clear evidence of this effect is offered by the CET derivatives of *trans,cis*-2,4-decadienal (**4a**) and *trans,trans*-2,4-decadienal (**3a**) that differ significantly for the chemical shift of H-1', H-2' and H-3' [respectively, δ 7.27, 6.48 and 6.84 in **4a** and at δ 7.20, 6.38, and 6.50 in **3a**] (Figure 2.3).

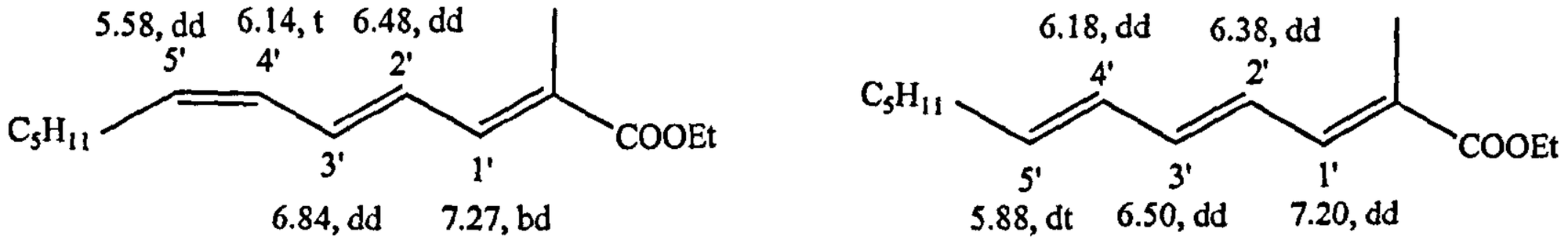

Figure 2.3: Chemical shifts of CET-derivatives of 2*E*,4*Z*-decadienal (**4a**) and 2*E*,4*E*-decadienal (**3a**). ^{1}H-NMR (400 MHz) data were recorded in $CDCl_3$ and are referenced to $CHCl_3$ (δ 7.26) as internal standard.

2.2. *Skeletonema costatum*

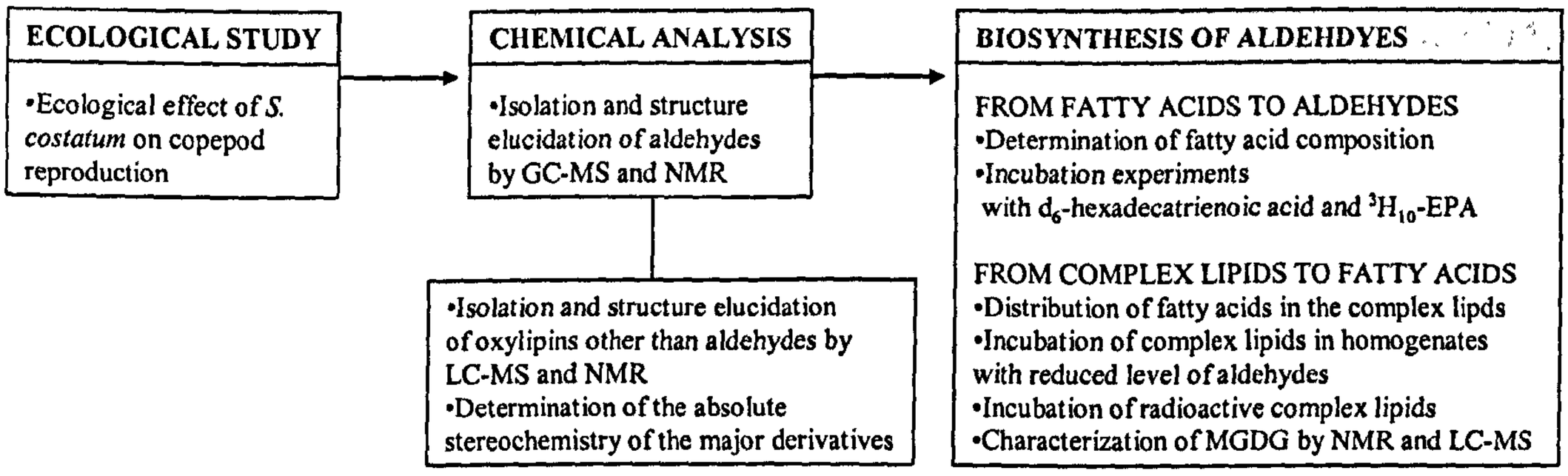

2.2.1. Ecological effect of *S. costatum* on copepod reproduction.

Egg production rates (Figure 2.4 A) and hatching viability (Figure 2.4 B) in the copepod *Temora stylifera* were strongly affected by diet. Fecundity diminished to 3.7% of initial values within only 4 days and to 0% hatching success within 7 days.

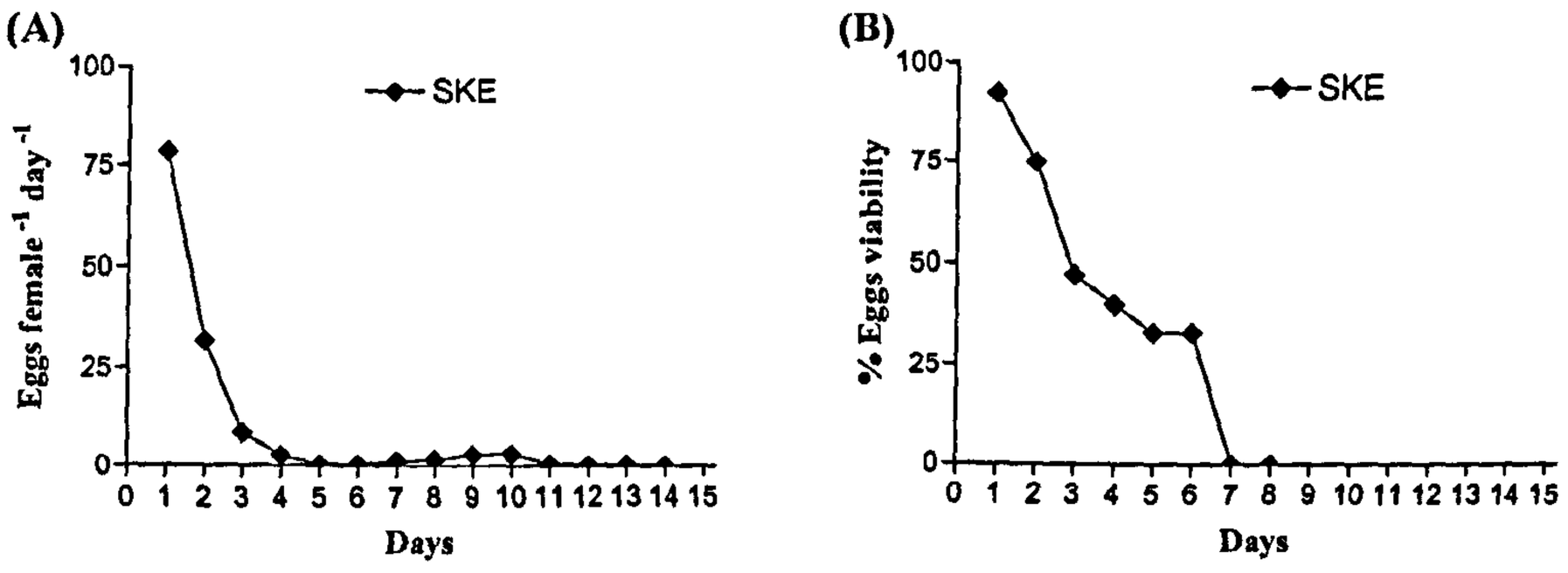

Figure 2.4: Laboratory experiments testing the effects of *S.costatum* on egg production rates (A) and hatching viability (B) in the copepod *T. stylifera*.

2.2.2. Aldehyde profile

The CET derivatization was applied to detect the production of short chain aldehydes in *S. costatum*. The microalgae (3 g) were sonicated in F/2 and after 30 minutes the resulting water suspensions were extracted with acetone and dichloromethane (Experimental Section). Direct derivatization of the organic extracts gave an enriched pool of CET derivatives that were examined after purification on mini-columns of silica gel. CET derivatives were resolved by GCMS in 2*E*,4*Z*-octadienal (**13**), 2*E*,4*E*-octadienal (**14**), 2*E*,4*E*,7-octatrienal (**16**) and 2*E*,4*E*-heptadienal (**18**), **14** being the main component. The

mixture of CET derivatives also contained a variety of saturated and monounsaturated compounds, including tridecanal (**9**), pentadecanal (**19**) and 8-pentadecenal (**20**) (d'Ippolito *et al.*, 2002a).

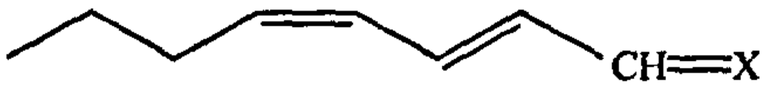

13. X=O; **13a.** X=$C_5H_8O_2$

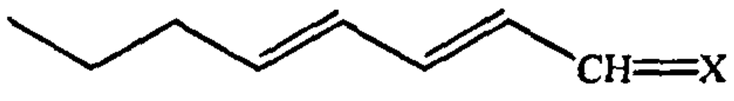

14. X=O; **14a.** X=$C_5H_8O_2$

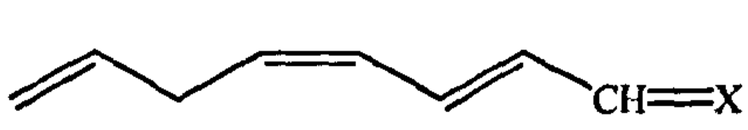

15. X=O; **15a.** X=$C_5H_8O_2$

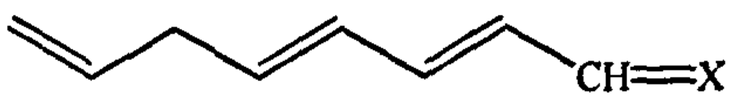

16. X=O; **16a.** X=$C_5H_8O_2$

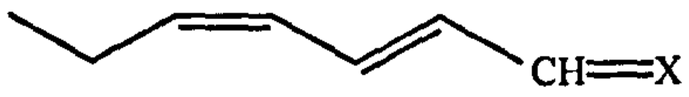

17. X=O; **17a.** X=$C_5H_8O_2$

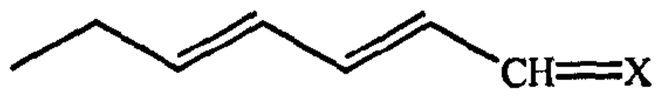

18. X=O; **18a.** X=$C_5H_8O_2$

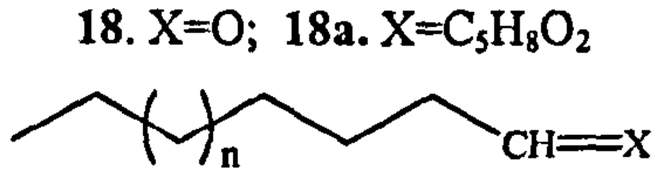

9. n=7, X=O; **9a.** n=7, X=$C_5H_8O_2$
19. n=9, X=O; **19a.** n=9 $C_5H_8O_2$

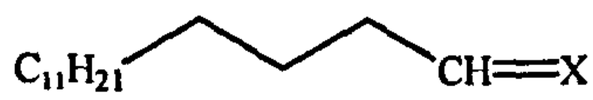

20. X=O; **20a.** X=$C_5H_8O_2$

All the described aldehyde compounds were unambiguously characterized by comparison of their NMR data with those of standard products. In fact, CET derivatives were purified on RP-HPLC in CH_3CN/H_2O 70/30 and further characterized by mono- and bidimensional NMR. Except for octatrienal (**16**), all of these compounds were already known as products of lipid oxidation. So, the structure of octatrienal (**16**) was unambiguously identified by 2D NMR spectroscopy.

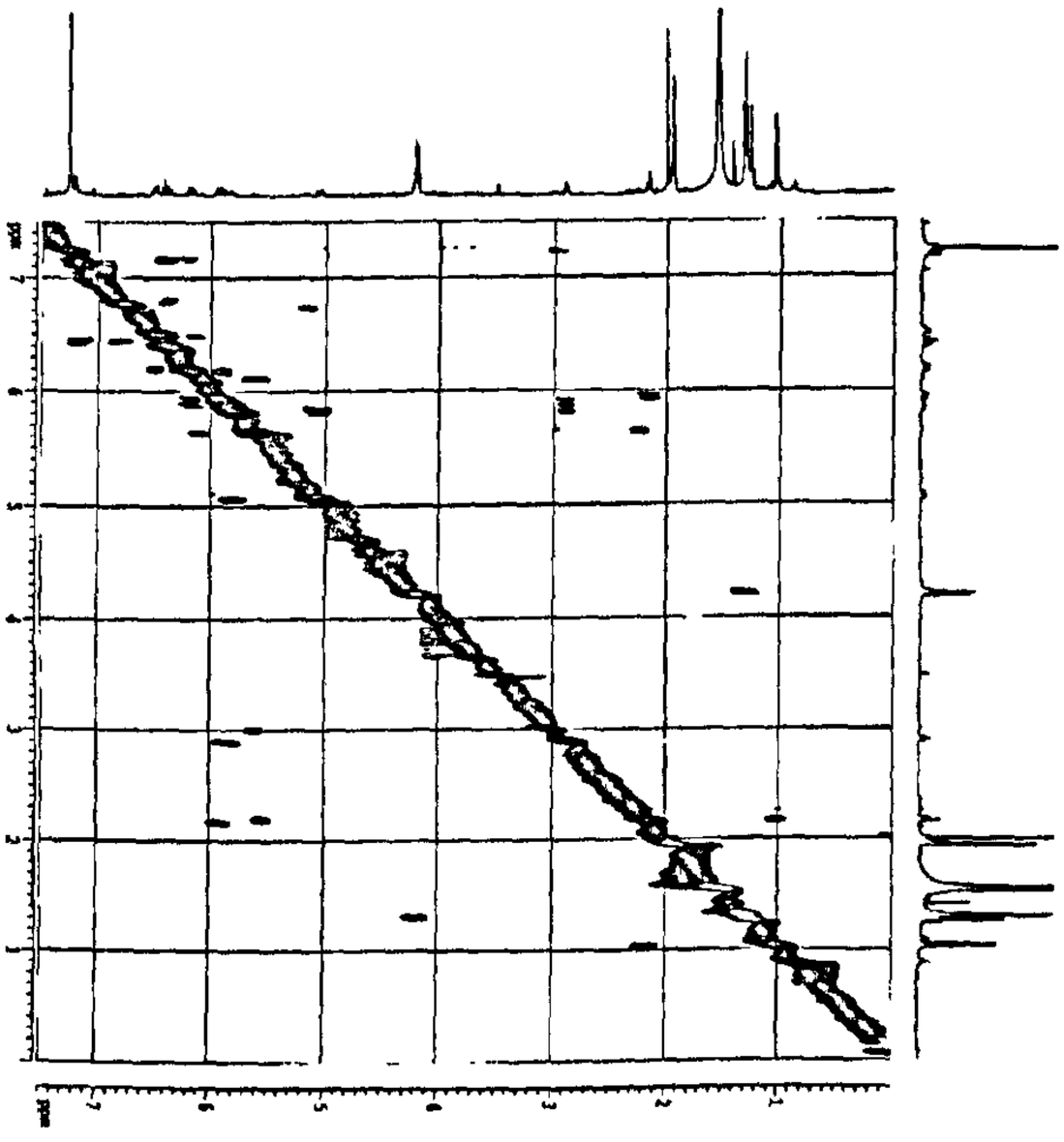

Figure 2.5: ^1H-^1H COSY of 2*E*,4*E*,7-octatrienal (**16**) ($CDCl_3$, 400 MHz).

In particular, ^1H-^1H COSY spectrum revealed a bis-allylic methylene group (δ 2.89) coupled to the vinyl protons at δ 5.92 and 5.74; this latter signal was in turn correlated to the methylene protons at δ 5.07 (H-8a, bd, J = 17.1 Hz) and 4.99 (H-8b, bd, J = 10.1 Hz) (Figure 2.5). The remaining part of the molecule, as well as the configuration of the double bonds in the other aldehydes, were assigned in analogy with CET derivative of 2*E*,4*E*-octadienal. No aldehyde was found in intact cells of *S. costatum*. The intact cells were obtained after treatment of fresh cell pellet with boiling methanol.

2.2.3. Fatty acid composition

Since aldehydes generally derive from fatty acid oxidation, the first step in approaching the biosynthesis of these compounds was the description of the fatty acid composition. A cell suspension was sonicated for 1 min and extracted with acetone and CH_2Cl_2 as described above. The extract was methylated with diazomethane and fatty acid methyl ester (FAME) analyzed in GCMS. In agreement with Bergè *et al.* (1995), the lipid profile of *S. costatum* showed a predominance of eicosapentaenoic acid (20:5 ω-3) (**21**) whereas neither ω-1 or ω-4 C_{20} fatty acids were detectable. *S. costatum* lipids contained also high levels of C_{16} compounds (almost 65% of the whole fatty acid content). In particular, significant amounts of 6,9,12-hexadecatrienoic (HTrA, 16:3ω-4, almost 26% of C_{16} content) (**22**) and 6,9,12,15-hexadecatetraenoic acids (HTA, 16:4ω-1, almost 12% of C_{16} content) (**23**) were found, which may be related to the production of octadienals and octatrienal, respectively.

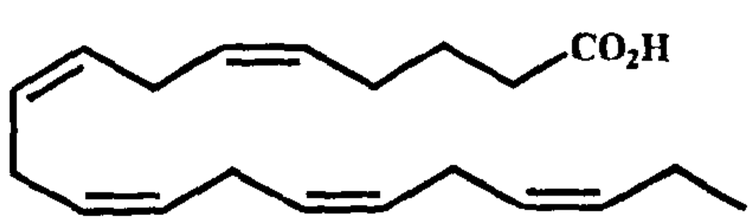

EPA (**21**)

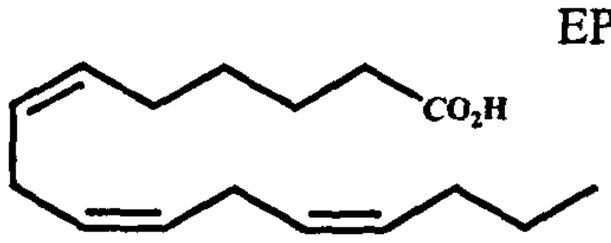

HTrA (**22**)

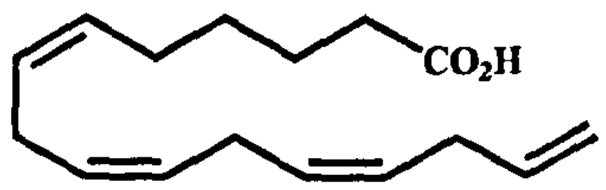

HTA (**23**)

It is worth noting that no other fatty acid with a terminal double bond was detected in the *S. costatum* extract and that the structure of 6,9,12,15-hexadecatetraenoic acid was

rigorously determined by NMR after purification of the product on RP-HPLC with MeOH/H_2O/TFA 85:15:0.3 (v/v/v). In addition to the typical signals of polyunsaturated fatty acids (PUFAs), the ^{1}H-NMR spectra (Figure 2.6) clearly showed the presence of the terminal double bond at δ 4.99 (H-16a), δ 5.04 (H-16b) and δ 5.79 (H-15).

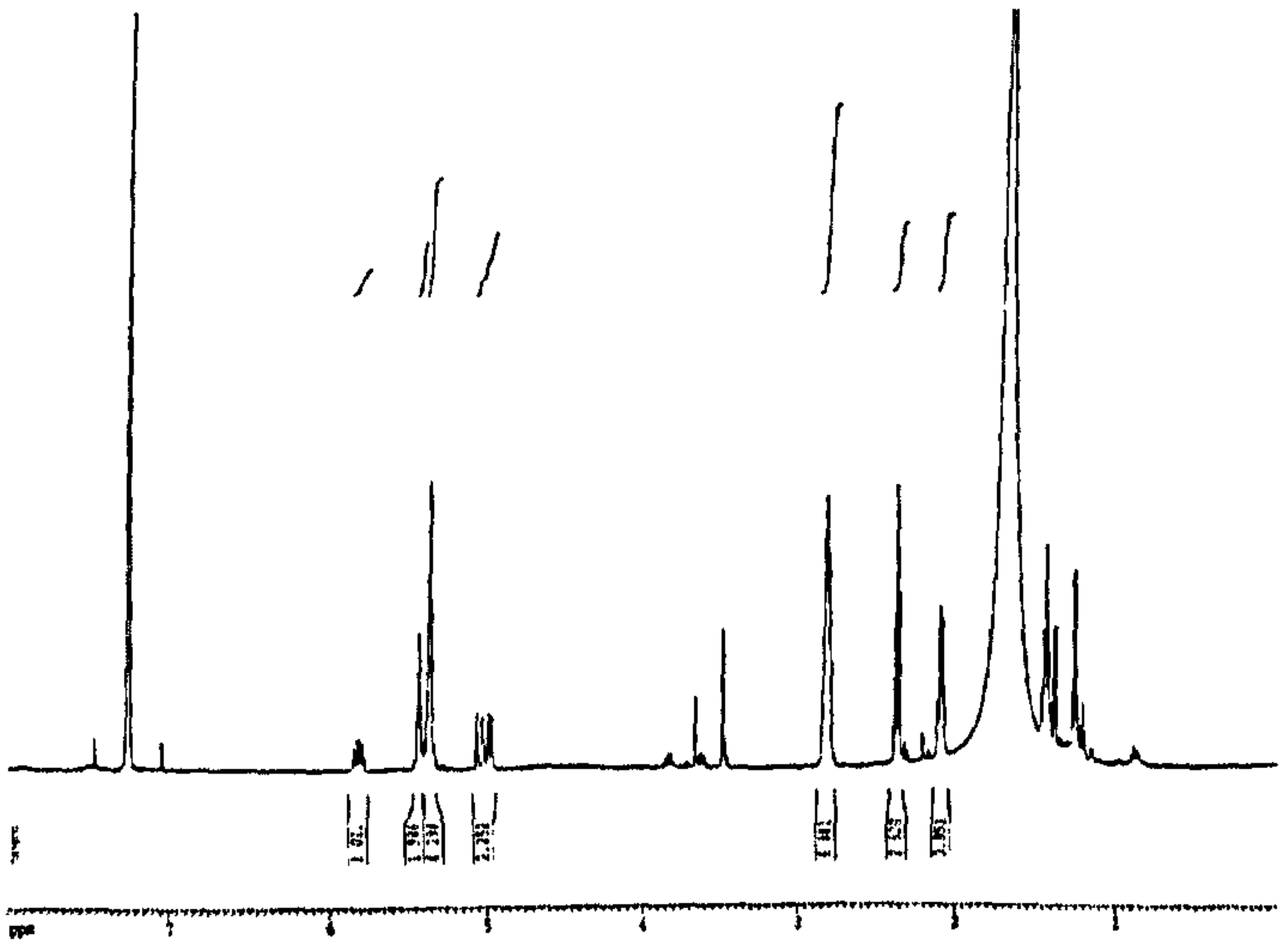

Figure 2.6: ^{1}H-NMR of 6,9,12,15-hexadecatetraenoic acid (**23**) ($CDCl_3$, 400 MHz).

2.2.4. Biosynthesis of octadienal from 6,9,12-hexadecatrienoic acid

To test the possibility that octadienal should derive from HTrA, the deuterated fatty acid was synthetized since this labelled fatty acid was not commercially available. [6,7,9,10,12,13-$^2H_6$]-6,9,12-Hexadecatrienoic acid (d_6-HTrA) was prepared as reported in Scheme 2.2, following a general procedure based on coupling of propargyl halide with terminal alkyne in the presence of cesium carbonate. Reduction of the resulting polyalkyne by $^2H_2$/Pd on $BaSO_4$ as catalyst gave good yield (77%) of the deuterated C_{16} methyl ester, from which pure d_6-HTrA (**22a**, D_6 91%) was quantitatively obtained by basic hydrolysis.

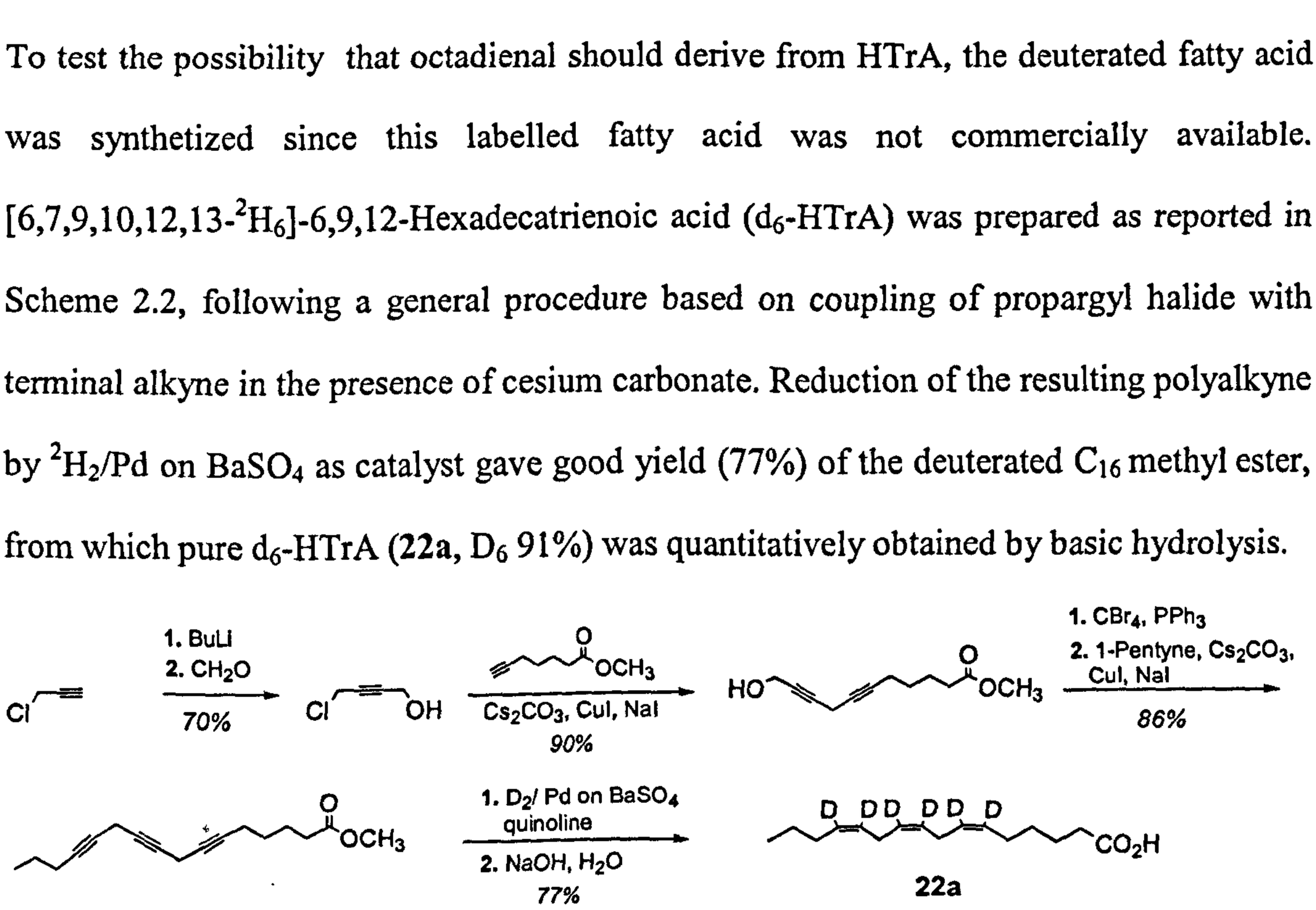

Scheme 2.2: Synthesis of d_6-hexadecatrienoic acid (**22a**)

Once the labelled precursor was synthesized, d_6-HTrA was incubated for 30 min in different suspensions of *S. costatum*, in concentration ranging from 8.3 to 15.6 μmol/g of wet cells. The suspension was extracted after 30 min, and derivatized with CET-triphenylphosphorane. The pool of CET aldehydes was purified on silica gel, and analyzed by GC-MS and NMR. GC-MS analysis of the mixture of CET derivatives obtained from cells treated with d_6-HTrA (**22a**) showed clear labelling of 2,4 octadienal (**13**) (d'Ippolito *et al.*, 2003). In fact, the MS spectra of this compound (Figure 2.7) showed significant M + 4 peaks (natural $C_{13}H_{20}O_2^+$, *m/z* 208; labelled $C_{13}H_{16}D_4O_2^+$, *m/z* 212) that agreed well with the retention of four deuterium atoms. The presence of these isotopomers was also confirmed by the isotopic clusters associated with fragments generated by the diagnostic loss of ethyl (natural $C_{11}H_{15}O_2^+$, *m/z* 179; labelled $C_{11}H_{11}D_4O_2^+$, *m/z* 183) and ethoxyl (natural $C_{11}H_{15}O^+$, *m/z* 163; labelled $C_{11}H_{11}D_4O^+$, *m/z* 167) radicals in the mass spectra of 2,4 octadienal (Figure 2.7). As expected, no trace of labelling was detectable in the other aldehydes, supporting the prediction of a substrate-specific process.

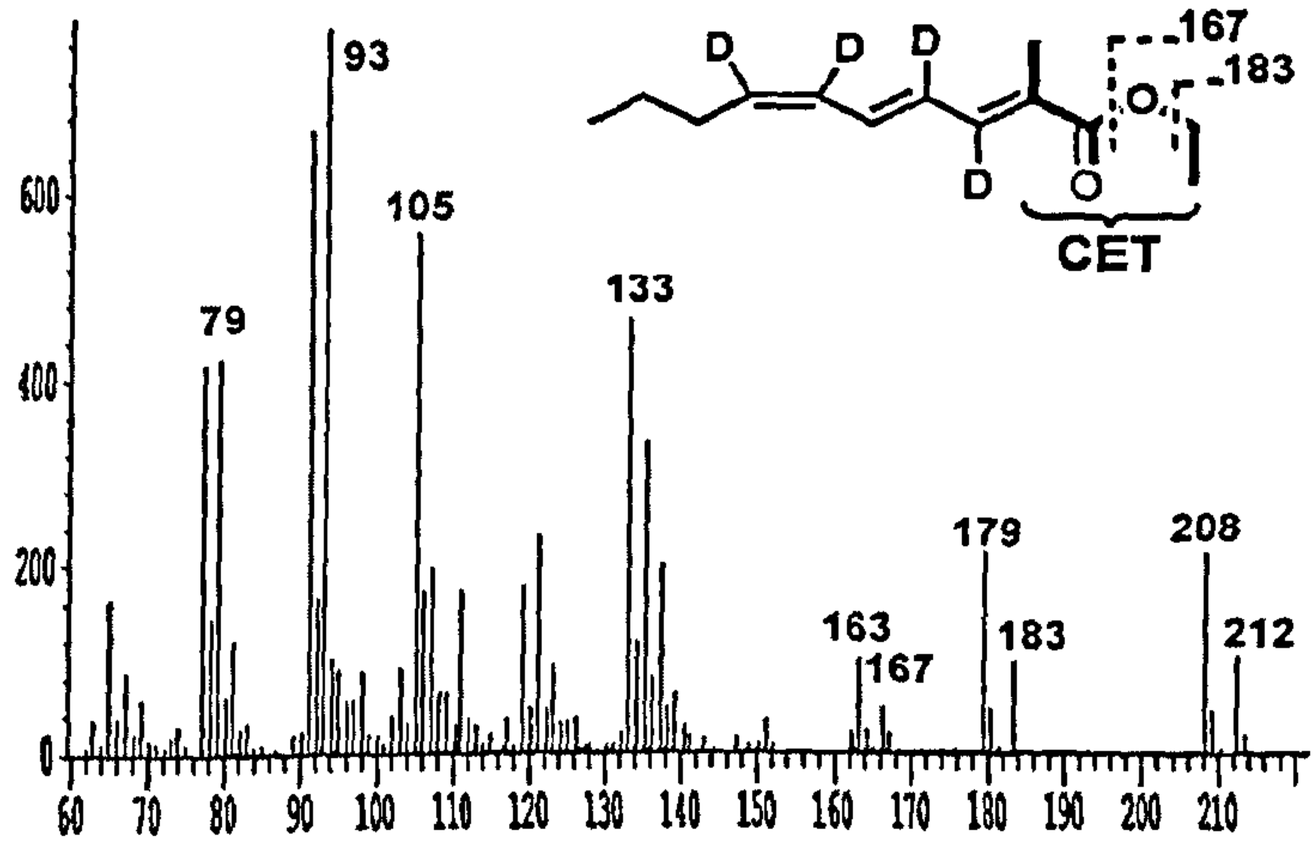

Figure 2.7: EI-MS spectrum of 2,4 octadienal from cells of *S. costatum* fed with D_6-hexadecatrienoic acid.

The localization of the deuterium atoms, on the other hand, was clearly established by NMR spectroscopy. In fact, the ^{2}H-NMR spectrum of derivatized 2,4 octadienal purified from treated cells showed three signals attributable to ^{2}H-2 (δ 6.42), ^{2}H-4 (δ 6.20), and ^{2}H-5 (δ 5.91) (Figure 2.8). The resonance of the fourth deuterium atom (^{2}H-1) was only

apparently missing, since it fell under the large peak of $CDCl_3$ (δ 7.26). The assignment was rigorously proved by comparison with the ^1H NMR spectrum of derivatized *trans,trans*-2,4-octadienal (**14a**) (Figure 2.8).

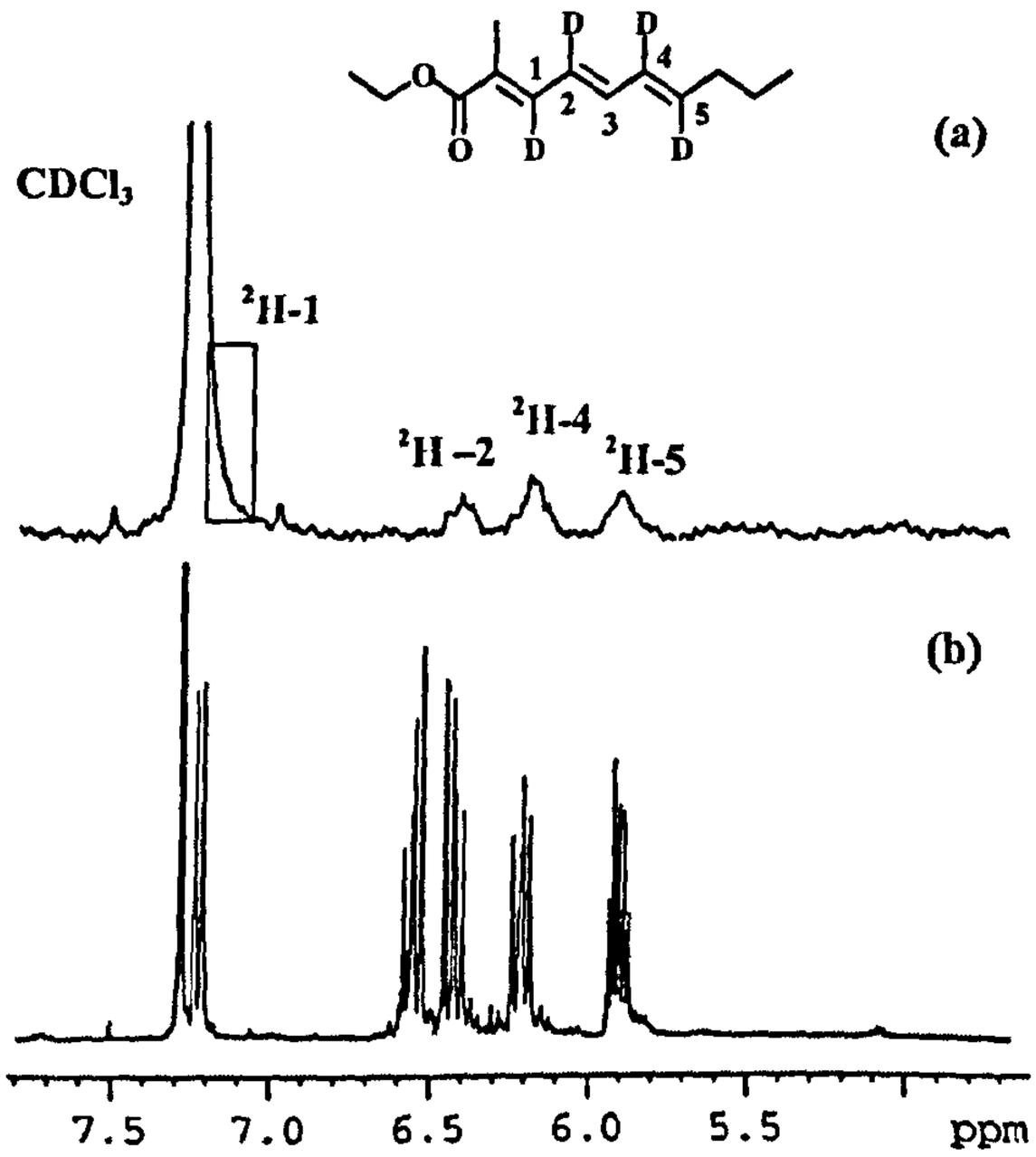

Figure 2.8: Downfield regions of ^2H-NMR (a) and ^1H-NMR (b) of the CET derivatives of labelled (a) and commercially available (b) *trans,trans*-2,4-octadienal.

On the basis of the labelling pattern, it was possible to hypothesize a mechanism of octadienal formation through the action of 9-lipoxygenase (9-LOX) and a hydroperoxide lyase (HPL) (Scheme 2.3).

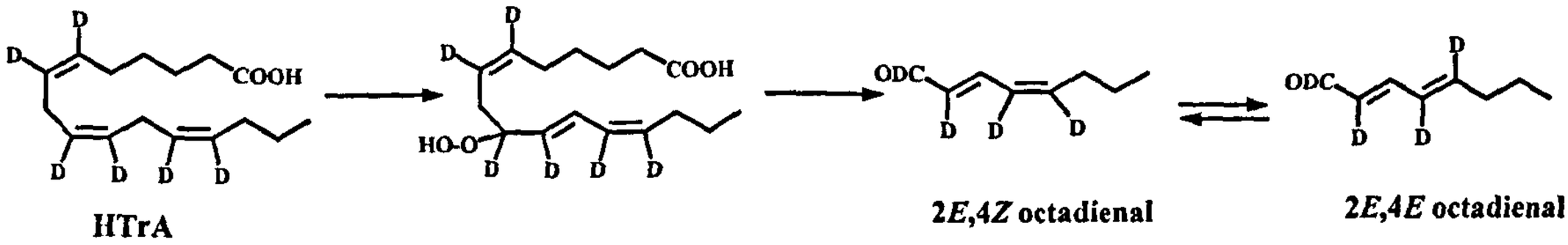

Scheme 2.3: Hypothesized mechanism of 2,4 octadienal formation from HTrA.

As previously reported, no detectable level of octadienal was found in intact cells of *S. costatum*. Analogously, octadienal production was totally inhibited when the deuterated

acid was added to a boiled sample of the diatom, suggesting that the aldehydes are not formed by a spontaneous, auto-oxidative process.

2.2.5. Incubation experiments with $^{3}H_{10}$-EPA

To test the origin of heptadienal in *S. costatum*, commercially available tritiated EPA was used. [5,6,8,9,11,12,14,15,17,18-^{3}H]-eicosapentaenoic acid ($^{3}H_{10}$-EPA) at concentration ranging from 0.5 to 3 μCi was incubated with cell homogenates of the diatom for 30 min at room temperature.

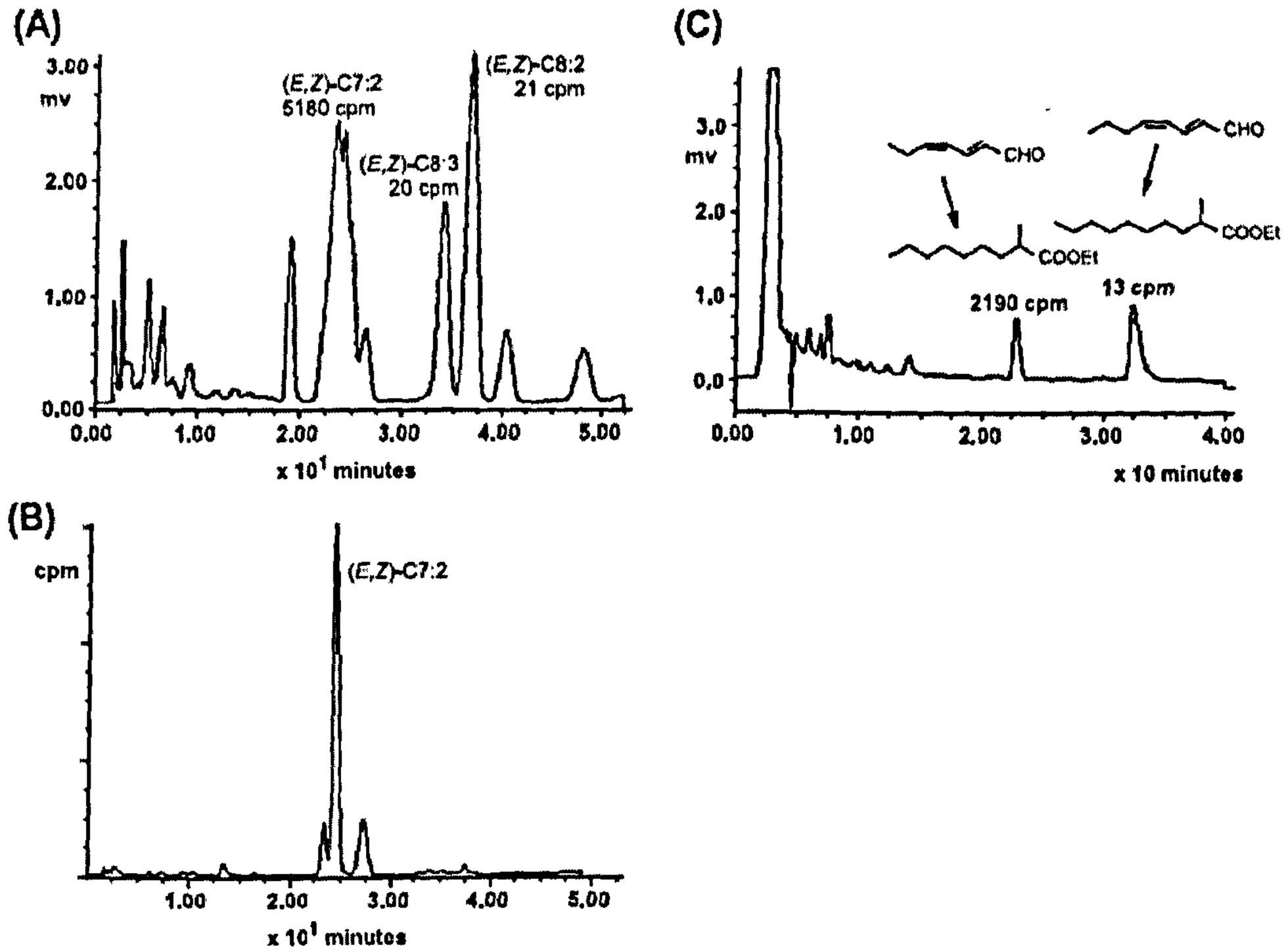

Figure 2.9: Conversion of $^{3}H_{10}$-EPA by cell homogenates of *S. costatum*. (A) RP-HPLC profile of PUAs produced by diatom cells incubated with 3 μCi of [$^{3}H_{10}$]-EPA; (B) radio-chromatogram of *Skeletonema* PUAs; (C) RP-HPLC of hydrogenated CET-PUAs produced by cells incubated with 3 μCi of [$^{3}H_{10}$]-EPA.

After extraction and derivatization of the mixture with CET-TPP, analysis of polyunsaturated aldehydes (PUAs) derivatives on RP-HPLC demonstrated the specific presence of radioactivity only in the two isomers 2*E*,4*Z* and 2*E*,4*E* of heptadienal (5180 cpm) (Figure 2.9A and B, T_R=23.1 and 24.2 min), whereas no labelling was found in the

peaks corresponding to octadienal and octatrienal (T_R=37.5 and 34.1 min) (d'Ippolito *et al.*, 2004).

The identity of these products was ascertained by co-elution with CET derivatives prepared from commercially available heptadienal. As further evidence of the labelling specificity, an aliquot of the mixture of PUAs was exhaustively hydrogenated and analysed by HPLC. Two distinct peaks were detected on reverse phase column (Figure 2.9C). These compounds derived by conversion of the different C_7 and C_8 stereoisomers of CET-PUAs into the corresponding saturated analogues 2-methyl-nonanoic acid ethyl ester (T_R=22.8 min) and 2-methyl-decanoic acid ethyl ester (T_R=32.8 min). The structures of these last compounds were unambiguously proved by NMR spectroscopy on hydrogenated CET-derivatives of commercially available C7:2 and C8:2 aldehydes, respectively. Radioactivity was found associated only with the peak of 2-methylnonanoic acid ethyl ester (2190 cpm), thus confirming the specific origin of heptadienal from EPA. The oxidizing activities leading to heptadienal were totally inhibited when radioactive precursor was added to boiled homogenates of diatom cells.

2.2.6. Lipid analysis

After demonstrating the origin of C_8 aldehydes from C_{16} fatty acids and heptadienal from EPA, the lipid analysis was carried out to understand the distribution of these fatty acids in the complex lipids of *S. costatum*, even though these data were already available in the literature (Bergè *et al.*, 1995). In fact, it has been reported that there is a certain variability of lipid pools within different strains of the same species (Pohnert *et al.*, 2002) and in response to different environmental parameters, including culture conditions and growth cycle (Lopez *et al.*, 2000). For simplicity, every experiment was carried out with cells at the stationary phase and the results should be considered within this specific frame. *S. costatum* cultures were gently centrifuged at 1200g before inactivating lipase activity with boiling MeOH. Extraction was performed following the Folch method (Hamilton *et al.*,

1993) and fractionation of this material was carried out on silica gel. Triacylglycerols (TAG) were eluted with petroleum ether/diethyl ether 90:10, whereas glycolipids (GL) and phospholipids (PL) were obtained with acetone/MeOH 9:1 and $CHCl_3$/MeOH/H_2O 65:25:4, respectively (Bergè *et al.*, 1995).

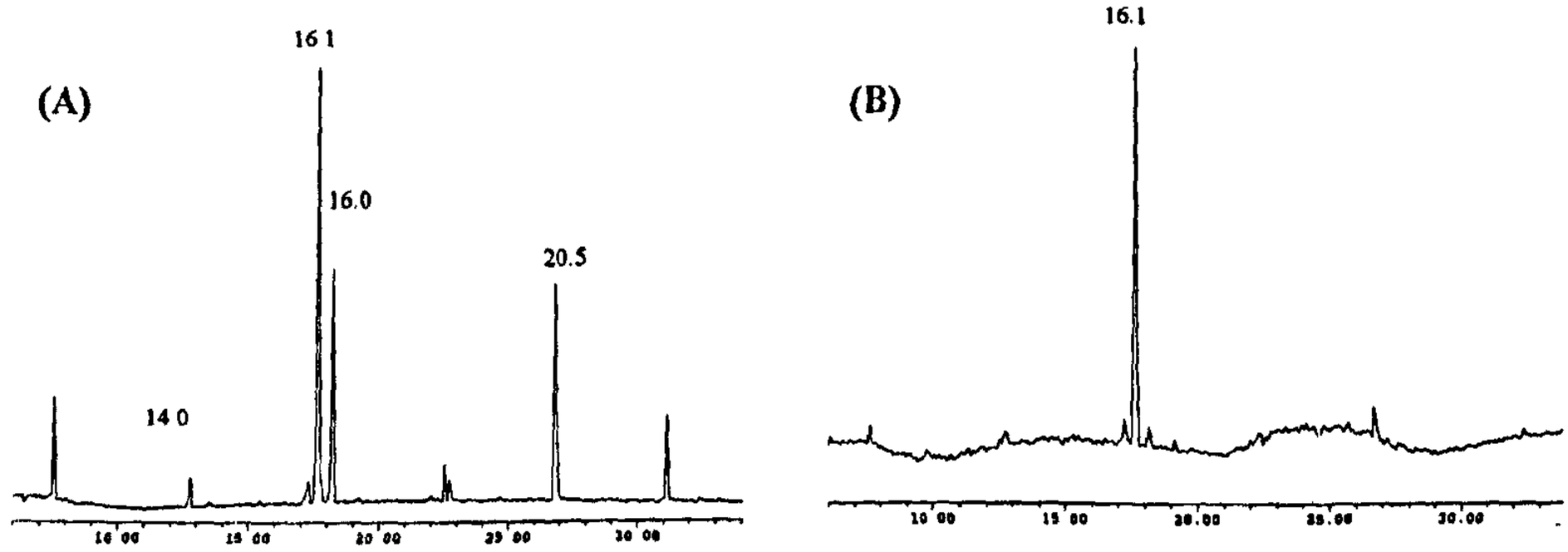

T_R	FAME	GL	PL	TAG
12.8	C14:0	25.9%	2.4%	-----
17.1	C16:4 ω1	11.8%	-----	-----
17.3	C16:3 ω4	19.3%	2.83%	1.9%
17.7	C16:1 ω5	-----	40.7% *	-----
	C16:2 ω4			
17.7	C16:1 ω7	15.23%	-----	86%
18.2	C16:0	1.98%	20.1%	4.6%
26.8	C20:5 ω3	22.46%	23.4%	7.19%

Figure 2.10: GCMS spectra of FAME from (A) phospholipids, (B) triacylglycerols and (C) glycolipids. (D) Relative composition of FAME in the three different classes of complex lipids. T_R is expressed in minutes.
* This peak is a mixture of C16:1 ω5 and C16: 2 ω4.

In this condition, *Skeletonema* lipids contained approximately 9% of TAG, 24% of PL and 67% of GL. HTrA and HTA were mainly present in the glycolipid fraction. On the contrary EPA was rather uniformly present in PL and GL (Figure 2.10). Other fatty acids, for the most part C_{16} and C_{14} saturated and monounsaturated species, occurred at lower levels in polar lipids. PUFAs, mainly EPA, did not reach 10% of the entire fatty acids present in TAG. The analysis indicated that GL was composed of monogalactosyldiacylglycerols (MGDG) (about 65%), digalactosyldiacylglycerols

(DGDG) (about 24%) and sulphoquinovosyldiacylglycerols (SQDG) (about 9%). MGDG were separated from DGDG and SQDG by a further SiO_2 column with $CHCl_3$/MeOH 95:5.

2.2.7. PUAs formation from glycolipids

The precursor of octadienal, 6,9,12-hexadecatrienoic acid, was present only in glycolipids, suggesting the active role of glycolipids in the process of PUAs formation. To investigate the role of glycolipids in the generation of aldehydes, the production of PUAs was measured after incubation of GL and MGDG with cell homogenates containing reduced levels of aldehydes. To achieve such a goal, prior to adding the exogenous substrates, PUA content was drastically lowered by keeping the cell homogenates under vacuum for 15 min at 4°C.

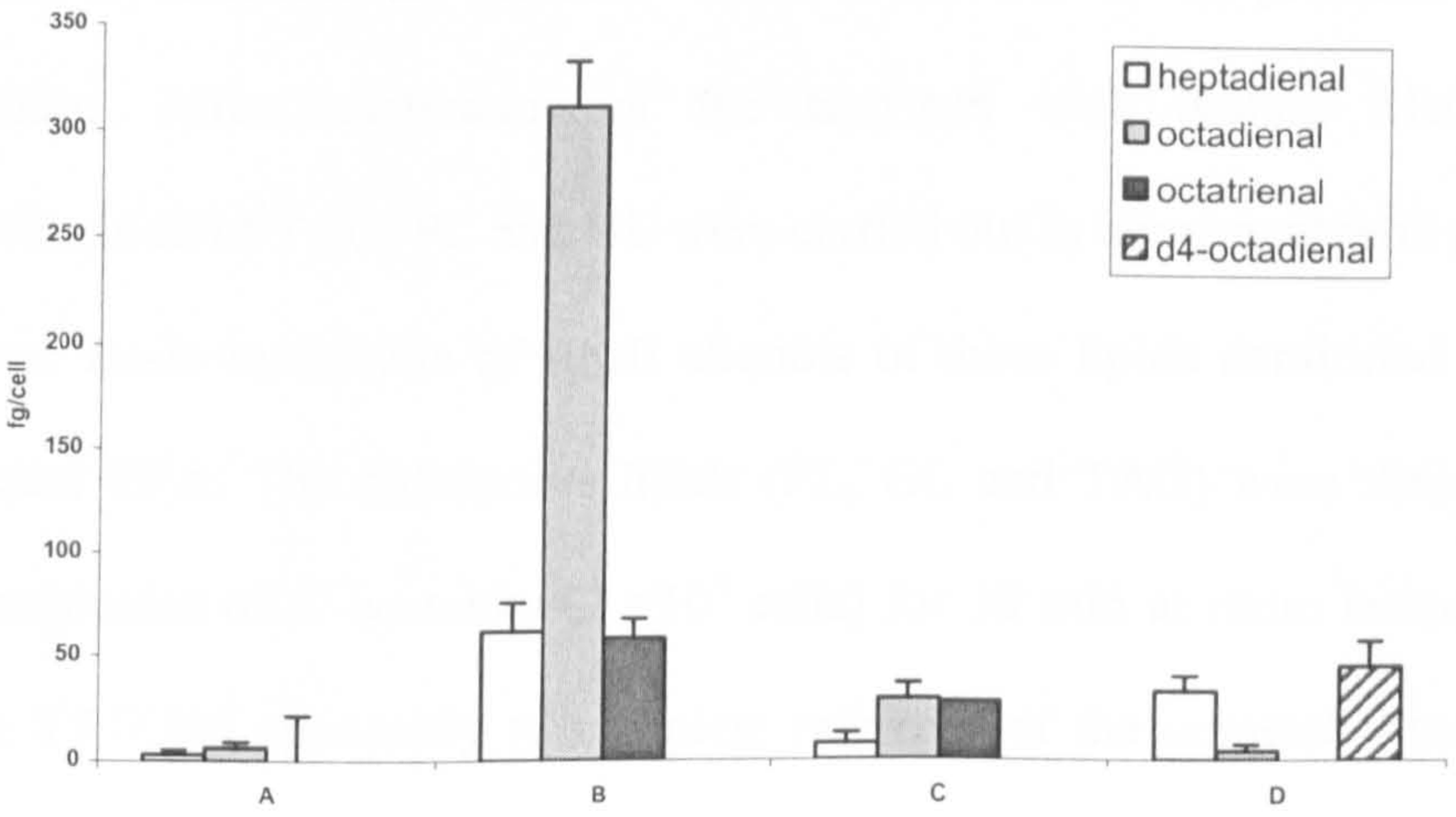

Figure 2.11: Incubation experiments with diatom homogenates kept under vacuum (5 torr) for 15 min (n=3). (A) Control; (B) incubation with MGDG; (C) incubation with GL; (D) incubation with d_6-HTrA and EPA.

The treatment did not cause any evident decrease in enzymatic activity and cell preparations maintained the capability of converting d_6-HTrA and EPA into d_4-octadienal and heptadienal, respectively. Incubations of both GL and MGDG increased the levels of octadienal, octatrienal and heptadienal (Figure 2.11). It is significant that the experiments with MGDG affected mainly the synthesis of octadienal (increased by about 300-fold after incubation), whereas incubation of the whole pool of glycolipids (MGDG, DGDG and

SQDG) had a generalized effect on PUA levels (increased by about 45–65-fold after incubation) (d'Ippolito *et al.*, 2004).

2.2.8. Metabolism of complex lipids containing radioactive EPA

Since the precursor of heptadienal, EPA, was present in both glycolipids and phospholipids, it was necessary to clarify the role of these complex lipids in the generation of heptadienal. A procedure was developed to label the natural complex lipids with $^{3}H_{10}$-EPA. Radiolabelling was achieved by growing the diatom for 20 h in culture media containing $^{3}H_{10}$-EPA (5 μCi). During this time the cells actively capture the labelled fatty acid from the medium, storing it in the complex lipids. Microalgal cells were then harvested at the stationary phase by gentle centrifugation, washing repetitively the cell pellets to eliminate the residual radioactivity due to the presence of $^{3}H_{10}$-EPA in the medium. After inactivation of the enzymes with boiling MeOH, extraction and fractionation of TAG, PL and GL were carried out in agreement with procedures described above. Basic hydrolysis of small aliquots of these lipids confirmed the incorporation of tritiated EPA. The radioactive lipids (PL, GL and TAG) were then incubated with cell homogenates of *S. costatum* (2 x10^{9} cells) for 30 min at room temperature. Experiments with TAG led apparently to complete recovery of the unmetabolised lipid (not shown), without detectable formation of labelled heptadienal. However, due to the low content of radioactive EPA, it was not possible to make a conclusion about the contribution of TAG to the synthesis of this oxylipin. On the other hand, incubations of radioactive GL and PL gave significant labelling of free fatty acid (FFA) (Table 2.2). Both lipid pools led to similar levels of labelling of FFAs (10818 dpm/mg from GL and 9486 dpm/mg from PL) although the initial content of radioactivity was significantly higher in PL (47856 dpm/mg) than in GL (4434 dpm/mg). This is consistent with a different rate of hydrolysis, suggesting that GL were metabolized with higher efficiency.

Glycolipids 181800 cpm (4434 dpm/mg)	**Extract**[a] 2460 dpm/mg	**CET-PUSCAs**[c] 2670 dpm/mg	**C7:2**[g] 2120 dpm/mg
	Water Residue 17790 dpm	**FFA**[d] 9486 dpm/mg	**C8:2 – C8:3**[g] n.d.
Phospholipids 933200 cpm (47856 dpm/mg)	**Extract**[b] 9096 dpm/mg	**CET-PUSCAs**[e] 12776 dpm/mg	**C7:2**[g] 420 dpm/mg
	Water Residue 3640 dpm	**FFA**[f] 10818 dpm/mg	**C8:2 – C8:3**[g] n.d.

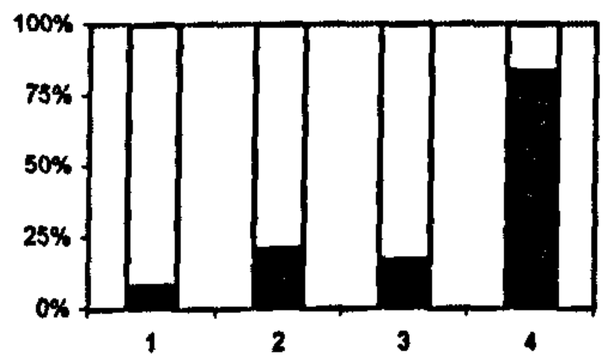

Synoptic picture of radioactivity distribution in lipid fractions after feeding experiments.
black column= glycolipids; white column= phospholipids; 1st column: supplemented radioactiviy; 2nd column = extract; 3rd column = CET-PUSCAs; 4th column=heptadienal (C7:2) after HPLC purification.

[a]82.0 mg; [b]83.0 mg; [c]2.7 mg after purification on column; [d]20.6mg after purification on column; [e]4.1 mg after purification on column; [f]38.1 mg after purification on column; [g]after purification on HPLC; n.d = value below the background.

Table 2.2: Radioactivity distribution through purification steps of *S. costatum* cell homogenates (4.4 g, $5.9x10^9$ cells) incubated with lipid-containing $^3H_{10}$-EPA.

After direct derivatization of the extracts with CET-TPP, the mixture of derivatized PUAs was then analysed by HPLC showing significant radiolabelling ($4x10^2$ dpm/mg from PL and $2x10^3$ dpm/mg from GL) associated to CET-heptadienal (Table 2.2). To find further confirmation that heptadienal can derive from the metabolism of both PL and GL, the fractions of PUAs prepared from incubation with radioactive PL and GL were also hydrogenated on Pd/C. As reported above for the experiments with free EPA, HPLC analysis of the resulting material corroborated the presence of radioactivity only in the peak of 2-methylnonaoic acid ethyl ester (T_R=22.8 min), the hydrogenated derivative of CET-heptadienal. This indicated clearly that both GL and PL contribute to the origin of this oxylipin.

2.2.9. Characterization of MGDG

Since MGDG was the most abundant part of glycolipids in marine diatoms, this class of lipids was analyzed using HPLC/ESI-MS/MS in agreement with a recent methodology proposed by Guella *et al.* (2003), in order to define *sn*-composition. Results are summarized in Table 2.3. MGDG showed a very large content of PUFAs that, on the

whole, represented almost 98% of the total fatty acids. The MGDG fraction was composed of four major molecular species, with 20:5/16:3 (26.7%) and 16:3/16:3 (25.9%) being the most abundant. A distinctive feature was the specific presence of HTA at the *sn*-2 position and EPA at the *sn*-1 position, whereas HTrA was uniformly present at both *sn*-1and *sn*-2 positions (Table 2.3), demonstrating that both the *sn*-positions were involved in the process.

Retention Time	$[M+Na]^+$	Formula	Fatty acid *sn*-1/*sn*-2	Abundance %
7.3 min	739	$C_{41}H_{64}O_{10}$	C16:3/C16:4	13.2
8.3 min	741	$C_{41}H_{66}O_{10}$	C16:3/C16:3	25.9
9.2 min	791	$C_{45}H_{68}O_{10}$	C20:5/C16:4	16.1
9.8 min	743	$C_{41}H_{68}O_{10}$	C16:2/C16:3	6.5
10.6 min	793	$C_{45}H_{70}O_{10}$	C20:5/C16:3	26.7
12.5 min	795	$C_{45}H_{72}O_{10}$	C20:5/C16:2	6.5
others				5.1

RP-HPLC profile of MGDG

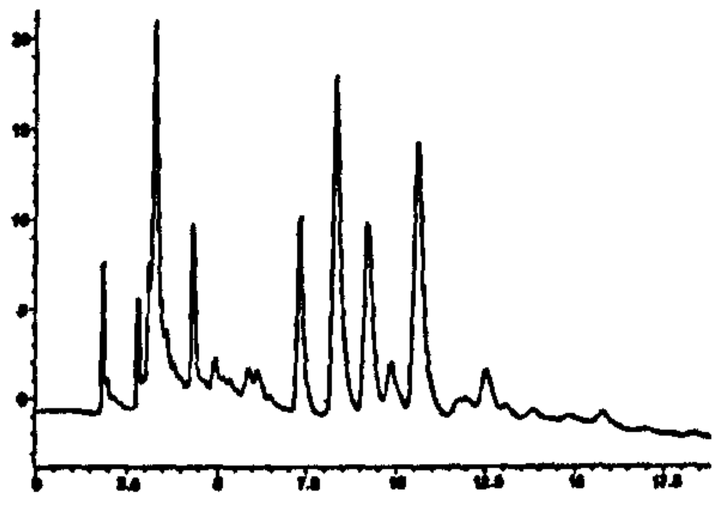

Table 2.3: Composition (mol%) of MGDG of *S. costatum*

Nuclear magnetic resonance (NMR) experiments supported the β-galactopyranosyl nature of the sugar in MGDG, showing a spin system in good agreement with the literature data of 3-(β-D-galactopyranosyl)-1,2-diacyl-*sn*-glycerol. The NMR data confirmed, furthermore, the large presence of PUFAs with the unequivocal signals due to the terminal double bond (δ 4.99, *dd*, H-16a; δ 5.04, *dd*, H-16b; δ 5.81, *m*, H-15) of HTA. The *Z* stereochemistry of the double bonds in this and in the other fatty acids was inferred on the basis of the chemical shift of the *bis*-allylic carbons centred around 24.8 ppm in the ^{13}C-NMR spectrum (not shown).

2.2.10. Structure elucidation of other oxylipins

In order to characterize oxylipin derivative other than aldehydes, extracts of *S. costatum* were methylated with ethylic diazomethane and analyzed by RP-LCMS. The analysis revealed the presence of a conspicuous pool of other oxylipins including hydroxy-fatty

acids (**25-27, 29**), hydroperoxy-fatty acids (**28**) and keto-fatty acids (**24**). All these compounds were purified as methyl ester, and characterized through LCMS and one- and two-dimensional NMR.

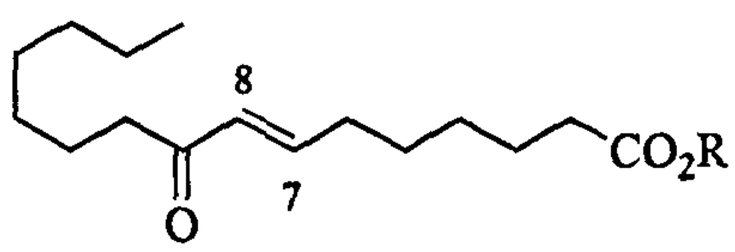

24. R=H; **24a.** R=Me

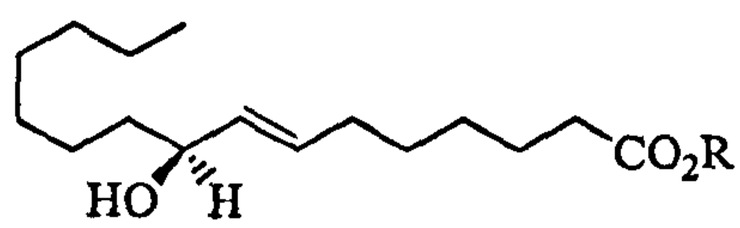

25. R=H; **25a.** R=Me

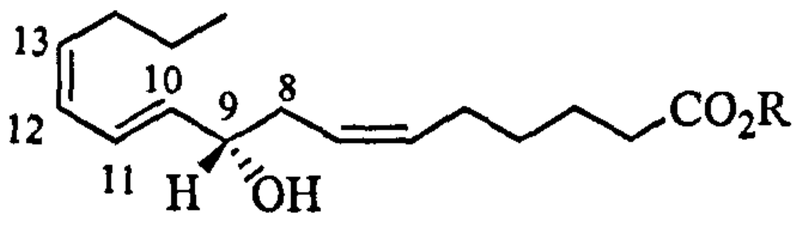

26. R=H; **26a.** R=Me

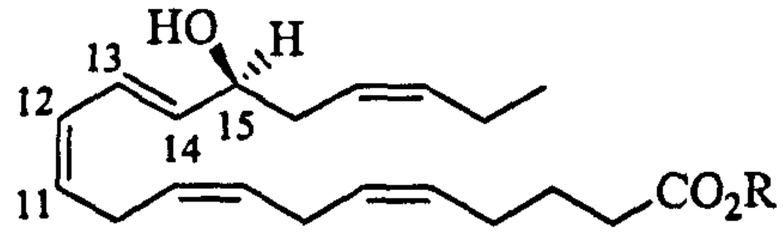

27. R=H; **27a.** R=Me

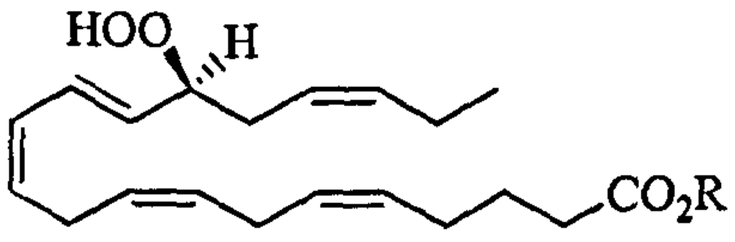

28. R=H; **28a.** R=Me

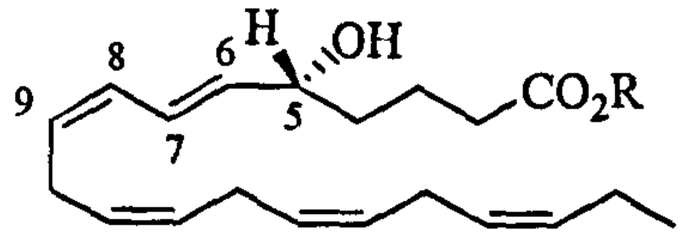

29. R=H; **29a.** R=Me

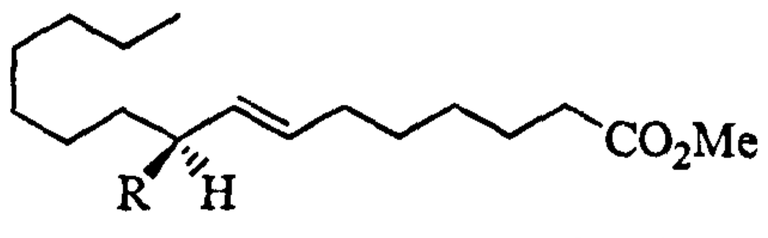

25b. R=*R*-PhTFE; **25c.** R=*S*-PhTFE

The structures of the two major derivatives **24a** and **25a** were determined as 9-keto-7*E*-hexadecenoic acid methyl ester and 9-hydroxy-7*E*-hexadecenoic acid methyl ester by ESI^+-MS spectrometry and NMR spectroscopy. In particular, in-source collision induced dissociation spectra (MacMillan and Murphy, 1995) (cone voltage = 90 V) of **24a** exhibited a diagnostic ion at *m/z* 165, which derives from the cleavage of the conjugated double bond between C-7 and C-8, as well as TOCSY and HMBC spectra clearly indicated the presence of two separate spin systems from C-2 to C-8 and from C-10 to C-16 (Table 2.4). The *trans* stereochemistry of the double bond was established on the basis of H-7/H-8 coupling constant (J=15.8 Hz). Similar results were obtained for **25a** and the structure relationship between the two oxylipins was proved by reduction of **24a** into racemic **25a** after reduction with diisobutylaluminium hydride (DIBAL).

Peak of compound **26a** exhibited UV absorbance (λ_{max} 235 nm) and ESI$^+$-MS pseudomolecular ion (*m/z* 303.5 for $[C_{17}H_{28}O_3+Na]^+$) indicative for a hydroxy derivative of HTrA methyl ester. NMR spectrum of this material after purification confirmed this suggestion, showing the typical signal of one hydroxylated methine group (H-9, δ 4.05) correlated to a *trans*, *cis*-diene moiety (H-10/H-13, δ 5.60, 6.65, 6.07 and 5.38) and diastereotopic allylic protons (H_2-8, δ 2.25 and 2.19) (Figure 2.12).

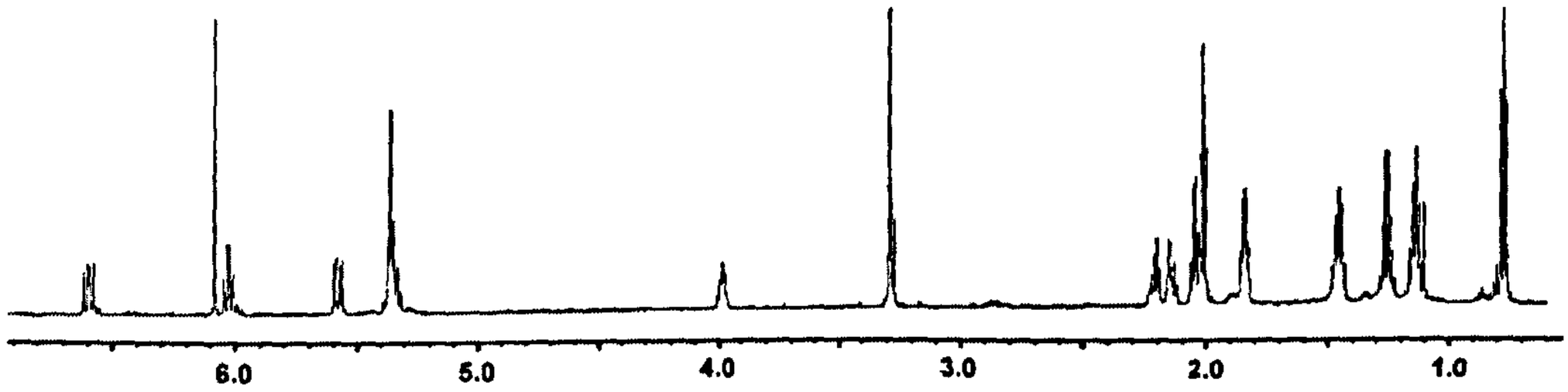

Figure 2.12: ^{1}H-NMR of 9-HHTrE methyl ester (**26a**) (C_6D_6, 600 MHz).

The lack of signals in the region 2.5-3 ppm confirmed the absence of *bis*-allylic protons in the molecule.

	24a ^{1}H δ, m, *J*	^{13}C	**25a** ^{1}H δ, m, *J*	^{13}C	**26a** ^{1}H δ, m, *J*	^{13}C
1		173.2		173.4		173.0
2	2.08, t, 7.4	33.4	2.09, t, 7.4	33.7	2.06, t, 7.4	33.7
3	1.48, q, 7.4	24.4	1.54, q, 7.4	24.9	1.51, q, 7.4	24.5
4	1.08, m	28.5	1.16, m	28.8	1.20, q, 7.4	29.4
5	1.15, m	27.9	1.25, m	29.5	1.90, q, 7.4	20.9
6	1.80, q, 7.0	31.8	1.91, q, 7.0	32.2	5.42, m	125.5
7	6.64, dt, 15.8; 7.0	145.5	5.50, dt, 15.3; 7.0	130.5	5.40, m	132.0
8	6.0, d, 15.8	130.5	5.43, dd, 15.3; 6.6	134.2	2.19, m2.25, m	35.8
9		198.6	3.93, m	72.7	4.05, m	71.8
10	2.27, t, 7.4	39.9	1.55, m 1.43, m	37.7	5.60, dd, 15.1; 5.9	136.0
11	1.64, m, 7.4	24.0	1.33, m	29.9	6.65, dd, 15.1; 10.9	125.2
12	1.22, m	28.8	1.24,[b] m	29.1	6.07, t, 10.9	128.5
13	1.20,[a] m	31.6	1.24,[b] m	32.2	5.38, m	132.0
14	1.20,[a] m	31.6	1.24,[b] m	32.2	2.09, q, 7.4	29.7
15	1.23, m	22.5	1.26, m	22.5	1.32, m	22.7
16	0.86, t, 7.4	13.8	0.88, t, 7.0	14.0	0.83, t, 7.4	13.4
OCH_3	3.36, s	50.8	3.35, s	50.8	3.34, s	50.8

Table 2.4: NMR data (C_6D_6, 600MHz) for oxylipins **24-26** from *S. costatum*. Complete assignments were determined on the basis of 1D- and 2D-NMR experiments.

The other NMR resonances (Table 2.4) were in agreement with the structure depicted, proving that compound **26a** is the methyl ester of 9-hydroxy-6*Z*,10*E*,12*Z*-hexadecatrienoic acid (9-HHTrE).

ESI$^+$-MS spectra of compound **27a** showed a pseudomolecular ion at *m/z* 355.0 accounting for a molecular formula $C_{21}H_{32}O_3Na^+$, indicative of a hydroxyl derivative of the EPA methyl ester. In fact, the ^{1}H-NMR spectrum of **27a** contained a typical signal of one hydroxylated methine (H-15, δ 4.08) coupled to a *trans, cis*-diene moiety H-14/H-11 (H-14 δ 5.65 *J*=15.1; H-13 δ 6.70 *J*=15.1-10.7; H-12 δ 6.05 *J*=15.1-10.7; H-11 δ 5.40 *J*=10.7) and to two diastereotopic allylic protons (H-12a, δ 2.22 and H-12b 2.28). The analysis of homonuclear 2D-NMR data allowed for the build up of the entire spin system depicted for 15-hydroxy-eicosa-5*Z*,8*Z*,11*Z*,13*E*,17*Z*-pentaenoic acid (15-HEPE) methyl ester. A complete chemical characterization was achieved through analysis of HSQC and HMBC data.

Molecular data of compound **28a** were almost identical to that of 15-HEPE (**27a**) except for the chemical shift of carbinolic proton (H-15) that in **28a** was down-shielded at δ 4.38, in respect to δ 4.08 of H-15 in 15-HEPE (Feussner *et al.*, 1997) and the ESI$^+$ MS peak at *m/z* 371 $(C_{21}H_{32}O_4+Na)^+$ instead of 355. Both changes were consistent with the presence of one hydroperoxy group at C15 and were unambiguously confirmed by COSY and TOCSY experiments that showed correlation of the proton at 4.46 ppm with two spin systems formed by the diene fragment from C-14 to C-11 and by the terminal pentenyl residue C-16/C-20. Co-injection of **27a** and **28a** in RP-LCMS gave rise to a single peak eluting at 33 min in the condition used for oxylipin analysis.

Peak of compound **29a** exhibited a pseudomolecular ion at *m/z* 355.0 accounting for a molecular formula $C_{21}H_{32}O_3Na^+$, indicative of a regioisomer of **27a**. The ^{1}H-NMR spectrum of **29a** contained the signal of hydroxylated methine (H-5, δ 3.86) up-field shifted with respect to that registered for **27a**, due to the absence on a side of the molecule of double bonds. This carbynolic proton was correlated to H-6 δ 5.50, from which *trans, cis*-diene moiety H-6/H-9 was constructed (H-6 δ 5.50 *J*=15.1; H-7 δ 6.54 *J*=15.1-10.7; H-8 δ 6.00 *J*=15.1-10.7; H-9 δ 5.35 *J*=10.7). Signal integration in ^{1}H-NMR spectra indicated the presence of three *bis*-allylic methylenes at δ 2.83 (4H, H_2-13 and H_2-16) and at δ 2.94

(2H, H_2-10). The analysis of all the bidimensional connectivities allowed the assignment of 5-hydroxy-6*E*,8*Z*,11*Z*,14*E*,17*Z*-eicosapentaenoic acid (5-HEPE) methyl ester to **29a**.

2.2.11. Absolute stereochemistry of 9-hydroxy-7*E*-hexadecenoic acid

The absolute stereochemistry at C9 of 9-hydroxy-7*E*-hexadecenoic acid (**25a**) was determined in agreement with the method recently proposed by Williamson and co-workers (2003). However, to achieve the determination on microscale, the methodology was slightly modified by inverting the order of the reactions reported in the literature. Therefore, dichlorodimethylsilane was first added to a solution of the hydroxy acid **25a** (1.4 μmol) in dry pyridine (200 μl) and then the resulting silyl derivative was reacted *in situ* with an excess of (*R*)- or (*S*)-α-trifluoromethyl benzyl alcohol to give the diastereomeric **25b** and **25c**.

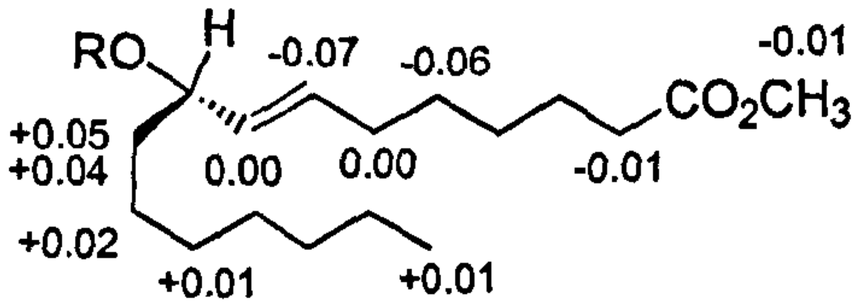

Figure 2.13: Absolute stereochemistry of alcohol **25a**. Δδ (δ*R*-δ*S*) are indicated. R = (*R*)- or (*S*)-PhTFE.

After purification on silica gel, both compounds were fully characterized by NMR spectroscopy. Differences (δ*R*-δ*S*) of the ^{1}H chemical shifts of the diastereomeric α-trifluoromethyl benzyl silyl derivatives (*R*- and *S*-PhTFE) **25b** and **25c** (Figure 2.13) indicated the *S* configuration of the secondary alcohol, thus characterizing compound **25** as 9(*S*)-hydroxy-7*E*-hexadecenoic acid.

2.2.12 Absolute stereochemistry of 9-hydroxy-6*Z*,10*E*,12*Z*-hexadecatrienoic acid

The absolute stereochemistry of 9-HHTrE (**26a**) was determined by applying of the strategy described in Scheme 2.4.

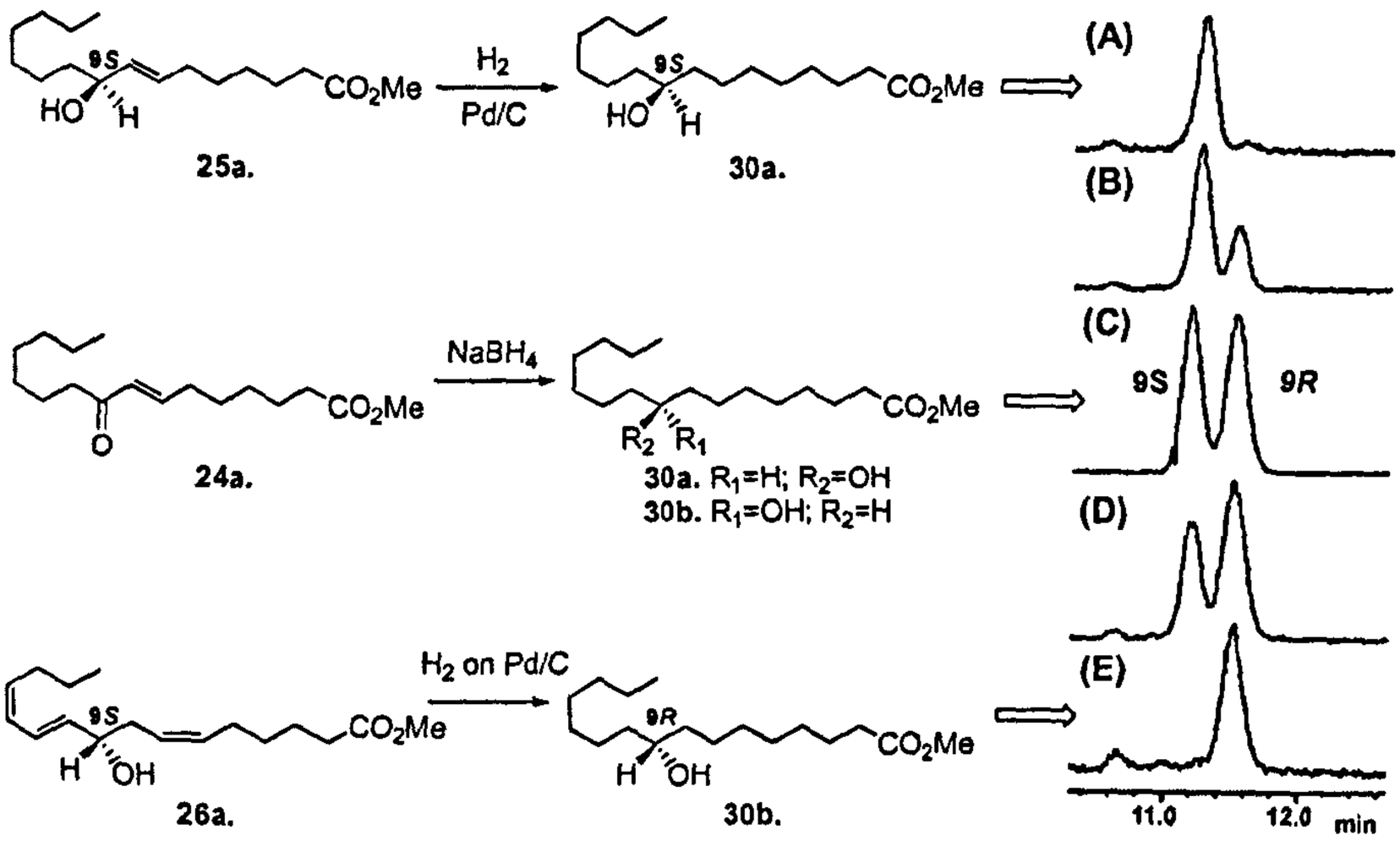

Scheme 2.4: Chiral analysis of *9S*-HHTrE (**26a**) from *T. rotula*. Enantiomers of hydroxyhexadecanoic acid methyl esters (**30a** and **30b**) were obtained by hydrogenation of **25a** and **26a**, respectively. Racemic hydroxyhexadecanoic acid methyl ester (**30a/30b**) was obtained by $NaBH_4$ reduction of **24a.** Chiral $APCI^+$ HPLC of (*A*) *9S*-hydroxyhexadecanoic acid methyl ester (**30a**); (*B*) racemic (**30a/30b**) and *9S*-hydroxyhexadecanoic acid methyl ester (**30ba**); (*C*) racemic (**30a/30b**) hydroxyhexadecanoic acid methyl ester; (*D*) racemic (**30a/30b**) and *9R*-hydroxyhexadecanoic acid methyl ester (**30b**); (*E*) *9R*-hydroxyhexadecanoic acid methyl ester (**30b**).

Hydrogenation of the 9*S*-alcohol **25a** by 5% Pd on C and $NaBH_4$ reduction of the ketone **24a** gave the *S*-enantiomer (**30a**) and racemic mixture (**30a** and **30b**) of the 9-hydroxyhexadecanoic acid methyl ester, respectively. Comparison of these products by chiral $APCI^+$ HPLC allowed to discriminate the enantiomeric peaks (Scheme 2.4), thus providing a tool suitable for the characterization of **26a**. In fact, Pd-catalysed hydrogenation of this last compound (**26a**) led to a single derivative that was recognized as the *R* isomer of 9-hydroxyhexadecanoic methyl ester (**30b**) by elution on the chiral column. This assigned the structure of 95% optically pure 9(*S*)-hydroxy-6*Z*,10*E*,12*Z*-hexadecatrienoic acid methyl ester to **26a**.

2.2.13 Absolute stereochemistry of 15-HEPE methyl ester and 5-HEPE methyl ester

The absolute stereochemistry of **27a** and **29a** was established as *S* and *R*, respectively, on the basis of the product elution on chiral HPLC. 15(*R*,*S*)-HEPE/15(*S*)-HEPE and 5(*R*,*S*)-HEPE/5(*S*)-HEPE were used as authentic standards. The chirality of the compounds was

confirmed by coelution with commercially available standards. Whereas 15(*S*)-HEPE is almost optically pure [enantiomeric excess (e.e.) 99%], 5(*R*)-HEPE presented an e.e. of 74% (Figure 2.14).

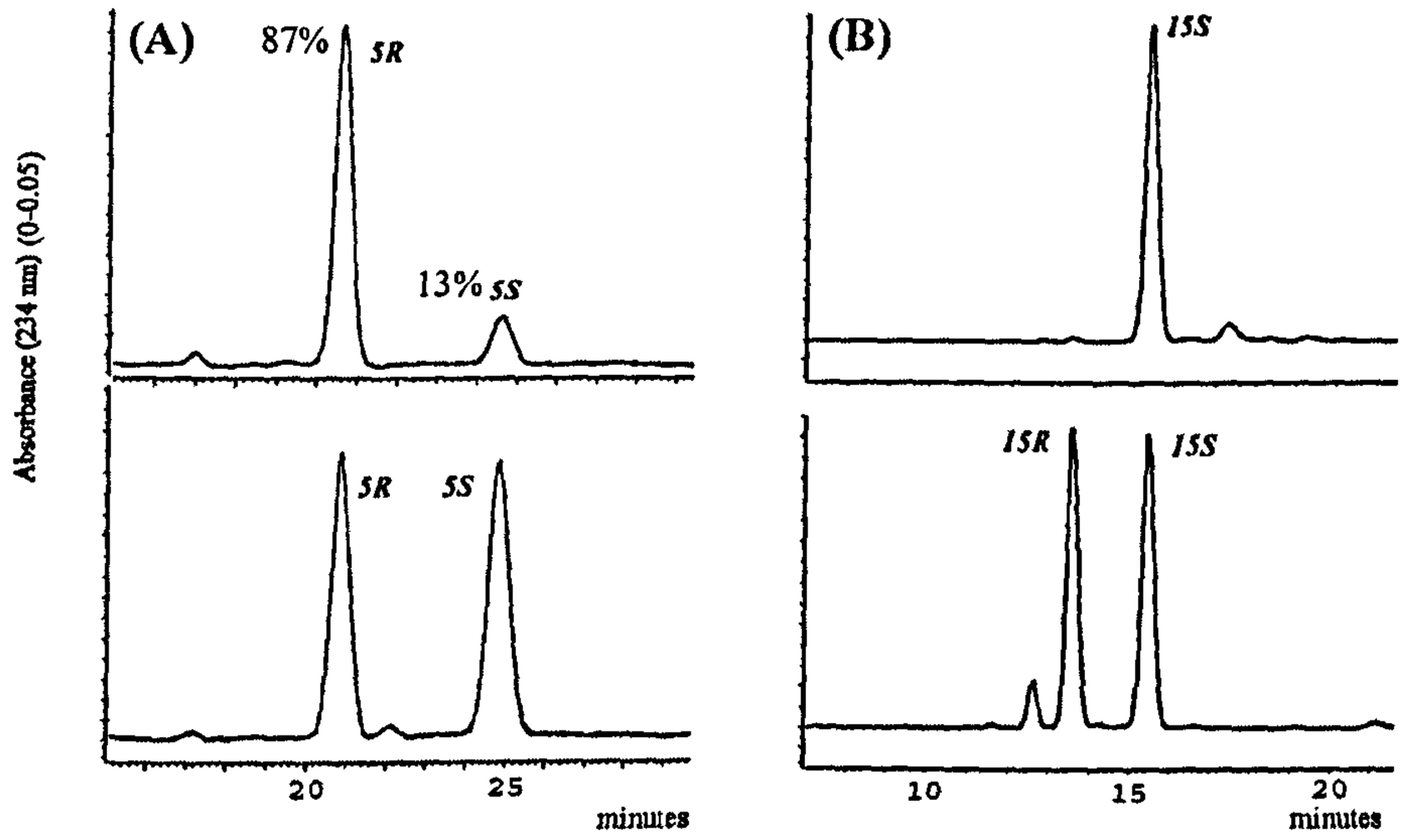

Figure 2.14: Chiral SP-HPLC analysis of 5-HEPE and 15-HEPE from *S. costatum.* All the products were analyzed after methylation. (A) Commercial 5(*R*,*S*)-HEPE (bottom); 5(*R*)-HEPE from *S. costatum* (top); (B) Commercial 15(*R*,*S*)-HEPE (bottom); 15(*S*)-HEPE from *S. costatum* (top).

2.3 *Thalassiosira rotula*

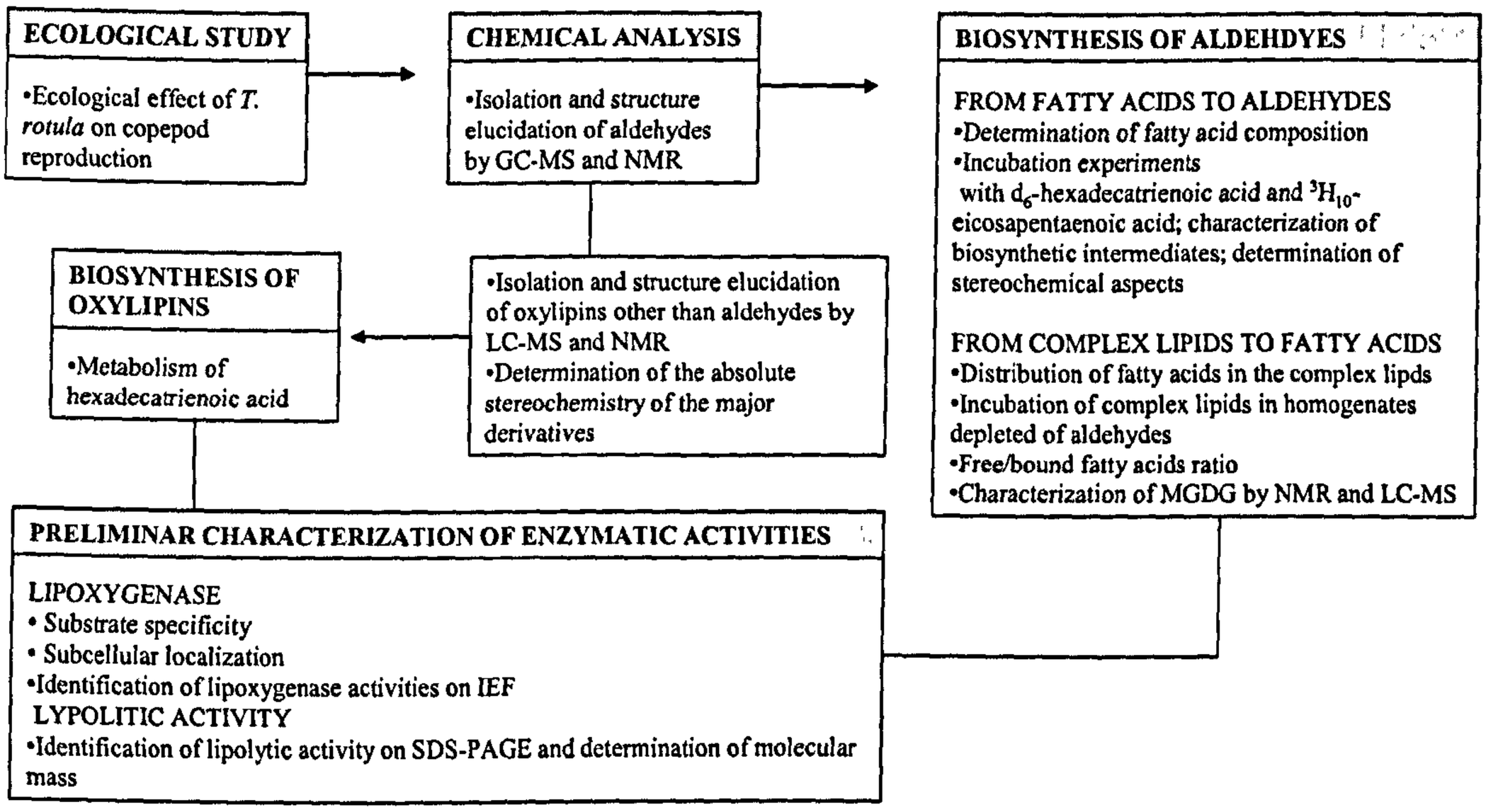

2.3.1 Ecological effect of *T. rotula* on copepod reproduction.

This species forms major blooms at Sea, especially in coastal regions of the Atlantic. *T. rotula* diet did not modify egg production rates, but hatching success of copepods eggs diminished to 10% within 15 days (Figure 2.15). This effect was less intense than the effect obtained with a diet of *S. costatum*.

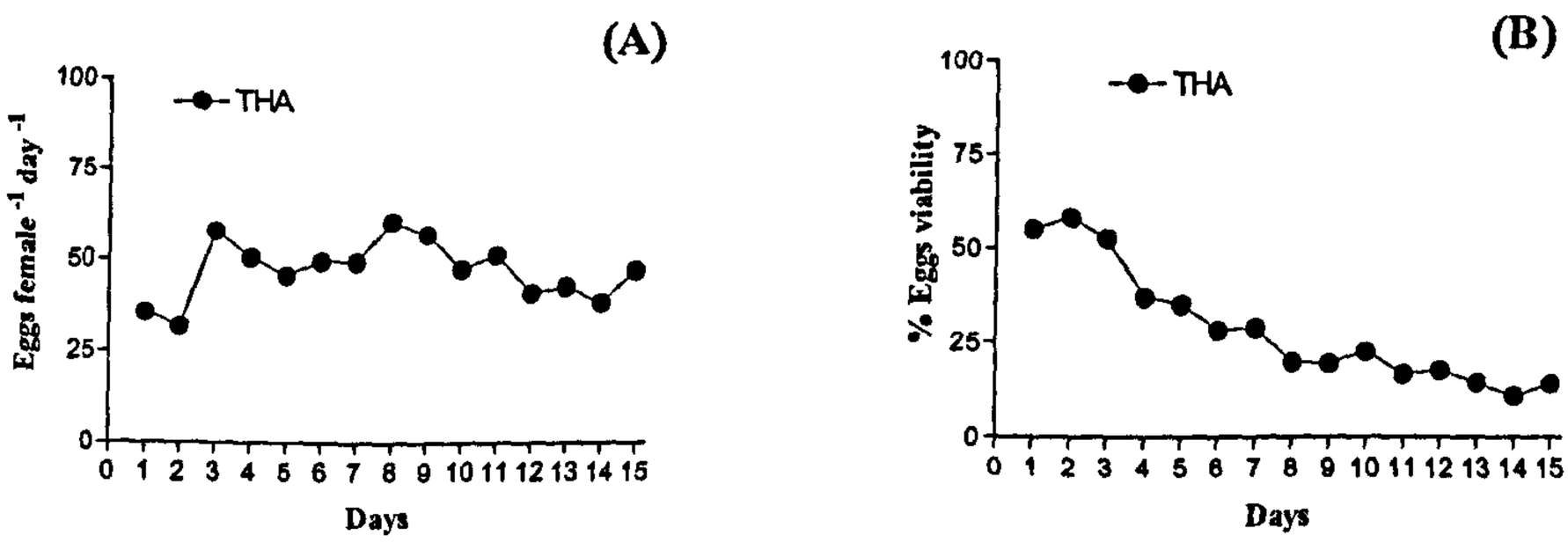

Figure 2.15: Laboratory experiments testing the effects of the diatom *T. rotula* on egg production rates (A) and hatching viability (B) in the copepod *T. stylifera*.

2.3.2. Aldehyde profile

GCMS analysis of *T. rotula* CET-derivatives showed the presence of unsaturated C_{10} compounds, 2*E*,4*Z*,7*Z* decatrienal (**1**) and 2*E*,4*E*,7*Z*-decatrienal (**2**). This finding confirmed

the results previously reported by Miralto *et al.*, (1999) although our strain of *T. rotula* did not contain 2,4 decadienal (**3**). The extracts also contained high levels of other aldehydes, including 2*E*,4*E*-octadienal (**14**), 2*E*,4*E*,7-octatrienal (**16**) and 2*E*,4*E*-heptadienal (**18**). As for *S. costatum*, the *trans/trans* isomers were predominant over the *trans/cis* isomers (d'Ippolito *et al.*, 2002a).

2.3.3 Production of octadienal and its intermediate from HTrA

The production of octadienal was investigated using d_6-HtrA. Sonicated diatoms (1.2×10^8 cells in 5 ml F/2 medium) were incubated for 30 min at room temperature (22 °C) with 0.5 mg d_6-HTrA. After extraction, the material was derivatized with CET-TPP and analyzed by GCMS. As in *S. costatum*, MS spectrum of the peak at 13.8 min indicated two series of signals consistent with the presence of octadienal [*m/z* 208 (M+), 179 (M-29), 163 (M-45)] and d_4-octadienal [*m/z* 212 (M+), 183 (M-29), 167 (M-45)] (d'Ippolito *et al.*, 2003) (Figure 2.16). The synthesis of the labelled aldehyde was further confirmed by high-resolution ^{2}H-NMR. Detailed LCMS analyses indicated that extracts of lysed cells of *T. rotula* contained minor components showing spectroscopic and chromatographic characteristics attributable to methyl ester of hydroperoxy derivative of HTrA [*m/z* 319 ($M+Na^+$), 303 ($M-O+Na^+$) UV λ_{max} = 236 nm]. However, the exceptionally low levels of these compounds in raw extracts did not allow the direct determination of their structures. To overcome this problem, diatom homogenates incubated with d_6-HTrA were reacted with trimethylphosphite (TMP) in order to reduce hydroperoxides to the corresponding hydroxy acids. After reaction, the total ion chromatogram (RP-LCMS) revealed a drastic simplification of the extract, with complete disappearance of the aforementioned peak.

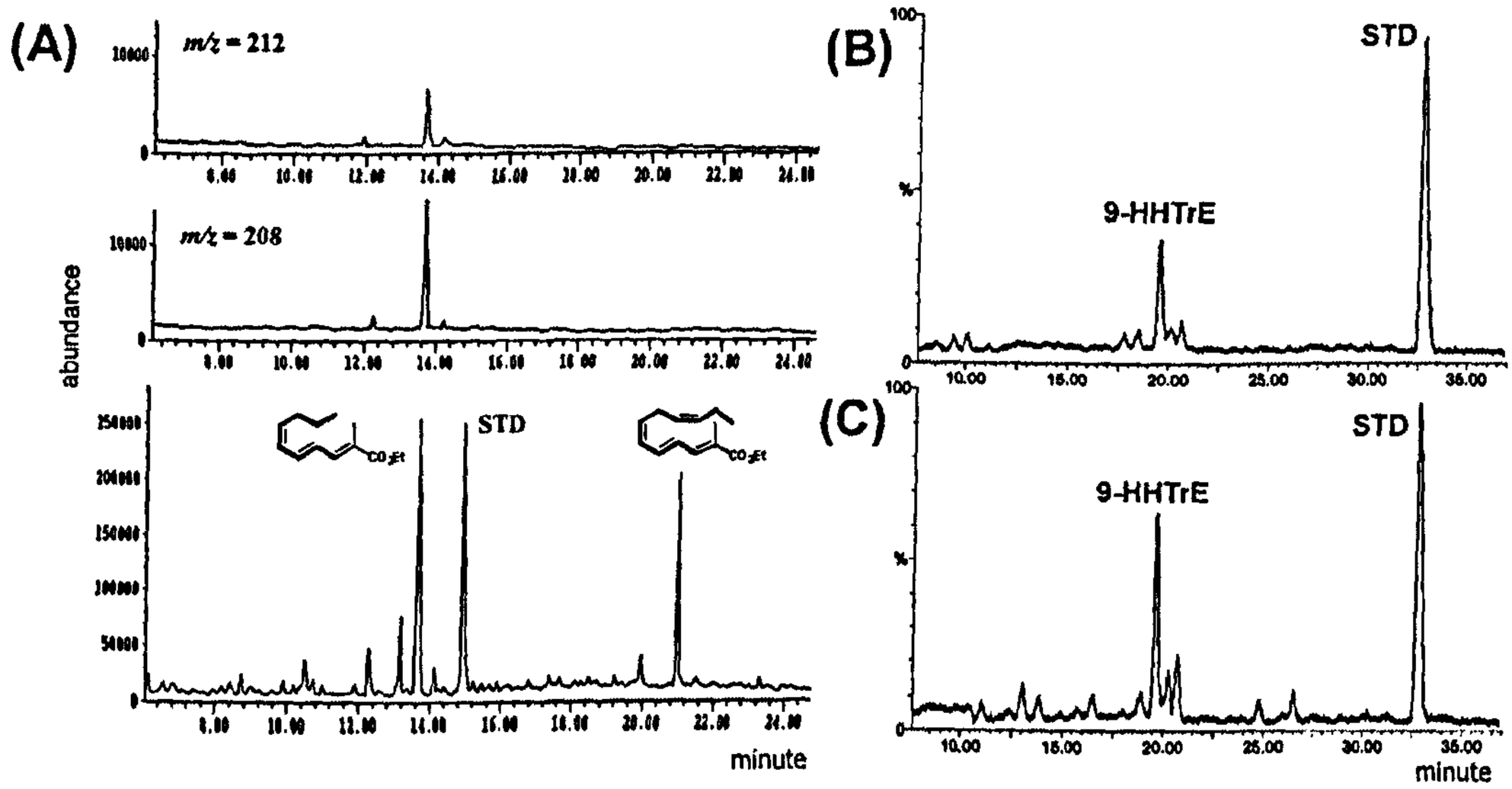

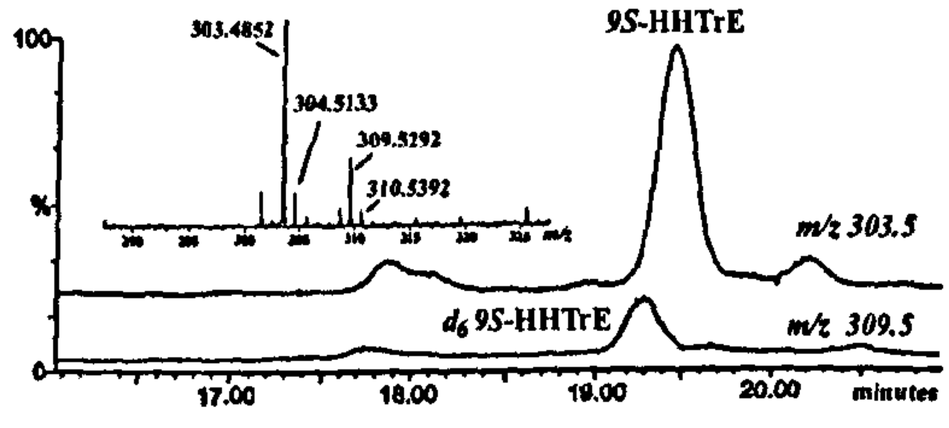

Figure 2.16: Biosynthesis of octadienal in cell homogenates of *T. rotula*. GCMS analysis (A) of PUAs from cells incubated with d_6-HTrA (STD = 4-*trans*-decenal as internal standard): Total GC profile (bottom), GC profile after ion extraction at *m/z* 212 for d_4-octadienal (top) and 208 for octadienal (middle). LC-MS/MS detection of deuterated 9-HHTrE before (B) and after (C) reduction of extract incubated with d_6-HTrA (STD = 16-hydroxyhexadecanoic acid methyl ester). The depicted profiles were obtained by ion extraction at *m/z* 309 corresponding to the pseudomolecular formulas of methylated d_6-HHtrE ($C_{17}H_{22}D_6O_3+Na^+$) and 16-hydroxyhexadecanoic acid ($C_{17}H_{34}O_3+Na^+$). (D) RP LC-MS analysis of *Thalassiosira* homogenates incubated with d_6-HTrA. ESI^+ MS spectrum of the peak eluted at 19.5 min (*insert*) and chromatographic profiles of methyl esters of 9*S*-HHTrE and [d_6]-9*S*-HHTrE obtained by ion extraction at *m/z* 303.5 ($C_{17}H_{28}O_3+Na^+$) and 309.5 ($C_{17}H_{22}D_6O_3+Na^+$), respectively.

In the presence of 16-hydroxyhexadecanoic acid as internal standard, LCMS analysis (Figure 2.16B and C) also proved a clear increase of the peak due to the deuterated derivative of 9-hydroxy-6*Z*,10*E*,12*Z*- hexadecatrienoic acid (9-HHTrE) (*m/z* 303, UV λ_{max} = 234 nm) (Figure 2.16D). In agreement with the method already described (d'Ippolito *et al.*, 2005), the absolute stereochemistry of this product was verified by injection or co-injection of standards, proving that 9(*S*)-HHTrE (95% e.e.) was the only detectable stereoisomer (data not shown). Considering the selectivity of TMP for hydroperoxide reduction and the stereospecificity of the hydroperoxy/alcohol conversion, the obtained data seem to confirm the stereospecific formation of 9(*S*)-HPHTrE in lysed cells of *T.*

rotula (d'Ippolito *et al.*, 2006). The characterization of this intermediate was the first circumstantial evidence of the mechanism of octadienal production through the action of a LOX and further action of a HPL (Scheme 2.5).

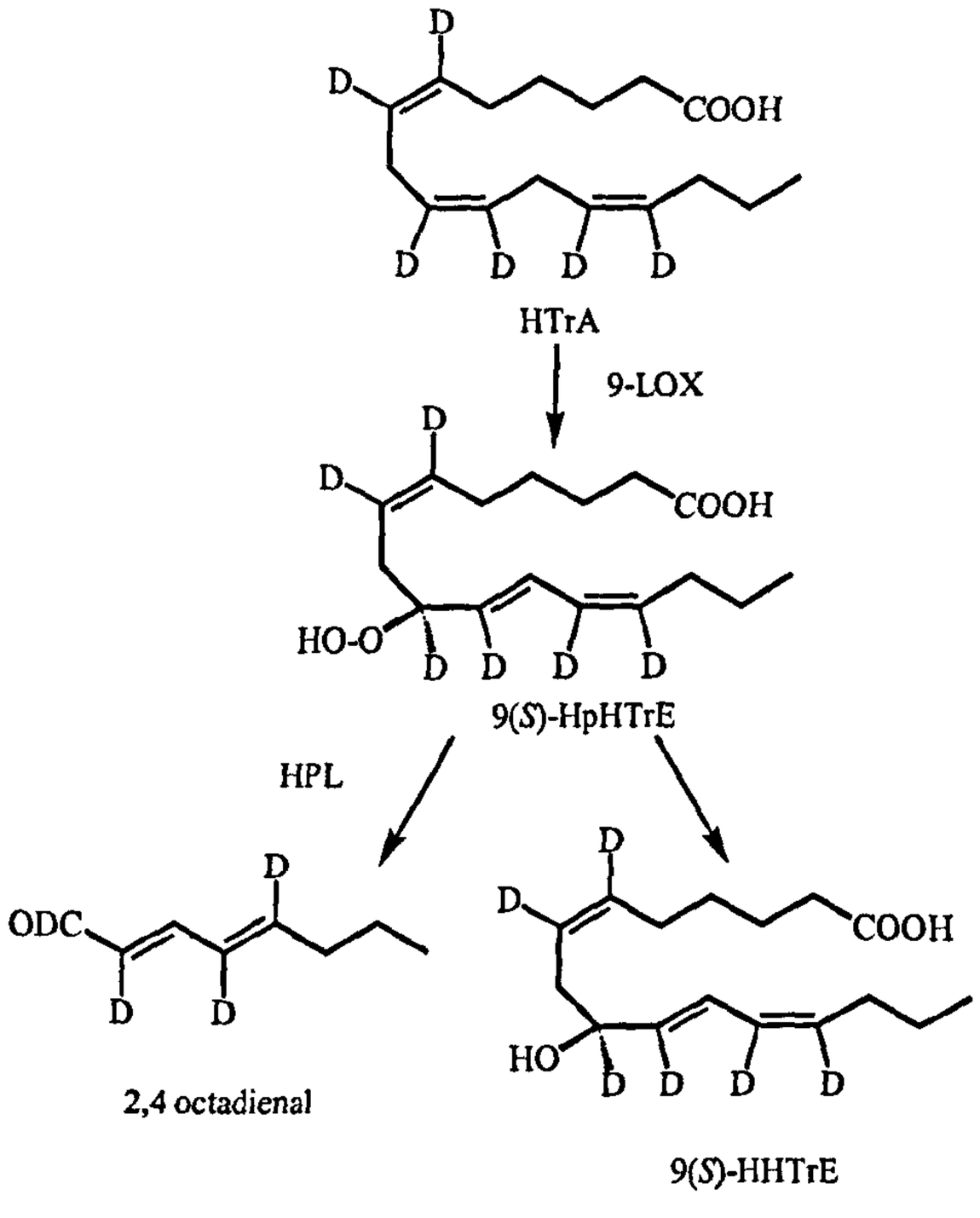

Scheme 2.5: Demonstrated mechanism of octadienal formation

2.3.4. Production of decatrienal and its intermediates from $^{3}H_{10}$-EPA

To investigate the origin of decatrienal, in triplicate, *Thalassiosira* homogenates were incubated with 0.6 mg of ($1.2x10^{7}$ cpm/mg) $^{3}H_{10}$-EPA. After extraction and derivatization, the radioactive material ($9.8x10^{5}$ cpm) was fractionated on silica gel. Except for the radioactivity recovered as unaffected EPA (about $5.8x10^{5}$ cpm, 59%), only two other fractions were significantly labeled. The less polar of these was clearly consistent with the aldehydic pool ($1.4x10^{5}$ cpm, 14%). As shown in Figure 2.17A, HPLC purification of this fraction indicated the presence of a major radioactive component ($1.2x10^{5}$ cpm, 12%) that had the same chromatographic and spectroscopic properties of the derivatized decatrienal.

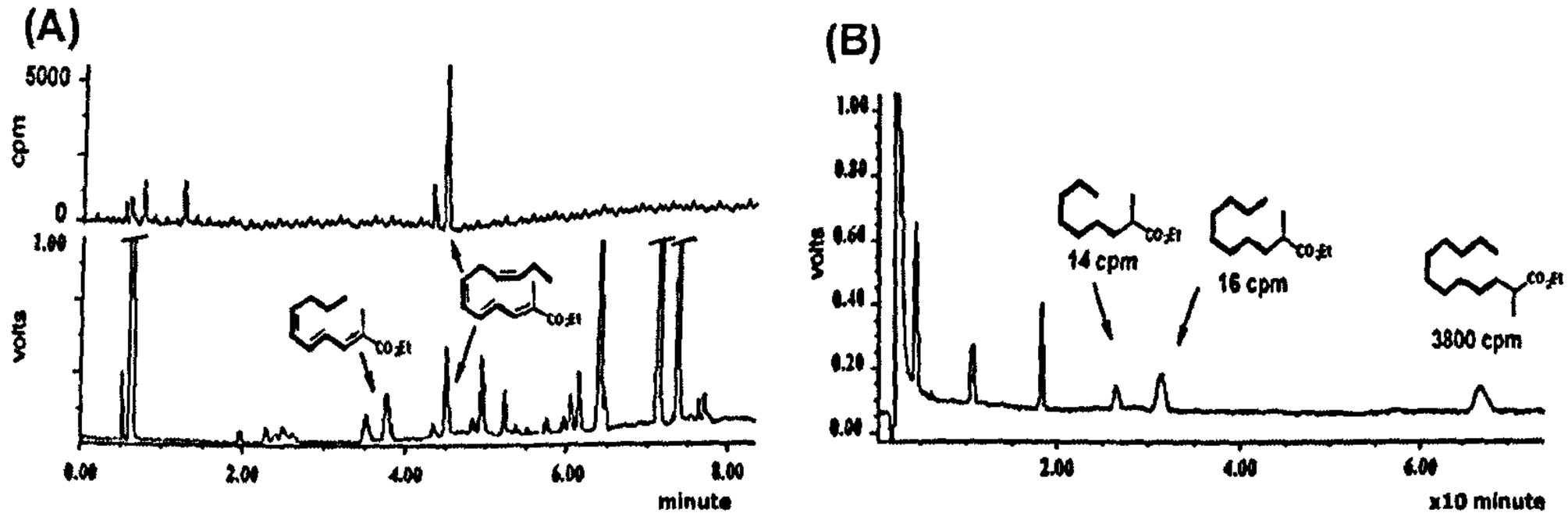

Figure 2.17: Biosynthesis of decatrienal in cell homogenates of *T. rotula* (A) HPLC analysis of CET-aldehydes from cells incubated with ^{3}H-EPA: elution followed by UV 210 nm (below) and radio detectors (top); (B) HPLC analysis of hydrogenated CET-aldehydes from cells incubated with ^{3}H-EPA. Derivative of CET-heptadienal (T_R = 26.8 min), CET-octadienal (T_R = 32.0 min) and CET-decatrienal (T_R = 67.2 min).

Peak identity was unambiguously determined by co-elution with a standard sample of CET-decatrienal (data not shown) and further verified by chemical conversion. To this aim, the derivatized pool of aldehydes was hydrogenated with 5% Pd on carbon and analyzed by HPLC again (Figure 2.17B). The chromatogram of the resulting mixture indicated labeling only of the peak corresponding to 2-methyl-dodecanoic acid ethyl ester (3800 cpm), the product derived by reduction of CET-decatrienal. No significant radioactivity was recorded for the hydrogenated derivatives of C_8 and C_7 aldehydes, namely 2-methyl-decanoic acid ethyl ester and 2-methyl-nonanoic acid ethyl ester.

The second radioactive fraction ($1.1x10^5$ cpm, 11%) obtained from silica gel separation was methylated and resolved in a series of labelled and unlabelled peaks by RP-HPLC. The major labelled product ($0.6x10^5$ cpm, 6%), co-eluted at 31.5 min with the methyl ester of 11-hydroxy-5*Z*,8*Z*,12*E*,14*Z*,17*Z*-eicosapentaenoic acid (11-HEPE), was a lipoxygenase product previously isolated from mussel ovarians (Coffa & Hill, 2000) To confirm this identification, a further RP-LCMS analysis on a fresh extract of *T. rotula* was conducted. The UV absorbance and the MS spectrum of the peak at 31.5 min were indistinguishable from authentic 11-HEPE with a maximum at 236 nm and molecular ion at *m/z* 355 ($C_{21}H_{32}O_3Na^+$). Traces of 11-hydroperoxy-5*Z*,8*Z*,12*E*,14*Z*,17*Z*-eicosapentaenoic acid (11-HPEPE) were also detectable in the chromatogram [R_t 31 min, ESI$^+$ *m/z* 371 ($M+Na^+$,

$C_{21}H_{32}O_4+Na^+$), 355 ($M-O+Na^+$, $C_{21}H_{32}O_3Na^+$)], but the extremely low levels of this metabolite did not allow a more accurate identification. Other labelled products were also present in radio-HPLC but the tiny amount prevented their identification. Among these compounds only the peak of 11-HEPE was still observable after treatment of *Thalassiosira* extracts with reducing agents (data not shown). To determine the stereochemistry of *Thalassiosira* 11-HEPE, the peak corresponding to this product was purified on RP-HPLC from raw extracts of the diatom and re-injected on chiral HPLC. The procedure was repeated several times both before and after reduction of the diatom material. Figure 2.18A shows the elution of racemic methyl esters of commercially available 11-HEPE. The *R* and *S* enatiomers were resolved in two well-separated peaks eluted at approximately 19 min. 11-HEPE methyl ester isolated from *Thalassiosira* was eluted as an asymmetric doublet at the same retention time of the commercial *R/S* 11-HEPE, indicating the presence of a non-racemic mixture containing a slight predominance of the *R* isomer (12% e.e.) (Figure 2.18B). This was fully confirmed by co-elution of the diatom product with standard 11*R*-HEPE (Figure 2.18C). In agreement with the enzymatic origin of this compound, synthesis of decatrienal and 11-HEPE was completely abolished in homogenates of boiled cells incubated with radioactive EPA.

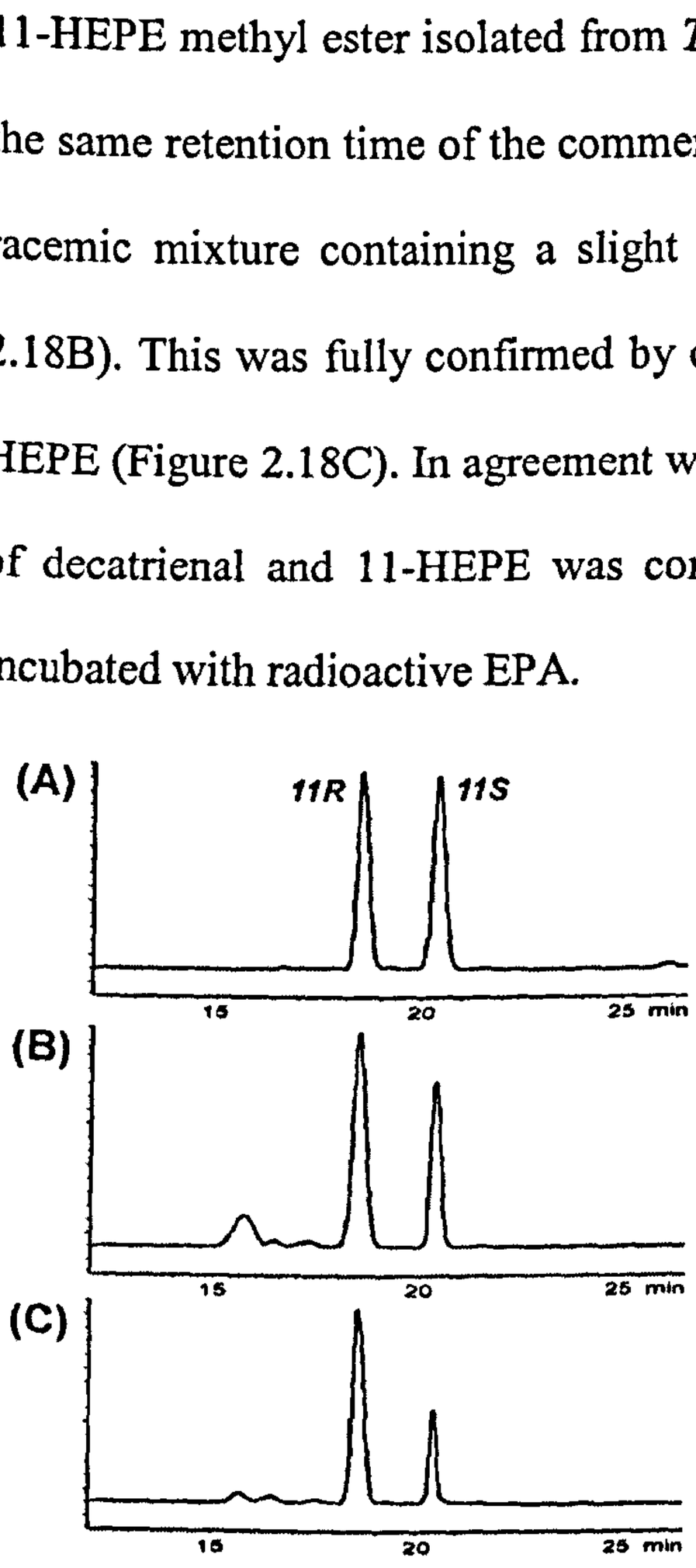

Figure 2.18: Chiral analysis of 11-HEPE from *Thalassiosira* homogenates. (A) resolution of enantiomers of racemic 11-HEPE methyl ester; (B) elution of 11-HEPE methyl ester from extract of *T. rotula*; (C) co-elution of 11-HEPE methyl ester from extract of *T. rotula* plus authentic 11*R*-HEPE methyl ester.

2.3.5. Substrate specificity

In support of the enzymatic origin of octadienal and decatrienal from HTrA and EPA, substrate specificity in the synthesis of these aldehydes was investigated. To this aim, fatty acid-depleted preparations of diatoms were prepared as described in the Materials and Methods by ultrafiltrating the 9600 g supernatant from 1.2 x 10^9 of diatom cells on membranes with 10'000 cut off. F/2 Suspension of these retents were then incubated with the following polyunsaturated free fatty acids (PUFAs): HTrA (12 µmol), EPA (10 µmol), arachidonic acid (AA) (10 µmol), linoleic acid (11 µmol), linolenic acid (11 µmol) and 6,9,12,15-octadecatetraenoic acid (C18:4 ω-3) (11 µmol) (Figure 2.19).

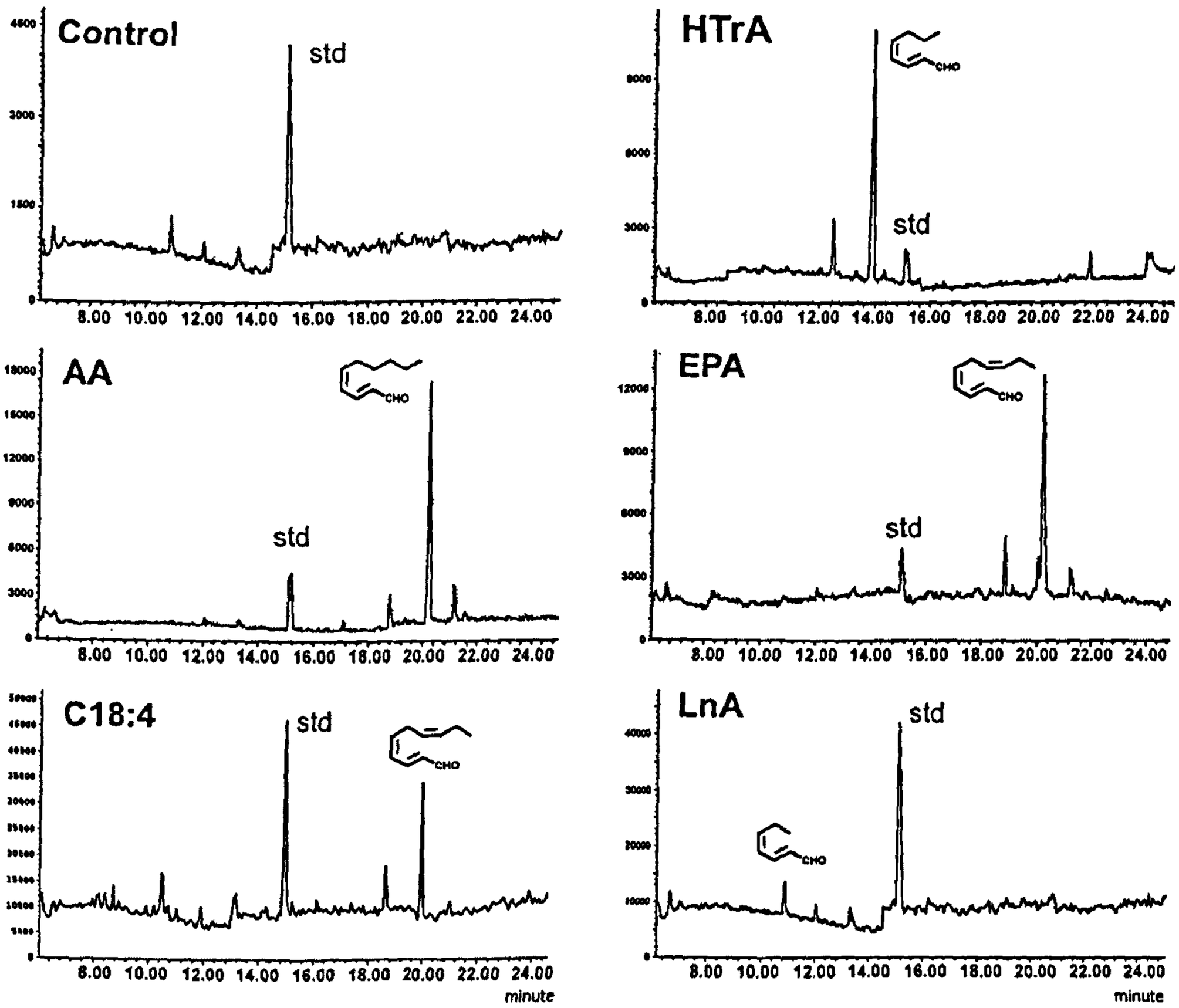

Figure 2.19: Conversion of free fatty acids by YM10 Amicon retents of *T. rotula*. GC profiles of aldehydes after incubation of: HTrA = 6,9,12-hexadecatrienoic acid; AA = arachidonic acid; EPA = eicosapentaenoic acid; C18:4 = 6,9,12,15-octadecatetraenoic acid; LnA = α-linolenic acid. 4-*trans*-Decenal was used as internal standard (std).

As expected, HTrA and EPA were mainly converted to 2*E*,4*Z*-octadienal (4.7±0.8 μmol) and 2*E*,4*Z*,7*Z*-decatrienal (3.9±1.1 μmol), respectively. The 4*E*-isomers of the two products were not detected, in sharp contrast with the results obtained with raw cell homogenates that showed pairs of isomeric compounds. The retents also catalysed production of 2*E*,4*Z*-decadienal (3.6 ±0.7 μmol) from arachidonic acid under conditions identical to those used for EPA. The absence of decadienal in lipid profiles of *T. rotula* is therefore explained by the deficiency of arachidonic acid in this diatom. Interestingly, octadecatetraenoic acid (C18:4 ω-3) was also converted to 2*E*,4*Z*,7*Z*-decatrienal in low rate (1.6±0.7 μmol). On the other hand, linoleic acid and α-linolenic acid were apparently not involved in the formation of PUAs, since their conversion did not occur or was very low (0.3±0.2 μmol for α-linolenic). Heat denaturation of the retents also abolished the generation of aldehydes.

2.3.6. Subcellular localization of enzymatic activities involved in the synthesis of aldehydes

To test the subcellular localization of enzymatic activities related to the synthesis of octadienal, cytosolic and microsomal fractions of *T. rotula* cells (1 x 10^9 cells) were prepared after sonication and successive centrifugation at 9,600 and 102,000 *g*. Pellets and supernatants were incubated with d_6-HTrA (0.5 mg) at room temperature for 30 min. The formation of aldehydes was monitored by GCMS analysis of the incubation mixture after extraction and derivatization with CET-TPP. As shown in Figure 2.20, octadienal synthesis was predominantly associated to the microsomal fraction, with a very evident formation of the deuterated aldehyde (192.3 ±7.2 fg/cell) in the 102,000 *g* pellet. The process was totally inhibited by boiling the preparations for 2 min. LOX activity of the subcellular fractions of *Thalassiosira* cells was also measured by the spectrophotometric method recently proposed by Anthon & Barrett (Anthon & Barrett, 2001) and adapted for using on diatom homogenate.

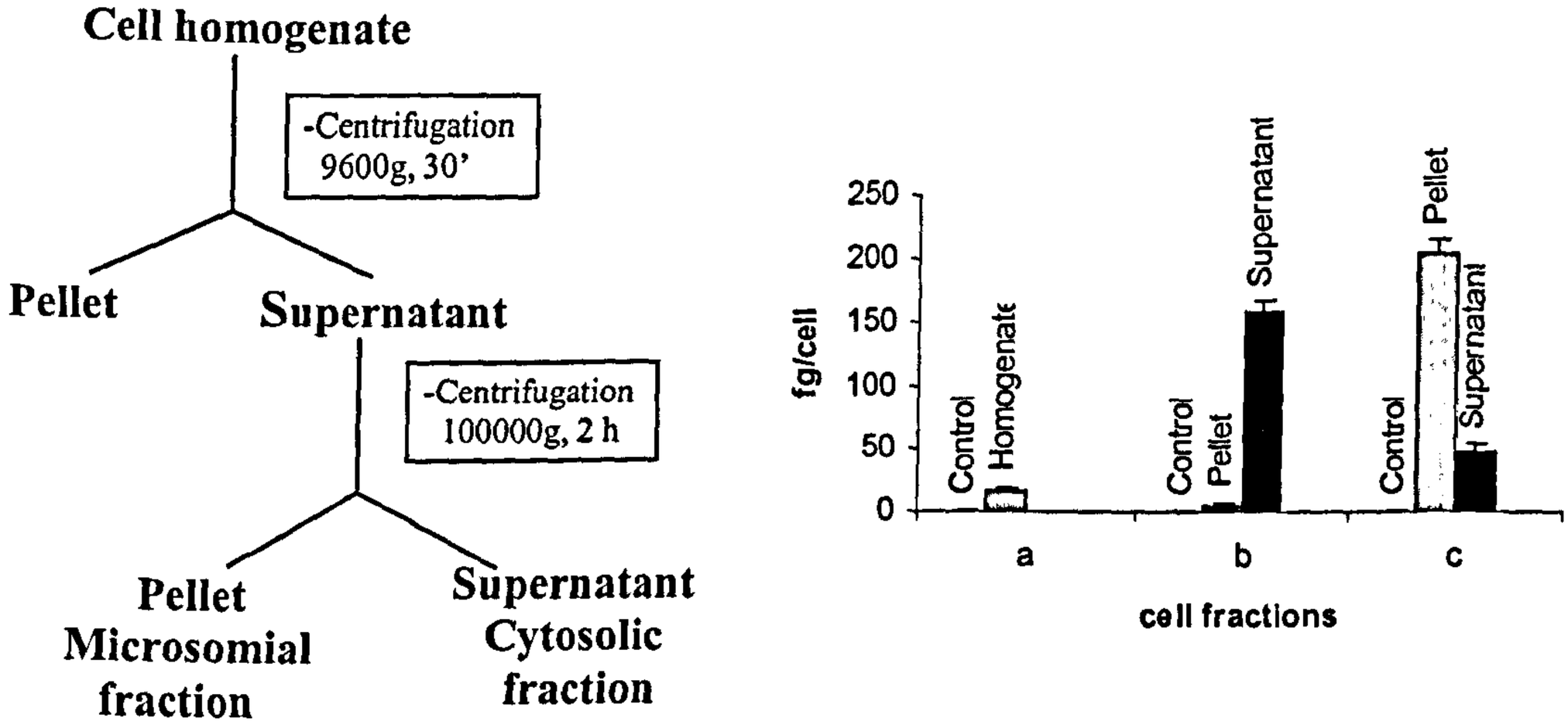

Figure 2.20: Fractionation of cell homogenate (left) and correspondent production of d_4-octadienal by cell fractions of *T. rotula* (right) derived by (a) crude homogenate + 0.5 mg of d_6-HTrA, (b) 9600 *g* centrifugation + 0.5 mg of d_6-HTrA, (c) 102,000 *g* centrifugation + 0.5 mg of d_6-HTrA. Control experiments were carried out by adding d_6-HTrA to boiled preparations.

Protein content was determined by the Lowry method. Using EPA as exogenous substrate, LOX analysis was carried out in triplicate on increasing concentrations of algal cells (1.42 x 10^6, 2.13 x 10^6, 2.84 x 10^6 and 4.26 x 10^6). As shown in Figure 2.21, the highest production of lipid hydroperoxides (expressed as absorbance at 598 nm per μg of total protein) occurred in the 102,000 *g* pellet, indicating distribution of aldehyde synthesis and lipoxygenase activity in the subcellular fractions of *T. rotula*.

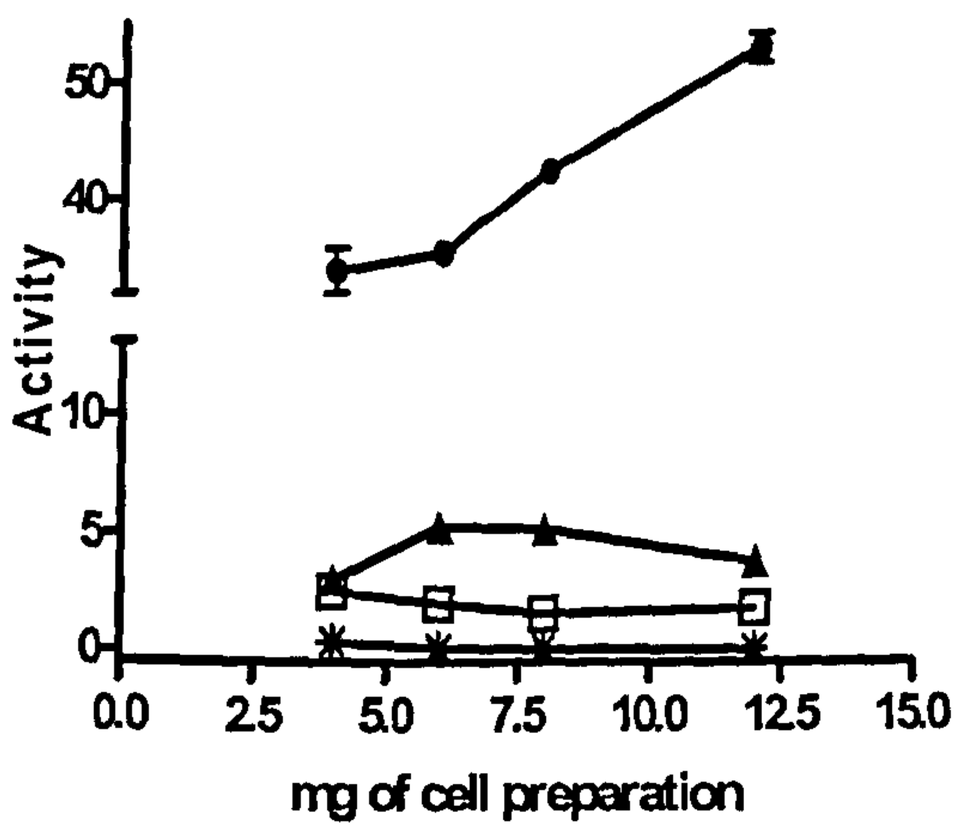

Figure 2.21: Lipoxygenase activity vs number of diatom cells. Assays were performed in triplicate in agreement with the spectrophotometric method of Anthon and Barrett (2001). Lipoxygenase activity = Δ_{598} /µg of protein. (●) = 102,000 *g* pellet; (▲)= 9600 g supernatant; (□)= 102,000 *g* supernatant; (•) = 9600 *g* pellet.

2.3.7. Lipid analysis

Qualitative composition and distribution of fatty acids in the major lipidic groups of *T. rotula* are reported in Figure 2.22.

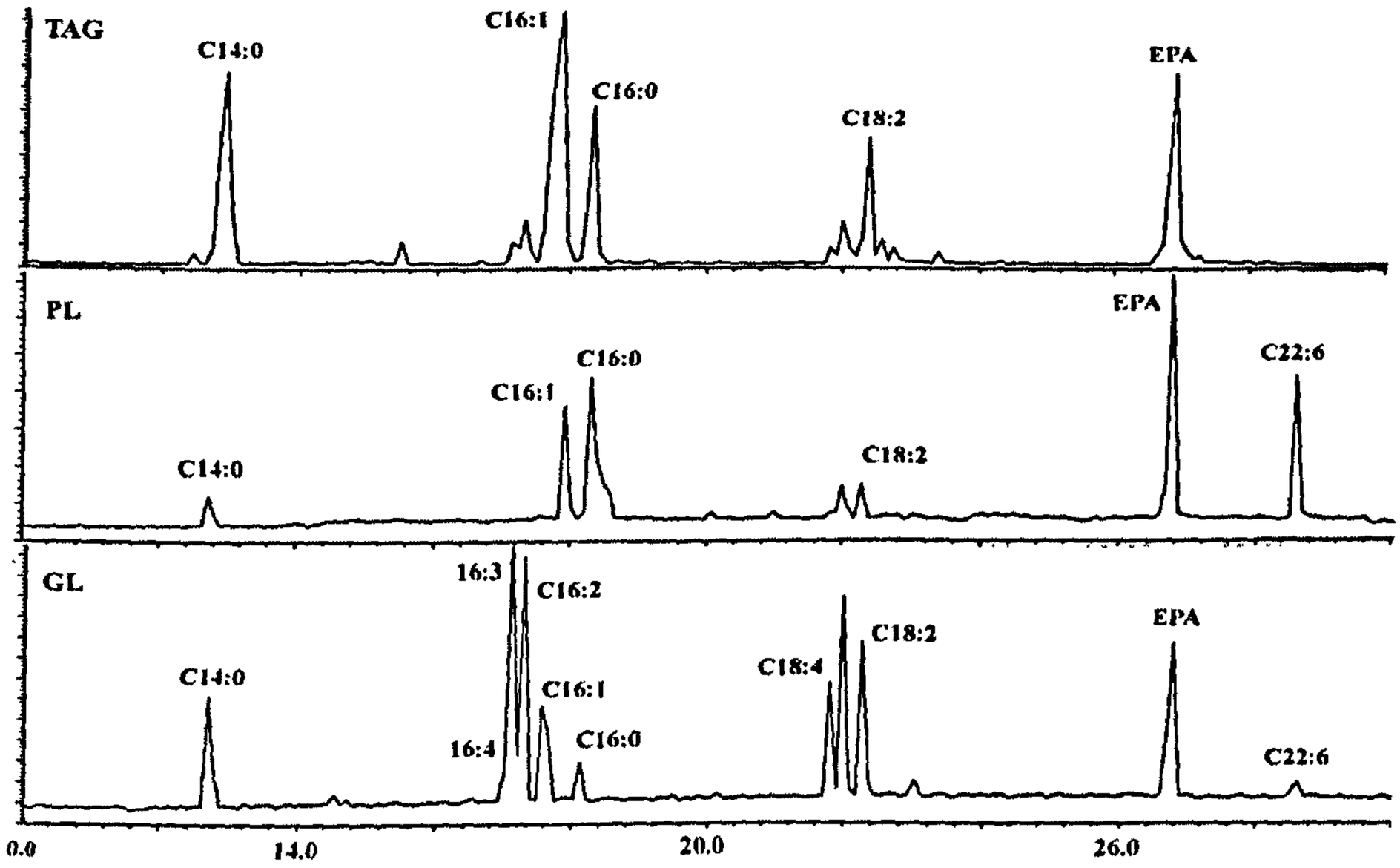

Figure 2.22: GCMS spectra of FAME from glycolipids (bottom), phospholipids (middle) and triacylglycerols (top) in *T. rotula*.

Except for EPA, which was uniformly distributed in the different classes of lipids, GCMS profiling revealed strict differences between triglycerides, phospholipids and glycolipid. The acyl chains linked to phospholipids and triglycerides of the diatom are mainly C20:5, C16:0 and C16:1 together with minor amounts of C14:0, C22:6 and C18:2. On the contrary, in agreement with the literature data on other diatoms, glycolipids contained a very large content of PUFAs, since the percentage of saturated fatty acids was lower than 10%. Furthermore, it was clearly evident that polyunsaturated C_{18} and C_{16} fatty acids, including HTrA and HTA, were only present in the glycolipid fractions.

2.3.8. Metabolism of complex lipids by cell preparations

Considering that HTrA is largely bound to glycolipids, the conversion of this fatty acid to octadienal implicitly suggested that this class of polar lipids could be the specific source of

PUAs *in vivo*. To test this process, aldehyde synthesis was evaluated after incubation of complex lipids in lipid-depleted preparations of *Thalassiosira* homogenate. All the preparations were also incubated with d_6-HTrA to control that the LOX/HPL pathway was active. As shown in Figure 2.23, 2*E*,4*Z*-octadienal (24.3 μg) and 2*E*,4*Z*,7*Z*-decatrienal (48 μg) were formed after 30 min incubation of glycolipid (8 mg) with the diatom's crude fractions retained on membrane (YM10 Amicon filter) with cut-off of 10,000 (Cutignano *et al.*, 2006). Similar results were obtained in experiments with MGDG, the major glycolipidic pool of the diatom (data not shown). On the other hand, in agreement with the fatty acid composition, PLs metabolism led only to formation of decatrienal (43 μg). TAG were apparently not metabolised by *Thalassiosira* retents and most of this lipidic fraction was recovered unaltered after the experiment, without any detectable formation of aldehydes.

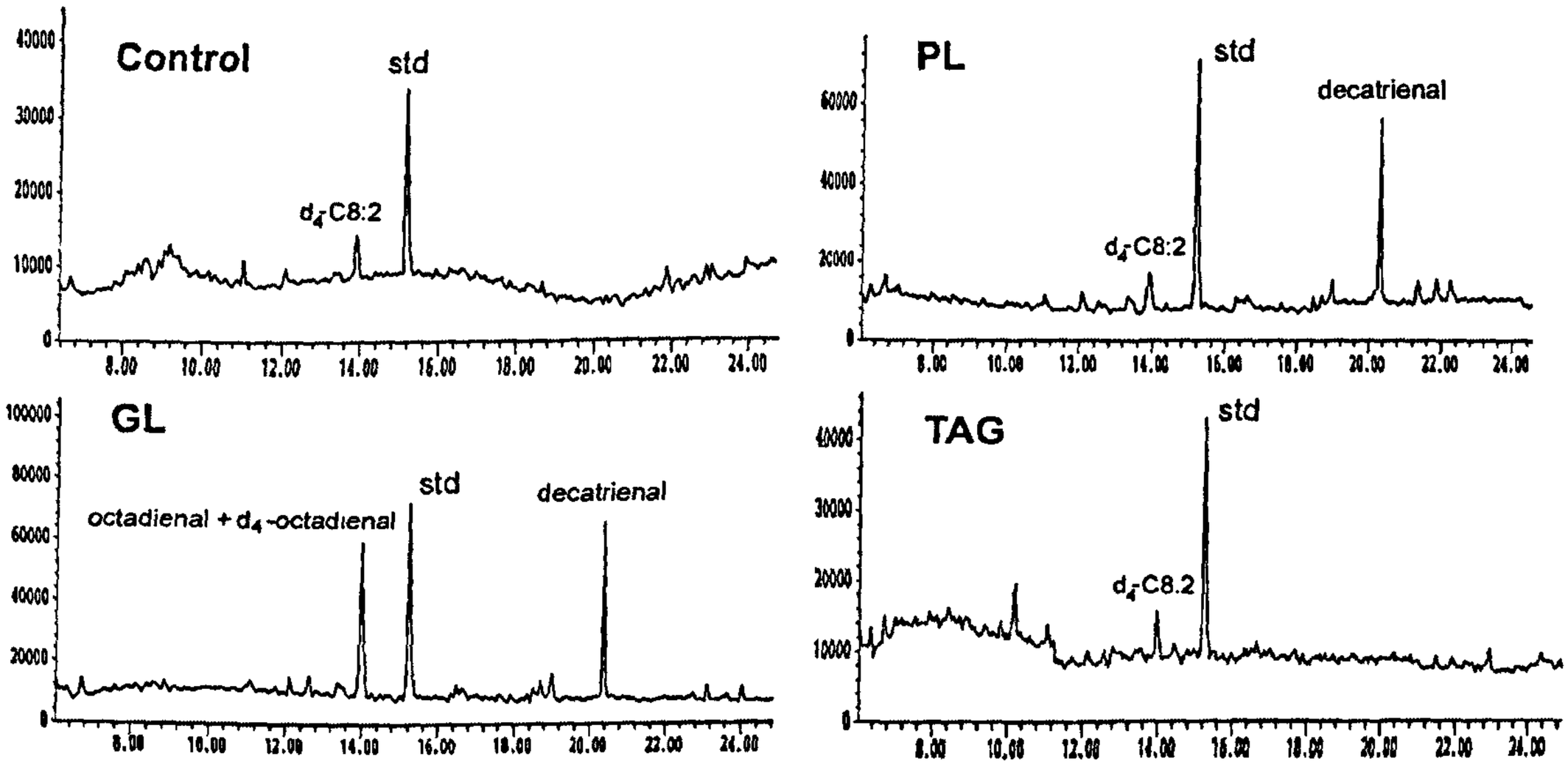

Figure 2.23. Conversion of complex lipids by YM10 Amicon retenates of *T. rotula*. GC profiles of aldehydes after incubation of: GL = glycolipids; PL = phospholipids; TAG = triglycerides. 4-*trans*- Decenal and d_6-HTrA were used as internal standard (std) and internal control, respectively. Aldehydes were analyzed as the corresponding CET-derivatives.

2.3.9. Free/bound fatty acids ratio

The hydrolysis rate of complex lipids was monitored in *T. rotula* by quantifying the levels of free and bound forms of fatty acids in sonicated cells of the microalga. To this aim, a simple methodology was designed based on formation of d_3-labelled methyl derivatives specifically from the lipid-bound fatty acids, hydrolyzing residual complex lipids in CD_3OD/Na_2CO_3, at 42 °C for 4 h. This allowed the GCMS comparison of the fatty acid methyl esters (FAME) from esterified and non-esterified pools, giving a direct value of the hydrolytic activity of the cell preparation. Quantification was performed by using erucic acid as an internal standard, whereas free/bound ratio was directly established by measuring for each compound the ratio between M and M+3 peak (Table 2.5). The fatty acids directly involved in the synthesis of aldehydes, namely HTrA, HTA and EPA, showed a free/bound ratio of about 3 to 1, thus supporting the hypothesis that they were largely present in a non-esterified form in the cell homogenates. The lipolytic process, however, does posses a certain degree of specificity since other components, such as palmitic and myristic acids, were almost found with the same distribution in the two pools (free/bound ratio 0.9. ± 0.1 and 0.8 ± 0.1, respectively).

Fatty Acid	Retention Time	μg/mg pellet (w/w)	Free Species (*m/z*)	Bound Species (*m/z*)	Free/Bound Ratio[b]
C14:0	12.59 min	2,931± 0,571	242	245	0.9 ± 0.1
C16:4	16.96 min	0,488 ± 0,177	262	265	3.0 ± 0.1
C16:3	17.05 min	1,832 ± 0,266	264	267	3.1 ± 1.3
C16:2	17.14 min	0,467 ± 0,156	266	269	1.3 ± 0.6
C16:1	17.40 min	5,164 ± 0,584	268	271	2.5 ± 0.3
C16:0	17.95 min	2,181 ± 0,168	270	273	0.8 ± 0.1
C18:5	21.29 min	trace	288	n.d.	n.c.
C18:4	21.82 min	0,718 ± 0,365	290	293	3.2 ± 0.4
C18:4	22.11 min	1,528 ± 0,234	290	293	3.8 ± 0.6
C18:2	22.25 min	1,288 ± 0,409	294	297	1.6 ± 0.4
C18:1	22.88 min	trace	296	n.d.	n.c.
C20:5	26.56 min	4,818 ± 0,369	316	319	2.6 ± 0.5
C22:6	30.87 min	0,117 ± 0,074	342	345	1.1 ± 0.4

Table 2.5. Composition of fatty acids occurring in free and esterified forms in elicited cells of *T. rotula*. Results are expressed as mean ± S.D. of three independent analyses. [b] Relative amount was established as described in the text by measuring the M/(M+3) ratio of each component. n.d. = not detectable; n.c. = not calculable.

2.3.10. Glycolipid composition

As in *S. costatum*, analysis of fatty acids linked to the *sn*-1 and *sn*-2 positions of the major glycolipid fraction (MGDG) was made in *T. rotula*. MGDG was composed of seven major molecular species, with 20:5/16:3 (20.5%) and 20:5/16:4 (15.6%) being the most abundant (Table 2.6). C_{16}-Fatty acids were largely predominant, with the sum of HTrA (C16:3 ω-4) (approximately 31% of the whole fatty acids) and HTA (C16:4 ω-1) (approximately 27% of the whole fatty acids) close to 60 % of the fatty acid content. The remaining PUFAs consisted in EPA (C20:5 ω-3) (approximately 19% of the whole fatty acids) and unusual penta-and tetra-unsaturated C18-fatty acids (approximately 16% of the whole fatty acids). In analogy with *S. costatum* (d'Ippolito *et al.*, 2004) a distinctive feature was the specific presence of HTA at the *sn*-2 position and EPA at the *sn*-1 position, whereas HTrA was uniformly present at both *sn*-1and *sn*-2 positions (Table 2.6).

Retention Time (min)	$[M+Na]^+$	$[M-H]^-$	Molecular formula	Fatty acids *sn*-1/*sn*-2	Abundance %
t_R=7.0	763	739	$C_{43}H_{64}O_{10}$	18:5/16:4	9.7±1.3
t_R=7.2	739	715	$C_{41}H_{64}O_{10}$	16:3/16:4	4.8±1.5
t_R=8.0	765	741	$C_{43}H_{66}O_{10}$	18:4/16:4 18:5/16:3	8.5±1.2 6.2±1.3
t_R=8.2	741	717	$C_{41}H_{66}O_{10}$	16:3/16:3	9.8±2.3
t_R=9.0	791	767	$C_{45}H_{68}O_{10}$	20:5/16:4	15.6±2.0
t_R=9.2	767	743	$C_{43}H_{68}O_{10}$	18:4/16:3	12.0±2.8
t_R=10.4	793	769	$C_{45}H_{70}O_{10}$	20:5/16:3 18:4/18:4	20.5±2.8 3.3±0.6

Table 2.6. Fatty acid distribution in *sn*-1/*sn*-2 positions of MGDG of *T. rotula*.

2.3.11. Preliminary characterization of the lipolytic activity

When the diatom extracts were processed through centrifugation at 102,000 g as reported in Figure 2.20, lipolytic activity towards 4-methylumbelliferone (MUF)-butyrate and genuine diatom MGDG was found to be associated with both the supernatants and pellets

(Figure 2.24). The reaction towards MUF-butyrate is an assay that allows to detect the lipase activity directly on SDS-PAGE. In fact, analysis on SDS-PAGE showed the presence of three protein bands positive to MUF-butyrate at approximately 45 kDa in both fractions, suggesting the formation of large aggregates (Cutignano *et al.*, 2006). The aggregation was concentration dependent as repetitive cycles of suspension and ultracentrifugation allowed to concentrate the fraction above 45 kDa in the pellet and the prominent activities at approximately 41-43 kDa in the supernatants (Figure 2.24).

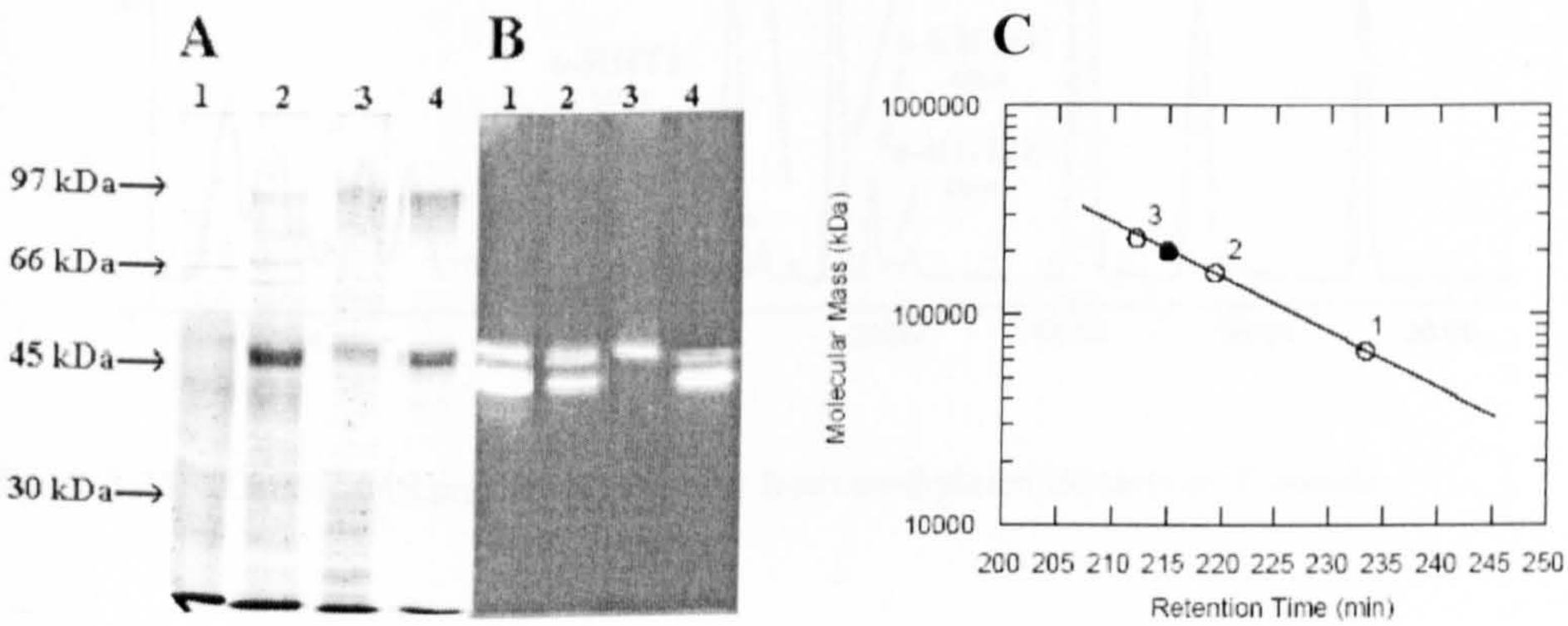

Figure 2.24: SDS-PAGE of *T. rotula* fractions stained in Comassie Brilliant Blue (A) and MUF for lipase activity (B). Each lane holds 15 μg of samples: (1) extract after sonication; (2) 9600 *g* supernatant; (3) 102'000 *g* pellet; (4) 102'000 *g* supernatant. Protein markers consisting of phosphorylase *b* (97,000), bovine serum albumin (66,000), ova albumin (45,000), carbonic anhydrase (30,000). (C) Native molecular mass of lipolytic activities (closed circle) determined by Superdex 200 size exclusion gel chromatography, using (1) bovine serum albumin, 67 kDa; (2) aldolase, 158 kDa; (3) catalase, 232 kDa.

These latter bands run very close on the gel and became undistinguishable a few seconds after staining or in the presence of higher protein concentrations. Native molecular mass determination of the lipolytic activity in the supernatant was carried out with a size exclusion column calibrated with standard proteins. Assuming a globular structure, the lipolytic activity appeared to have a molecular mass at around 200 kDa (Figure 2.24C). The 102'000 g supernatants and 200 kDa material displayed hydrolytic activity using GL fractions isolated from *T. rotula* extracts as substrate.

2.3.12. Structure elucidation of other oxylipins

Axenic cultures of *T. rotula* were obtained and worked out as already described in the Experimental section. The analysis of methylated extract in RP-LCMS revealed the presence of keto- and hydroxy- fatty acid derivatives mainly derived from C_{16} fatty acids (Figure 2.25).

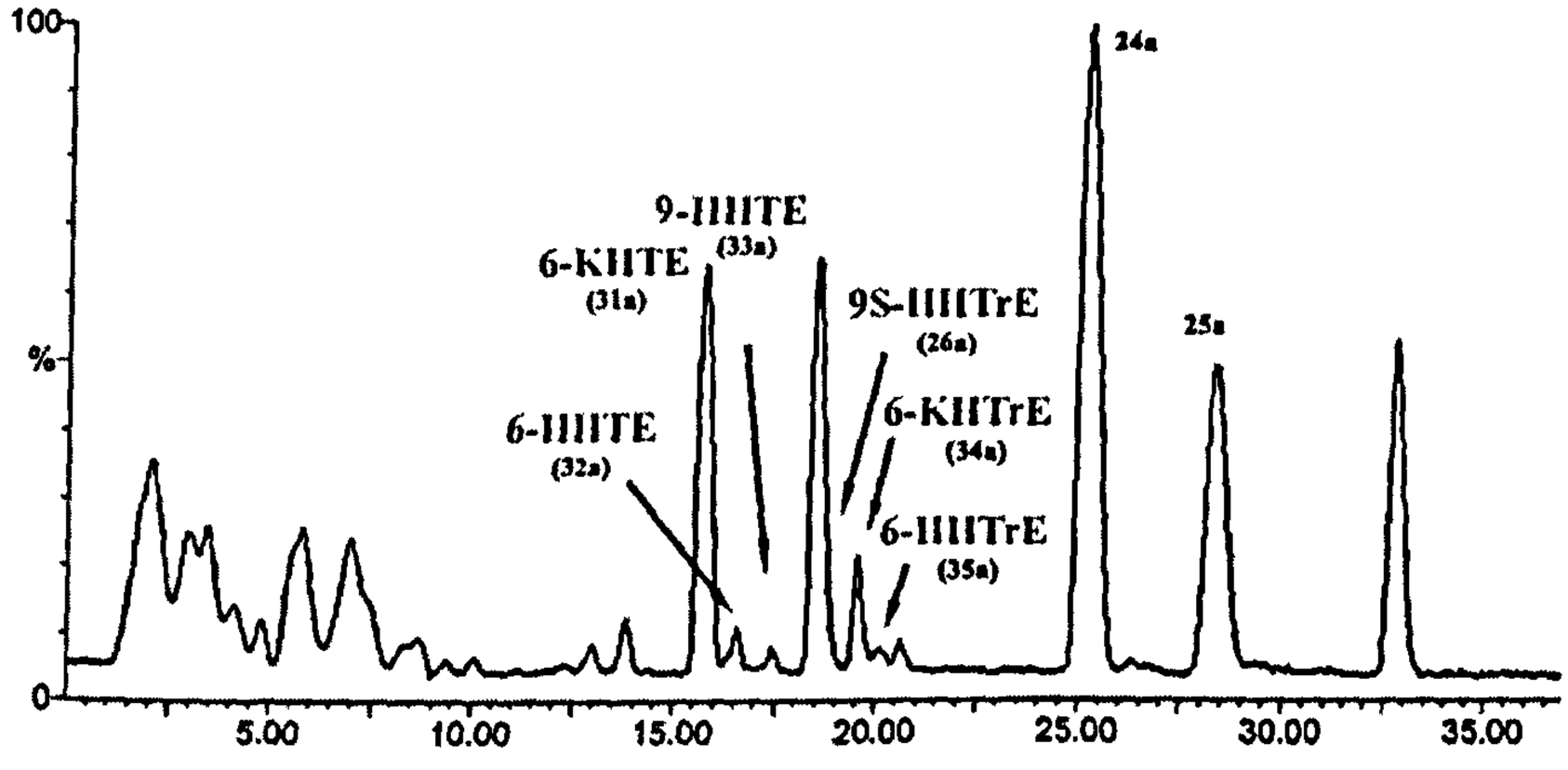

Figure 2.25: LC-ESI$^+$-MS profile of oxylipins from methylated extracts of *T. rotula*.

In particular, the structures of some products were identical to that already described for *S. costatum*. In fact, in analogy with this diatom, *T. rotula* contained 9-keto-7*E*-hexadecenoic acid methyl ester (**24a**), 9(*S*)-hydroxy-7*E*-hexadecenoic acid methyl ester (**25a**), 9(*S*)-HHTrE (**26a**), with the same stereochemical characteristics (d'Ippolito *et al.*, 2005). In addition, *T. rotula* also contained other C_{16} derivatives (**31-35**).

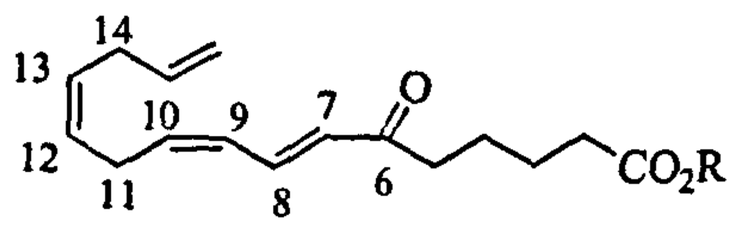

31. R=H; **31a.** R=Me

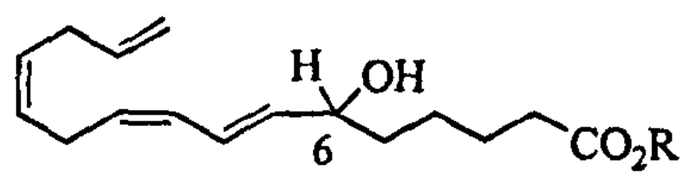

32. R=H; **32a.** R=Me

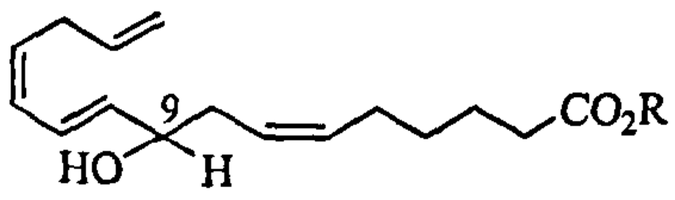

33. R=H; **33a.** R=Me

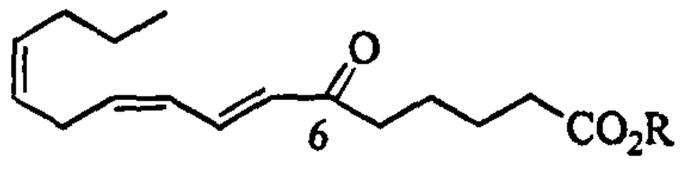

34. R=H; **34a.** R=Me

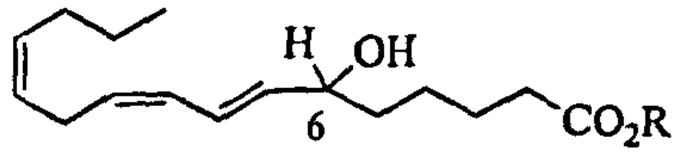

35. R=H; **35a.** R=Me

Peak of compound **31a** showed an ESI$^+$-MS pseudomolecular ion at *m/z* 299 ($[M+Na]^+$) consistent with the formula $C_{17}H_{24}O_3$. The strong UV maximum at 282 nm indicated the presence of an extended conjugation suggestive of a α,β,γ,δ-unsaturated ketone. Consistently, NMR experiments (Table 2.7) indicated the presence of a keto group at δ 198.2 (C-6) that separated two independent spin systems.

	31a ^{1}H δ, m, *J*	^{13}C	**32a** ^{1}H δ, m, *J*
1		172.9	
2	2.04, t, 6.9	33.8	2.03, t, 7.2
3	1.48, m	24.4	1.48, m
4	1.53, m	28.9	1.26, m
5	2.13, t, 7.2	40.6	1.36, m
6		198.2	3.88, q,
7	5.95, d, 15.3	129.9	5.52, dd, 14.9; 6.0
8	7.58, dd, 15.3; 11.5	135.4	6.53, dd, 14.9; 10.8
9	5.88, t, 11.5	127.1	6.0, t, 10.8
10	5.55, dt, 11.5; 7.5	138.8	5.40,[f] m
11	2.76, t, 7.5	26.0	2.90, t, 6.3
12	5.27, m	127.4	5.40,[e] m
13	5.38, m	127.9	5.40,[e] m
14	2.63, t, 6.2	31.2	2.73, t, 6.0
15	5.70, m	136.2	5.72, m
16	4.97, dd, 10.1; 1.5	115.0	4.98, dd, 10.1; 1.5
	5.02, dd, 17.1; 1.5		5.05, dd, 17.1; 1.5
OCH_3	3.31, s	50.5	3.33, s

Table 2.7: NMR data (C_6D_6, 600MHz) for oxylipins **31a** and **32a** from *T. rotula*. Complete assignments were determined on the basis of 1D- and 2D-NMR experiments

One of these embraced most of the deshielded signals, including the diene residue H-7/H-10, one disubstituted double bond H-12/H-13 (δ 5.27 and 5.38) and the terminal methylene H-15/ H_2-16 (δ 5.70, 4.97 and 5.02) (Figure 2.26). The second fragment extended between two methylene groups at δ 2.04 (H_2-2) and 2.13 (H_2-5) through two shielded signals attributable to H_2-3 (δ 1.48) and H_2-4 (δ 1.53). The stereochemistry of the double bonds was identified as 7*E*, 9*Z*, 12*Z* on the basis of the coupling constants of the vinyl protons (15.3, 11.5 and 7.5 Hz, respectively), thus yielding the total structure of compound **31** as the methyl ester of 6-keto-7*E*,9*Z*,12*Z*,15-hexadecatetraenoic acid (6-KHTE).

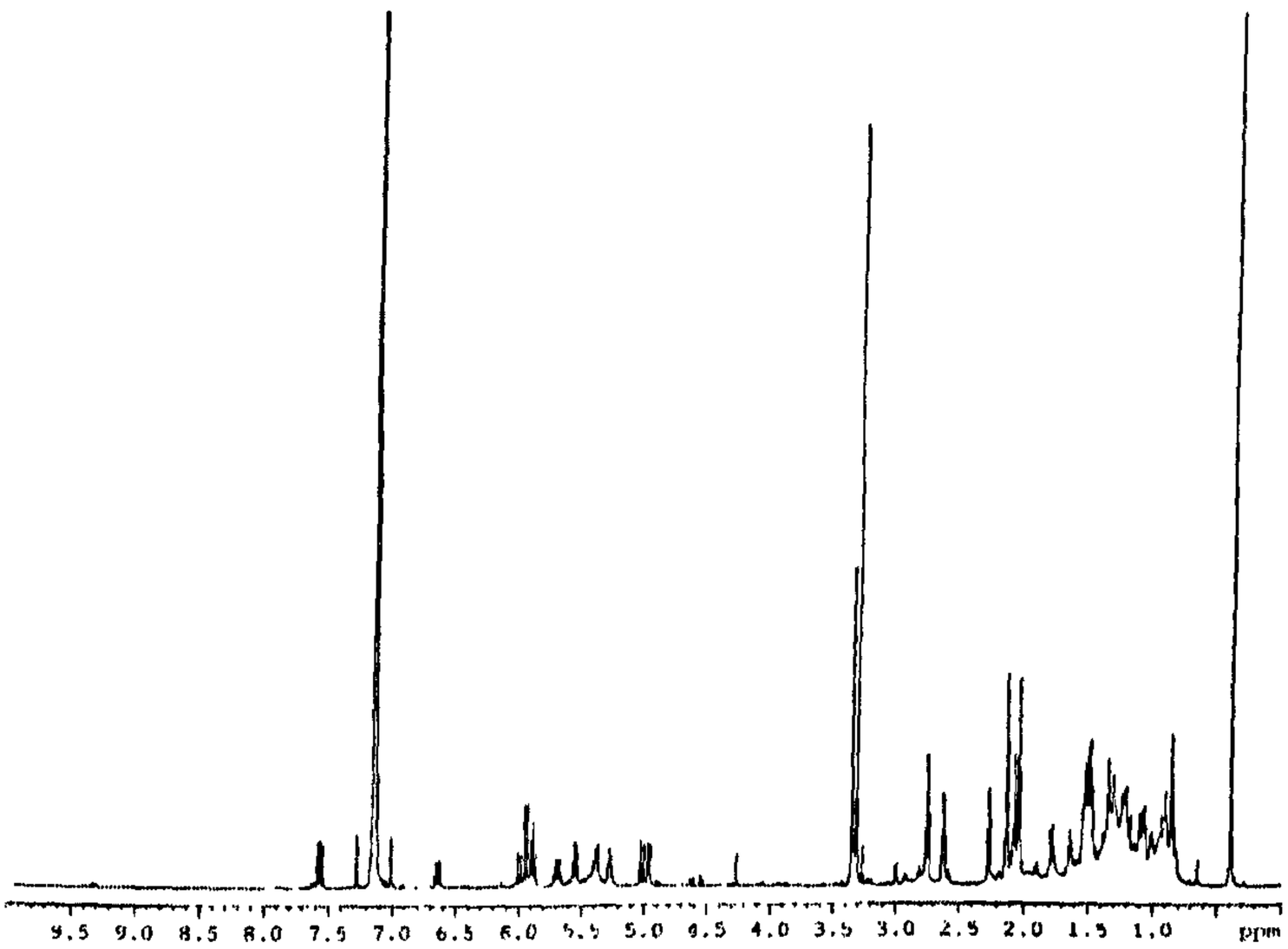

Figure 2.26: ^{1}H-NMR of 6-KHTE methyl ester (**31a**) (C_6D_6, 600 MHz).

^{1}H-NMR data (Table 2.6) of compound **32a** show a strong resemblance with that of 6-KHTE (**31a**), providing evidence for the presence of one *cis*, *trans* diene system, one isolated double bond and one terminal olefin. Clear differences in the spectra of the two compounds were only evident in the high-field region that in compound **32a** is featured by the distinctive resonance due to an allylic alcohol (H-6, δ 3.88). Considering the molecular formula $C_{17}H_{26}O_3$, calculated from the ESI$^+$ MS molecular ion at *m/z* 301 [M+Na$^+$] and the hypsochromic shift of the UV absorption (λ_{max} at 236 nm), these data established for **32** the structure of 6-hydroxy-7*E*,9*Z*,12*Z*,15-hexadecatetraenoic acid (6-HHTE). 6-HHTE purified from *T. rotula* eluted as a single enantiomer using chiral HPLC but the absence of reference compounds and the little amount of the compound did not allow for the determination of the absolute stereochemistry.

In addition to compound **24-26** and **31-32**, lysis of *T. rotula* cells produce a complex group of minor oxylipins. Although these compounds occur at levels too low to allow their isolation, a combination of LC-MS/MS and NMR techniques proved to be suitable to recognize, at least, three major classes of metabolites derived by oxidation of HTrA and HTA. In particular, the chemical investigations of raw methylated extracts of the microalga were consistent with the presence of 9-hydroxy-6*Z*,9*E*,12*Z*,15-hexadecatetraenoic acid (9-

HHTE) (**33a**), 6-keto-7*E*,9*Z*,12*Z*-hexadecatrienoic acid (6-KHTrE) (**34a**) and 6-hydroxy-7*E*,9*Z*,12*Z*- hexadecatrienoic acid (6-HHTrE) (**35a**). Notably, synthesis of these compounds was drastically inhibited when diatom cells were boiled prior to lysis.

2.3.13 Metabolism of HTrA

In the light of the other oxylipins identified in *T. rotula*, HTrA metabolism was assayed. After incubation of crude homogenates of the diatom with d_6-HTrA as previously described, the production of deuterated 9*S*-HHTrE (**26a**), 6-KHTrE (**34a**) and 6-HHTrE (**35a**) was observed. In fact, LCMS analysis of the peak at 19.5 min indicated the presence of 9*S*-HHTrE methyl ester [*m/z* 303.5 ($M+Na^+$)] together with its hexadeuterated analogue [*m/z* 309.5 ($M+Na^+$)] (Figure 2.16 D), thus proving the enzymatic conversion of HTrA to 9*S*-HHTrE. Also 6-KHTrE (**34a**) and 6-HHTrE (**35a**) were labelled after incubation with d_6-HTrA. In particular, MS/MS analysis of the pentadeuterated derivative of 6-KHTrE (ESI^+ *m/z* 306 $[M+Na]^+$, $C_{17}H_{19}D_5O_3$) indicated a fragmentation in α to the keto function, consistent with the LOX-derived structure of **34a**. No product was obtained by incubating the deuterated precursor with boiled preparations of the diatom, thus further supporting the enzymatic origin of **26a**.

2.3.14. Identification of lipoxygenase activities on SDS-PAGE

In order to identify the presence of lipoxygenase activities in the diatom *T. rotula*, preliminary data were obtained by native isoelectric focusing (IEF) of the diatom proteins partially purified by ammonium sulfate precipitation. The lipoxygenase activities were directly localized on the polyacrylamide gels by a specific staining technique using o-dianisidine as developer and HTrA (lane B), linoleic acid (lane C) and EPA (lane D) (Figure 2.27). One single band was observable with HTrA, while the gel revealed more activities specifically associated with EPA metabolism. The stained bands presented average pH values of 5.63 suggesting a pI near this value. A more detailed pI's

determination was carried out using the same ampholyte pH gradient in the PROTEAN II apparatus, doubling the gel length (about 13 cm), and obtaining values in the range 5.61-5.76 (data not shown), in agreement with other known lipoxygenases from rabbit reticulocyte (pI=5.5) (Kuribayashi *et al.*, 2002), from *Pleurotus ostreatus* (pI=5.1) (Doderer *et al.*, 1992) and lipoxygenase isoenzymes from *germinating barley* (pI=5.2-5.3) (Reisner, 1984).

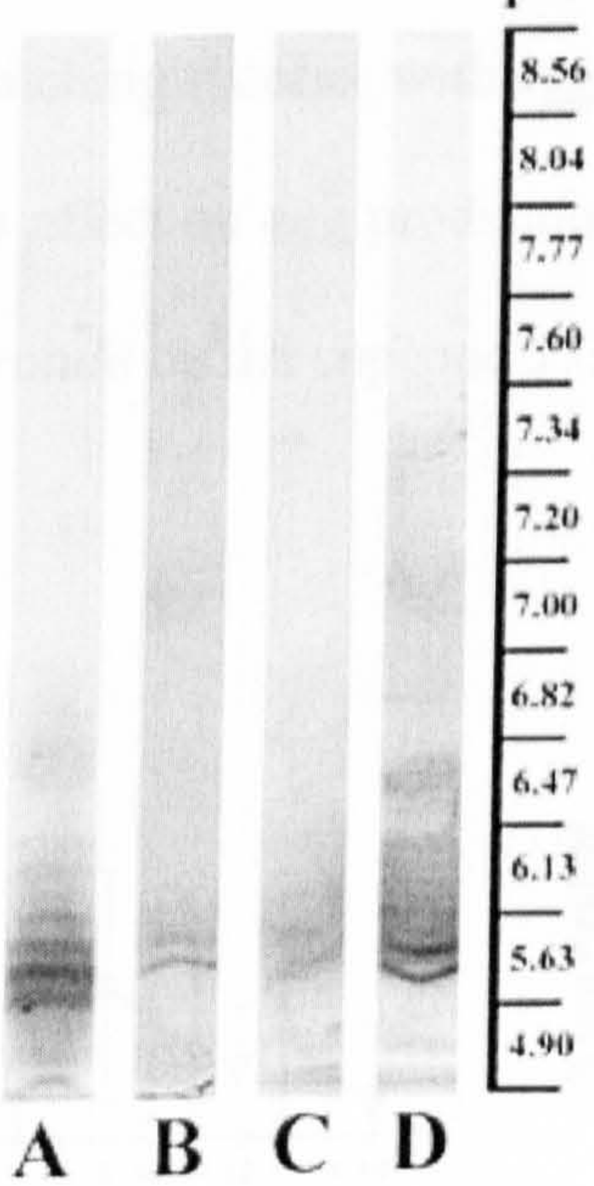

Figure 2.27: IEF-PAGE of *T. rotula* lipoxygenases. Lane A = total protein; lane B = HTrA-dependent LOX activity; lane C = linoleic-dependent LOX activity; lane D = EPA-dependent LOX activity. Gel was stained with Comassie for total protein and with o-anisidine and fatty acid for LOX activity.

Non-specific oxidation by heme proteins cannot be excluded for the absence in the assay of KCN, but the different patterns obtained for the three fatty acids, suggest the absence of these proteins in the pre-fractionated protein samples.

2.4. *Pseudonitschia delicatissima*

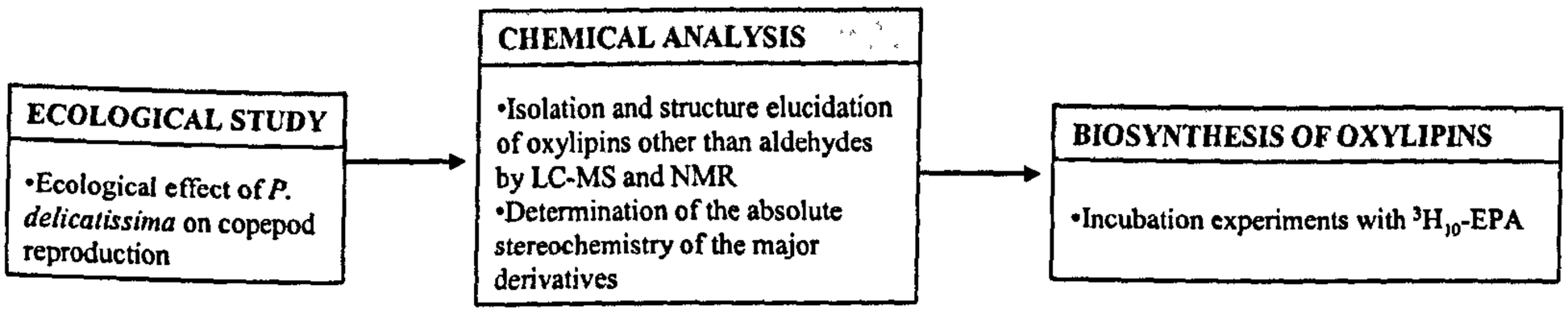

2.4.1. Ecological effect of *P. delicatissima* on copepod reproduction

The effect of a *P. delicatissima* diet was evaluated on the copepod *Calanus helgolandicus*. This diatom modified hatching success, with egg viability dropping to 0% after two weeks; the same diatom had no effect on egg production. These characteristics were very similar to those reported for *T. rotula* on the copepod *T. stylifera*.

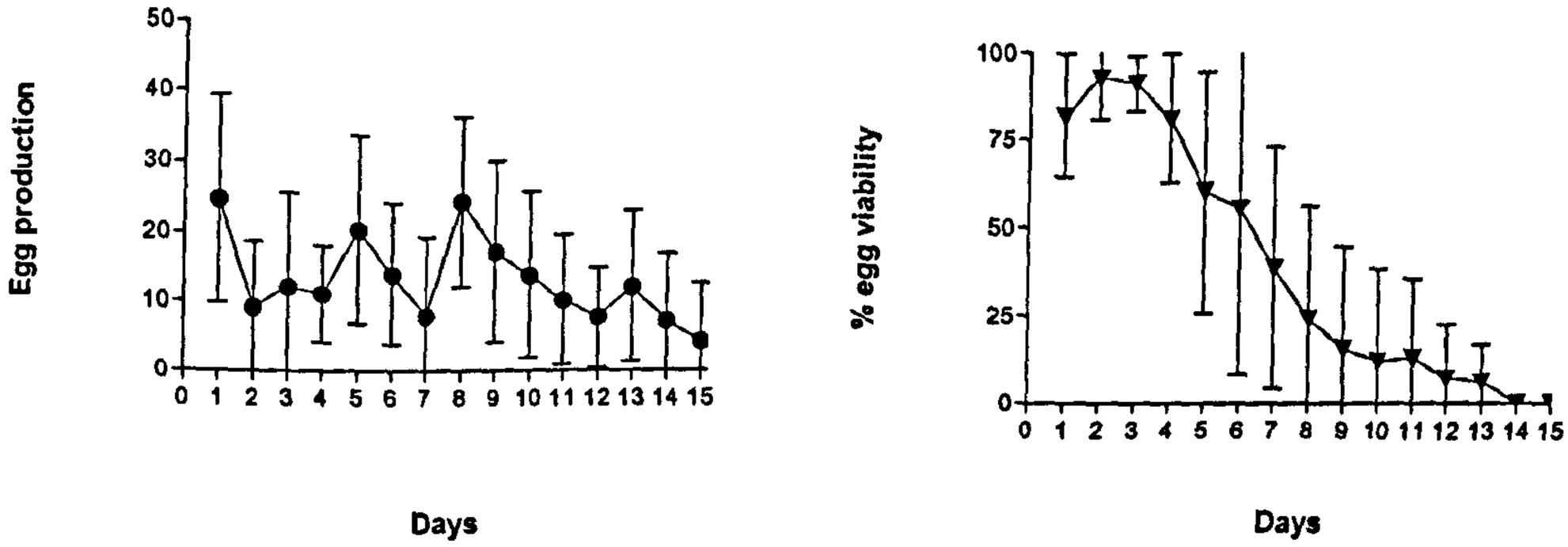

Figure 2.28: Laboratory experiments testing the effects of the diatom *P. delicatissima* on egg production rates (left) and hatching viability (right) in the copepod *C. helgolandicus*.

2.4.2 Structure elucidation of oxylipins

Axenic cultures of *P. delicatissima* were pelletted and extracted as already described. GC-MS analysis revealed the absence of short-chain aldehydes. The extract was methylated and analysed in RP-LCMS. The HPLC profile immediately showed the presence of 3 major peak components (Figure 2.29). The extract was successively fractionated on silica gel column by a polarity gradient system (Et_2O in petroleum ether).

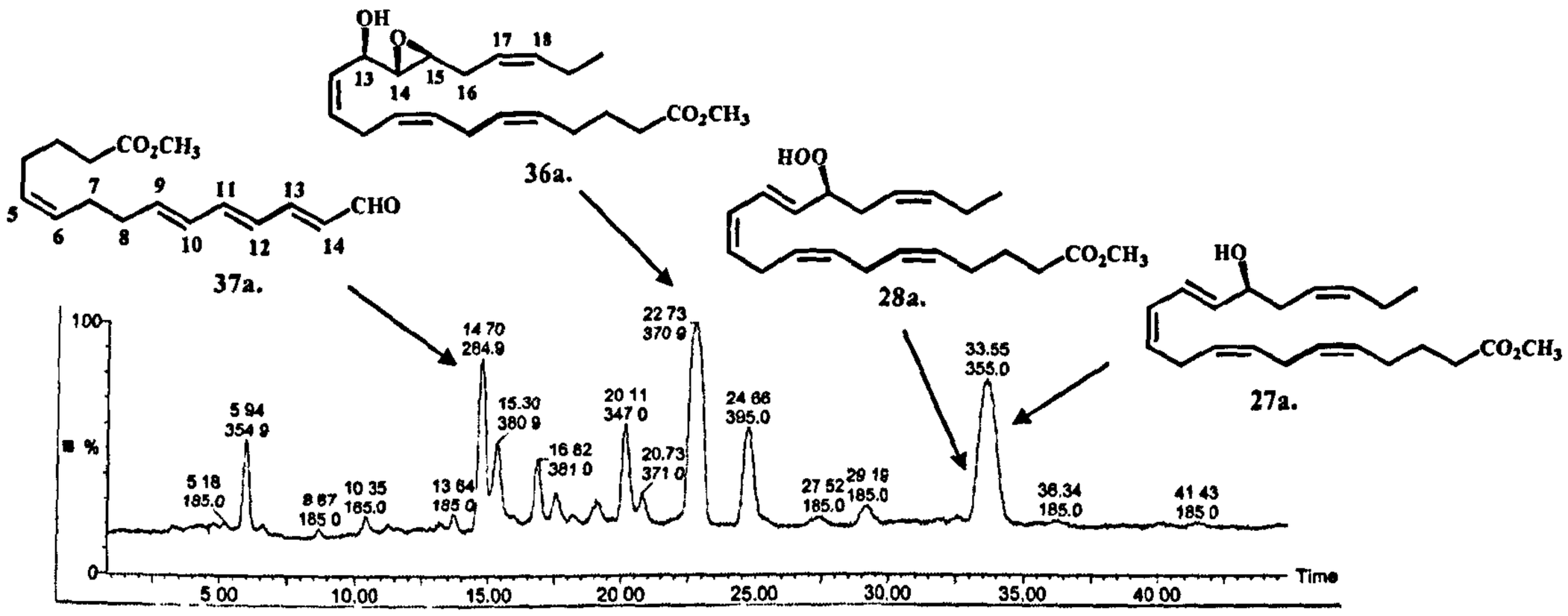

Figure 2.29: ESI$^+$ LCMS profile of oxylipins from methylated extracts of *P. delicatissima*

Each fraction was analyzed by NMR and LCMS, and when required, the fractions were ulterior purified on RP-HPLC. ESI$^+$-MS and NMR spectra of the major compound was identical to that of 15-HEPE (**27a**) previously characterized from extracts of *S. costatum*. The absolute stereochemistry of this metabolite was established as *S* on the basis of the product elution on chiral HPLC, using 15(*R*,*S*)-HEPE and 15(*S*)-HEPE as authentic standards.

Due to the great instability of **28a**, 15-hydroperoxyeicosapentaenoic acid (15-HPEPE), it was not possible to purify a sufficient amount of the product for the NMR analysis. The presence of this metabolite in the extract was however confirmed by ESI$^+$ MS that showed a molecular ion at *m/z* 371 ($M+Na^+$). This MS peak disappeared after the reduction of the extract with TMP. As in *S. costatum*, the peak corresponding to 15-HPEPE was coeluted with that of 15-HEPE in RP-HPLC, giving rise to a large peak with a retention time of 33.5 min (Figure 2.30) with a *m/z* of 355 and 371.

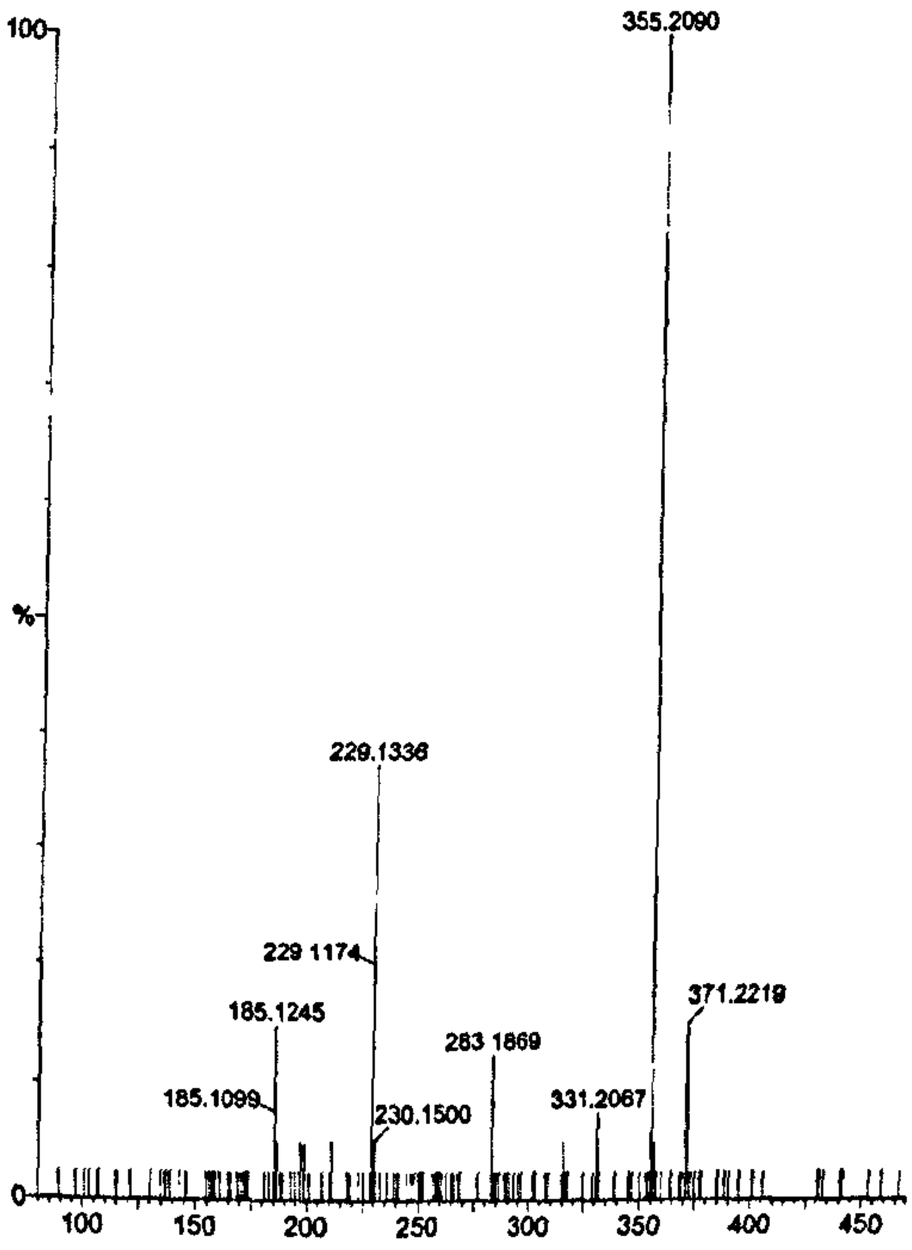

Figure 2.30: ESI^+/MS spectra of RP-LCMS peak eluted at 33.5 min, showing the *m/z* peak (355) corresponding to 15-HEPE methyl ester and the *m/z* peak (371) corresponding to 15-HPEPE methyl ester.

Peak of compound **36a** exhibited UV absorbance (λ_{max}=210 nm) and ESI^+-MS pseudomolecular ion (*m/z* 371.19 for $[C_{21}H_{32}0_4+Na]^+$) indicative for a di-oxygenated derivative of EPA methyl ester. ^{1}H-NMR spectrum of this material after purification showed the typical signal of one hydroxylated methine group (H-13, δ 4.27) (Figure 2.31).

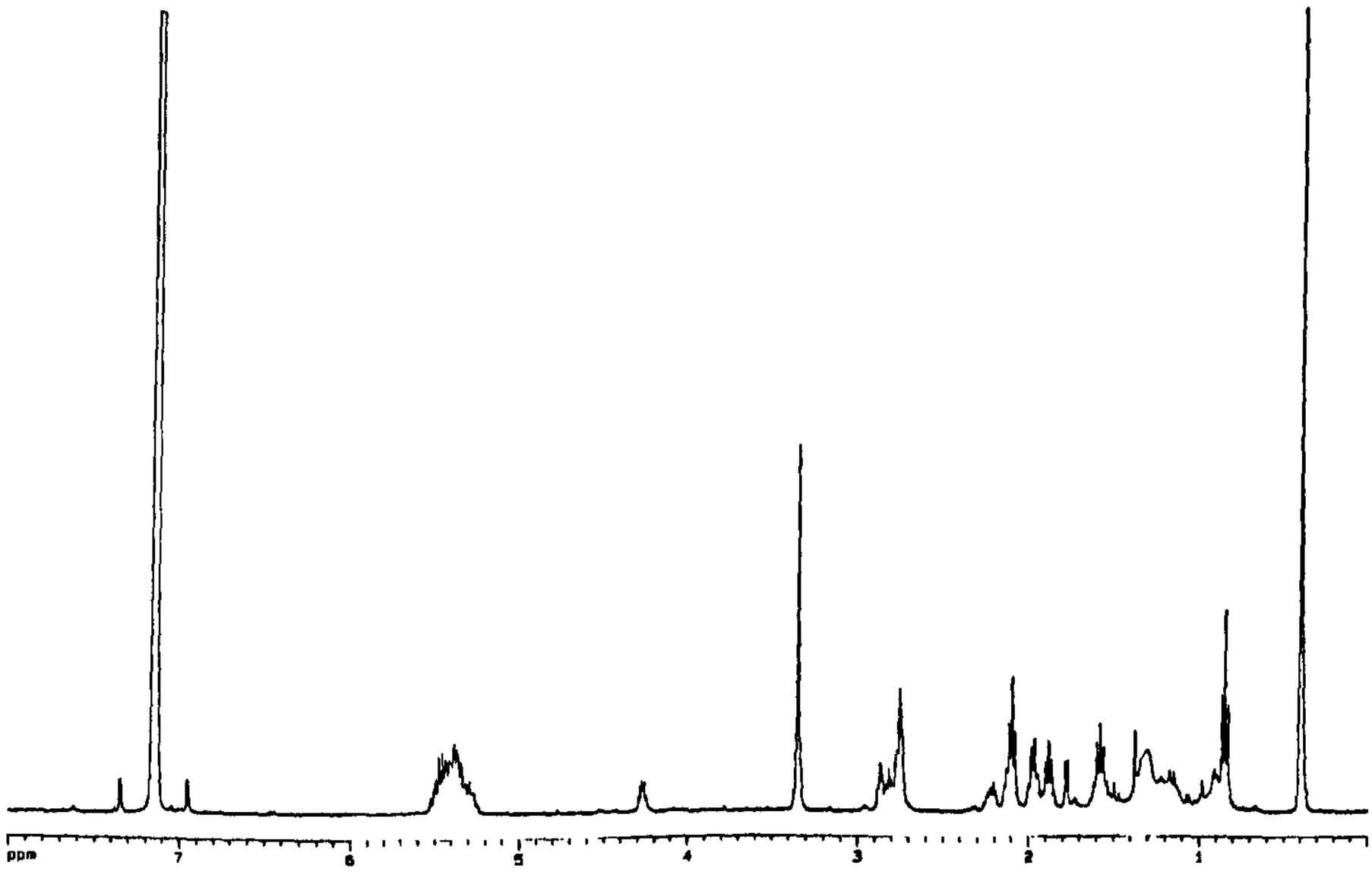

Figure 2.31: ^{1}H-NMR of 13-hydroxy-14,15-epoxyeicosa-5*Z*,8*Z*,11*Z*,17*Z*-tetraenoic acid methyl ester (**36a**) from *P. delicatissima*.(C_6D_6, 600 MHz).

In the COSY spectrum this resonance was correlated to one olefinic proton (H-12) δ 5.50 and to one proton (H-14 δ 2.74) on an oxygenated carbon (C-14 60.3 ppm). The chemical shift of C-15 was diagnostic for epoxide moiety, whose spin system was assigned by the signals of C-15 (56.0 ppm) and H-15 (δ 2.88). This latter proton in the COSY spectrum was further coupled to two methylene protons at δ 2.21 and δ 2.11 in α position to double bond (H-17 δ 5.35; H-18 δ 5.44). All the remaining signals were unambiguously assigned, on the basis of the connectivities observed in the homonuclear (COSY and TOCSY) and heteronuclear (HSQC and HMBC) 2D-NMR spectra, to 13-hydroxy-14,15-epoxyeicosa-5*Z*,8*Z*,11*Z*,17*Z*-tetraenoic acid methyl ester. Furthermore, the chemical structure was confirmed by ESI-MS/MS spectra containing fragments ions corresponding to the breaking of the epoxide moiety (loss of $C_6H_{10}^+$, M-82$^+$; loss of $C_6H_{10}O^+$, M-98$^+$) and between the epoxide and alcohol functions (loss of $C_7H_{12}O^+$, M-112$^+$), as showed in the Figure 2.32.

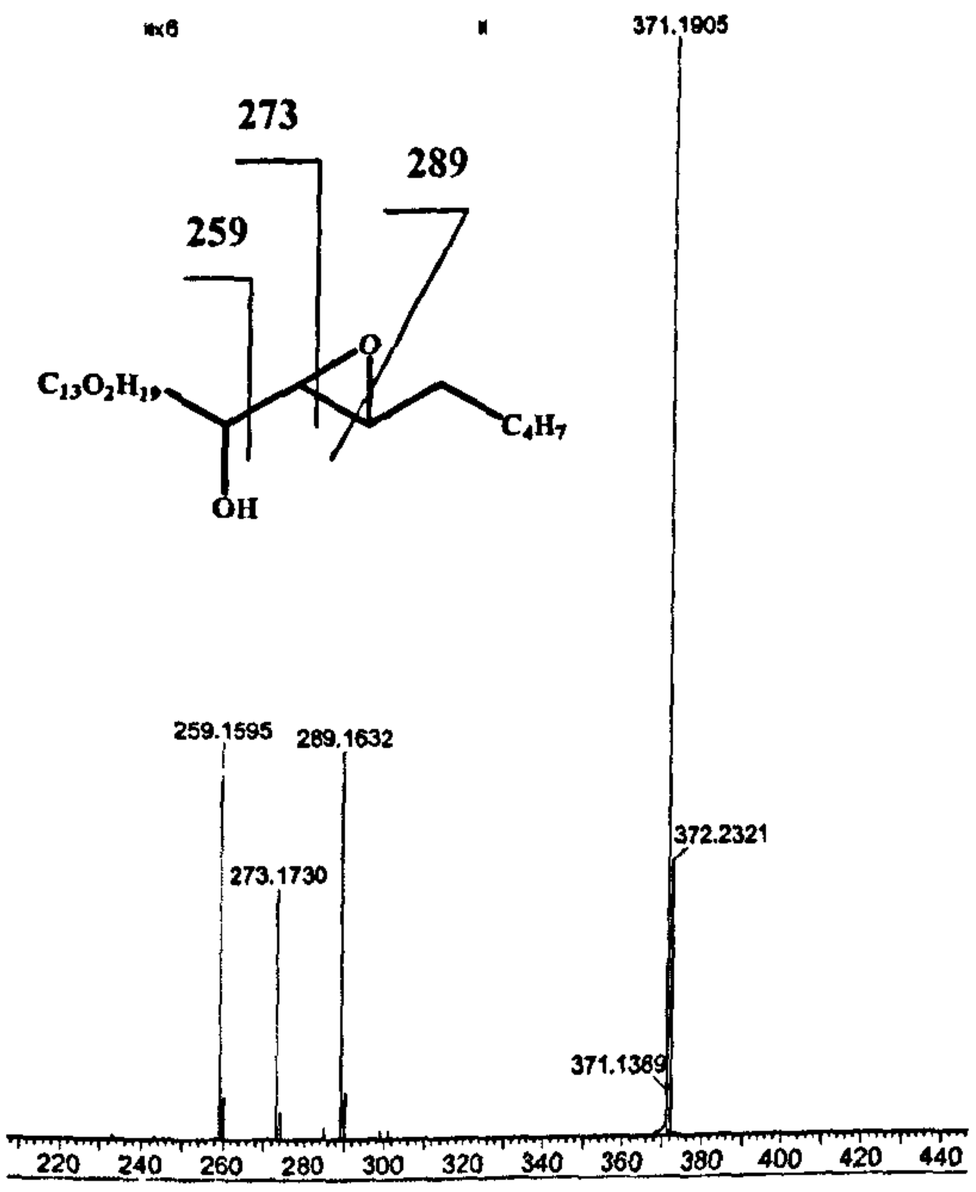

Figure 2.32: ESI$^+$-MS/MS spectrum of 13-hydroxy-14,15-epoxyeicosa-5*Z*,8*Z*,11*Z*,17*Z*-tetraenoic acid **(36a)** from *P. delicatissima*.

The main stereochemical features of the product were established by ^{1}H-NMR. The *trans* configuration of the 14,15 epoxide was established on the basis of the coupling constant $J_{14,15}$= 1.9 Hz (the coupling costant of *cis* epoxide is 4-5 Hz). The relative *threo*

configuration was assigned on the basis of the coupling constant measured between the α-hydroxyl group and the epoxide moiety (Mercier & Agoh, 1974) ($J_{13,14}$ = 7.46 Hz in *threo* product, $J_{13,14}$= 2.7 Hz in *erythro*). The absence of reference compounds prevented the determination of the absolute stereochemistry, even if it eluted as a single enantiomer on chiral-HPLC.

Compound **37a** showed a pseudomolecular ion in the ESI$^+$MS spectrum at *m/z* 284.9 accounting for a molecular formula $C_{16}H_{22}O_3$+Na^+. The strong UV maximum at 318 nm clearly indicated the presence of a highly conjugated carbonyl system. In particular, on the basis of the correlations observed in the COSY and TOCSY spectra it has been possible to assign the entire spin system from the aldehydic proton at δ 9.4 to the protons of three conjugated double bonds (H-14 δ 5.95; H-13 δ 7.04; H-12 δ 5.64; H-11 δ 6.1; H-10 δ 6.46; H-9 δ 5.84). The signal at 5.84 ppm (H-9) was also coupled to methylene protons at δ 2.0 in turn coupled to signals at δ1.94 in α position to the double bond H-6/H-5. The presence of two additional allylic groups in the ^{1}H NMR spectrum together with correlation data contained in homo and heteronuclear 2D NMR experiments allowed for the build up of the structure of 15-oxo-5*Z*,9*E*,11*E*,13*E*-pentadecatetraenoic acid.

2.4.3 Incubation experiments with $^3H_{10}$-EPA

All the products identified in the diatom *P. delicatissima* should derive from a 15-LOX pathway starting from EPA. To test this hypothesis, 1 μCi of $^3H_{10}$-EPA was incubated with cell homogenates of the diatom for 20 min at room temperature. The incubation mixture was extracted and methylated. An aliquot of the extract was reduced with TMP. The untreated and the reduced extract were injected on RP-HPLC coupled with a radiodetector, obtaining no substantial variations in the labelling values.

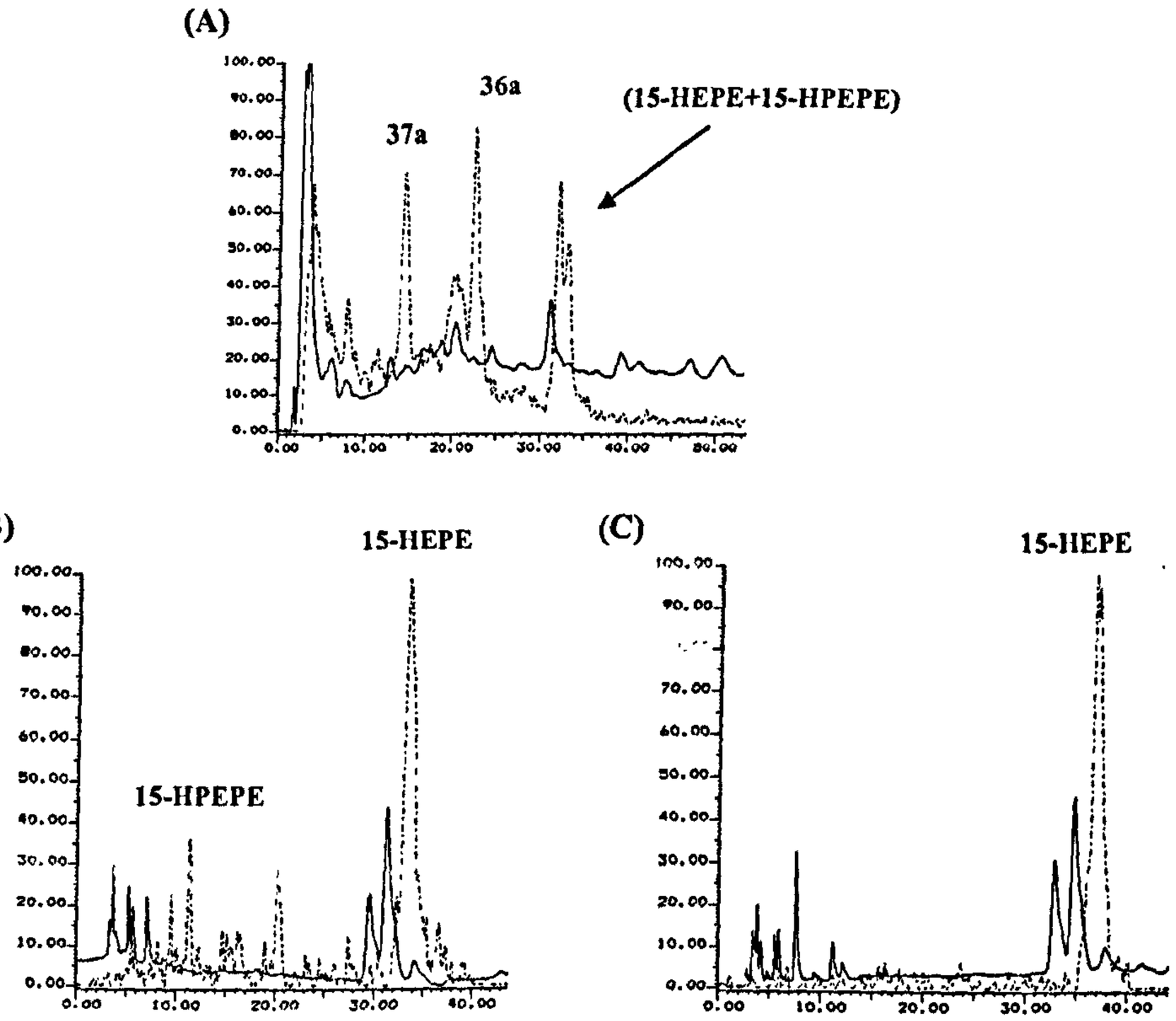

Figure 2.33: Incorporation of $^{3}H_{10}$ EPA in cell homogenates of *P. delicatissima*. The bold line indicate the HPLC profile at 210nm. The dashed line indicate the radio profile obtained with a radiodetector coupled to the HPLC. (A) RP-HPLC chromatogram of total extract. (B) SP-HPLC chromatogram of untreated mixture of 15-HEPE and 15-HPEPE. (C) SP-HPLC chromatogram of reduced mixture of 15-HEPE and 15-HPEPE.

The chromatograms revealed the clear labelling of 15-oxo-acid (T_R= 13 min, 464 cpm, 2.1%), 15-epoxyalcohol (T_R=22 min, 813 cpm, 3.7%) and 15-HEPE/15-HPEPE (T_R= 32 min, 3743 cpm, 17%) (Figure 2.33). Since 15-HPEPE and 15-HEPE were coeluted in RP-HPLC, the large peak corresponding to these oxylipins (T_R= 32 min) was collected either from TMP reduced and untreated extracts. Both fractions were injected on SP-HPLC (n-hexane/diethyl ether 85:15 v/v), leading to resolution of 15-HPEPE and 15-HEPE components. The radioactive analysis revealed the clear labelling of 15-HPEPE (T_R= 11 min, 279 cpm, 6.3%) and 15-HEPE (T_R=33 min, 1890 cpm 43%) in the untreated extract, and the unique labelling of 15-HEPE (T_R=33 min, 3537 cpm, 73.6%) in the reduced extract, showing the indirect labelling of 15-HPEPE in the cells.

2.5. The genus *Chaetoceros*

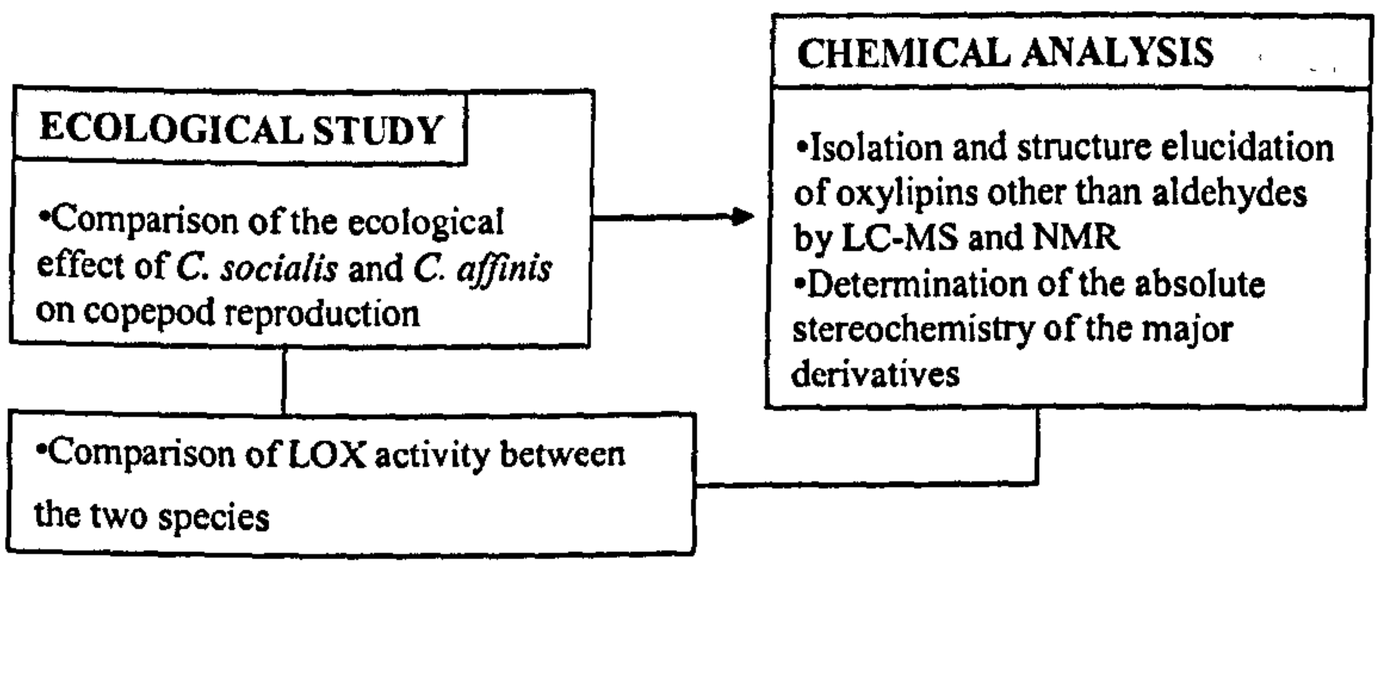

2.5.1. Effect of *C. socialis* and *C.affinis* on copepod reproduction

The effect of two diatom species belonging to the same genus, *C. socialis* and *C. affinis*, was tested on the reproduction and development of early larval stages of the calanoid copepod *T. stylifera*.

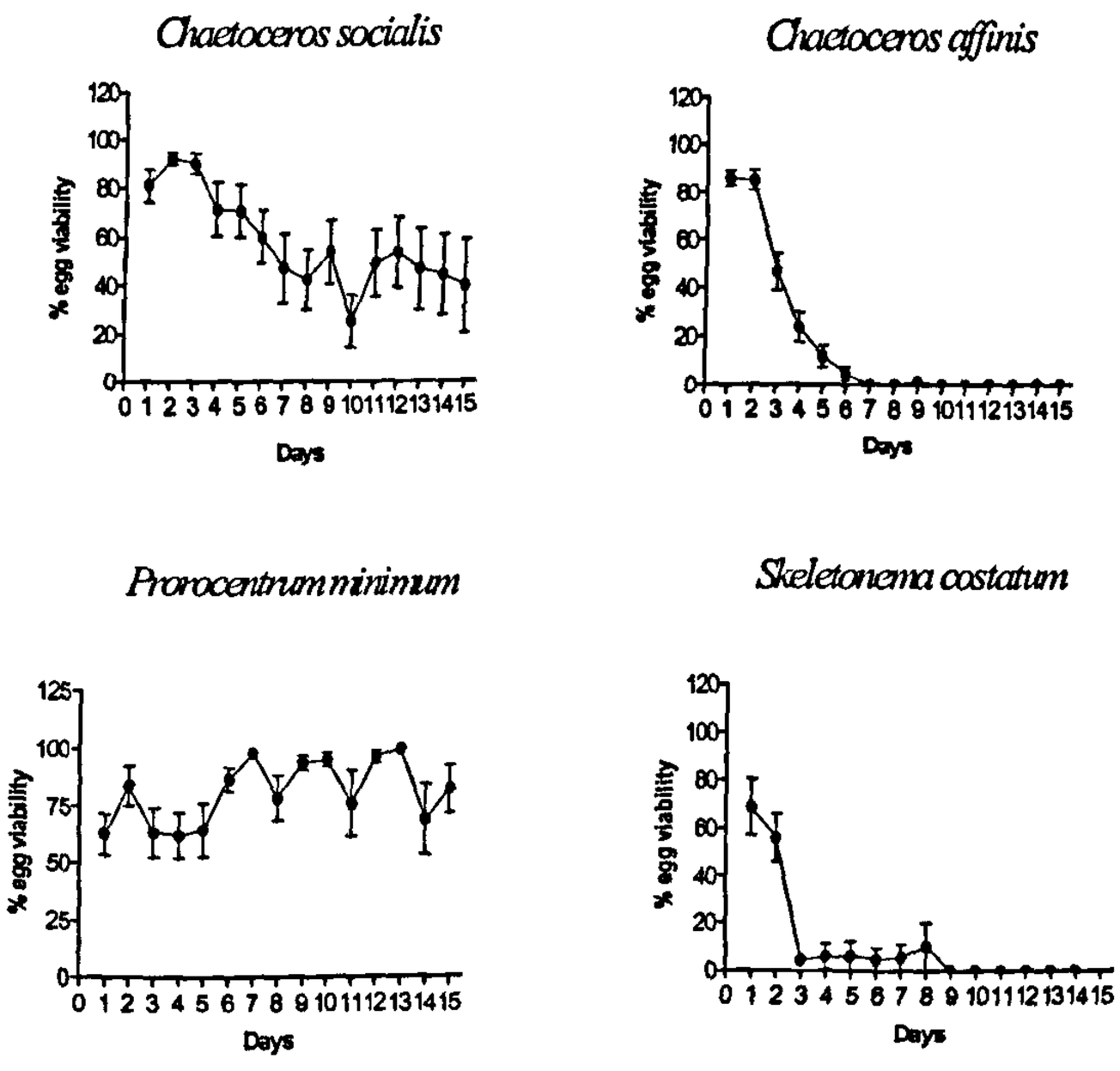

Figure 2.34: Effect of *C. socialis*, *C. affinis*, *P. minimum* and *S. costatum* on hatching success in *T. stylifera*.

The dinoflagellate *P. minimum* and the diatom *S. costatum* were used as negative and positive control, respectively. *C. socialis* did not affect copepod egg viability that remained high after 15 day experiments; no abnormal nauplii were generated with this diet. In contrast, with the *C. affinis* diet, copepod egg viability declined dramatically decreasing to

0% after the first week (Figure 2.34). The nauplii produced during experiments were assessed for morphological anomalies and for apoptosis (labelling techniques TUNEL) using confocal laser scanning microscope. TUNEL staining is a specific cytochemical reaction that labeled the ends of DNA fragments produced by apoptosis. Females reared with negative control diet produce only morphologically normal nauplii that showed a low value of fluorescence.

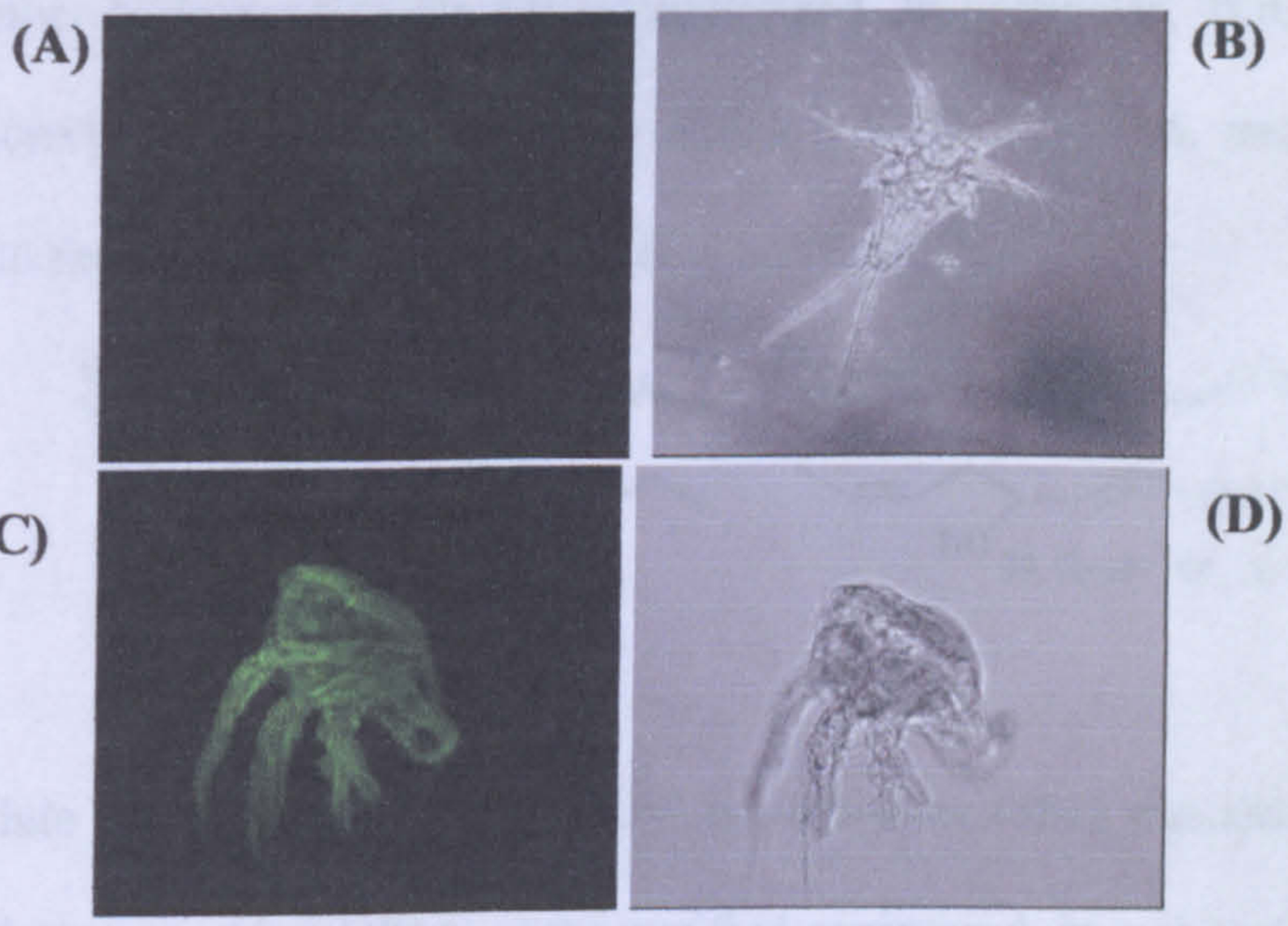

Figure 2.35: (A) and (B) Control copepod reared with *P. minimum*; (C) and (D) copepod reared with *C. affinis*. The images were obtained with a laser confocal microscope; copepods in (A) and (C) were stained with TUNEL.

Nauplii produced by females reared with positive control diet displayed strong morphological anomalies and wide apoptotic areas. Nauplii produced by females reared with *C. affinis* showed incomplete development of swimming appendages with segments that differed from normal both in number and shape. The fluorescent light image of the same specimen showed apoptotic areas corresponding to these morphological anomalies (Figure 2.35 D).

2.5.2. Oxylipins in *C. socialis* and *C. affinis*

GCMS analysis of derivatized extracts showed the absence of aldehydes in both species. The LCMS of methylated extracts showed the main presence of two hydroxyacids, 9-

hydroxy- 5*Z*,7*E*,11*Z*,14*E*,17*Z*-eicosapentaenoic acid (9-HEPE) (**38a**) in *C. socialis*, and 14-hydroxy-5*Z*,8*Z*,11*Z*,15*E*,17*Z*-eicosapentaenoic acid (14-HEPE) (**39a**) in *C. affinis*. The peaks of the compounds **38a** and **39a** exhibited UV absorbance (λ_{max}=236 nm) and ESI$^+$-MS pseudomolecolar ion (*m/z* 355.2 for $[C_{21}H_{32}O_3+Na]^+$ indicative for a hydroxyderivatives of EPA methyl ester. Complete structure assignments were obtained on the basis of the COSY connectivities and TOCSY spectrum, and in analogy with NMR data of other hydroxyacids already characterized. In particular, TOCSY spectra revealed all the correlations from the hydroxy-function to H-3 in **38a**, and from the hydroxy-function to the terminal methyl in **39a** (data not shown).

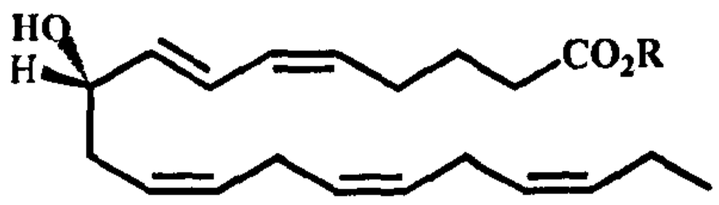

38. R=H; **38a.** R=Me

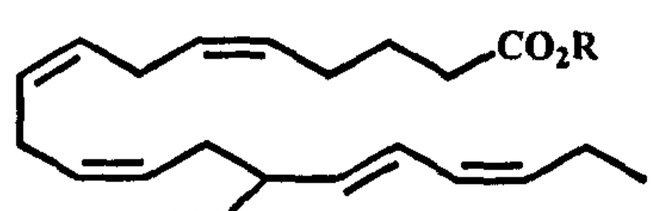

39. R=H; **39a.** R=Me

The absolute stereochemistry of 9-HEPE methyl ester (**38a**) was determined as *S* on the basis of elution on chiral-HPLC of the purified compound, in comparison with commercial 9(*R*,*S*)-HEPE and 9(*R*)-HEPE. Due to the absence of reference compounds, the absolute stereochemistry of 14-HEPE methyl ester (**38a**) was not determined, even if **38a** eluted as single enantiomer on chiral-HPLC.

2.5.3. Comparison of LOX activity between the two species.

Lipoxygenase activity in *C. socialis* and *C. affinis* cell homogenates was determined using a rapid and sensitive colorimetic assay, in agreement with Anthon and Barrett (2001). The assay is based on the detection of the lipoxygenase reaction products, fatty acid hydroperoxides, by the oxidative coupling of 3-methyl-2-benzothiazolinone (MBTH) with 3-(dimethylamino) benzoic acid (DMAB) in a haemoglobin catalyzed reaction.

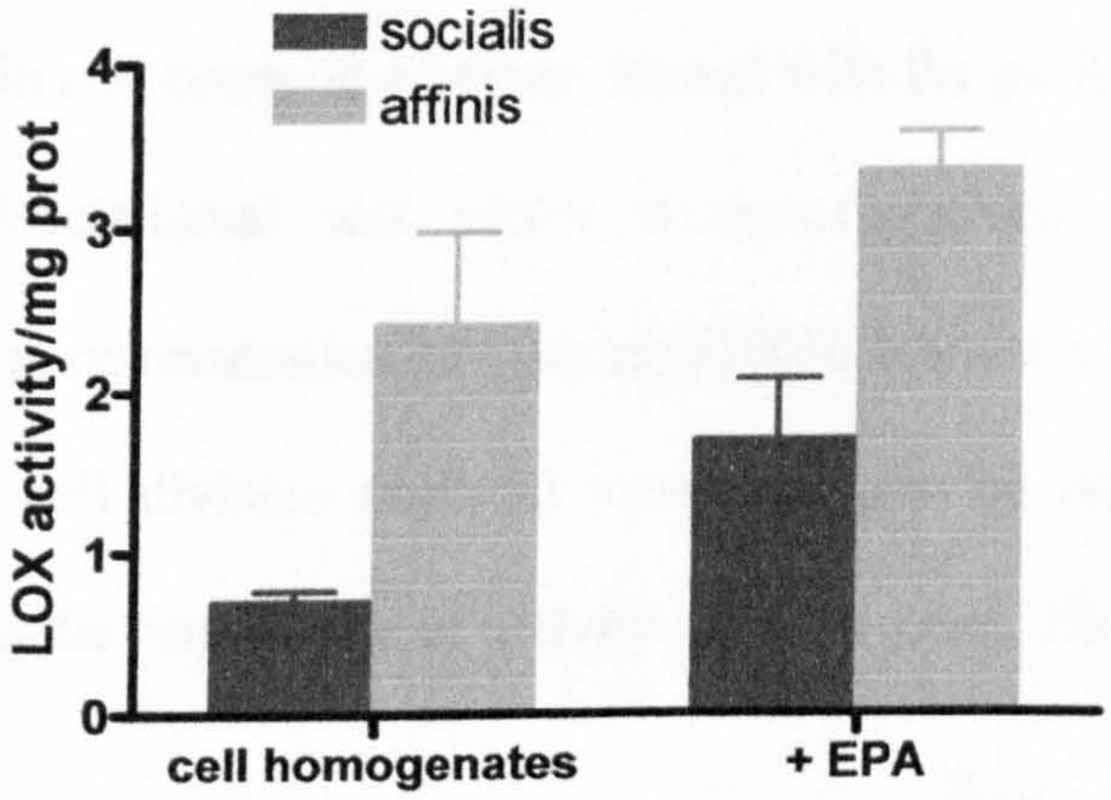

Figure 2.36: LOX activity expressed as Δ_{598}/mg protein in *C. affinis* and *C. socialis* homogenates in absence and in presence of EPA as exogenous substrate.

Lipoxygenase activity is almost 3 times higher in *C. affinis* than in *C. socialis*, both in the absence and presence of the exogenous substrate (EPA) (Figure 2.36).

2.6. Antimitotic assay of oxylipins

To detect the compounds responsible of the antiproliferative effet of diatoms on copepod reproduction, a test of antimitotic activity on sea urchin embryos of *Paracentrotus lividus* was used. The extracts blocked the division at concentration ranging from 25 to 100 µg/ml. The effect of diatom extracts on sea urchin embryos is the result of the action of various and differently active molecules. The treated embryos in fact were blocked in a dose-dependent manner and among them, some undergo to apoptosis, estimated by the analysis of morphological changes as cell blebbing and nuclear disorganization, and some other show cell swelling identical to that induced in the same kind of assay by free fatty acid, due to the alteration of cell membrane integrity and stability.

After a first fractionation on silica gel, the antimitotic assay identified two main active fractions recognized as aldehydes and oxylipins in *T. rotula* and *S. costatum*, and only oxylipins in *P. delicatissima*, *C. socialis* and *C. affinis* which lacked of PUAs. The purified aldehydic pools from both *T. rotula* and *S. costatum* were able to inhibit the cleavage of sea urchin embryos (100% inhibition) at concentration of 0.75 µg/ml for the first and 1 µg/ml for the latter diatom (Figure 2.37), and to induce apoptosis as already demonstrated

in sea urchin and copepod embryos treated with the purified aldehydes. Among aldehydes, natural 2,4-octadienal was active at concentrations of 1.3 μg/ml, commercial 2,4-decadienal at concentration of 1 μg/ml (100% inhibition), and the saturated tridecanal did not inhibit cell division until 50 μg/ml, suggesting that the reactive Michael-acceptor element was the responsible of activity (Adolph *et al.*, 2003)

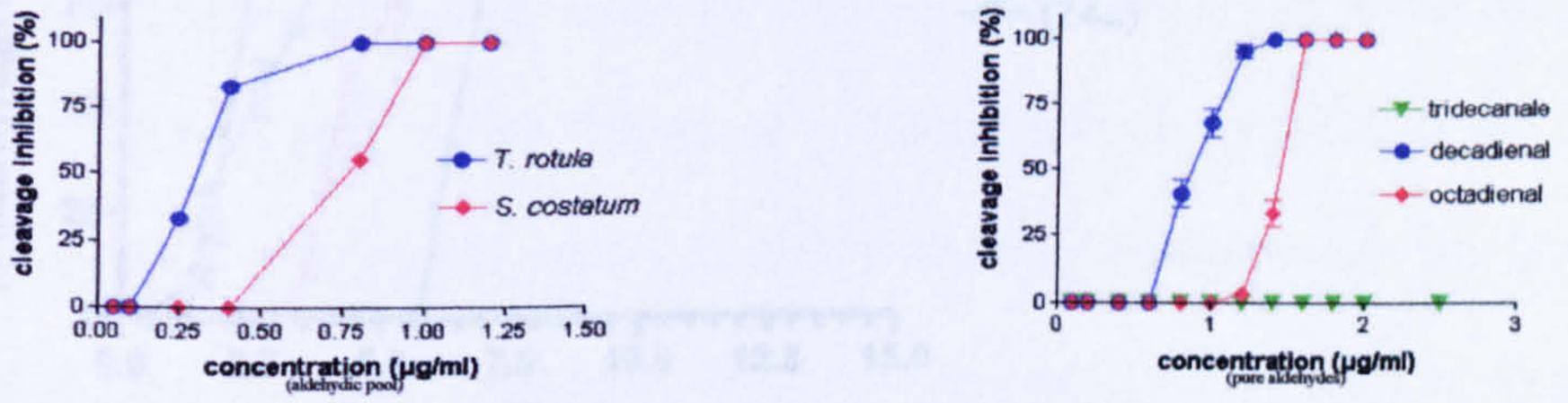

Figure 2.37: Effect of the aldehyde mixture obtained from *S. costatum* and *T. rotula* on the first division of sea urchin eggs (left). Effect of purified decadienal, octadienal and tridecanal in the same assay (right).

The active oxylipin fractions induced effects similar to that observed in assays with the extracts. The oxylipin fractions were active at concentrations ranging from 5 to 50 μg/ml. For example the pure oxylipin pool isolated from *C. affinis* was able to induce 100% of blockage at concentration of 8 μg/ml, while the oxylipin fraction from *C. socialis* induced the total block at concentrations of 50 μg/ml (Figure 2.38).

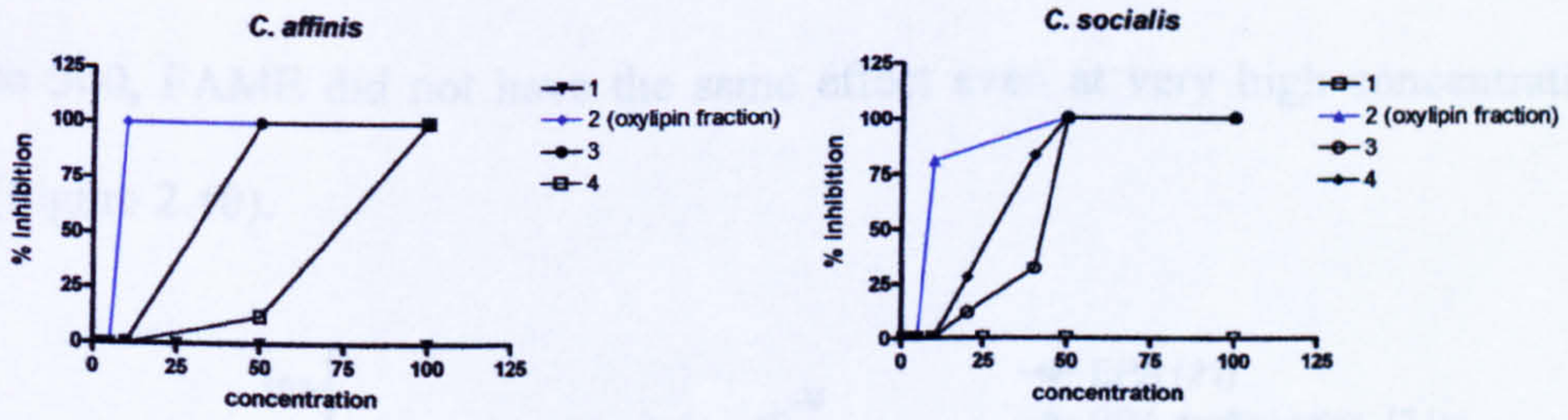

Figure 2.38: Bioactivity guided screening on purified fractions from methylated extracts of *C. socialis* and *C. affinis*. 1,2,3,4 represented fractions obtained from silica gel column in a gradient from petroleum ether to petroleum ether/diethyl ether 10/90.

Some pure oxylipins were initially tested as methylated molecules, since they were purified in this form after methylation of the extracts. In particular, the hydroxyacid 15(*S*)-HEPE (**27a**) inhibited cell division at concentration 3.3 μM, and it was more active than decadienal (4.95 μM). The ketoacid 6-KHTE (**31a**) induced the same effect at

concentration 6.3 μM. The 9-keto-7*E*-hexadecanoic acid (**24a**) blocked cell division at concentration 7 μM, whereas the correspondent 9-hydroxy-7*E*-hexadecanoic (**25a**) was active at concentration 53 μM (Figure 2.39).

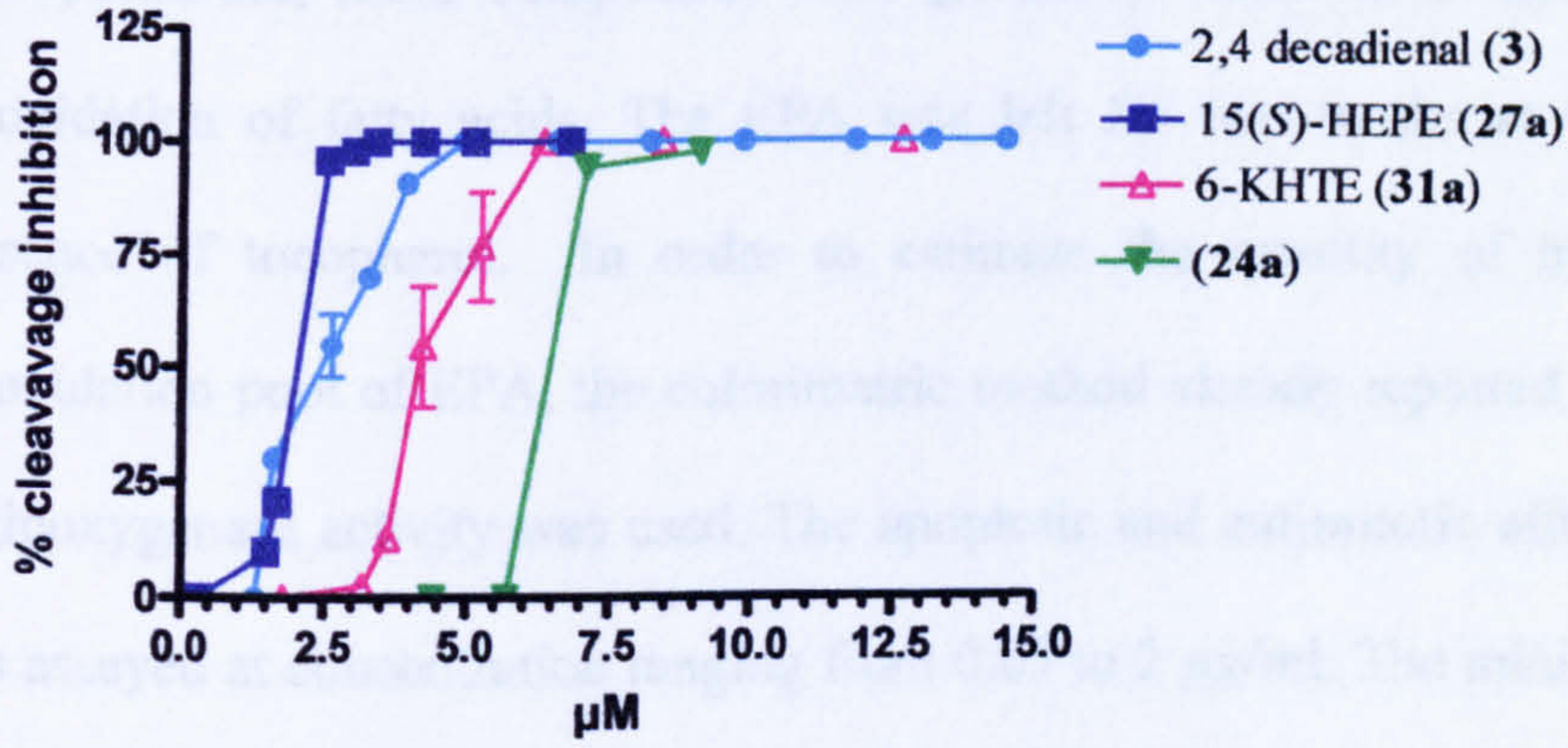

Figure 2.39 Effect of methylated 15(*S*)-HEPE (**27a**), 6-KHTE (**31a**), 9-keto-7*E*-hexadecanoic acid (**24a**) on the cleavage of sea urchin embryos, in comparison with 2,4-decadienal.

The epoxyalcohol (**36a**) isolated from *P. delicatissima* was not active at concentrations from 0.7 to 20 μM Surprisingly, the same metabolites active as methyl ester lost their antimitotic activity after hydrolysis at concentrations ranging from 0.7 to 30 μM. It is important to note that the influence of methylation on the molecule activity is opposite in FFAs. In fact, whereas FFAs had an antimitotic effect at concentrations ranging from 100 to 300, FAME did not have the same effect even at very high concentrations (300 μM) (Figure 2.40).

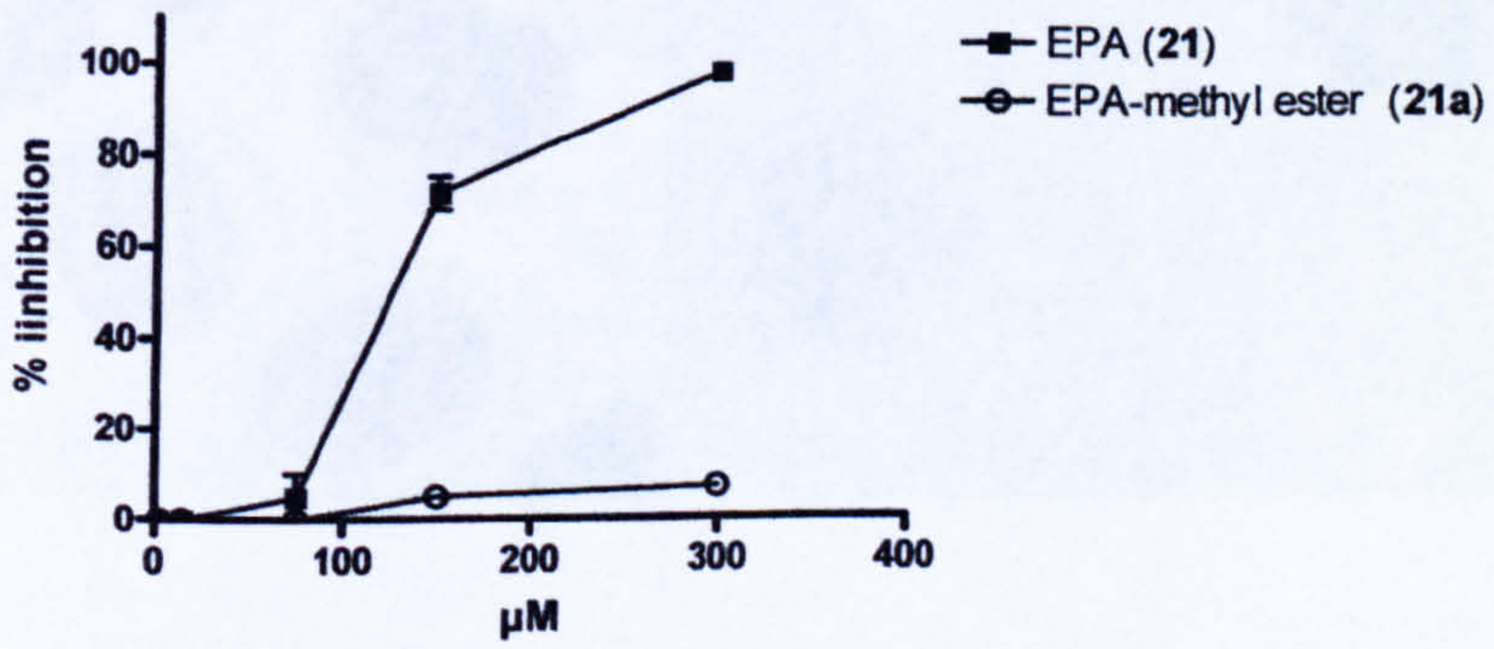

Figure 2.40: Effect of EPA and EPA methyl ester on the cleavage of sea urchin embryos.

In mammals and terrestrial plants, hydroperoxides, the primary intermediates in the biosynthesis of oxylipins, are reported as apoptotic agents (Knight *et al.*, 2001; Kalyankrishna *et al.*, 2002; Tang *et al.*, 2002). Due to the instability of pure hydroperoxides, these compounds were generally tested in a mixture obtained by the autoxidation of fatty acids. The EPA was left for two weeks at 42°C, in the dark, in presence of tocopherol. In order to estimate the quantity of hydroperoxides in the autoxidation pool of EPA, the colorimetric method already reported for the determination of lipoxygenase activity was used. The apoptotic and antimitotic effect of hydroperoxides was assayed at concentration ranging from 0.05 to 2 μg/ml. The minimal dose required for total block of mitotic events is 0.9 μg/ml of hydroperoxides. The apoptotic effect was evaluated morphologically using an inverted microscope observing the arising of membrane and cellular blebbing in treated sea urchin embryos. As shown in Figure 2.41B, treated embryos did not undergo to cell cleavage (control embryos in figure 2.41A), and they remained blocked at zigote stadium, presenting therefore a total block of mitosis that precede induction of apoptosis. The embryos were totally destroyed presenting various degree of vesciculation and cell fragmentation typical of the final steps of apoptosis

(A) **(B)**

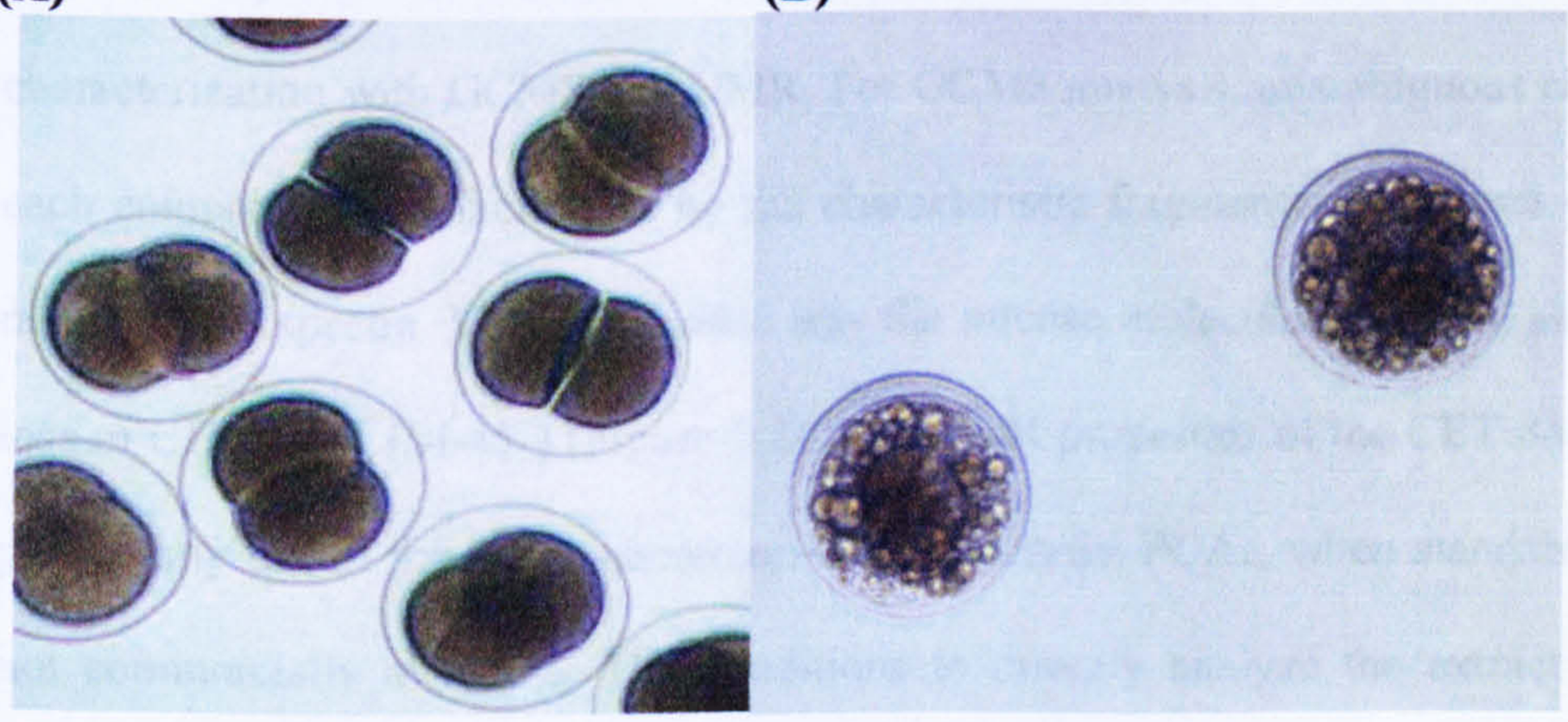

Figure 2.41: (A) Control sea urchin embryos at two blastomere stage, 90 minutes after fertilization; (B) embryos treated with 0.25 μg/ml of hydroperoxides, 90 minutes after fertilization. They were blocked at zygote stage and presented cell fragmentation following the blebbing, typical of the final stage of apoptosis.

3. DISCUSSION

3.1. Chemistry

After the isolation of C_{10} aldehydes using a large-scale purification approach (Miralto *et al.*, 1999), studies focused on the analysis of volatile compounds in diatoms. Aldehyde-containing compounds are generally very unstable and prompt to decompose, thus aldehydes are generally analyzed in GCMS after transformation into more stable products (Vogel *et al.* 2000; Schulte-Ladbeck *et al.* 2001). In the literature, different methods have been introduced to analyze these volatile molecules in diatoms. A sensitive protocol with the use of solid-phase microextraction (SPME) allowed rapid screening for the production of volatiles from small culture samples (Pohnert, 2000). This method, however, does not allow samples to be stored or derivatized, so structural elucidation is limited to metabolites that are available as reference compounds.

For the analysis described in this thesis, an alternative procedure based on the conversion of aldehyde into ethyl ester by Wittig reaction with (Carbethoxyethylidene)-triphenylphosphorane was developed (Scheme 2.1) (d'Ippolito *et al.*, 2002b). This method is useful to improve the stability of the derivatives, allowing their purification and unequivocal characterization with GCMS and NMR. For GCMS analysis, unambiguous characterisation of each component was facilitated by the characteristic fragmentation pattern of the high mass range in MS spectra. Very diagnostic was the intense molecular ion (M^+) and ion formed by loss of $CH_3CH_2O^\bullet$ ($M\text{-}45^+$) (Figure 2.2). The NMR properties of the CET derivatives resulted particularly useful for the characterization of unknown PUAs, when standard compounds are not commercially available. The conditions to directly analyze the extract in GCMS were assessed for routine analysis.

Using this method, the presence of aldehydes was tested in the diatoms *S. costatum*, *T. rotula*, *P. delicatissima*, *C. socialis* and *C. affinis*. As summarized in the Table 3.1, *T. rotula*, in

addition to the unsaturated C_{10} compounds 2*E*,4*Z*,7*Z*-decatrienal (**1**), 2*E*,4*E*,7*Z*-decatrienal (**2**) already described by Miralto *et al.* (1999), contained aldehydes with eight carbon atoms, 2*E*,4*Z*/2*E*,4*E*-octadienal (**13/14**), 2*E*,4*Z*,7/2*E*,4*E*,7-octatrienal (**15/16**), and 2*E*,4*Z*/2*E*,4*E*-heptadienal (**17/18**) with a C_7 skeleton (d'Ippolito *et al.*, 2002b). Unlike previously reported by Miralto *et al.*, (1999), 2,4 decadienal (**3**) was absent in this strain of *T. rotula*. In *S. costatum*, the aldehydic pool was resolved in 2*E*,4*Z*/2*E*,4*E*-octadienal (**13/14**) (the main components), 2*E*,4*Z*/2*E*,4*E*-heptadienal (**17/18**), and 2*E*,4*Z*,7/2*E*,4*E*,7-octatrienal (**15/16**) (d'Ippolito *et al.*, 2002a). The mixture of CET derivatives also contained a variety of saturated and monounsaturated compounds, including tridecanal, 8-pentadecenal and pentadecanal. In contrast to that already reported (Miralto *et al.*, 1999) this diatom interestingly lacked C_{10} aldehydes, suggesting a certain degree of diversity from the process observable in *T. rotula*. It is worth noting that 2-*trans*-4-*trans* isomers were significantly predominant over the corresponding 2-*trans*-4-*cis* analogues. Since the derivatization procedure did not cause *Z*/*E* isomerization, this may be due to the extraction of the sample. However, the 4-*trans*/4-*cis* ratio was rather variable in different preparations suggesting that the process might be due to a non-enzymatic mechanism.

	T. rotula	*S. costatum*	*P. delicatissima*	*C. socialis*	*C. affinis*
 **2,4,7 decatrienal (1)**	+	–	–	–	–
 **2,4 octadienal (13)**	+	+	–	–	–
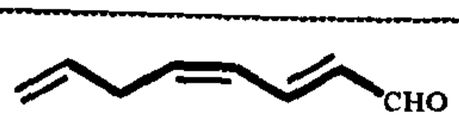 **2,4 octatrienal (15)**	+	+	–	–	–
 **2,4 heptadienal (17)**	+	+	–	–	–

Table 3.1: Distribution of short-chain polyunsaturated aldehydes in *T. rotula*, S. *costatum*, *P. delicatissima*, *C. socialis* and *C. affinis*. For simplicity, only the isomers 2*E*,4*Z* are reported.

P. delicatissima was shown to have an ecological effect on copepod reproduction similar to that already described for *T. rotula* (Figure 2.28). But interestingly, although *P. delicatissima* was reported as a producer of 2,4,7-decatrienal and 2,4-decadienal (Miralto *et al.*, 1999), our strain did not contain PUAs. In the same way, *C. socialis* and *C. affinis* lacked any of the aldehydes identified in *T. rotula* and *S. costatum*.

This implies that not every diatom has the metabolic capacity to carry out synthesis of aldehydes, in agreement with the recent paper in which 71 diatom strains belonging to 50 species were analyzed for PUA formation upon cell damage by sonication (Witchard *et al.*, 2005). Of these, 27 PUA producers were identified. So, more than half of the investigated species did not produce aldehydes. In the light of the ongoing discussion about the influence of diatoms on copepods, this result stressed that a general aldehyde-mediated effect cannot be assumed for any given diatom, but that a species and strain-specific analysis is required.

Moreover, a deep chemical analysis revealed that oxylipin pathways in marine diatoms can be more complex, and that the aldehydes could be only a part of fatty acid derivatives produced by diatoms. In fact many other derivatives, such as hydroxyacids, oxoacids, ketoacids and epoxyalcohols were isolated and characterized using ESI^+-MS and NMR spectroscopy.

In particular, *T. rotula* revealed the presence of a series of products with 16 carbon atoms and oxidation at C-9, including two major derivatives 9-keto-7*E*-hexadecenoic acid (**24**) and 9-hydroxy-7*E*-hexadecenoic acid (**25**), 9(*S*)-HHTrE (**26**) and 9-HHTE (**33**). Also C_{16} derivatives with an oxidation at C-6 were isolated, characterizing 6-KHTE (**31**) and 6-HHTE (**32**) together with the 6-KHTrE (**34**) and the corresponding alcohol 6-HHTrE (**35**) (Table 3.2) (d'Ippolito *et al.*, 2005a). The single C_{20} derivative isolated from extract of *T. rotula* was 11-HEPE, indicating that the enzymatic activities of this diatom have a strong preference for C_{16} fatty acids.

	T. rotula	*S. costatum*	*P. delicatissima*	*C. socialis*	*C. affinis*
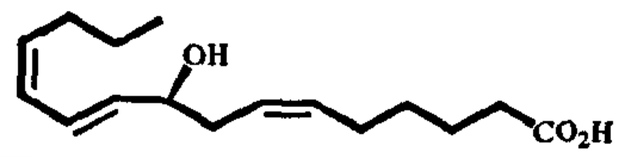	+	+	–	–	–
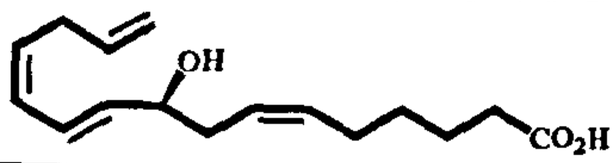	+	–	–	–	–
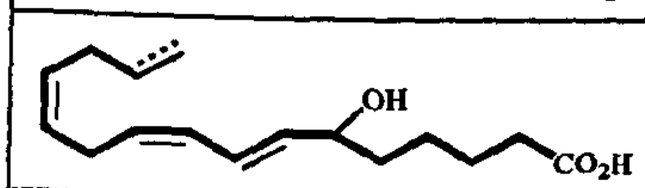	+	–	–	–	–
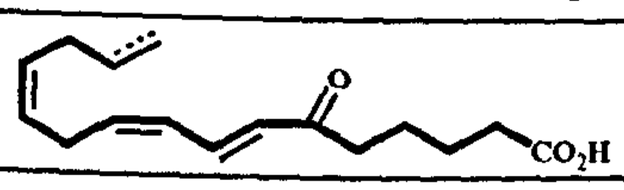	+	–	–	–	–
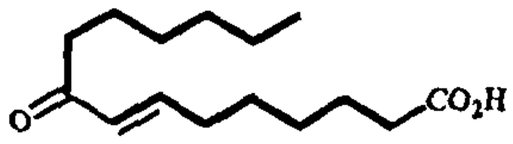	+	+	–	–	–
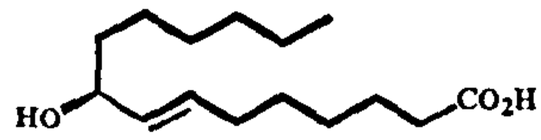	+	+	–	–	–
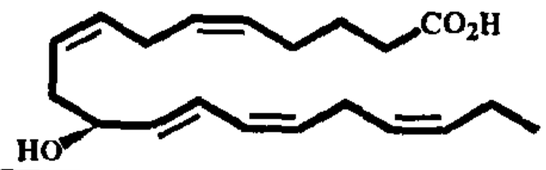	+	–	–	–	–
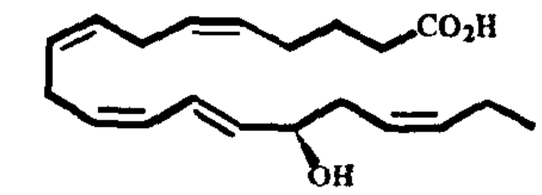	–	+	+	–	–
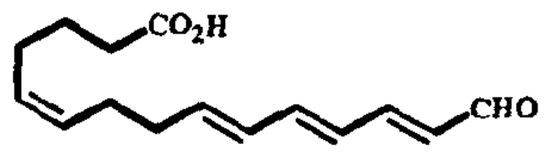	–	–	+	–	–
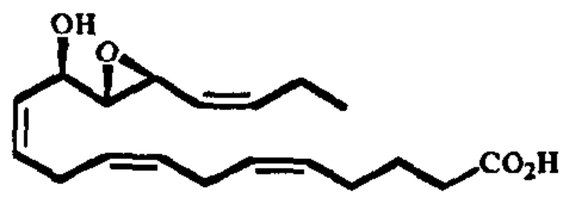	–	–	+	–	–
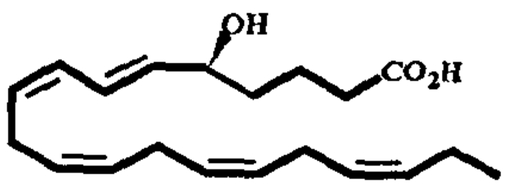	–	+	–	–	–
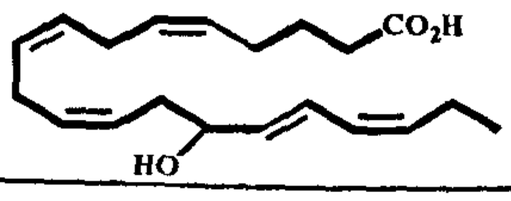	–	–	–	–	+
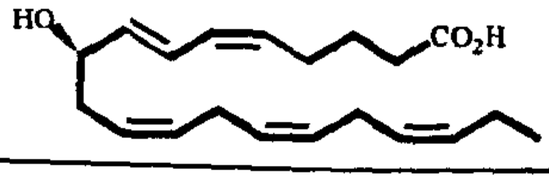	–	–	–	+	–

Table 3.2: Distribution of oxylipins other than PUAs in *T. rotula*, S. *costatum*, *P. delicatissima*, *C. socialis* and *C. affinis*.

The oxylipin profile of *S. costatum* was very similar to that already described for *T. rotula*. The essential difference with *T. rotula* was due to the lack of C_{16} derivatives with four

insaturations and of products derived from the oxidation at position C-6 of C_{16} fatty acids. In fact, in *S. costatum* the formation of C_{16} derivatives oxidized at position C-9 such as 9-keto-7*E*-hexadecenoic acid and 9(*S*)-hydroxy-7*E*-hexadecenoic acid and 9(*S*)-HHTrE was predominant. Interestingly, C_{20} hydroxyacids 5(*R*)-HEPE (**29**) and 15(*S*)-HEPE (**27**) were characterized.

In contrast with *S. costatum* and *T. rotula*, the other studied species did not show any occurrence of C_{16} derivatives, containing preferentially C_{20} derivatives. In fact, oxylipin profile of *P. delicatissima* revealed the presence of at least 3 compounds: 15-oxo-5Z,9*E*,11*E*,13*E*-pentadecatetraenoic acid (**37**), 15(*S*)-HEPE (**27**), 13(*R*)-hydroxy-14(*S*),15(*S*)-epoxyeicosa-5*Z*,8*Z*,11*Z*,17Z-tetraenoic acid (**36**). All these compounds were C_{20} derivatives, and the structural features suggested they could be produced by EPA. In the same way, two C_{20} hydroxyacids were characterized as main oxylipin products into two species of the genus *Chaetoceros*. In particular *C. socialis* was mainly characterized by the presence of 9(*S*)-HEPE (**38**), and *C.affinis* by 14-HEPE (**39**).

Since enzymes generally lead to the formation of chiral products, an important aspect in the characterization of the oxylipins of marine diatoms was the determination of the absolute stereochemistry of the final products to corroborate their enzymatic origin. The majority of characterized hydroxyacids showed an *S* configuration, and an elevated enantiomeric excess (e.e. 97-99 %). The hydroxyacids showing an *R* configuration were 5(*R*)-HEPE in *S. costatum* (e.e 74%) (Figure 2.14) and 11(*R*)-HEPE in *T. rotula* (e.e 12%) (Figure 2.18). The epoxyalcohol eluted as a single enantiomer on chiral HPLC, even if it was possible to define only its relative stereochemistry by ^{1}H-NMR. The stereochemistry of 9-hydroxy-7-hexadecenoic acid (**25a**) was determined on the basis of differences (δR-δS) in the ^{1}H chemical shifts of the diastereomeric α-trifluoromethyl benzyl silyl derivatives (*R*- and *S*-PhTFE) (Figure 2.13). The absolute stereochemistry of 9-HHTrE (**26**) was demonstrated by

applying of the strategy described in Scheme 2.4. 6-HHTE eluted as a single enantiomer using chiral HPLC but the absence of reference compounds did not allow for the determination of the absolute stereochemistry. The absolute stereochemistry of C_{20} derivatives was established by comparison with commercially available standards after elution on chiral HPLC. The chirality of these metabolites was the first direct demonstration that the process of formation of oxylipins in marine diatoms is enzymatic.

3.2. Biochemistry

Since α,β,γ,δ-unsaturated aldehydes produced by marine diatoms were correlated to the antiproliferative effect of diatoms on copepod reproduction, the key bio-organic aspects concern the clarification of the biosynthetic pathway leading to the formation of oxylipins and the regulating factors of the process. In fact, understanding the relationship between diatom lipids and oxylipins is important for several reasons. First, it can serve for the characterization of the enzymes or proteins involved in the biosynthetic pathway, permitting the development of a molecular approach to study field and lab samples. Second, in absence of the genetic and biochemical data, it aids in building up a model of the biochemical processes necessary to address a number of points concerning the physiological and ecological significance of these molecules.

3.2.1. Biosynthesis of oxylipins

In plant, algal and animal kingdoms, structurally related unsaturated aldehydes are known to be break-down products from the oxidative transformation of fatty acids (Gerwick, 1994; Gerwick *et al.*, 1999; Feussner and Wasternack, 2002; Brash, 1999; Yamamoto *et al.*, 1997). Higher plants use only the pool of C_{18} fatty acids that are transformed by lipoxygenases (LOX) to form intermediate hydroperoxides. These then serve as substrates for a family of

hydroperoxide lyases (HPL) that release aldehydes with shorter chain lengths (Noordermeer *et al.*, 2001). In general, HPL-mediated reactions result in short-chain aldehydes such as 3(*Z*)-hexenal (Figure 3.1), which is a component of the so-called green leafy volatiles, or 3(*Z*)-nonenal with a cucumber-like odor.

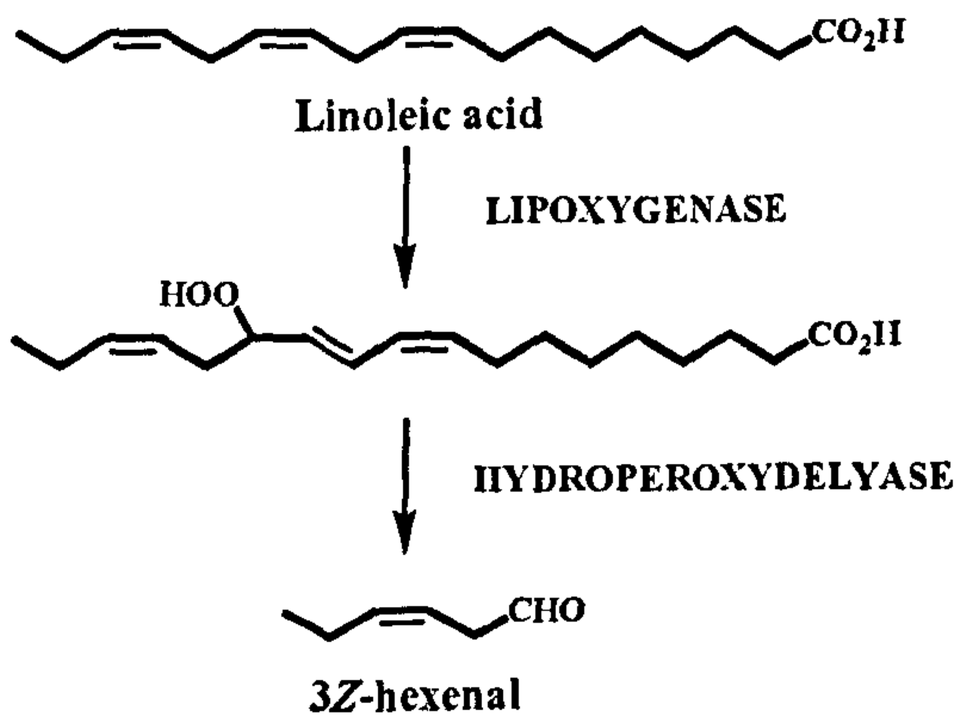

Figure 3.1: Lipoxygenase mediated formation of 3(*Z*)-hexenal from linolenic acid in plants

A characteristic structural feature of these HPL-derived products is that they contain only isolated double bonds and lack a Michael acceptor element. In plants, further transformations by 3*Z*:2*E*-enal isomerases result in α,β-conjugated aldehydes such as the phytohormone traumatic acid (Phillips *et al.*, 1979)

Essentially, oxylipins in marine diatoms derived from the oxidation of three fatty acids: C_{20} EPA (**21**) and C_{16} fatty acids HTrA (**22**) and HTA (**23**). The first biosynthetic study in marine diatoms was in 2000, when Pohnert demonstrated the production of decadienal from arachidonic acid in *T. rotula* (Pohnert, 2000). Even if these experiments could not be considered because, as subsequently demonstrated, the arachidonic acid and decadienal are not physiological components of this marine diatom, he proposed that aldehydes may derive from the breakdown of C_{20} polyunsaturated fatty acids by lipoxygenase/hydroperoxide lyase. However, an intriguing question regarded the origin of 2,4-octadienal and 2,4,7 octatrienal in

S. costatum and *T. rotula*, since the double-bond position of these compounds (belonging to ω-4 and ω-1 series) was not consistent with the composition of LOX-sensititive C_{20} fatty acids in these diatoms. In fact, the fatty acid profile of these diatoms showed a predominance of EPA (20:5 ω-3), and high levels of C_{16} compounds (almost 65% of the whole fatty acid content). In particular, significant amounts of HTrA (16:3ω-4) and HTA (16:4 ω -1) were found, which may be related to the production of octadienal and octatrienal, respectively. Experiments with the deuterated precursor d_6-HTrA demonstrated the labelling of d_4-octadienal in *S. costaum* and *T. rotula* (d'Ippolito *et al.*, 2003). In fact, the GCMS spectrum of 2,4-octadienal revealed the retention of four deuterium atoms both in the molecular ion and in the fragmentation pattern of this aldehyde (Figure 2.7 and 2.16). The localization of the four deuterium atoms in C-1, C-2, C-4 and C-5 of octadienal was established by NMR with a deuterium probe in comparison with ^{1}H-NMR of the standard octadienal (Figure 2.8). So, these experiments not only proved the biosynthesis of octadienal, but the labeling pattern was fully consistent with the mechanism involving the oxidation of HTrA by 9-LOX and the further action of an HPL, giving the final octadienal (Scheme 2.3). Even if the incorporation patterns found in transformations of deuterated precursors were in accordance with mechanisms involving lipoxygenase, this assumption remained an hypothesis since neither the intermediate hydroperoxides nor the acidic cleavage products that should have resulted as a second fragment from the hydroperoxide transformation had yet been detected.

The first direct proof of a mechanism involving lipoxygenases was obtained with the characterization of the intermediate 9-hydroperoxy-hexadecatrienoic acid in *T. rotula*. This unstable intermediate was detected only in fresh diatom extracts, and convincing evidence of its presence was obtained after the selective reduction of the incubation mixture with trimethylphosphite (TMP). This treatment led to complete disappearance of the hydroperoxide peak and induced a clear increase in the peak due to the deuterated derivative of 9(*S*)-HHTrE

(Figure 2.16 B and C). Considering the selectivity of TMP for hydroperoxide reduction and the stereospecificity of the hydroperoxy/alcohol conversion, the obtained data accurately reflected the 9*S* lipoxygenase activity of the cell lysates, and represents the first direct proof of the existence of a lipoxygenase pathway (d'Ippolito *et al.*, 2006).

On this ground, it was possible to assume that octatrienal derived from HTA, since this fatty acid was the only ω-1 precursor present in *S. costatum* and *T. rotula*. This biosynthetic step has been independently demonstrated in a successive work (Pohnert *et al.*, 2004) in the diatom *T. rotula*. The same author proposed the origin of decatrienal from EPA on the basis of feeding experiments with an unlabeled precursor, observing an increase in the peak of decatrienal (Pohnert, 2002). His biogenetical proposal was rigorously proved by using labeled $^{3}H_{10}$-EPA (d'Ippolito *et al.*, 2006). The clear labelling of decatrienal was demonstrated after its purification in HPLC coupled with a radiodetector, and further hydrogenation to ensure that the radioactivity was only associated with the peak of decatrienal (Figure 2.17). Interestingly in *S. costatum*, the same feeding experiment with $^{3}H_{10}$-EPA led to the specific labelling of heptadienal (Figure 2.9) (d'Ippolito *et al.*, 2004).

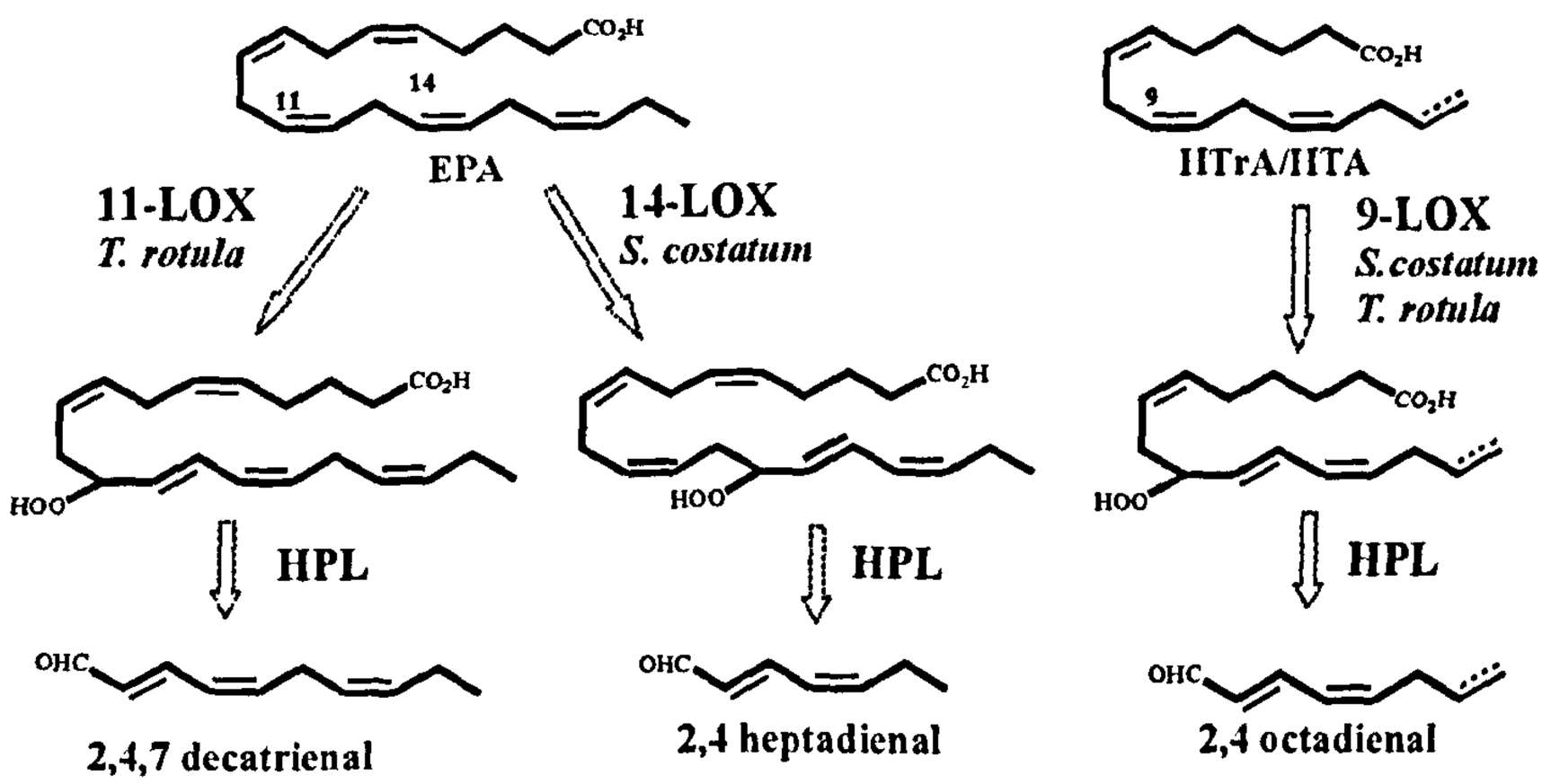

Scheme 3.1: Results of the first biosynthetic studies in the marine diatoms. EPA was converted in decatrienal in *T. rotula*, whereas it was converted to heptadienal in *S. costatum*. In both species the C_{16} fatty acids HtrA and HTA were converted to 2,4-octadienal and 2,4,7-octatrienal, respectively.

So, a common substrate such as EPA (20:5 ω3) in *T. rotula* is metabolized to decatrienal by a 11-LOX, whereas in *S. costatum* it is oxidized to heptadienal by a 14-LOX. This observation revealed the specificity of the biochemical pathway leading to aldehyde production. Instead, C_{16} substrates such as HTrA (16:3 ω4) and HTA (16:4 ω1) were metabolized in both species to octadienal and octatrienal, respectively (Scheme 3.1). Formation of octadienal in *S. costatum* and *T. rotula* is the first evidence of oxidation of 6,9,12-hexadecatrienoic acid (d'Ippolito *et al.*, 2003). Even if this fatty acid is structurally related to 7,10,13-hexadecatrienoic acid found in plants, 6,9,12 hexadecatrienoic acid has never been described in sources other than diatoms.

Labelled aldehyde production was totally inhibited when the labelled fatty acids were added to a boiled sample of the diatoms, suggesting the enzymatic origin of octadienal, excluding its production by a spontaneous process. As outlined in the biogenetic proposal (Scheme 2.3), *trans,cis*-2,4-octadienal (**13**) is the former product of the oxidation of hexadecatrienoic acid, whereas *trans,trans*-2,4-octadienal (**14**) is probably derived by a nonenzymatic process involving the isomerization of the C-4/C-5 double bond of **13**.

The recovery of 9(*S*)-HHTrE in *T. rotula* and *S. costaum* was an important step to corroborate the presence of a 9(S)-lipoxygenase in these marine diatoms, since this compound was the direct derivative of the corresponding 9-hydroperoxy-6*Z*,10*E*,12*Z*-hexadecatrienoic acid (9-HPHTrE) (Scheme 2.5). The important role of C_{16} fatty acids in diatoms was further demonstrated by the characterization in *T. rotula* of other oxylipins derived from this class of fatty acids (Table 3.2) . On the basis of incorporations of deuterated hexadecatrienoic acid in *T.rotula*, it was possible to demonstrate the presence also of another lipoxygenase, a 6-LOX specific for the oxidations at position C-6 of C_{16} fatty acids (Scheme 3.2).

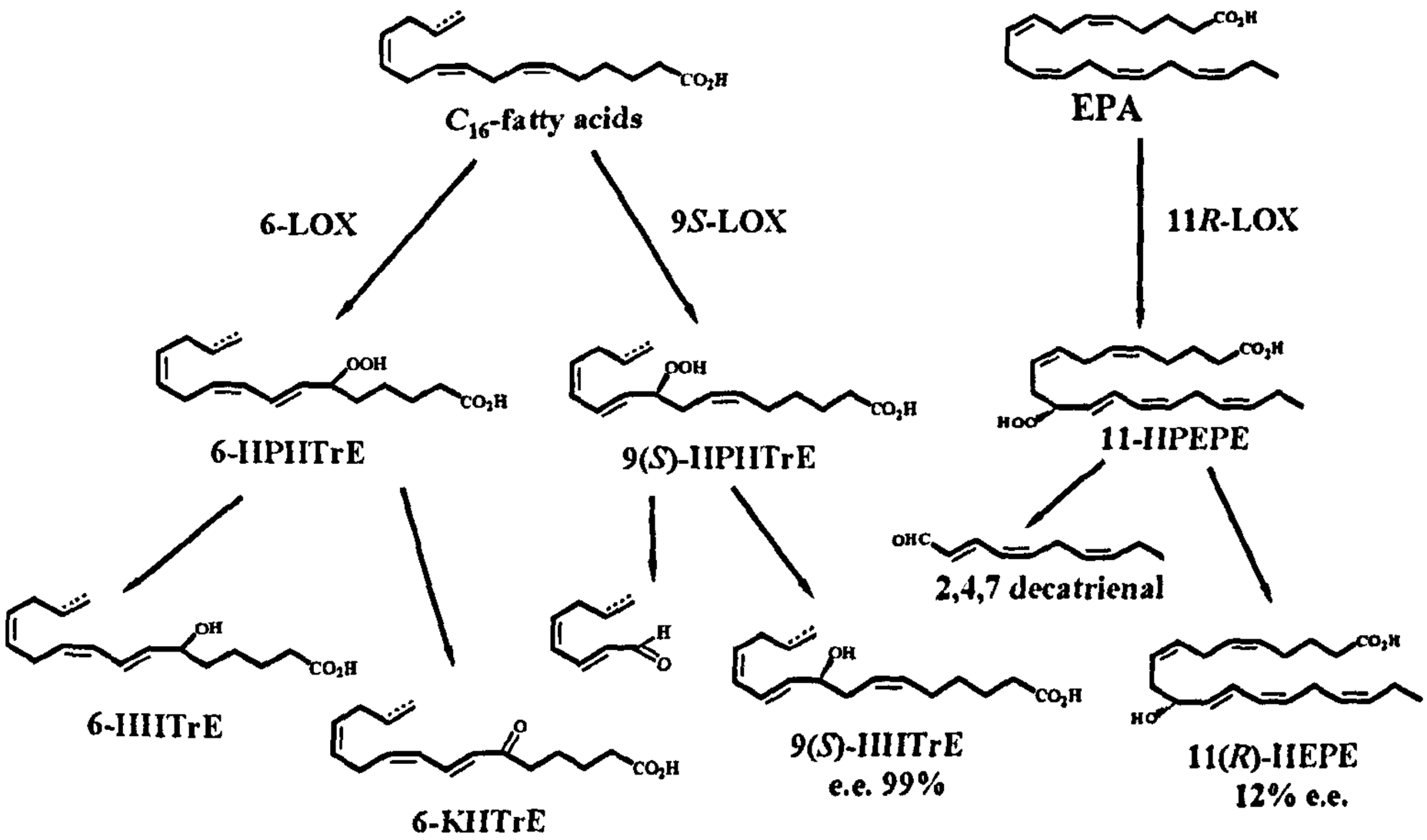

Scheme 3.2: Oxylipin pathway from C_{16} fatty acids C_{20} fatty acid EPA in *T. rotula*.

In *T .rotula* HTrA and HTA were metabolized in the same rate to hydroxyacids and keto derivatives by these lipoxygenases. This is the first time that a complete oxylipin pathway involving the oxidation of C_{16} fatty acids in the marine environment has been demonstrated (d'Ippolito *et al.*, 2005). Also the synthesis of 2,4,7-decatrienal is associated to the production of the hydroxyacid 11(*R*)-HEPE, with 12% e.e, demonstrating the low stereospecificity of the putative 11-LOX for EPA (Figure 2.18). This low stereospecificity is also associated to the putative 5*R*-LOX in *S. costatum*, since the 5(*R*)-HEPE (**29**) is formed with an entiamoric excess of 74% (Figure 2.14). This is consistent with *R*-lipoxygenases described in plants, where the synthesis of *R*-hydroperoxides is invariably accompanied by the formation of *S*-hydroperoxides (Coffa and Hill, 2000).

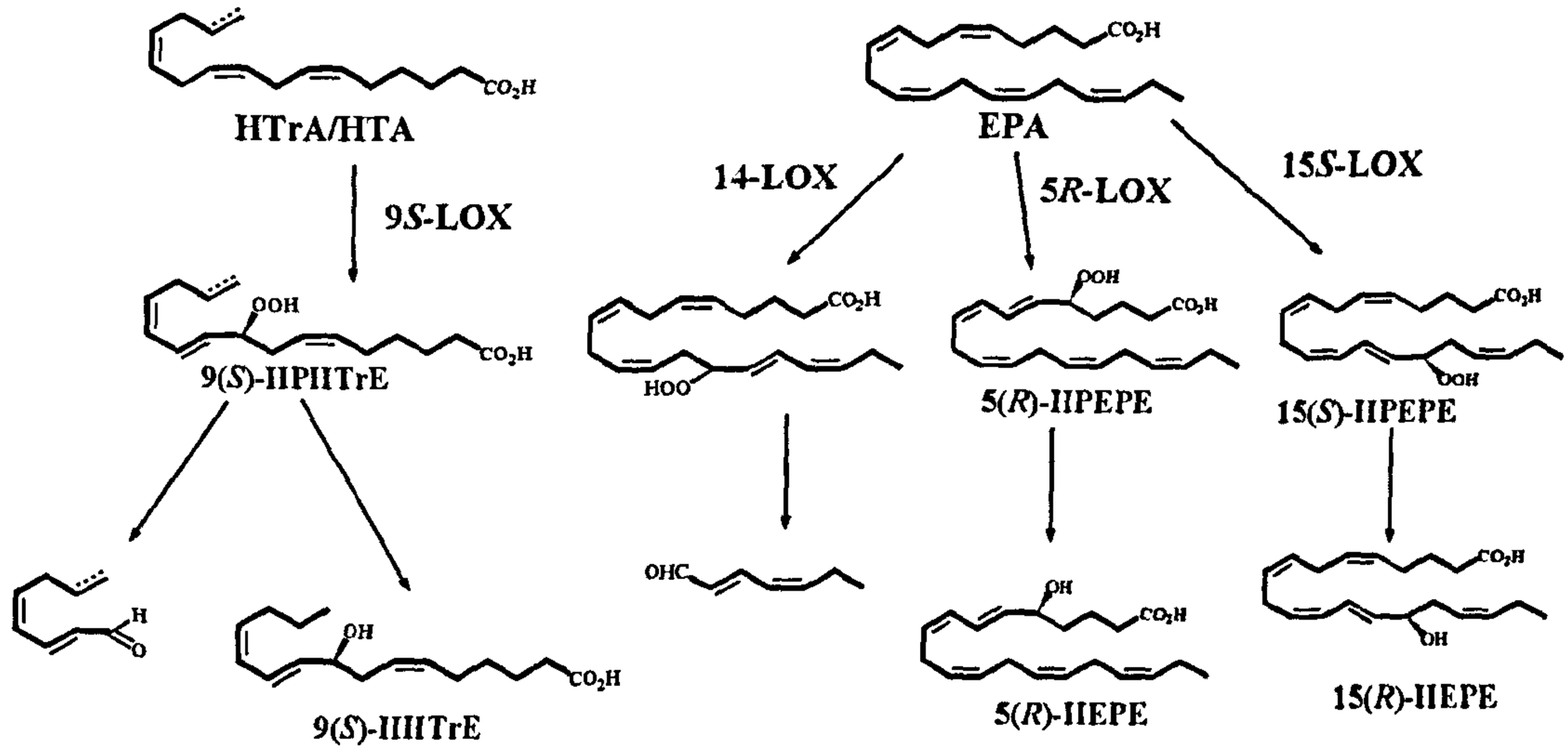

Scheme 3.3: Oxylipin pathway from C_{16} fatty acids C_{20} fatty acid EPA in *S. costatum*.

As for *T. rotula*, the synthesis of octadienal is associated to the production of 9-HHTrE in *S. costatum*. But in this diatom 9(*S*)-LOX preferentially oxidized HTrA compared to HTA. The synthesis of heptadienal from EPA is not associated to the production of the corresponding 14-HEPE, although the presence of other enzymatic activities such as 5*R*-LOX and 15*S*-LOX could be inferred on the basis of the recovery of the correspondent hydroxyacids in *S. costatum* extract (Scheme 3.3). The existence of 15*S*-LOX pathway was also confirmed by complete characterization by NMR of the intermediate 15(*S*)-HPEPE (**28**), that strongly support a mechanism involving lipoxygenases.

15*S*-LOX activity specific for EPA was also demonstrated in *P. delicatissima* through the use of $^{3}H_{10}$-EPA, but in this case the corresponding hydroperoxide was metabolised not only to the hydroxyacid 15(*S*)-HEPE (**27**), but it was also cleaved to 15-oxo-acid and metabolized by a putative epoxyalcohol synthase giving raise to the epoxyalcohol **36** (Scheme 3.4)

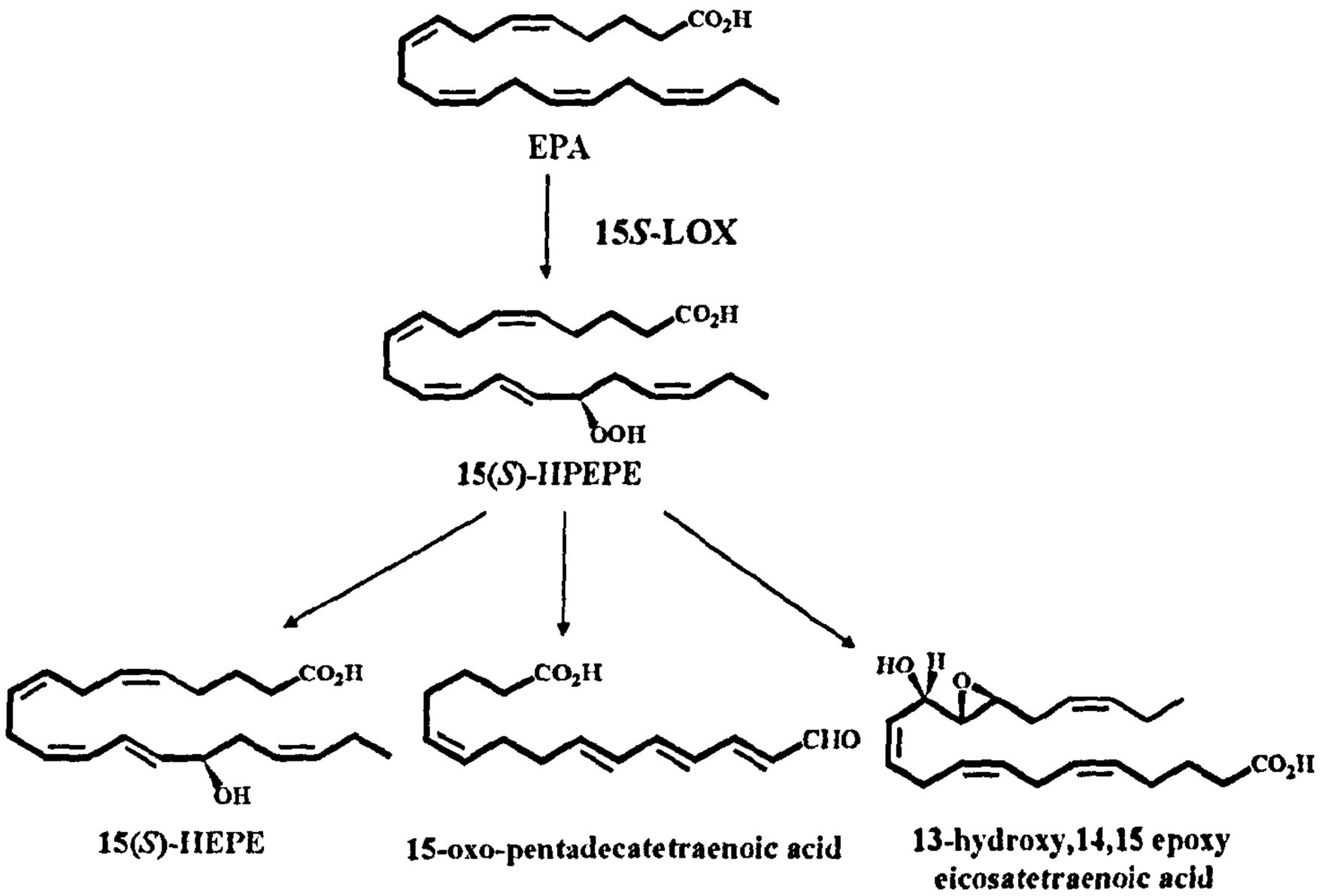

Scheme 3.4: Oxylipin pathway in *P.delicatissima*

It was interesting that although this species possesses the polyunsaturated C_{16} substrates, no compounds derived from these fatty acids was recovered. This could be due to the lack or the inactivity of the enzyme that recognizes C_{16} substrates. The preferential oxidation of EPA in *P. delicatissima* was similar to the fatty acid metabolism in the genus *Chaeotoceros*.

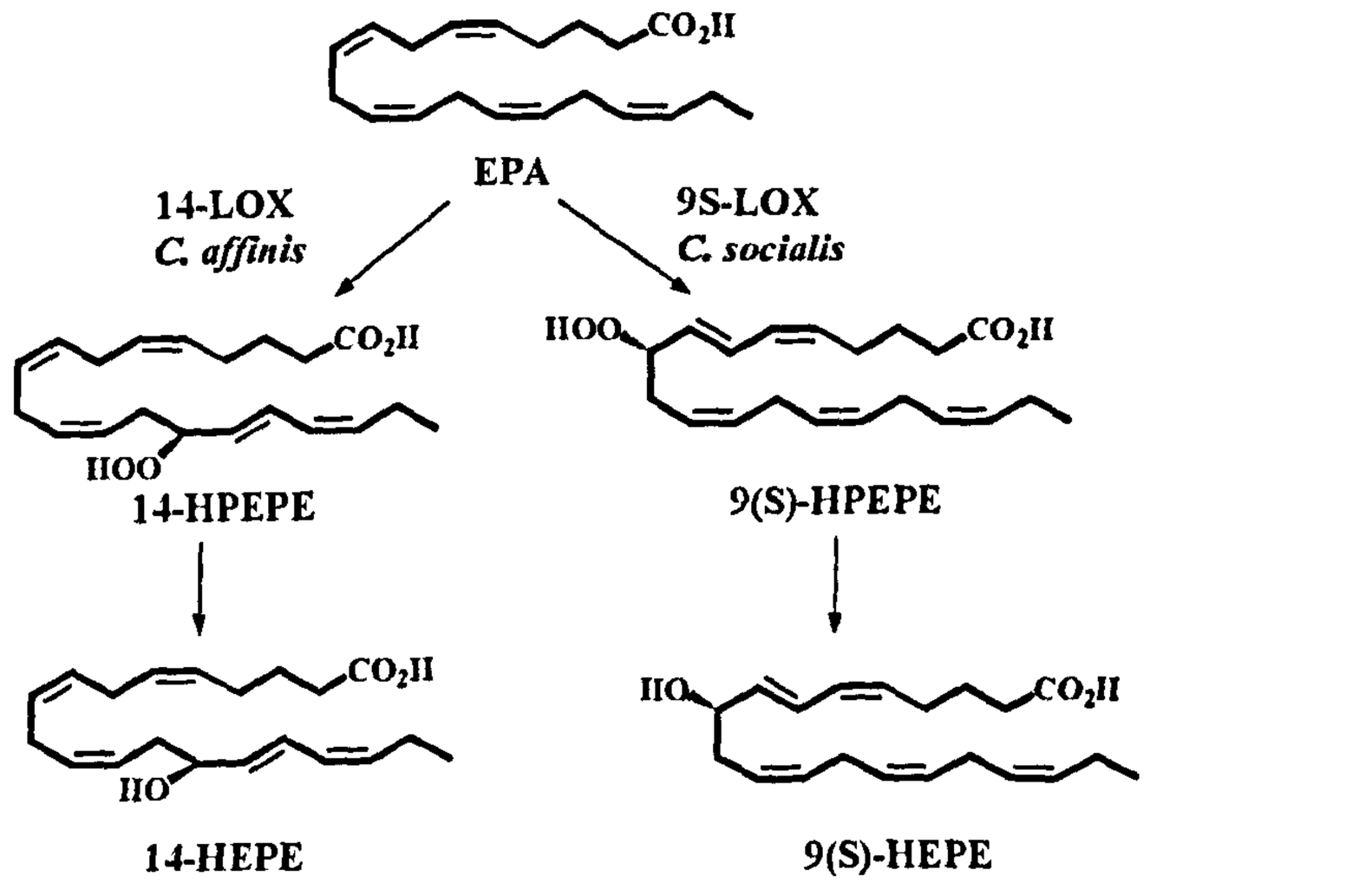

Scheme 3.5: Oxylipin pathway in *C.affinis* and *C. socialis*

In fact, *C. socialis* is mainly characterized by a 9*S*-LOX and *C. affinis* by a 14-LOX, both specific for EPA (Scheme 3.5) .

The oxylipin pathway in different diatoms revealed their species-specific distribution, either for the preferential substrate involved (HTrA, HTA and EPA), either for the regio- and stereo-specificity of LOXs, or considering the different metabolic fate of hydroperoxides in dependence of the enzymatic activities able of metabolizing these unstable intermediates (hydroperoxidelyase, peroxygenase or epoxyalcohol synthase).

3.2.2 Molecular characterization of lipoxygenases in *T. rotula*

Since no information is available on the genome of these diatoms, a biochemical approach was adopted. The production of aldehydes in *T. rotula* was used as a tool to obtain molecular data on enzymatic activities. In fact, further information about the oxidizing activities were obtained after fractionation of cell homogenates at different centrifugation speeds (9600g and 100000g). Each of these subcellular fractions was incubated with deuterated hexadecatrienoic acid quantifying the rate of incorporation in d_4-octadienal (Figure 2.20). LOX/HPL activities were found predominantly within the microsomial fraction with a very evident formation of aldehydes (d'Ippolito *et al.*, 2006). Interestingly, synthesis of octadienal significantly increased in the subcellular fractions. Although a partial inactivation of enzymatic activities in the raw homogenates cannot be excluded, it was more plausible that the apparently low conversion of HTrA into d_4-octadienal in these preparations was due to a rapid degradation of the aldehydic pool as a result of reaction with nucleophiles (for example, amine groups of protein) largely present in these fractions. These preparations were also assayed for the capability of producing lipid hydroperoxides in homogenates and subcellular fractions of the diatom (Figure 2.21). LOX activity was measured using a spectrophotometric method recently

proposed by Anthon & Barrett (2001). It revealed that LOX-mediated formation of fatty acid hydroperoxides in 102,000 *g* pellet of *T. rotula* is ten times higher than in other fractions. The general agreement between the assay for lipoxygenase activity and fatty acid/aldehyde conversion revealed that microsomes are capable of transforming fatty acids to aldehydes through the corresponding hydroperoxides.

To test substrate specificity, the soluble fraction at 9600g was ultrafiltered on Amicon. In this way, the enzymatic system is completely depleted of aldehydes and all type of secondary metabolites, allowing the use of unlabelled fatty acids (Figure 2.19). As already demonstrated, HTrA was transformed to 2,4-octadienal. EPA was metabolized to 2,4,7-decatrienal, and, in the same way, AA was converted to 2,4-decadienal.

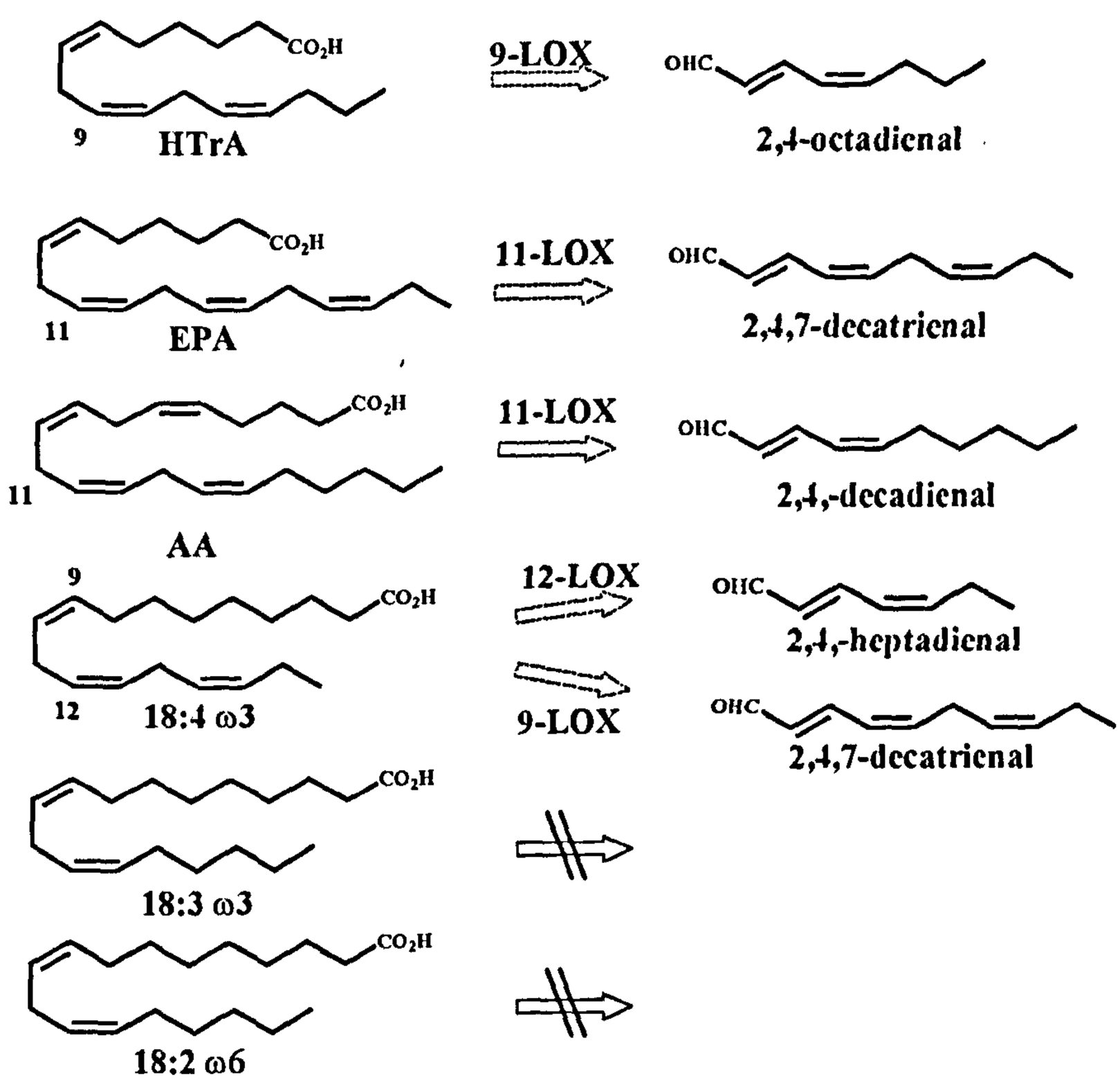

Scheme 3.6: Substrate specificity in partial purified enzymatic system of *T. rotula*.

Even if arachidonic acid is not a physiological component of *T. rotula*, it was probably recognized by the same enzyme, a 11-LOX, that was active on eicosapentaenoic acid (Scheme

3.6). The absence of decadienal in our strain of *T. rotula* was essentially due to the absence of the precursor, arachidonic acid. Among C_{18} fatty acids, 5,8,11,14-octadecatetrenoic acid (18:4ω3) was partly converted to 2,4-heptadienal and 2,4,7-decatrienal, whereas linolenic acid (18:3ω3) and linoleic acid (18:2ω6) were not recognized by the enzymatic system even if they have similar structural characteristics to other ω-3 and ω-6 fatty acids recognized by the enzymatic system. The difference in positional specificity of lipoxygenases is generally due to a ''frame shift'' of the substrate, where the position of oxygenation is determined by how deeply the substrate enters into the active site (Kühn *et al.*, 1990; Sloane *et al.*, 1991; Borngräber *et al.*, 1999). Positional specificity is also determined by the substrate orientation, whereby different oxygenation products are formed if the substrate enters the active site with the carboxylic or the methyl end first (Prigge *et al.*, 1998; Hornung *et al.*, 1999; Jisaka *et al.*, 2000). So, without the purification of enzymes is not possible to give definitive proof of enzyme specificity.

However, the incorporations in the purified enzymatic system provided important information about the isomerization of the double bond in the extract. In fact, in raw homogenates the incorporation of labelled fatty acids led to a mixture of 2-*trans*/4-*cis* and 2-*trans*/4-*trans* isomers (Figure 2.8 and Scheme 2.3). In the purified enzymatic system only the 2-*trans*/4-*cis* isomers were found, in the same conditions of incubation, extraction and derivatisation (Figure 2.19). This aspect demonstrates that the natural isomers of aldehydes were 2-*trans*/4-*cis* also inferred on the basis of the configuration of the double bond in the fatty acid precursors. The isomerization could be due to the possible presence in the raw homogenates of isomerase (eliminated in the purified enzymatic system) capable of converting the natural isomers *trans/cis* in the *trans/trans* isoforms. Another possibility was that in the raw extracts the environment (proteins or metabolites) caused the isomerization of *trans/cis* into the more stable *trans/trans* isoform.

The presence in diatom extracts of interference due to other enzymatic activities involved in the lipoxygenase pathway (e.g., hydroperoxide lyases) and organic compounds, make the isolation and characterization of LOXs very difficult. The existence of lipoxygenase activities with a different substrate specificity was consistent with preliminary molecular studies of the protein extract on isoeletric focusing (IEF) (Figure 2.27). Preliminary results suggested the presence of different activity bands for HTrA and EPA, and no activity for linoleic acid, in agreement with the chemical data. IEF bands (pI=5.61-5.76) are too near to discriminate between them. Unfortunately, the low protein quantities and lipophilic nature of *Thalassiosira* LOXs have so far prevented the purification of these activities, as well as the determination of the molecular weight in SDS-PAGE.

3.2.3 Lipolytic activity in marine diatoms

Once information about the LOX pathway in diatoms was accumulated, it was necessary to clarify how the free fatty acids were released from complex lipids. As already mentioned, in intact cells there are no free fatty acids, but they are physiologically bound to complex lipids. So it is necessary the activation of hydrolytic enzymes to liberate free fatty acids from complex lipids to initiate the enzymatic cascade. In analogy to mammals, phospolipase A_2 has been suggested as a key enzyme to trigger the release of free fatty acids (Pohnert, 2002). This was demonstrated with the use of fluorescent phospholipids (BODIPY- phospholipids) labelled in the *sn*-2 position. These experiments with labeled phospholipids and triacylglycerols do not rule out the possibility of other lipid hydrolyzing activities to be involved in the activated defence of marine diatoms. Because the presence of other polar lipids rich in PUFAs, such as MGDG, DGDG and SQDG have been reported from other diatoms (Arao *et al.*, 1987; Yongmanitchai and Ward, 1993), these sources have also been taken into account.

The data regarding the distribution of fatty acids in complex lipids was already present in the literature (Bergè *et al.*, 1995) for *S. costatum*, whereas no information about the distribution of fatty acids in complex lipids was present for *T. rotula*. In both cases, it was important to perform these analyses, due to the extreme variability of these lipidic pools in response to different environmental parameters including culture conditions and growth cycle (Lopez *et al.*, 2000). From the fatty acid distribution in complex lipids of *S. costatum* and *T. rotula* (Figure 2.10 and 2.22), it was immediately clear that HTrA and HTA (the precursors of octadienal and octatrienal, respectively) were only present in the glycolipids of both species. On the contrary, EPA was present both in phospholipids and glycolipids of both species. These observations immediately suggested the active role of glycolipids in this process, because C_{16} fatty acid precursors of octadienal and octatrienal as well as other important oxylipins, were present only in the glycolipids. To address how phospholipids are involved in the synthesis of decatrienal in *T. rotula* and heptadienal in *S. costatum*, different approaches were used, leading essentially to similar results. In *S. costatum*, two series of experiments were prepared using either radiolabelled precursors or cell preparations with a low content of volatile components. In the first approach, a procedure was developed to label the natural complex lipids of the diatom with EPA, since these were not commercially available; ^{3}H-PL and ^{3}H-GL were incorporated in cell homogenates. Although there was a major radioactivity associated to phospolipids rather than glycolipids at the beginning, the percentage of radioactivity recovered in heptadienal was three times higher with glycolipids than phospholipids (Table 2.2) (d'Ippolito *et al.*, 2004). This is consistent with a higher affinity of hydrolytic enzymes for glycolipids. Furthermore, incubation of radioactive pools of complex lipids indicate that the ability of *Skeletonema* homogenates to promote release of $^{3}H_{10}$-EPA is higher in experiments with GL rather than PL (Table 2.2). In a second approach, an enzymatic system completely depleted of aldehydes was prepared, and this was tested with natural

complex lipids. Diatom cells have indeed the capability of forming a whole set of aldehydes upon incubation with glycolipids, whereas metabolism of phospholipids led only to the production of heptadienal (Figure 2.11).

In *T. rotula*, the partially purified enzymatic system depleted of natural secondary metabolites was used. The natural three classes of complex lipids, isolated from *T. rotula*, were incubated in this enzymatic system. Incorporations with triglycerides gave no detectable products and did not serve as precursors for aldehyde production, in agreement with Pohnert (Pohnert, 2002). Incorporation of phospholipids led only to the formation of decatrienal, whereas the only class of complex lipids that gave rise to all the aldehydic pattern of *T. rotula* was glycolipid that led to the formation of the major compounds octadienal and decatrienal, and the minor compounds heptadienal and octatrienal (Figure 2.23) (Cutignano *et al.*, 2006). In contrast to Pohnert's conclusion, the role of phospholipids is apparently less crucial, being only involved in the partial formation of decatrienal. Only the hydrolysis of glycolipids is capable of supplying all the aldehydic pool. Both in *T. rotula* and *S. costatum*, the results indicated clearly that glycolipids were the major pool involved in the production of aldehydes. It should be noted that glycolipids have been considered as precursors of plant oxylipins (Matsui, 2000), but their involvement in the biosynthesis of diatom aldehydes has been never demonstrated to date.

To understand what position between *sn*-1 and *sn*-2 is preferred by the hydrolytic enzymes, a recent powerful technique (Guella *et al.*, 2003) was used to analyze the distribution of fatty acids in MGDG (Table 2.3 and 2.6). In both species similar patterns were obtained: HTrA was present in both *sn*-1 and *sn*-2 positions. EPA was exclusively present in *sn*-1, while HTA was exclusively present in the *sn*-2 positions. So both the positions were involved in the hydrolytic process. On these grounds, although the presence of other lipolytic activities cannot be ruled out, the release of fatty acids from both glycolipids and phospholipids may be catalysed by the

same enzyme or class of enzymes. In summary, even if the hydrolytic activity was active on both glycolipids and phospholipids, it possessed a major affinity toward glycolipids, and it was active on both *sn* positions of glycolipids. Finally, it did not have activity on tryglicerides. All these characteristics were consistent with a class of enzymes, called lypolitic acyl hydrolases (LAHs), the activity of which has been reported in plant leaves and tubers (Andrews *et al.*, 1988; Matos *et al.*, 2001; Banerji and Flieger, 2004). Since galactolipids are restricted to diatom chloroplasts, the data indirectly implicate these organelles in the production of oxylipins in marine diatoms.

Purification and characterization of galactolipid-hydrolyzing enzymes in *T. rotula* are currently in progress. Preliminary results show the presence of a lipolytic protein band at approximately 42 kDa, whereas native gel filtration indicates an apparent molecular weight of 200 kDa (Figure 2.24). The different mass values suggest the association of the putative galactolipase(s) in an oligomeric structure composed of either five identical subunits of the lipolytic polypeptide or a multi-molecular aggregate that includes also the lipolytic enzyme(s).

3.2.4 Dynamics of oxylipin pathway in marine diatoms

Extracts of intact cells of *S. costatum* and *T. rotula* did not show any presence of volatile aldehydes, nor hydrolysis of complex lipids. In the laboratory, this process was triggered by the mechanical rupture of the cells through sonication. The formation of aldehydes begins soon after the sonication, increasing after 16 minutes to the maximum level, in agreement with data already published (Pohnert, 2000 and 2002). But, interestingly, when the aldehydes were eliminated by treating the cell suspension for 15 minutes with a vacuum pump, the process of production re-initiated, giving rise to higher levels.

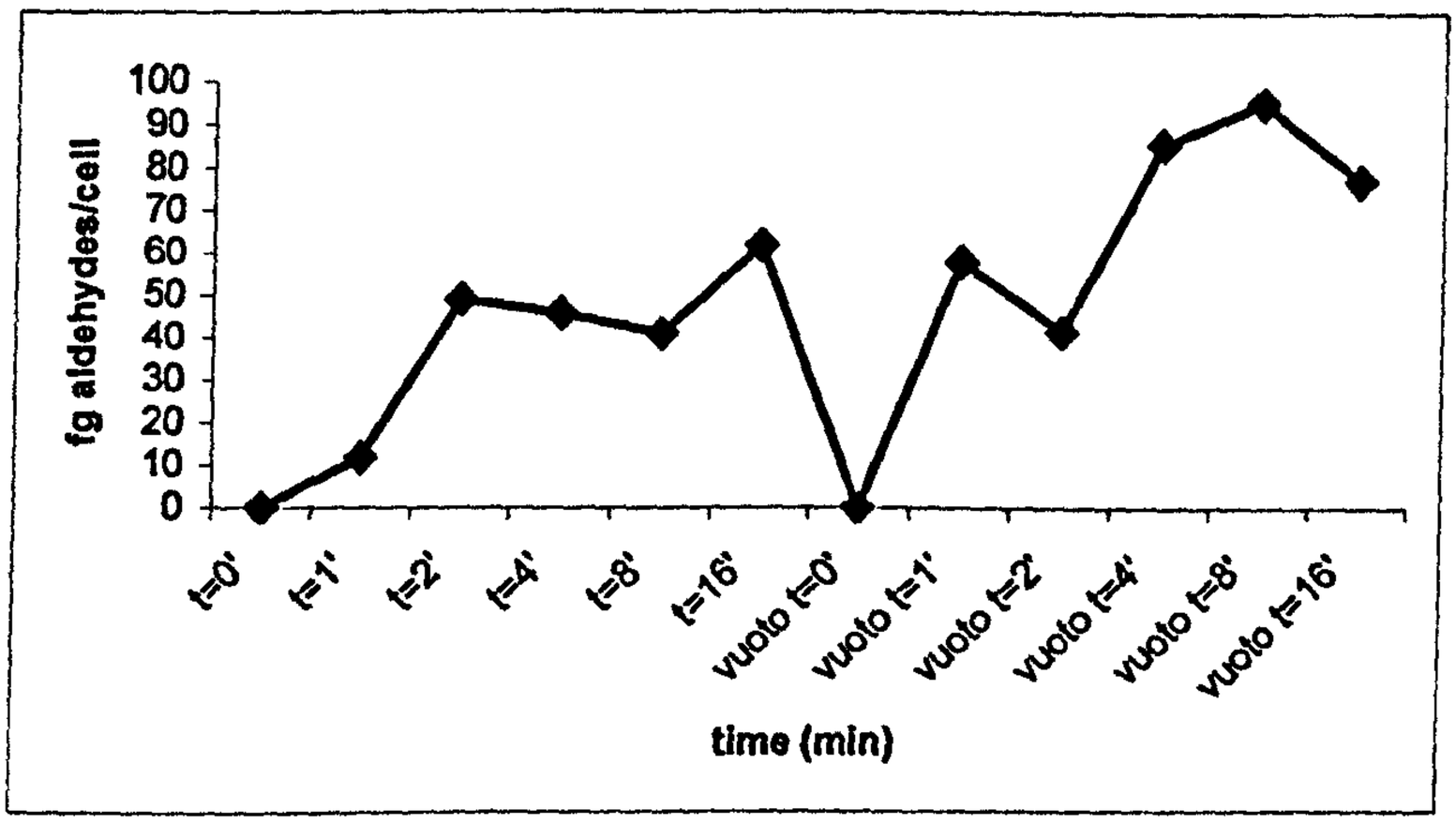

Figure 3.2: Formation of PUAs aldehydes on time. After 16 minutes, the homogenates were treated with a vacuum pump for 15minutes, and then the quantity of aldehydes newly measured at different time.

This experiment provides some important information. First of all it explains the difficulty in determining the precise quantity of aldehydes per cell, because it depends by the moment in which the cells were analyzed. It is only possible to define the order of magnitude of aldehydes/diatom cell. The second important point regards the dynamics of the process. At each concentration tested, the substrates were always available for the process (the amount of fatty acids remained more or less constant). It is possible that, as for many enzymatic processes, the enzymes reached a steady state, establishing an equilibrium between the substrates (fatty acids) consumed and the final products (aldehydes) produced. When the aldehydes were eliminated, the equilibrium was moved, leading to the formation of new aldehydes, until a new equilibrium was reached. This model for the production of aldehydes in *T. rotula* and *S. costatum* fit in general for the production of oxylipins in all the studied marine diatoms.

Since intact diatom cells do not show any presence of fatty acids or oxylipins, the process become active immediately after lyses of the cells in an aqueous medium. A wound activated defence strategy for diatoms has been proposed (Pohnert, 2000). When diatom cells are eaten by copepods, the cells are broken, generating the production of oxylipins. Probably, it is too

early to speak of a wound-activated defence in diatoms. This phenemonon has been well studied in plants.

Plants have developed a complex response to wounding that dramatically alters the cellular physiology of plant tissues and results in the production of defences. The wounding response is essentially the result of two set of events: direct defence and signalling. Behind the mechanical barriers, chemical defences against invading pathogens and herbivores are also produced in response to wounding, both in the wounded leaf and at systemic sites. These chemical defences can be separated into two major categories, secondary metabolites and proteins (de Bruxelles *et al.*, 2001). Although secondary metabolites with defensive functions may be present constitutively, the majority are induced by wounding and/or pathogens. These include terpenoids, alkaloids, and phenolics and are collectively known as phytoalexins. Wound-inducible proteins with direct defensive properties include protease inhibitors, α-amylase inhibitors, polyphenol oxidase and lectins, all of which have proposed roles as insect anti-feedants. There are also many other wound-inducible genes which do not have direct defensive roles (Zhou and Thomburg, 1999). Defence gene expression is mediated primarily through the synthesis and action of the oxylipin jasmonic acid (JA). Other hormones with important roles in regulating wound gene expression are ethylene and abscisic acid (ABA). Other elicitors of wound responses have also been identified, the most important of which include cell wall glycans such as oligogalacturonides (OGAs), and, in solanaceous plants at least, a peptide hormone called systemin. These elicitors of wound responses may either be primary signals released upon cellular damage, or may function to amplify the response in the wounded leaf. Finally, plants under attack from herbivores produce characteristic blends of volatile compounds that serve to attract predators and parasitoids of those herbivores. The complexity of the events involved in plant defence is hinted at from analysis of the genome of *Arabidopsis thaliana*. It is estimated that 2005 genes (11.5% of the total number of genes) are

involved in defence, whilst a further 1855 (10.4%) genes are involved in signalling (The *Arabidopsis* Genome Initiative, 2000).

On the other hands, diatoms are unicellular microorganisms, so they lack much of the complexity found in multicellular organisms. As already mentioned, it is necessary the rupture of the cells to initiate the enzymatic cascade leading to the formation of oxylipins. Oxylipin production starts within seconds after cell rupture, a fact that makes regulation through transcription and de novo protein biosynthesis of the required LOX very unlikely. So, the enzymes responsible for this pathway must be constitutively expressed. On these grounds, it is reasonable to assume a simple compartmentalization of enzymes and substrates. When the cells are broken or in response to stress conditions, the enzymes and substrates are mixed, activating the oxylipin pathway. In the laboratory, the process is activated by the mechanical rupture of the cells through the sonication. The products are released simply as a consequence of the decompartimentalization and mixing of enzymes and substrates. The data available to date are not sufficient to justify a wound-activated defence since it has not yet been demonstrated in diatoms that oxylipins can act as elicitors on the gene expression of oxylipin pathway, an important component of the wound response observed in plants.

3.3 Biochemical ecology

The studied diatoms had a similar effect on copepod reproduction. *S. costatum* affected both egg production and egg viability within 7 days (Figure 2.4); *T. rotula* and *P. delicatissima* had a less intense effect since hatching success decreased within 15 days (Figure 2.15 and 2.28). But whereas *C. socialis* had a moderate effect on copepod reproduction, *C. affinis* had a strong effect on the hatching success of copepod eggs (Figure 2.34). Since only *T. rotula* and *S. costatum* produced aldehydes, the only compounds that were initially correlated to the antiproliferative effect of diatoms on copepod reproduction, it appeared immediately clear that

they could not be the only molecules able to explain the ecological effect. In general the production of oxylipins can probably interfere with copepod reproduction, independently by the type of final products and enzymatic activity involved. To address the possibility that oxylipins could be involved in the insidious effect of diatoms on copepod reproduction, a biological assay based on ability of the molecules to block cell divisions in sea urchin embryos was used. This test should mimic *in vitro* the antiproliferative effect of diatoms on copepod reproduction *in vivo*. A typical bioactivity guided screening revealed that oxylipins other than aldehydes were also active. Some methylated pure oxylipins, such as 15(*S*)-HEPE (**27a**), 6-KHTE (**31a**), 9-keto-7*E*-hexadecenoic acid (**24a**), showed antimitotic activity from 3 to 50 μM (Figure 2.39). Surprisingly, the same metabolites active as methyl ester lost their antimitotic activity after hydrolysis, at concentrations ranging from 0.7 to 30 μM. This could be due to the difficulty of the non-methylated molecules to pass through the membrane or to a receptorial mechanism, since the molecules with a free carboxylic function did not reach the receptors. It is important to note that the influence of methylation on the molecule activity is opposite in FFAs. In fact, whereas FFA induced the necrosis of cells due to the loss of the cell membrane integrity, FAME failed to induce any morphological changes in sea urchin embryos, neither influence mitotic division and development even at very high concentrations. These results support the idea of an active role of oxylipins in apoptosis initiation, since the functionalitation of the chain is essential for this kind of biological activity.

Since intermediate in the oxylipin pathway, hydroperoxides, are reported in mammals and terrestrial plants as inducer of apoptosis (Knight *et al.*, 2001; Kalyankrishna *et al.*, 2002; Tang *et al.*, 2002), this possibility was also tested on sea urchin embryos. EPA hydroperoxides, tested in a mixture of autoxidation, induced severe morphological changes resembling those occurring in apoptotic events such as cell fragmentation and blebbing at concentration of 0.25 μg/ml (Figure 2.41), clearly discernable in respect of the effect of pure fatty acids. The

ecological role of hydroperoxides as inducer of apoptosis can be well explained considering the case of the genus *Chaetoceros*. In comparison with a C. *socialis*, a *C. affinis* diet induced abnormality in copepod development, with extensive areas of the body showing malformations. In fact, when abnormal nauplii were stained with TUNEL for the detection of apoptosis, wide apoptotic areas compared to controls were evident (Figure 2.35). The analytical parameter that reproduce well the different ecological activity between *C.socialis* and *C. affinis* was the lipoxygenase activity, a measure of the lipoxygenase process.

	Effect on copepod reproduction	Apoptotic effect	Aldehydes	Hydroperoxides levels
C. socialis	+	+	--	+
C.affinis	+++	+++	--	+++

Table 3.3: Summary of the relationships between ecological and biochemical data in *C. socialis* and *C. affinis*

In fact, in this way the rate of hydroperoxides was measured, understanding how the lipoxygenase is expressed and how the cells is ready to activate the LOX-pathway. LOX acitivity was three times higher in *C.affinis* than in *C. socialis*, both in the absence or in the presence of an exogenous substrate (EPA) (Figure 2.36), in perfect agreement with the ecological data (Table 3.3). This laboratory data are supported by *in situ* data. In fact also during phytoplankton bloom in North Adriatic Sea, it was possible to observe a modulation in the lipoxygenase activity, independently by the rate and type of secondary oxygenated products.

The apoptotic and antimitotic effect due to the autoxidation pool fit well what happen *in vivo*, because when copepods fed on diatoms they ingested a great quantity of fatty acids miscelated to oxidation products, in part due to enzymatic activity and in part due to autoxidation phenomena.

4. CONCLUSIONS

Summarizing the oxylipin pathway observed in marine diatoms, the lipase activity triggers the release of C_{16} and C_{20} fatty acids. These substrates are metabolized by lipoxygenases with different regio- and stereo-specificity, leading to the formation of hydroperoxides, the primary products of oxidation, that are further converted to different types of secondary oxygenated compounds, whose structures depend on the enzymes involved in the process (lyase, peroxygenase, epoxyalcohol synthase) (Scheme 4.1). Many of these final products are chiral, proving that the process is mostly enzymatic.

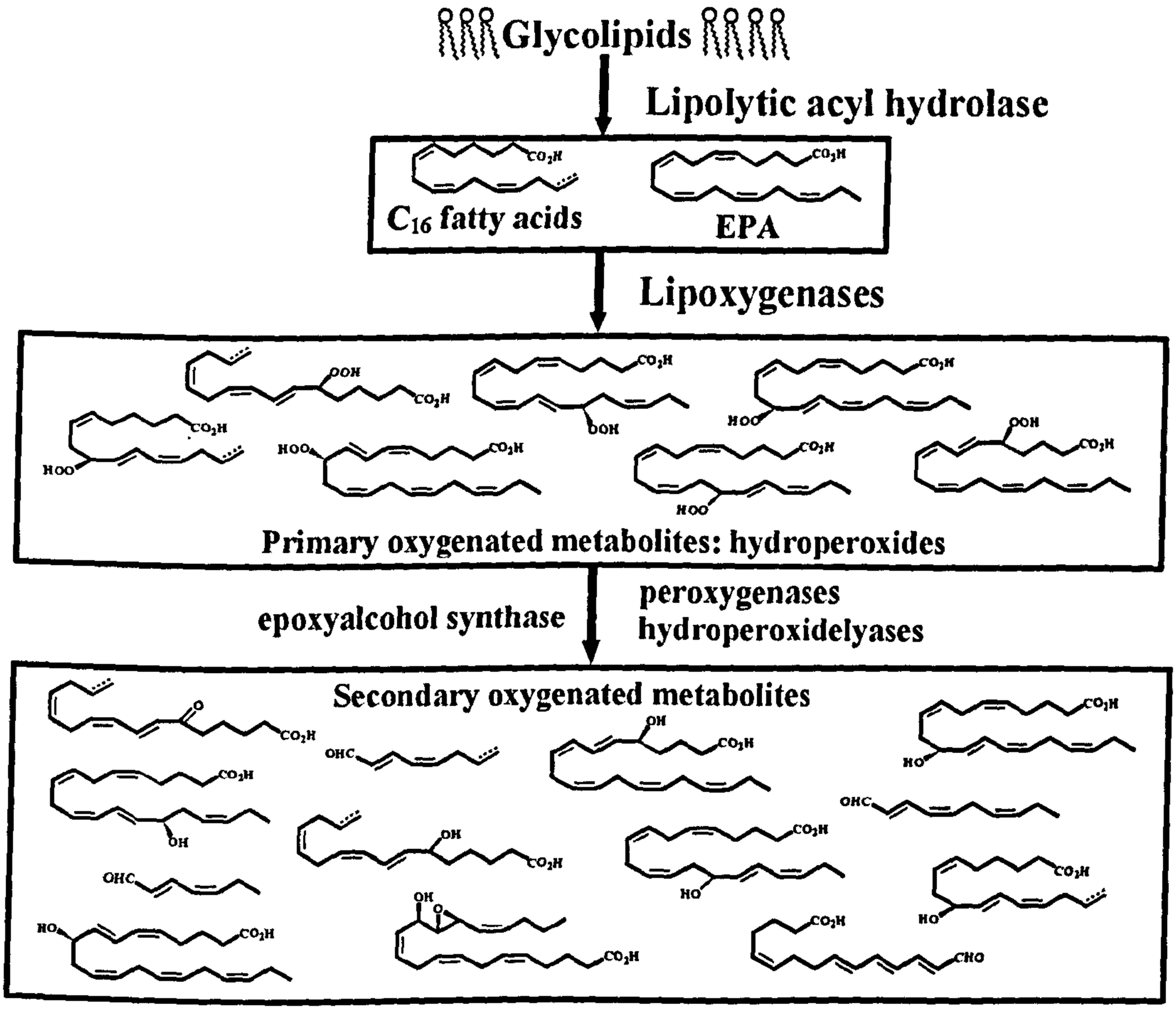

Scheme 4.1: Summary of the oxylipin pathway in marine diatoms.

So, in analogy with terrestrial systems, oxylipin production in marine diatoms can be divided in two phases (Scheme 4.2). In the first phase there is the generation of primary oxygenated products (hydroperoxides) with a transient life. In the second phase, hydroperoxides are

metabolized to secondary oxygenated products, such as aldehydes, oxo-acids, hydroxyacids, keto-acids, epoxyalcohol. The peculiarity of the oxylipin pathway in marine diatoms regards the starting fatty acids and the set of enzymatic activities. In fact, it is the first time that was reported an organic network involving oxidation of C_{16} substrates in marine environment as well LOX activities specific for these fatty acid pool, such as 9S-LOX and 6-LOX, have been reported. Also the biochemical characterization of lypolitic acyl hydrolase activity able to release free fatty acids from complex lipids has never been described in marine organisms.

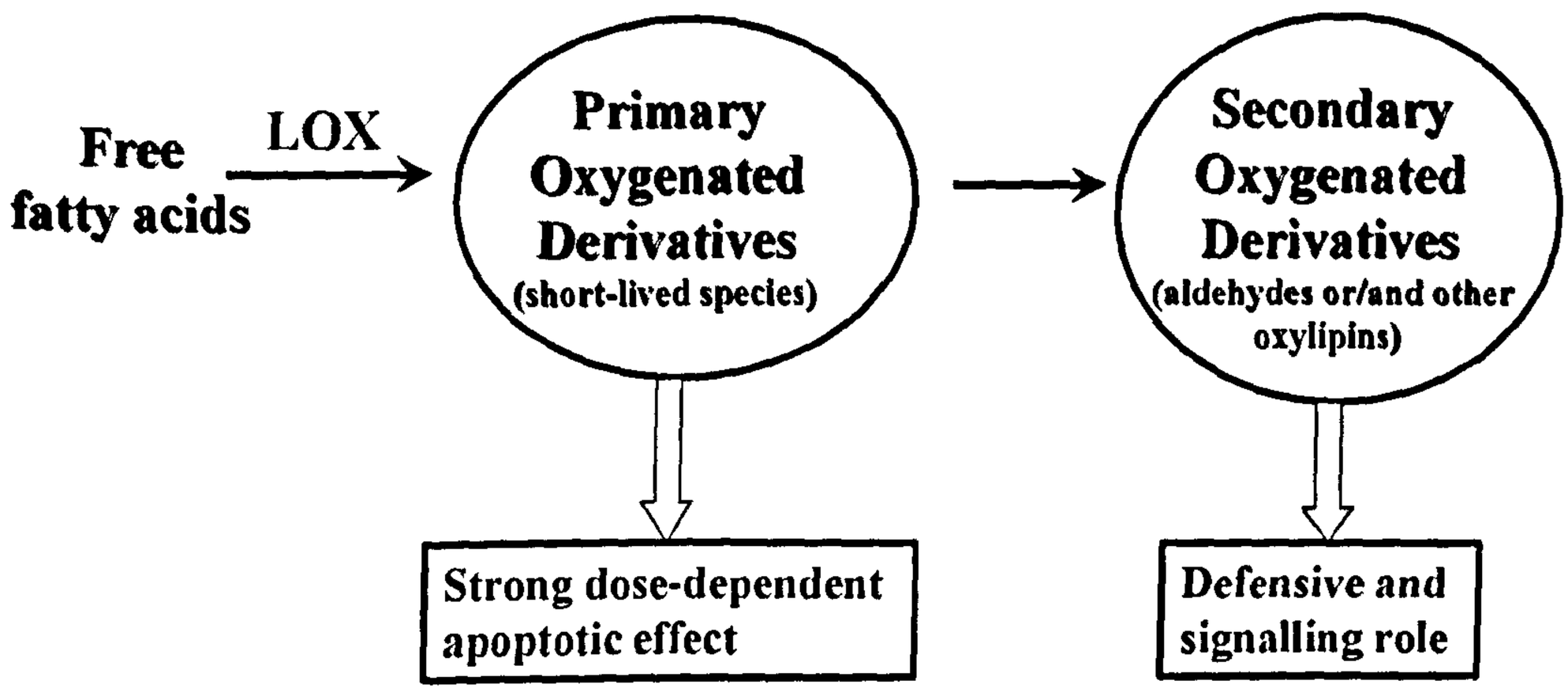

Scheme 4.2: Diagram representing the two step in the production of oxylipins and their biological activity in terrestrial organisms

Although there has been little experimental investigation about the function of oxylipins in marine environment, a number of possible roles have been advanced. Largely, these ideas build on the known properties of oxylipins in mammals and plants. The conceivable function of oxylipins in marine organisms, such as red algae, include defence from predation, osmoregulation, detoxification of reactive oxygen species, regulation of plant growth and mediation of wound responses (Gerwick *et al.*, 1991 and 1999).

A strong apoptotic effect has been demonstrated for the primary oxygenated products in marine diatoms, that could be responsible of the apoptotic effect on copepod reproduction. The secondary products may play a role *in vivo* as chemical defence and as chemical

messengers in diatom-diatom communication and as a part of a signal transduction system that serves to protect diatom cells from various stresses (oxidant injury, predation, pathogen interaction) (Blee, 1998). Anyway, independently from the oxylipin pathway that seem to be specie-specific, the rupture of the diatom cells generates an high oxidative potential that is able to interfere with copepod reproduction. Attention has to move from a single compound to a complex biochemical process that is important to measure in its entirety. The deleterious effect on copepod reproduction could be due to a complex biochemical process such as the generation of a high oxidative potential, rather than only by aldehydes or other secondary oxygenated products, that when present can co-occur to produce the final effect.

Copepods are known to be generalist feeders, as opposed to insects, which are highly specialized. Since copepods are potentially capable of filtering as much as 500% of their body weight per day, these small crustaceans can graze and eliminate phytoplankton blooms within only a few days (Paffenhoffer, 1988). Copepods are also highly prolific, with some species producing well over 100 eggs per female per day, and have very short development times, reaching adulthood within 2–3 weeks in warm temperate areas of the world's oceans (Ianora, 1998). So how do phytoplankton cope with such formidable predators? The probable answer is through chemical defence and the evolution of secondary metabolites that serve as feeding deterrents to reduce grazing pressure by herbivores. We are only now beginning to understand the chemistry of algal defence in microalgae (Paffenhöfer *et al.*, 2005). Until recently, most of the attention on metabolites produced by phytoplankton was devoted to the neurotoxins produced by a number of dinoflagellate species, such as the brevetoxins (Turner & Tester 1997). Diatoms were not known to produce such toxins until the discovery of domoic acid production by *Pseudo-nitzschia australis* and other diatoms of this complex (Turner & Tester 1997). However, diatoms are capable of producing another interesting class of molecules that interfere with the reproductive capacities of the animals that ingest them. Although the effect

of such toxins is less catastrophic than that of toxins that induce acute lethal poisoning, the effect is nonetheless considerable and insidious, becoming manifest in abortions, birth defects, poor development rates and high mortalities. This biological model is new and has no equivalent in marine plant– herbivore systems, since most of the known antipredator defensive compounds generally induce repellence or poisoning, but never reproductive failure.

At a first view, this type of defence might not be make evolutionary sense for unicellular algae that have no tissue to sacrifice and do not survive the ingestion process that triggers oxylipin production. However, it has to be taken into account that, during diatom blooms, algae proliferate predominantly asexually and thus the proportion of genetically identical algae can be high. The whole population could very well benefit from a reduction of the pool of grazers, even if certain individuals are sacrificed. Nevertheless, this concept lacks experimental verification since the molecular analysis of phytoplankton population is still in its infancy.

MATERIALS AND METHODS

5.1. General

Solvents were purchased from Carlo Erba (Milano) and distilled prior to use. $^{3}H_{10}$-EPA was obtained from ICN Pharmaceuticals. (±)11-HEPE, 11(R)-HEPE, (±)15-HEPE, 15(*S*)-HEPE, (±)5-HEPE, 5(*S*)-HEPE, (±)9-HEPE and 9(*S*)-HEPE were purchased from Cayman Chemicals. Except where noted, all other chemicals were obtained from Sigma-Aldrich. Si-gel chromatography was performed using precoated Merck F254 plates and Merck Kieselgel 60 powder. HPLC purifications were carried out on a Waters chromatograph equipped with R401 differential refractometer and 490E UV multiwavelength detector. A Packard 1600TR liquid scintillation analyser monitored ^{3}H-incorporation. GCMS data were obtained by a Hewlett & Packard 5989B mass spectrometer equipped with a 5890 Series II Plus gas chromatograph and with a HP 5MS column. LCMS analysis was performed on a Qtof-*micro* mass spectrometer (Waters) equipped with an ESI or APCI source and coupled with an 2695HPLC Alliance system. NMR spectra were registered on a Bruker Avance DPX 300, Bruker AMX 400, Bruker DRX 600 equipped with inverse TCI Cryoprobe®. Amicon YM10 were purchased by Millipore S.p.A. Protein content was determined using Lowry protein assay, following the protocol of the manufacturer's instructions (Bio-Rad), with bovine serum albumin as standard. SDS-PAGE was performed using a continuous buffer system of Laemmli, in a miniprotean vertical slab gel apparatus (Bio-Rad). Acrylamide stock contained 29.8% (w/v) acrylamide, 0.2% (w/v) N,N'-methylenebisacrylamide. Low molecular weight standards for SDS-PAGE (Amersham Biosciences) were used as calibration proteins: phosphorylase b (97,000), bovine serum albumin (66,000), ovalbumin (45,000), carbonic anhydrase (30,000).

5.2. Cell culturing

Axenic cultures of marine diatoms were prepared as described in Miralto et al. (Miralto et al., 1999). Briefly, diatom was grown in Guillard's (F/2) Marine Enrichment Basal Salt Mixture Powder (Sigma-Aldrich) medium, on a 12L:12D cycle, and a light intensity of 175

μmol μm^{-2} sec^{-1}. Cells were kept in 10 L carboys for 1 week and then harvested in the stationary phase by centrifugation at 1200 g in swing-out rotor. The cell pellets were immediately worked or frozen at –80°C.

5.3. Extraction of aldehydes

The cell pellet was suspended in F/2 medium (1ml/g cell pellet, sonicated 1 minute, and left at room temperature. After 30 minutes, acetone was added (1ml/g cell pellet) and internal standards were added. The sample was sonicated 1 minute and centrifuged at 2000 g for 5 minute at 5°C. The pellet was resuspended twice in H_2O/acetone 1:1 (2 ml/g cell pellet), sonicated 1 minute and centrifuged at 2000 g for 5 minutes. The supernatants were combined and extracted two times with equal volume of CH_2Cl_2. The organic layers were combined, dried over dry Na_2SO_4, filtrated and evaporated at reduced pressure. In this way an oil extract was obtained.

5.4. Derivatization procedure of aldehydes

(CarbethoxyEThylidene)-triphenylphosphorane [CET-triphenylphosphorane] was used as derivatizing agent. CH_2Cl_2 and C_6H_6 were tested as solvents, at different temperatures from 15°C to 80°C, and different reaction times. The derivatization procedure was developed on commercially available aldehydes (saturated aldehydes: octanal, decanal, undecanal, dodecanal, tetradecanal; monounsaturated: 2-*t*-octenal, 4-*t*-decenal; polyunsaturated: 2,4-*t,t*-heptadienal, 2,4-*t,t*-octadienal, 2,4-*t,t*-decadienal). Reaction with 1.1 equivalents of derivatising agent in CH_2Cl_2 at room temperature for 18 hours, under agitation were the most advantageous conditions for derivatization (d'Ippolito et al., 2002b). The reaction mixture was evaporated to dryness. The derivatization reaction was also directly applied to extracts. The extract was re-dissolved in 1 mL of CH_2Cl_2 and treated with CET-triphenylphosphorane (3mg/mg extract). The reaction was stirred at room temperature for 18h and then evaporated to dryness.

5.5. Purification of CET-aldehydes

The derivatized extracts were purified on silica gel with a gradient from petroleum ether to petroleum ether/Et_2O 1:1. The CET aldehydes were eluted with petroleum ether/Et_20 95:5.

5.6. GCMS analysis of CET-aldehydes

After derivatization, the purified aldehydes or raw extracts were analyzed by GCMS on OV-1 column, temperature gradient from 130 to 220°C at 3°C/min; injector temperature 240°C; detector temperature 260°C, N_2 flow 1 ml/min. Electron voltage was set at 70 eV.

5.7. Total fatty acid composition

The diatom cells were extracted with acetone and CH_2Cl_2 as described above for the extraction of aldehydes. The extract was methylated with a saturated solution of diazomethane in ethyl ether. The reaction mixture was dried and analyzed directly in GCMS. Alternatively, fatty acids methyl ester (FAME) were purified on silica gel with petroleum ether/diethyl ether 95/5.

5.8. GCMS analysis of FAME

FAME mixtures were dissolved in CH_2Cl_2 to a final concentration of 0.5 µg/µL, and analyzed by GCMS on OV-1 column, temperature gradient from 135 to 260°C at 3,5°C/min; injector temperature 260°C; detector temperature 260°C, N_2 flow 1,4 ml/min.

5.9. Isolation of HTA from *S. costatum*

Cells of *S. costatum* were suspended in F/2, sonicated 1 min. After 30 min the suspension was extracted in agreement with the modified Folch Method (Hamilton and Hamilton, 1993). The organic material was then fractionated on a silica gel column with light petroleum/Et_2O 85:15 (v/v) to give a clean fraction of free fatty acids. Reverse phase HPLC [column KR 100-5 C18; flow 1 mL/min; isocratic elution with MeOH/H_2O/TFA 85:15:0,3 (v/v/v)] of this fraction gave pure 6,9,12,15-hexadecatetraenoic acid (2.1 mg; CIMS *m/z* 249 [$M+H^+$]).

5.10. Synthesis of d_6-HTrA

6,9,12-Hexadecatriynoic acid methyl ester (0.82 mmol) was added to 10 mL of MeOH containing a catalytic amount of 5% Pd on $BaSO_4$ and quinoline. The reaction was vigorously stirred under D_2 atmosphere for 16h. After filtration on paper, the clear solution was evaporated. The reaction mixture was purified on silica gel and then hydrolyzed by 10% NaOH in EtOH to give [6,7,9,10,12,13-$^2H_6$]-6,9,12-hexadecatrienoic acid.

5.11. Incubation experiments with d_6-HTrA

The microalgae harvested in stationary phase were centrifuged at 1200 g for 10 min at 16°C and the resulting cell pellet (1.2 x 10^8 cells) was suspended at 4° C in 2 mL of F/2 medium prior to the addition of appropriate amounts of precursors ([6,7,9,10,12,13-$^2H_6$]-6,9,12-hexadecatrienoic acid (d_6-HTrA) (15.6 µmol/g of wet cells). The suspension was sonicated for 1 min and incubations were performed for 30 min at room temperature. The suspension was extracted and derivatized as described above. The derivatized aldehydes were purified on silica gel and analyzed in GCMS and NMR with a deuterium probe.

5.12. Incubation experiment with $^3H_{10}$-EPA in *S. costatum*

$^3H_{10}$-EPA (1 µCi/g cells) was added to sonicated suspensions of diatom cells. The incubation mixtures were extracted and derivatized as described above. The CET-aldehydes were purified on silica gel with petroleum ether/Et_20 95:5. Incorporation of $^3H_{10}$-EPA in derivatized heptadienal was determined by RP-HPLC (Phenomenex RP-18) eluting with CH_3CN/H_2O 70:30 (1 ml/min) and equipped with both Flo-One (Perkin Elmer) radiodetector and UV detector at 210 nm. The derivatized aldehydes were further hydrogenated on 5% Pd/C to give the corresponding saturated derivatives. After filtration on paper, the residue was analysed by HPLC with CH_3CN/H_2O 78:22 (1 ml/min), UV at 210 nm. The identity of each component was ascertained by co-elution with authentic standards.

5.13. Incubation experiment with $^{3}H_{10}$-EPA in *T. rotula*

In triplicate, 0.6 mg of radioactive EPA ($1.2x10^{7}$ cpm/mg) was added to a F/2 suspension of a fresh pellet (3 g wet weight) of diatoms harvested at the stationary phase. The pellet was sonicated for 1 min, and let to stand for 30 min prior to extraction with acetone (1 ml/g of cells). The suspension was centrifuged at 2000 g for 5 min. The supernatant was transferred and the pellet was washed twice with fresh acetone/H_2O (2 ml/g of cells). The supernatants were combined and a small amount (1/100 of the whole suspension) was diluted with scintillation cocktail (Perkin Elmer Optiphase High Safe, 10 ml) and counted for radioactivity ($3.9x10^{6}$ cpm). Analogously, the pellet was suspended in F/2 (12 ml), diluted with the scintillation cocktail, and counted ($1.7x10^{6}$ cpm). The supernatant was partitioned against CH_2Cl_2 to give 15 mg of organic extract ($6.5x10^{4}$ cpm/mg) that was directly derivatized by CET-TPP, as described above. Silica gel fractionation of the resulting material led to six fractions containing: #1 apolar compounds (0.3 mg, below blank), #2 pigment (0.5 mg, below blank), #3 CET-aldehydes (1.2 mg, $1.3x10^{5}$ cpm/mg, 14.0% of yield), #4 sterols and fatty acids (1.5 mg, 8253 cpm/mg), #5 fatty acids (7.2 mg, 80185 cpm/mg, 58.6%), #6 polar components (1.7 mg, $6.9x10^{4}$ cpm/mg, 12.0%). Each fraction was characterized by ^{1}H-NMR in $CDCl_3$. Fraction #3 was dried at reduced pressure and part of this material ($5.0x10^{4}$ cpm) was further fractionated on RP-HPLC (gradient H_2O/CH_3CN from 35:65 to 15:85 v/v, flow 1.0 ml/min) equipped with both a Flo-One (Perkin Elmer) radiodetector and UV detector. The remaining part of fraction #3 (about $6.7x10^{4}$ cpm) was hydrogenated with 5% Pd/C as described above. After 6 h, the reaction was stopped and filtered on paper. The resulting solution was dried at reduced pressure, dissolved in 0.5 ml of CH_3CN and analyzed on RP-HPLC (Kromasil C-18) eluting with CH_3CN /H_2O 78:22, flow 1.0 ml/min, and monitored by UV detector at 210 nm and radio-detector. Fraction #6 was methylated with ethereal diazomethane and further analyzed on RP-HPLC (isocratic H_2O/MeOH from 20:80 v/v, flow 1.0 ml/min) equipped

with both Flo-One (Perkin Elmer) radiodetector and UV (210 nm) detector. 11-HEPE methyl ester was used as a reference.

5.14. Inactivated enzymatic preparations

Diatom homogenates were kept in a boiling water bath for 10 min.

5.15. Localization of LOX/HPL activities in *T. rotula*

All procedures were carried out at 4 °C unless otherwise indicated. Frozen diatom pellets (1×10^9 cells) were sonicated in 30 ml of F/2 medium for 1 min. The homogenate (about 27 ml) was centrifuged for 30 min at 9600 *g*. The pellet was suspended in F/2 and centrifuged again. The resulting supernatants were pooled together (about 40 ml of suspension) and centrifuged for 2 h at 102000 *g*. The pellets of 9600 *g* and 102000 *g* were suspended in 8 ml of F/2. These suspensions together with crude homogenate and supernatants at 9600 *g* and 102000 *g* were used for the LOX assay and protein quantification. The same preparations were incubated for 30 min at 22 °C with 0.5 mg of d_6-HTrA. After addition of the internal reference (30 µg of 4-decenal), the reaction mixtures were extracted with dichloromethane and directly derivatized with CET-TPP. Analysis of the product was carried by GCMS as described previously. Inactivated enzymatic preparations were obtained by boiling the preparations for 10 min before adding HTrA. Their processing was identical to that described for the active fractions.

5.16. LOX assay

LOX activity was determined in agreement with the recent method proposed by Anthon and Barrett (Anthon and Barrett, 2001). The colorimetric response was optimized by two-step assay using hemoglobin, 32.5 µl of 25mM EPA and algal suspensions containing different number of cells (1.42×10^6, 2.13×10^6, 2.84×10^6 and 4.26×10^6) in 200 µl F/2. LOX activity was expressed as absorbance at 598 nm (Δ_{598}) X μg^{-1} of protein and normalized with respect to control without EPA. All experiments were performed in triplicate and data are presented as mean ± SD. The detection limits of LOX assay were determined using a concentration range of pure HpETE from 0.108 µmoli to 0.217 nmoli.

TMP was added to one series of samples to reduce the hydroperoxides to the corresponding non-reactive hydroxide derivatives and was used to authenticate the signal generated in the samples .

5.17. Substrate specificity in *T. rotula*

Diatom cells (about 1.2 x 10^9 cells) were lysed in F/2 medium as described above. Debris was removed by centrifugation at 9600 *g* for 30 min at 4 °C, and clarified lysate was ultrafiltrated on Amicon YM10 membranes under N_2 flow. The retent was extensively washed with F/2 medium, diluted to 10 ml in the same medium and divided in different aliquots. Part of this material, together with the corresponding filtrates, were incubated with d_6-HTrA (0.5 and 2.0 mg) at 24 °C for 30 min. After addition of the internal reference (30 µg of 4-decenal), the reaction mixture was extracted, derivatized with CET-TPP, and analyzed by GCMS as reported above.

To evaluate the capability of metabolizing different substrates, the remaining filtrate was divided in different aliquots and incubated (21 °C for 30 min) with free fatty acids [EPA (3.0 mg), arachidonic acid (3.0 mg), linoleic acid (3.0mg) and α-linolenic acid (3.0 mg) and [6,9,12,15]-octadecatetraenoic acid (3.0 mg)]. After extraction with organic solvent (CH_2Cl_2), the analysis of the incubation products was carried out by GCMS on CET-derivatives prepared as previously described. 4-Decenal (30 µg) was used as internal reference for the quantitative analysis.

5.18. Lipid extraction

Fresh diatoms were harvested by gentle centrifugation at 1200 g for 10 min at 16°C. The resulting pellet was suspended in F/2 and added in boiling MeOH. The suspension was then extracted with $CHCl_3$/MeOH 2:1 following the modified Folch method (Hamilton and Hamilton, 1993). The lipid classes were fractionated by silica gel column. Neutral lipids (TGA) were eluted with petroleum ether/ethylic ether 90:10, and glycolipids (GL) and phospholipids (PL) were obtained with acetone/MeOH 9:1 and $CHCl_3$/MeOH/H_20 65:25:4,

respectively (Bergè et al., 1995). Monogalactosyldiacylglycerols (MGDG) were separated from digalactosyldiacylglycerols (DGDG) and sulphoquinovosyldiacylglyecrols (SQDG) by a further SiO_2 column with $CHCl_3$/MeOH 95:5. Products were identified by NMR in $CDCl_3/CD_3OD$ 1:1.

5.19. Composition of complex lipids

The level and composition of fatty acids from each lipid class were determined by GC-MS on the corresponding methyl esters (fatty acid methyl ester, FAME) obtained after saponification with Na_2CO_3 in MeOH (42°C) for 4 h. The analysis of *sn*-composition of MGDG was carried out on silica gel purified fractions using HPLC/ESI-MS/MS in agreement with a recent methodology proposed by Guella et al. (Guella et al., 2003)

5.20. Direct in vivo preparation of labelled TAG, GL and PL in *S. costatum*

[5,6,8,9,11,12,14,15,17,18-$^3H_{10}$]-eicosapentaenoic acid ($^3H_{10}$-EPA) (5 µCi) was added to a suspension of the microalga ($9.5x10^6$ cells) in 2 ml of F/2 medium. After 1 h, the culture was transferred to a 250 ml flask and diluted with 200 ml of F/2 medium. The diatom was kept in this volume for another 20 h before harvesting by gentle centrifugation (1200g for 10 min, at 16°C). In order to remove excess quantities of free ^{3}H-EPA, the pellet was washed four times prior to being added to a fresh pellet of "cold" cells (3.3 g wet weight). The resulting material was suspended in boiling MeOH (3.5 ml) and then extracted and fractionated as described above to give 41 mg of glycolipids (1.8×10^5 cpm), 19.5 mg of phospholipids (9×10^5 cpm) and 7 mg of triglycerides (8.1×10^4 cpm).

5.21. Incubation experiments with $^3H_{10}$-EPA-containing lipids in *S. costatum*

To study the lipid pool involved in the formation of PUAs, feeding experiments were carried using GL (181800 cpm), PL (933200 cpm) and triacylglycerol (81500 cpm). Each radioactive fraction was dissolved in 2.5 ml MeOH (2.5 ml acetone for TAG) and transferred to a conical flask. After removing the organic solvent, each oily residue was incubated for 30 minutes with 4 ml of *S. costatum* homogenate ($2 x10^9$ cells) at 18 °C under constant stirring. Then each suspension was extracted and derivatized as described

above. The derivatized aldehydes were purified on silica gel with petroleum ether/diethyl ether 95:5. The rate of incorporation of $^{3}H_{10}$-EPA in derivatized heptadienal was determined by RP-HPLC (Phenomenex RP-18) eluting with CH_3CN/H_2O 70:30 (1 ml/min) and equipped with both Flo-One (Perkin Elmer) radiodetector and UV detector at 210 nm. The derivatized aldehydic mixture was further hydrogenated on 5% Pd/C and analysed as described above.

5.22. Incubation experiments with aldehyde-depleted homogenates of *S. costatum* cells

Skeletonema homogenates were prepared by sonication of diatom cells (in 12 ml distilled water for 1 min) harvested at the stationary phase. After 30 min, the suspension was kept under vacuum (5 torr) for 15 min at 4°C and then split into four aliquots (3 ml each). The first aliquot was used as control and kept untreated at 18°C. The other aliquots were incubated at 18°C with MGDG (7 mg) and GL (6 mg), prepared from a fresh culture of the microalgae as described above, and d_6-HTrA (1 mg) and EPA (1.8 mg) to test LOX activity. After 30 min, acetone (2 ml per fraction) was added to the control and incubated homogenates and the resulting solutions were extracted, derivatized and analysed by GCMS as described above for analysis of PUAs.

5.23. Incubation experiments of lipids in ultrafiltered fractions of *T. rotula*

All procedures were carried out at 4 °C unless otherwise indicated. Typically, a frozen diatom pellet (6×10^8 cells) was sonicated in 30 ml of F/2 medium for 1 min. The homogenate (about 27 ml) was centrifuged for 30 min at 9600 *g* at 6 °C, and the clarified supernatant was ultrafiltrated on Amicon YM10 membranes under N_2 flow. The retent was extensively washed with F/2 medium, diluted in the same medium (10 ml). This solution was divided in different aliquots and incubated with GL (8 mg), PL (6 mg) and neutral lipids (2 mg), which had been previously purified from other extracts of *T. rotula*. The incubation experiments were performed in triplicate and d_6-HTrA (0.2 mg) was added as internal control. Each incubation was kept at 22°C for 30 min, unless otherwise mentioned, and terminated by adding an equal volume of acetone. After addition of the internal

reference (30 μg of 4-decenal), half of each reaction mixture was extracted with dichlomethane, derivatized with CET-TPP and analyzed by GCMS as described above. The remaining parts of the incubation mixtures were extracted with $CHCl_3$/MeOH 2:1 and filtered. The filtrates were combined, quantitatively transferred to glass tube, and allowed to stand for 10 min at 4 °C for phase separation. The lower chloroform phase was collected, and the upper alcohol phase was re-extracted with 10 ml of chloroform. The combined chloroform extracts were washed twice with 0.9% (w/v) NaCl solution. The extract was concentrated by rotary evaporation under reduced pressure at 30°C and kept under vacuum until a constant weight was obtained. This material was then dissolved in chloroform/methanol and analyzed on TLC (silica Gel 60 F-254) using one of the following solvent systems: chloroform:methanol:water (65:25:4, v/v), chloroform/methanol/ammonia (65:30:4, v/v), petroleum ether/diethyl ether/acetic acid, (70:30:1, v/v). In each experiment boiled retentates (supplemented with lipids) and retenate controls were included.

5.24. Quantification of lipid hydrolysis in lysed diatoms of *T. rotula*

Cell pellet (about 5 x 10^7 cells) was suspended in 2 ml F/2 medium and sonicated for 30 s. Suspension was transferred to a flask and 0.4 mg of erucic acid (13*Z*-docosenoic acid) was added as internal standard prior to homogenization with 3.6 ml $CHCl_3$/MeOH 2:1 v/v. Sample was then filtered on paper, washing the residue with 2 ml of $CHCl_3$/MeOH 2:1 v/v. Filtrate was transferred to separatory funnel to obtain phase separation. The lower layer was recovered and the aqueous residue was re-extracted with 2 ml chloroform. Organic phases were combined and washed with ¼ H_20/MeOH 1:1. Organic solvent was then removed at reduced pressure and the resulting residue was dissolved in 2.5 ml CD_3OD and saponified under argon with 12 mg dry Na_2CO_3. After stirring at 42 °C for 4 h, the reaction mixture was neutralized (pH = 6) by 1N H_2SO_4 and extracted against diethyl ether. Organic solution was dried on Na_2SO_4, filtered on paper and methylated with an ethereal solution of diazomethane. After removing the excess of diazomethane under N_2 stream, the

solution was evaporated at reduced pressure and dissolved in *n*-hexane at a final concentration of 1.5 μg/μl. Fatty acid analysis was carried out by GCMS as reported above.

5.25. Fractionation of the lipolytic activity of *T. rotula*

About 20 g of wet cells of *T. rotula* were suspended in 50 mM sodium phosphate buffer, pH 7.0. Suspension was sonicated for 3 cycles of 30 s and the cell extract was centrifuged at 9,600 g (6 °C) for 30 min. The pellet was re-suspended in the same buffer and centrifuged twice. Supernatants were combined (60 ml) and centrifuged at 102,000 g for 4 h (6 °C). Lipolytic activity was qualitatively monitored on the resulting supernatants and pellets by assaying small aliquots of sample with 5 μl of 25 mM MUF-butyrate spotted onto filter paper (Prim et al., 2003). After that, glycolipid hydrolysis was monitored on the same fractions by incubating 6 mg MGDG previously purified from *T. rotula* lipids under the conditions illustrated above for the experiments with retenates. Reactions were monitored by SiO_2-TLC using chloroform/methanol/water (65:25:4, v/v) as eluent, and by GCMS.

5.26. Preliminary characterization of the lipolytic activity and zymograms in *T. rotula*

Supernatant and pellet were obtained by centrifugation at 102,000 g as described above. These fractions were analysed on SDS-PAGE containing 10% or 15% total acrylamide in 0.375 M Tris/HCl, pH 8.8, 0.1% SDS. Samples were dissolved in 0.01 M Tris/HCl, pH 6.8, 1% SDS, 0.7 M β-mercapto-ethanol, 1.36 M glycerol, 0.005% bromophenol blue as tracking dye, without heating. Electrophoresis was performed at 25 °C at 24 mA for 1 h. The pellet was repetitively washed with 50 mM sodium phosphate buffer (pH 7.0) and centrifuged at 102,000 g. The combined supernatants were concentrated on Centriplus YM10 (Amicon) and dialyzed against 2 liter of 20 mM diethanolamine pH 8.4. Aliquots of these fractions were analyzed by SDS-PAGE. In agreement with Prim (Prim et al., 2003) resolved gels were soaked in 2.5% Triton X-100 at room temperature for 30 min, washed

for 5 min in 50 mM sodium phosphate buffer (pH 7.0), and incubated in 10 ml of 100 µM MUF-butyrate or 200 µM MUF-oleate in 50 mM sodium phosphate (pH 7.0). After incubation of 1 min with the MUF-butyrate or 15 min with the MUF-oleate, the lipase activity was visualized by using the Chemidoc System (BIO-RAD). Following zymogram analysis, the same gel was stained with 0.1% Coomassie Brilliant Blue R-250 in 25% (v/v) methanol. The proteins were monitored spectrophotometrically at 280 nm or were assayed with Bio-Rad protein dye assay reagent.

5.27. Native gel filtration of 102'000 g supernatants of *T. rotula*

Lipolytic activity was also evaluated by gel filtration in native conditions. To this aim, supernatant from 102,000 g centrifugation was concentrated on Centricon 10® as described above and dialyzed at 6 °C against 150 mM NaCl in 50 mM sodium phosphate buffer, pH 7.0. The sample was loaded onto a Superdex 200 HR 26/60 (Amersham Lifescience) FPLC column, equilibrated in 50 mM sodium phosphate buffer pH 7.0, containing 0.15 M NaCl. Gel filtration chromatography was performed with the same eluent at a flow rate of 1.0 ml/min and adsorbance was monitored at 280 nm. A high molecular weight gel filtration calibration kit (Amersham Biosciences) was employed, using as markers the proteins catalase (232 kDa), aldolase (158 kDa) and bovine serum albumin (67 kDa). Apparent molecular weights of the aggregate proteins were determined by comparing their elution peaks (calculated as the ratio of elution volume [*V*e] to void volume [*V*0]) against a calibration curve generated by the elution peaks of the protein standards. *V*0 was determined by gel filtration of blue dextran. Fractions of 5.0 ml were collected and analyzed for protein content and lipolytic activity with MUF-butyrate on paper filter. The active fractions were concentrated on Centricon 10® and assayed for galactolipid-hydrolyzing activity, using authentic GLs purified from *T. rotula* extracts. In Teflon screw-top glass tubes, 100 µl of enzymatic preparation were diluted at 1 ml with 50 mM sodium phosphate buffer (pH 7.0) and incubated with 3 mg of GL (dissolved in 20 µl of methanol). After the addition of pentadecanoic acid (C15:0) as internal standard, the

organic solution were methylated by ethereal diazomethane, dried under nitrogen and analyzed by GCMS as described above.

5.28. Extraction, purification and analysis of oxylipins

About 25 g of frozen cells were extracted as previously described for the aldehydes. The raw extracts were methylated with ethereal diazomethane and successively fractionated on silica gel column by a polarity gradient system (Et_2O in petroleum ether). Further purification steps were performed by reverse phase HPLC (Phenomenex C-18, 100A, 5µm, 250 x 4.6 mm) eluting with a gradient from MeOH/H_2O 70/30 to MeOH/H_2O 80/20 in 15 minutes, followed by isocratic elution MeOH/H_2O 80/20 (1 ml/min) and monitoring the elution at 210 nm. Every purified fraction was analyzed by LC-ESI$^+$-MS in the same conditions. The column flow was split approximately 9:1 before ESI source. Alternatively, raw extracts were dissolved in MeOH at a final concentration of 1 mg/ml and directly analyzed by LC-ESI$^+$-MS/MS as described above.

5.29. Absolute stereochemistry of 9-hydroxy-7*E*-hexadecenoic acid

Dimethyl dichlorosilane (54 µmol) was added by a syringe to a solution of the alcohol **25a** (0.4 mg, 1.4 µmol) in dry pyridine (200 µl) under Argon atmosphere. The reaction was kept at 75 °C for 45 min and then split into two identical parts. These aliquots were then reacted with (*R*)- and (*S*)-α-trifuoromethyl benzyl alcohol (108 µmol) dissolved in 200 µl of dry pyridine. After 30 min. at 75 °C, the reactions were quenched by addition of 400 µl of MeOH. The resulting solutions were dried under reduced pressure and purified on silica gel by eluting with petroleum ether/diethyl ether 95:5. The absolute stereochemistry was determined on the basis of the differences (δR-δS) of the ^{1}H chemical shifts of the diastereomeric α-trifluoromethyl benzyl silyl derivatives (*R*- and *S*-PhTFE) (**25b** and **25c**)

5.30. Absolute Stereochemistry of 9-HHTrE

Racemic (**30a/30b**) and (*S*)-enantiomer (**30a**) of 9-hydroxyhexadecanoate methyl esters were prepared by $NaBH_4$ reduction of 9-keto-7-hexadecanoate (**24a**) and hydrogenation of (9*S*) methyl-9-hydroxy-7-hexadecenoate (**25a**), respectively. Methyl 9-keto-7-hexadecenoate (**24a**) (0.8 mg) in MeOH was stirred overnight with excess $NaBH_4$. The reaction mixture was acidified with 5% H_2SO_4 and extracted with diethyl ether for three times. The ethereal fractions were combined and evaporated at reduced pressure to give 0.4 mg of (±) 9-hydroxyhexadecanoic acid methyl ester (**30a/30b**). 9(*S*)-Hydroxy-7*E*-hexadecenoic acid methyl ester (0.3 mg) and 9-HHTrE (0.2 mg) were purified from diatom extracts as described above and hydrogenated on 10% Pd on activated carbon in MeOH (0.5 ml). The reactions were stirred under H_2 for 6 h and then filtered on paper to give the saturated derivatives. For the chiral analysis, the above products were first purified on RP-HPLC (Kromasil C-18, MeOH/H_2O 80/20, flow 1 ml/min) and then injected on Chiralcel OD-H column (Baker) using *n*-hexane-isopropanol (98:2) (flow 1 ml/min) monitoring the elution by APCI-MS.

5.31. Chiral analysis of 6-HHTrE in *T. rotula*

6-HHTE was purified from raw extracts of *T. rotula* by RP-HPLC eluting with MeOH/H_2O 80/20 (1 ml/min), λ=236 nm. The peak was collected and re-injected on chiral-HPLC (Chiralcel OD-H column) by using a mixture of hexane/isopropanol (98:2) at a flow rate of 1 ml/min, (detection λ=236 nm).

5.32. Conversion of d_6-HTrA into d_6-9-HHTrE in *T. rotula*

Microalgae harvested in stationary phase were centrifuged at 1200 g for 10 min at 16°C and the resulting cell pellet (1.2×10^8 cells) was suspended at 4° C in 2 mL of F/2 medium prior to the addition of d_6-HTrA (15.6 µmol /g of wet cells). The suspension was sonicated for 1 min and incubations were performed for 30 min at room temperature. The incubation mixture was divided in three different aliquots and extracted as described above. The first aliquot was used for GCMS analysis after derivatization with CET-TPP. The second

aliquot was used as control, and the third one was treated with 20 wt% of TMP in CH_2Cl_2 at 4°C for 30'. The organic extracts were evaporated and methylated with diazomethane prior to the analysis on RP LC-MS (Kromasil C-18) with MeOH /H_2O 80:20, flow 1.0 ml/min (detction UV at 236 nm). 16-hydroxyhexadecanoic acid was used as internal standard.

5.33. Absolute stereochemistry of 11-HEPE, 15-HEPE, 9-HEPE and 5-HEPE.

HEPEs were purified from raw extracts by RP-HPLC eluting with H_2O/MeOH 20:80 (1 ml/min), λ=236 nm. The peaks corresponding to the retention time of authentic HEPEs were collected and re-injected on chiral-HPLC (Chiralcel OD-H column) by using a mixture of hexane/isopropanol (98:2) at a flow rate of 1 ml/min, (detection λ=236 nm). The absolute stereochemistry was determined in comparison with authentic (±)11-HEPE and 11(*R*)-HEPE, (±)15-HEPE and 15(*S*)-HEPE, (±)9-HEPE and 9(*S*)-HEPE, and (±)5-HEPE and 5(*S*)-HEPE.

5.34. Incorporation of $^3H_{10}$-EPA in *P. delicatissima*

In triplicate, radioactive EPA ($2.2x10^6$ cpm) was added to a F/2 suspension of a fresh pellet (1,5 g wet weight) of diatoms harvested at the stationary phase. The pellet was sonicated for 1 min, and let to stand for 30 min prior to the extraction with acetone and CH_2Cl_2 as described above. The extract (extract 241300 cpm/mg, residual water 369292cpm) was in part (144780 cpm) reduced with TMP in CH_2Cl_2. After 30 min, the reaction was dried, and lipids were extracted with Et_2O/water four times. The organic extract was evaporated to dryness (160650 cpm). An aliquot (1/25) of untreated extract and reduced extract were analyzed in RP-HPLC (MeOH/H20 80:20 v/v, λ=210 nm, flow 1 ml/min) equipped with both Flo-One (Perkin Elmer) radiodetector and UV detector. Peaks corresponding to 15-HEPE and 15-HPEPE were coeluted in this condition, giving rise to a large peak with a retention time of 33.5 min. This peak was collected from these different extracts. The compounds of interest were extracted from MeOH/H_2O with *n*-hexane for four times. The

n-hexane extracts were injected in SP-HPLC (n-exane/ethylic ether 85:15 v/v, flow 1 ml/min, λ=210 nm) equipped with the radiodetector.

5.35. Autoxidation of EPA

EPA was methylated with ethereal diazomethane and autoxidated at 42°C in the dark for two weeks in presence of α-tocopherol (Peers and Coxon, 1983). Isolation of the hydroperoxide mixture of was performed by SP-HPLC with a solvent system of hexane/Et_2O 85/15, flow 1 ml/min, λ=236 nm. Part of the purified hydroperoxide mixture was hydrolyzed by 10% NaOH in EtOH.

5.36. Antimitotic assay on sea urchin embryos of *Paracentrotus lividus*.

For egg development tests, specimens of the sea urchin *Paracentrotus lividus* were collected in the bay of Naples. Gamete ejection was induced by injecting 2 ml of 0.5 M KCl solution into the perivisceral cavity. Spawned eggs were allowed to settle and washed three times with 0.22 μm filtered sea water (FSW), then diluted to a final concentration of 1000 eggs/ml. Concentrated sperm was collected with a Pasteur pipette and diluted immediately prior to fertilization (20 μl of sperm in 5 ml FSW). An aliquot of 20 μl of sperm suspension was added to the egg suspension (50 ml). Five minutes after fertilization, 200 μl of egg suspension was added to each of 12-well plates containing increasing concentrations of the sample to be tested, ranging from 0.1 to 10 μg/ml. Samples were diluted in methanol and <10 μl of methanol/ml of FSW was added to assays, a concentration that had no effect on developing embryos. A control sample was incubated in the same conditions in FSW and another control was performed in the presence of 10 μl methanol/ml FSW. Eggs were incubated in a final volume of 2 ml at constant room temperature (20°C). After 90 min, 100 eggs or embryos were counted for each concentration, to obtain the percentage of cleavage inhibition.

6. REFERENCES

- Adolph S., Poulet S. and Pohnert G. 2003. *Tetrahedron* 59:3003–3008

- Andrews D.L., Beames B., Summers M.D., Park W. D. 1988. *Biochem J.* 252:199–206

- Anthon G.E. and Barrett D.M. 2001. *J. Agri. Food Chem.* 49, 32-37.

- Arao T., Kawaguchi A., Yamada M.1987. *Phytochemistry* 26: 2573–2576

- Ban S., Lee H.-W., Shinada A., Toda T. 2000. *J.Plankton Res.* 22: 907–922.

- Ban C., Burns J., Castel Y., Chaudron E., Christou R., Escribano S. F., Umani S., Gasparini F., Ruiz G., Hoffmeyer M., Ianora A., Kang H. K., Laabir M., Lacoste A., Miralto A., Ning X. R., Poulet S. A., Rodriguez V., Runge J., Shi J. X., Starr M., Uye S., Wang Y. J., 1997. *Mar. Ecol. Prog. Ser.* 157:287– 293.

- Banerji S., Flieger A., 2004. *Microbiology* 150:522-525.

- Berge J.P.,. Gouygou J.P, Durand P., Dubacq J.P.1995. *Phytochemistry* 39:1017– 1021.

- Blée E.1998. *Prog. Lipid Res.* 37(1):33-72

- Borngräber S., Browner M., Gillmor S., Gerth C., Anton M., Fletterick R., Kühn, H. 1999. *J. Biol. Chem.* 274:37345–37350.

- Brash A. R. 1999. *J. Biol. Chem.* 274:23679 –23682.

- Chaudron Y., Poulet S.A., Laabir M., Ianora A. and Miralto A. 1996. *Mar. Ecol. Prog. Ser.* 144: 185–193.

- Coffa G. and Hill E.M. 2000. *Lipids* 35:1195-1204.

- Cutignano A., d'Ippolito G., Cimino G., Febbraio F., Nucci R., Romano G., Fontana A. 2006. *ChemBioChem*, 7(3), 450-456

- d'Ippolito G., Romano G., Iadicicco O., Miralto A., Ianora A., Cimino G., Fontana A. 2002a. *Tetrahedron Lett.* 43:6133–6136.

- d'Ippolito G., Romano G., Iadicicco O., Fontana A. 2002b *Tetrahedron Lett.*, 43:6137–6140.

- d'Ippolito G., Romano G., Caruso T., Spinella A., Cimino G., Fontana A. 2003. *Org. Lett.* 5:885-887.

- d'Ippolito G., Tucci S., Cutignano A., Romano G., Cimino G., Miralto A., Fontana A. 2004. *BBA* 1686:100– 107

- d'Ippolito G., Cutignano A., Briante R., Febbraio F., Cimino G., Fontana A. 2005a. *Org. Biomol. Chem.* 3: 4065-4070

- d'Ippolito G., Cutignano A., Tucci S., Romano G., Cimino G., Fontana A. 2005b. *Phytochemistry*, 2006, 67 (3), 314-322

- de Bruxelles G. L. and Roberts M. R. 2001. *Crit. Rev. Plant Sci.* 20(5):487-521

- Doderer A., Kokkelink I., van der Veen S., Valk B.E., Schram A.W., Douma A.C. 1992. *BBA* 1120:97-104.

- Falciatore A. and Bowler C. 2002. *Annu. Rev. Plant Biol.* 53:109–130

- Falkowski P.G., Barber R.T., Smetacek V. 1998. *Science* 281:200–206

- Feussner I., Balkenhohl T. J., Porzel A., Kuhn H., Wasternack C. 1997. *J. Biol. Chem.* 272(34):21635–21641

- Gerwick W. H. 1994. *BBA* 1211:243 –255.

- Gerwick W. H., Roberts M. A., Vulpanovici A., Ballantine D. L.1999. In Advances in Experimental Medicine and Biology, Plenum, New York, pp.211 – 218

- Gerwick W. H., Moghaddam M. F., Hamberg M. 1991. *Arch. Biochem. Biophys.* 290: 436-444.

- Guella G., Frassanito R., Mancini I. 2003. *Rapid Commun. Mass Spectrom.* 17:1982–1994.

- Hamilton S., Hamilton R.J., Sewell P.A. 1993. In: R.J. Hamilton, S. Hamilton (Eds.), Lipid Analysis: A Practical Approach, IRL Press, Oxford, pp. 13– 14.

- Harkes P.D. and Begemann W.J. 1974. *J. Am. Chem. Soc.* 51: 356–359.

- Heath M.C. 2000. *Plant Mol. Biol.* 44:321–334.

- Hornung E., Walther M., Kuhn H., Feussner I. 1999. *Proc. Natl. Acad. Sci. USA* 96:4192–4197.

- Ianora A. 1998. *J. Mar. Syst.* 15: 337–349.

- Ianora A., Poulet S.A., Miralto A., Grottoli R. 1996. *Mar. Biol.* 125: 279–286.

- Ianora A., Poulet S. A., Miralto A. 2003. *Phycologia* 42:351–363.

- Ianora A. and Poulet S.A. 1993. *Limnol. Oceanogr.* 38:1615–1626.

- Irigoien X., Harris R.P., Head R.N., Harbour D. 2000. *Limnol. Oceanogr* 45:1433–1439.

- Irigoien X., Harris R.P., Verheye H.M., Joly P., Runge J., Starr M., Pond D., Campbell R., Shreeve R., Ward P., Smith A.N., Dam H.G., Peterson W., Tirelli V., Koski M., Smith T., Harbour D., Davidson R. 2002. *Nature* 419:387–389

- Isaacs 1969. *Sci. Amer.* 221(3):146-162

- Jisaka M., Kim R. B., Boeglin W. E., Brash A. R. 2000. *J. Biol. Chem.* 275:1287–1293.

- Kalyankrishna S., Parmentier J.-H., Malik K. U. 2002. *Prostaglandins Other Lipid Mediat.* 70:13–29

- Kemp A.E.S., Pike J., Pearce R.B., Lange C.B. 2000. *Deep-Sea Res.* 47:2129–54.

- Knight V.I., Wang H., Lincoln J.E., Lulai E., Gilchrist D.G., Bostock R.M. 2001. *Phys. Mol. Plant Phat.* 59:277-286

- Kühn H., Sprecher H., Brash A.R. 1990. *J. Biol. Chem.* 265.16300–16305.

- Kuribayashi T., Kaise H., Uno C., Hara T., Hayakawa T., Joh T. 2002. *J Agric Food Chem.* 50:1247-53.

- Laabir M., Poulet S.A., Ianora A., Miralto A., Cueff A. 1995. *Mar. Ecol. Prog. Ser.* 129: 97–105.

- Lacoste A., Poulet S.A., Cueff A., Kattner G., Ianora A., Laabir M. 2001. *J. Exp. Mar. Biol. Ecol.* 259:85–107.

- Lee R.E. 1999. In Phycology, ed. RE Lee, Cambridge, UK: Cambridge Univ. Press., pp. 415–458.

- Leon J., Rojo E., Sanchez-Serrano J.J. 2001. *J. Exp. Bot.* 52:1-9.

- Lopez D.A.,. Belrabi E.H, Fernandez-Sevilla J.M., Rodriguez Ruiz J., Molina Grima E. 2000. *Phytochemistry* 54:461–471.

- MacMillan D.K. and Murphy R.C.1995. *J. Am. Soc. Mass Spectrom.* 6:1190.

- Matos A.R., d'Arcy-Lameta A., França M., Pêtres S., Edelma L., Kader J-C., Zuily-Fodil Y., Pham-Thi A.T. 2001. *FEBS Lett.* 491:188-192.

- Matsui K., Kurishita S., Hisamitsu A., Kajiwara T.2000 *Biochem. Soc. Trans.* 28:857-860.

- Mercier J. and Agoh B.1974. *Chem. Phys. Lipids* 12:239-248.

- Miralto A., Ianora A. and Poulet S.A. 1995. *J. Plankton Res.* 17: 1521–1534.

- Miralto A., Barone G., Romano G., Poulet S.A., Ianora A., Russo G.L., Buttino I., Mazzarella G., Laabir M., Cabrini M., Giacobbe M.G. 1999. *Nature* 402:173-176.

- Muralidhar B., Carpenter K.L.H., Muller K., Skepper J.N., Arends M. 2004. *Prostaglandins Leukot. Essent. Fatty Acids* 71:251-262.

- Nejstgaard J.C., Hygum B.H., Naustvoll L.J. and Banamstedt U. 2001. *Mar. Ecol. Progr. Ser.* 221:77–91.

- Noordermeer M. A., Veldink G. A., Vliegenthart J. F. 2001. *ChemBioChem* 2:494–504.

- Norton T.A., Melkonian M., Andersen R.A. 1996. *Phycologia* 35:308–26.

- Ohman M. and Hirche H.J. 2001. *Nature* 412: 638–641.

- Paffenhöfer G.-A. 1988. *Bull. Mar. Sci.* 43:430–445.

- Paffenhöfer G-A., Ianora A., Miralto A., Turner J.T., Kleppel G.S., Ribera d'Alcala M., Casotti R., Caldwell G.S., Pohnert G., Fontana A., Müller-Navarra D., Jonasdottir S., Armbrust V., Bamstedt U., Ban S., Bentley M.G., Boersma M., Bundy M., Buttino I., Calbet A., Carlotti F., Carotenuto Y., d'Ippolito G., Frost B., Guisande C., Lampert W., Lee R.F., Mazza S., Mazzocchi M.G., Nejstgaard J.C., Poulet S.A., Romano G., Smetacek V., Uye S., Wakeham S., Watson S., Wichard T. 2005. *Mar. Ecol. Prog. Ser.* 286: 293-305.

- Paffenhöfer G.A. 1970. *Helgoländer wissenschaftliche Meeresuntersuchungen* 20:346–359.

- Peers K. E. and Coxon D. T. 1983. *Chem. Phys. Lipids* 32:49-56

- Phillips D. R., Matthew J. A., Reynolds J., Fenwick G. R., 1979. *Phytochemistry* 18:401–404.

- Pohnert G. 2000. *Angew. Chem.* 112:4506–4508

- Pohnert G. 2002. *Plant Physiol.* 129:103–111.

- Pohnert G., Lumineau O., Cueff A., Adolph S., Cordevant C., Lange M., Poulet S.A. 2002. *Mar. Ecol. Prog. Ser.* 245:33–45.

- Pohnert G., Adolph S., Wichard T. 2004. *Chem. Phys. Lipids.* 131:159 –166.

- Poulet S., Laabir M., Ianora A. and Miralto A. 1995. *Mar. Ecol. Prog. Ser.* 129:85–95.

- Poulet S.A., Ianora A., Miralto A., Meijer L. 1994. *Mar. Ecol. Prog. Ser.* 111:79–86.

- Prigge S. T., Gaffney B. J., Amzel L. M. 1998. *Nat. Struct.* Biol. 5:178–179.

- Prim N., Sanchez M., Ruiz C.R., Pastor J.F.I., Diaz P. 2003. *J. Mol. Catal.:B Enzym.* 22: 339-346.

- Reisner A.H., *Methods Enzymol.*, 1984, 104, 439-441.

- Scala S. and Bowler C. 2001. *Cell. Mol. Life Sci.* 58:1666–73

- Schulte-Ladbeck R., Lindahl R., Lewin J.O., Karst U. 2001. *J Environ Monit.* 3:306-310.

- Sloane D. L., Leung R., Craik C. S., Sigal E. 1991 *Nature* 354 :149–152.

- Smetacek V. 1999. *Protist* 150:25–32

- Smetacek V. 2001. *Nature* 411:745

- Spiteller D. and Spiteller G. 2000. *Angew. Chem. Int. Ed.* 39:583–585.

- Starr M., Runge J.A., Therriault J.C. 1999. *Sarsia* 84:379–389.

- Tang D.G., La E., Kern J., Kehrer J. 2002. *Biol. Chem* 383:425-442.

- Treguer P., Nelson D.M., Van Bennekom A.J., DeMaster D.J., Leynaert A.1995. *Science* 268:375–79

- Turner J.T. and Tester P.A. 1997. *Limnol. Oceanog.* 42:1203–1214.

- Vogel M., Buldt A., Karst U. 2000. *Fresenius J. Anal. Chem.* 366:781-791.

- Wendel T. and Jüttner F. 1996. *Phytochemistry* 41:1445–1449.

- Wichard T., Poulet S. A., Halsband-Lenk C., Albaina A., Harris R., Liu D., Pohnert G. 2005. *J. Chem. Ecol.* 31(4):949.

- Williamson R.T., Barrios Sosa A.C., Mitra A., Seaton P.J., Weibel D.B., Schroeder F.C., Meinwald J., Koehn F.E. 2003. *Org. Lett.* 5:1745.

- Yamamoto S., Suzuki H., Ueda N. 1997. *Prog. Lipid Res.* 36:23–41.

- Yongmanitchai W., Ward O.P. 1993. *J. Gen. Microbiol.* 139: 465–472.

- Zhou L. and Thornburg R. Wound -Inducible Genes in Plants Inducible Gene Expression cap. 8, CAB International 1999, (ed. P.H.S. Reynolds).